UNIVERSIDAD COMPLUTENSE DE MADRID

FACULTAD DE CIENCIAS BIOLÓGICAS

Departamento de Bioquímica y Biología Molecular I

TESIS DOCTORAL

Relaciones estructura-función de la proteína SP-C del surfactante pulmonar: efectos sobre la estructura de membranas y papel del colesterol

Structure-function relationships of lung surfactant protein SP-C : effects on membrane structure and role of cholesterol

MEMORIA PARA OPTAR AL GRADO DE DOCTOR

PRESENTADA POR

Nuria Roldán López

Directores

Begoña García Álvarez
Jesús Pérez Gil

Madrid, 2017

UNIVERSIDAD COMPLUTENSE DE MADRID

FACULTAD DE CIENCIAS BIOLÓGICAS

Departamento de Bioquímica y Biología Molecular I

RELACIONES ESTRUCTURA-FUNCIÓN DE LA PROTEÍNA SP-C DEL SURFACTANTE PULMONAR: EFECTOS SOBRE LA ESTRUCTURA DE MEMBRANAS Y PAPEL DEL COLESTEROL

STRUCTURE-FUNCTION RELATIONSHIPS OF LUNG SURFACTANT PROTEIN SP-C: EFFECTS ON MEMBRANE STRUCTURE AND ROLE OF CHOLESTEROL

MEMORIA PARA OPTAR AL GRADO DE DOCTOR

PRESENTADA POR

Nuria Roldán López

DIRECTORES

Begoña García Álvarez
Jesús Pérez Gil

Madrid, 2017

The research for this Thesis has been conducted in the Department of Biochemistry and Molecular Biology I of Complutense University of Madrid, under the supervision of Prof. Jesús Pérez Gil and Dr. Begoña García Álvarez. Part of the experimental work was conducted in collaboration with Prof. Erik Goormatigh, from the Laboratory for the Structure and Function of Biological Membranes (Université Libre de Bruxelles, Brussels, Belgium); at the Laboratory of Lipid and Membrane Biochemistry (Åbo Akademi, Turku, Finland) in collaboration with Prof. J. Peter Slotte and Dr. Thomas Nyholm; at the Department of Physics and Physical Oceanography (Memorial Univesity of Newfoundland, Saint John's, Newfoundland, Canada) in collaboration with Prof. Michael Morrow and at the Institute for Functional and Applied Anatomy (Hannover Medical School, Hannover, Germany) under the supervision of Dr. Elena López Rodríguez and Prof. Matthias Ochs. Funding for short-term stays was provided by the European Biophysical Societies' Association (EBSA), European Molecular Biology Organization (EMBO, ASTF 241-2014) and the Spanish Ministry of Education, Culture and Sport (EST15/00594).

The financial support to complete this Thesis was provided by the Spanish Ministry of Education, Culture and Sport (FPU- AP2012-5099) and research grants from Spanish Ministry of Economy and Competitiveness (BIO2012-30733, BIO2015-67930-R) and the Regional Government of Madrid (S2013/MIT-2807).

Table of contents

1. List of abbreviations

^{2}H: Deuterium
ABC: ATP-Binding cassette transporter
Amφ: Alveolar macrophage
AP: Application point (TLC)
AT1: Alveolar type 1 Cells
AT2: Alveolar type 2 Cells
ATR-FTIR: Attenuated total reflectance Fourier transformed infrared spectroscopy
BALF: Bronchoalveolar Lavage Fluid
BPC: Bodipy Phosphatidyl Choline
CB: Composite bodies
CD14: Cluster of differentiation 14
CD36: Cluster of differentiation 36 also known as fatty acid translocase
CD45: Cluster of differentiation 45, also known as receptor-type tyrosine-protein phosphatase C
Ch/Chol: Cholesterol
CH25H: Cholesterol 25-hydroxylase
Chl: Chloroform
CTL: Cholestatrienol
CYP27A1: Sterol 27-hydroxylase
DHCR24:24-dehydrocholesterol reductase
DPH: Diphenylhexatriene
DLS: Dynamic light scattering
DPPC: 1,2-dipalmitoyl-sn-glycero-3-phosphocholine
ESR: Spin electron microscopy
GM-CSF: Granulocyte-macrophage colony-stimulating factor
H_I: Direct hexagonal phase
H_{II}: Inverse hexagonal lipid phase
HMGCR: 3-Hydroxy-3-methylglutaryl-CoA reductase
IRE: Internal reflectance element
K_X: Partition coefficient
L_α: Liquid crystalline phase
L_β: Gel phase
LAL: Lysosomal acid lipase
LB: Lamellar body
L_d: Liquid disordered lipid phase
LDL-R: Low density lipoprotein receptor
L_e: Liquid expanded phase
L_o: Liquid ordered phase
LPLA2: Lysosomal phospholipase A2
LUV: Large unilamellar v
LXR: Liver X receptor
MeOH: Methanol
ML: Multilayer
MLV: Multilamellar Vesicle
MβCD: Methyl-β-cyclodextrin
N: Neutral lipid fraction of NS
NPC: Niemann-Pick type C protein
NMR: Nuclear magnetic resonance
n-PCSL: n-phosphatidylcholine spin label
NS: Native surfactant
OE: Organic extract
PE: Phosphatidylethanolamine
PG: Phosphatidylglycerol
PI: Phosphatidylinositol
PL: Phospholipid fraction of NS
POPC: 1-palmitoyl-2-oleoyl-sn-glycero-3-phosphocholine
POPG: 1-palmitoyl-2-oleoyl-sn-glycero-3-phosphoglycerol
PARγ: Peroxisome proliferator-activated receptor γ
Prot: Hydrophobic protein fraction of NS
rSP-C: Recombinant SP-C
SDS: Sodium Dodecyl Sulfate
SM: Sphingomyelin
S_o: Solid ordered phase
SP: Surfactant protein
SRA-I: Scavenger receptor A I
SREBP: Sterol regulatory-element binding Protein
SUV: Small unilamellar vesicle
TEM: Transmission electron microscopy
TFC: Topfluor-cholesterol
TLC: Thin layer chromatography
T_m: Melting temperature
TM: Tubular myelin
TxR: Texas red

2. Summary

Resumen

The respiratory function is supported by a lipid-protein complex produced and secreted by alveolar type II cells. This material is termed lung surfactant, and their main functions include the alveolar stabilization along the respiratory cycles and the regulation of the innate immune response against foreign particles and microorganisms entering the lung. Upon secretion, lung surfactant is rapidly adsorbed into the alveolar air-liquid interface, where it constitutes a continuum non-soluble film in charge of reducing surface tension in a proportional way to area reduction. Doing so it prevents atelectasis (alveolar collapse), and optimizes the amount of energy required to open the respiratory surface when inhalation takes place.

Lung surfactant is compositionally optimized to fulfil the functions described above, being phospholipids its main constituents. A lipid rarely found in most biological membranes, dipalmitoyl phosphatidyl choline (DPPC), accounts for 40 wt% of lung surfactant. This disaturated phospholipid can attain highly packed structures upon area reduction, becoming the main responsible for the extremely low surface tensions reached during exhalation. Other surfactant components, such as unsaturated phospholipids including phosphatidyl choline (PC) and phosphatidylglycerol (PG) species, and neutral lipids, mainly cholesterol, confer surfactant membranes and films optimal properties in terms of fluidity and viscosity. Nevertheless, although surfactant is 90 wt% lipids, it requires the presence of surfactant associated proteins (SP) to perform its specific associated activities. Surfactant protein A and D (SP-A and SP-D), are large hydrophilic proteins principally involved in the innate immune response in the lung. Both proteins belong to the collagenous calcium-dependent lectin (collectin) family, and exhibit different functions depending on their oligomeric state. Surfactant protein B and C (SP-B and SP-C), on the contrary, are small hydrophobic proteins that strongly associate to surfactant membranes. These two proteins are essential for surfactant to achieve a proper biophysical function, and they are responsible for the structural rearrangements of surfactant lipid assemblies involved in a fast lipid adsorption into the air-liquid interface, and the efficient re-spreading of surfactant material along the interface during area expansion (inhalation). The re-spreading ability of surfactant films is associated with 3D structures promoted by the proteins, which lead to the generation of multilayer structures that serve to store lipid material excluded from the interfacial film during compression, and newly secreted surfactant complexes. Thus, the action of SP-B and SP-C support the generation of an intricate meshwork of lipid structures connecting different surfactant extracellular forms, from secreted lamellar bodies to the interfacial film. All these structures contribute to provide active surfactant-forms to the interfacial film, which once exhausted, are recycled or degraded by lung homeostatic mechanisms involving type II alveolar cells and alveolar macrophages.

The function of SP-B and SP-C is essential for lung surfactant interfacial activity, but whereas SP-B absence is lethal, proving its essential activity for the breathing function, the role SP-C is still under discussion. SP-C is a small polypeptide (35 amino acids, 4.2 kDa) with an α-helical structure and a dually palmitoylated N-terminal segment. Some authors have suggested that it is the most hydrophobic protein of the proteome, and it adopts a transmembrane configuration in surfactant membranes. At the interfacial film, *in vitro* studies have suggested that SP-C

orientates with the α-helical segment exposed to the air and the positively charged N-terminal region interacting with phospholipid headgroups. SP-C is processed from a large precursor in alveolar type II cells in a SP-B dependent manner. Besides, it is prone to turn into amyloid aggregates, which are responsible for lung cytotoxicity and conformational lung disease. Together with the specific tissue-localization of SP-C and its highly conserved sequence, this evidence suggests that SP-C has a specific role that has not been elucidated yet.

Interestingly, SP-C function becomes especially relevant in cholesterol-containing surfactant films, an effect particularly associated to SP-C palmitoylation. Considering cholesterol is involved in lung surfactant adaptive response to different breathing conditions (i.e. temperature, pressure or exercise), mechanisms for cholesterol sensing and mobilization become apparent. This is directly linked to the role of cholesterol in modulating surfactant structures and properties, which over certain cholesterol/phospholipid ratios, result in lung surfactant dysfunction and the development of respiratory disorders. According to recent evidence, SP-C is a promising candidate involved in cholesterol regulatory mechanisms, which would explain the long-term stabilization of the lung associated to SP-C function.

Taking into account this evidence, the general objective of the present Thesis has been to characterize SP-C properties to a molecular detail in the lung surfactant context. Particularly, we have focused on SP-C effects on surfactant membrane structure and properties in the presence of cholesterol. This general objective has been approached through the following specific objectives:

1. Examination of the role of SP-C palmitoylation on SP-C structure and lipid-protein interactions in membrane multilayers.
2. Analysis of the effect of SP-C on cholesterol dynamics in native surfactant-derived and surfactant-mimicking membranes.
3. Evaluation of the effect of SP-C and cholesterol on membrane structure and lateral phase segregation.
4. Validation of selective SP-C/lipid interactions in membranes concerning SP-C/phospholipid, SP-C/cholesterol and protein palmitoylation.
5. Study of the effect of SP-C and cholesterol on surfactant homeostasis regarding lipid endocytosis and metabolism by alveolar macrophages.

OUTCOMES AND CONCLUSIONS

The experimental work presented in this Thesis reveals specific SP-C modulating activities on surfactant membrane structure which, together with cholesterol effects, contribute to the understanding of the physiological relevance of SP-C in the framework of lung surfactant function and homeostasis. A summary of the main conclusions and outcomes is presented below.

Initially, the role of SP-C palmitoylation on protein structure and protein/lipid interactions was investigated by Attenuated Total Reflectance Fourier Transformed Infrared spectroscopy (ATR-FTIR). Membrane multilayered films were generated using different membrane compositions: DPPC/POPC/POPG 50:25:15 w/w/w, DPPC/POPC 50:40 w/w and POPC/POPG 75:15 w/w and the behavior of a native palmitoylated SP-C form was compared to that of a recombinant non-palmitoylated version, rSP-C. We observed that SP-C palmitoylation did not affect protein structure incorporated in any of the lipid systems analyzed, but it contributed to SP-C α-helix stabilization. In general terms, N-terminal acylation of SP-C leaded to a greater protein tilting degree with respect to the membrane normal, increasing the polarity at the phosphate region of the lipid bilayer and maximizing SP-C-lipid interactions at this level. Thus, it could be concluded that SP-C palmitoylation is an important element defining a functionally optimal SP-C configuration in lipid bilayers and monolayers.

To analyze the potential SP-C/cholesterol interaction including SP-C effects on cholesterol dynamics, vesicles with different compositions, including surfactant-derived lipid fractions, were generated and approached by a partitioning assay. This methodology is based on the extraction of a cholesterol fluorescent analog, cholestatrienol (CTL), from membranes by the solubilizing agent methyl-β-cyclodextrin. A partitioning coefficient (K_X) can be calculated according to fluorescence anisotropy measurements, which indicates the affinity of the sterol (CTL or cholesterol by analogy) for a certain membrane. Our results demonstrated that SP-C and the native hydrophobic protein fraction of surfactant, incorporating SP-B and SP-C, specifically affected cholesterol mobilization in lipid bilayers, an effect detected by a decreased partition coefficient. The same behavior was observed for different lipid compositions including POPC model membranes, surfactant-derived lipids or surfactant mimicking systems such as DPPC/POPC/POPG 50:25:15 w/w/w. This effect suggests a role for SP-C in cholesterol mobilization and regulation in surfactant membranes, which could be involved in lung homeostasis.

Particularly, a SP-C-induced membrane-fragmenting behavior was identified, which correlated with effects on cholesterol mobilization as detected by the partitioning assay. SP-C activity resulted in the generation of small and highly curved vesicles (~30 nm) derived from larger liposomes, an effect non-dependent on membrane composition or SP-C palmitoylation. SP-C activity was counteracted by the presence of SP-B, which alone exhibited effects that could be associated to liposome fusion. This is indicative of either a direct protein/protein interaction or balanced SP-B and SP-C modulating effects on membrane structure.

To further characterize structural effects on membranes derived from SP-C incorporation, Deuterium Nuclear Magnetic Resonance (^{2}H-NMR) and Electron Spin Resonance (ESR) studies were performed. ^{2}H-NMR studies demonstrated that, in the absence of cholesterol, SP-C induced phase segregation in lung surfactant-mimicking membranes (DPPC/POPC/POPG 50:25:15 w/w/w) at 37^{o}C. From the two generated phases, one behaved as a liquid crystalline phase, which remained essentially unaltered upon SP-C incorporation in comparison with pure lipid systems. However, the ordered phase was indicative of restricted lipid motion, exhibiting

features consistent with an interdigitated phase. SP-C effects on restricting lipid motion were also confirmed by ESR. The ordered "interdigitated" structure accommodated DPPC, POPC and POPG to different extents, an effect dependent on protein palmitoylation. SP-C acylation maximized the differences between lipid species involved in the ordered phase, in agreement with the palmitoylation-derived effects reported by ATR-FTIR. This differential accommodation could be involved in structural transformations between different surfactant forms, such as those occurring during the generation of the surfactant reservoir with selectively sorted lipid species. Cholesterol addition resulted in membranes that exhibited phase segregation at 30^{o}C, which also appeared to involve certain lipids differently. This indicates a SP-C contribution on cholesterol modulating activity on surfactant structures.

With the aim of describing particular SP-C/lipid interactions that could particularly contribute to the structural membrane modifications induced by the protein, native surfactant suspensions and vesicles with varying compositions were analyzed by TLC. Surprisingly, when membranes were applied as aqueous suspensions on the silica-plate and left to dryness, selective lipid/lipid and lipid/SP-C interactions were preserved upon TLC development with an organic phase. This was detected as the generation of particular lipid or SP-C bands, which configured a defined migration pattern that we report here for the first time. Thus, we can conclude that the effects on membrane structure induced by SP-C are associated to strong protein/lipid interactions that can resist organic solvent solubilization. The TLC-based method developed in the present Thesis permits the identification of selective lipid/lipid and different lipid/protein interactions such as those described for SP-C.

Lastly, we aimed to study the importance of the SP-C and cholesterol combined action on surfactant membranes in a physiological context. With that purpose, we analyzed the effect of different lipid, cholesterol and protein composition in a cell type involved in lung homeostasis, the alveolar macrophage. It was observed that SP-C and cholesterol increased lipid uptake by a murine alveolar macrophage cell line, MH-S. However, cell treatment with different endocytosis inhibitors and a CD14 blocking antibody revealed that lipid uptake did not follow a unique mechanism, in which processes including receptor-unspecific and receptor-specific pathways could be involved. After the engulfment event, fluorescently labeled SP-C was detected in defined regions of the plasma membrane. This indicates a role for SP-C in lipid uptake and/or vesicle endocytic processing. Lipids, however, were accumulated intracellularly in the form of lipid droplets as detected by transmission electron microscopy. Lipid uptake elicited alterations in the transcriptional estate of alveolar macrophages that depended on vesicle composition. Affected genes included those coding for lipid and cholesterol transporters, enzymes implicated in lipid metabolism or different transcription factors.

In conclusion, the evidence presented in this Thesis illustrates how specific SP-C-induced membrane reorganizations contribute to the complex and dynamic behavior of lung surfactant structures, supporting a physiological role for SP-C and cholesterol relationships in lung homeostasis involving alveolar macrophages. SP-C could then be considered as a pivotal

molecule linking surfactant biophysics and lung homeostasis, which would explain its particular features, lung tissue specific localization and sequence conservation along evolution.

2. Resumen

La función respiratoria depende del establecimiento de una interfase aire-líquido que tiene lugar en los alveolos pulmonares. La estabilización de dicha interfase requiere la presencia de un complejo lipoproteico que es sintetizado y secretado por las células epiteliales alveolares de tipo II, también llamadas neumocitos tipo II. Este material se denomina surfactante pulmonar y sus funciones principales implican la estabilización de los alveolos a lo largo de los ciclos respiratorios, así como la regulación de la respuesta inmunológica innata frente a partículas y microorganismos exógenos que acceden al organismo por vía pulmonar. Una vez secretado, el surfactante pulmonar se adsorbe rápidamente a la interfase aire-líquido respiratoria, donde da lugar a una película interfacial continua e insoluble responsable de reducir la tensión superficial de manera proporcional a la reducción de área. De esta forma, el surfactante pulmonar previene la atelectasis (o colapso alveolar), minimizando la energía requerida para abrir la superficie respiratoria durante la inspiración.

El surfactante pulmonar tiene una composición optimizada para llevar a cabo las funciones descritas anteriormente, y en su mayoría está constituido por fosfolípidos. La dipalmitoil fosfatifil colina (DPPC), un lípido poco frecuente en membranas biológicas, representa el 40% en peso del surfactante. Este lípido insaturado es capaz de soportar altos grados de empaquetamiento, por lo que es el principal responsable de los bajos valores de tensión superficial que se adoptan durante la espiración. Otros componentes del surfactante, como fosfolípidos insaturados tales como especies moleculares de fosfatidil colina (PC) y fosfatidil glicerol (PG), y lípidos neutros, mayoritariamente colesterol, proporcionan al surfactante una fluidez y viscosidad apropiadas. Sin embargo, aunque los lípidos constituyen el 90% en peso del surfactante, para una correcta función tensioactiva depende de la presencia de proteínas asociadas (SP). La SP-A y SP-D son proteínas de gran tamaño e hidrófilas relacionadas con la función inmunológica del surfactante. Ambas pertenecen a la familia de las colectinas (lectinas dependientes de calcio con un dominio similar a colágeno) y exhiben diferentes grados de oligomerización. La SP-B y SP-C, por el contrario, son proteínas de bajo peso molecular altamente hidrófobas que se asocian fuertemente a las membranas de surfactante. Estas dos proteínas son esenciales para la función biofísica del surfactante. Ambas son responsables de las transformaciones estructurales de los complejos lipoproteicos implicadas tanto en la rápida adsorción interfacial del material, como en su eficaz re-extensión a lo largo de la interfase durante la inspiración (incremento de área). La re-extensión del surfactante tras la inspiración está asociada con las estructuras tridimensionales propiciadas por la actividad de las proteínas SP-B y SP-C, las cuales dan lugar a estructuras multilamelares que sirven como reservorio de surfactante. Este reservorio incluye aquellos componentes excluidos de la película interfacial durante la compresión, y además, los complejos de surfactante recién secretado. De esta forma, mediante la acción de las proteínas SP-B y SP-C, se genera una compleja red de estructuras lipídicas que conectan las distintas formas extracelulares de surfactante, desde los cuerpos lamelares secretados hasta la película interfacial. Todas esas estructuras proporcionan formas

activas de surfactante a la película interfacial, que tras varios ciclos de compresión-expansión, da lugar a formas inactivas que son recicladas o degradadas mediante los mecanismos homeostáticos del pulmón. Tales mecanismos incluyen la participación de las células alveolares de tipo II y los macrófagos alveolares.

La función de las proteínas SP-B y SP-C es esencial para la actividad biofísica del surfactante. Sin embargo, mientras que la ausencia de SP-B resulta letal, demostrando que su actividad es esencial para la función respiratoria, el papel de la SP-C es más controvertido. La SP-C es un polipéptido con estructura α-helicoidal de pequeño tamaño (35 aminoácidos, 4.2 kDa) cuyo extremo N-terminal posee dos residuos de palmitoil-cisteína. Algunos autores han sugerido que es la proteína más hidrofóbica del proteoma, y adopta una configuración transmembrana en bicapas de surfactante. En la película interfacial, experimentos *in vitro* sugieren que el segmento helicoidal de la proteína se orienta hacia el aire, mientras que el segmento N-terminal, que está cargado positivamente, interacciona con las cabezas polares de los fosfolípidos. La SP-C es expresada como un precursor de mayor tamaño, el cual se sintetiza y se procesa en los neumocitos tipo II. Dicho procesamiento requiere la presencia de SP-B. Además, debido a su particular secuencia de aminoácidos, la SP-C es propensa a precipitar formando agregados β-amiloides, los cuales son responsables de la citotoxicidad en el pulmón y de enfermedades crónicas pulmonares. Teniendo en cuenta la localización tejido-específica de la SP-C y el elevado grado de conservación de su secuencia, esta información sugiere que la SP-C tiene un papel específico en el pulmón que a día de hoy aún no se ha demostrado.

Cabe destacar que la función de la SP-C es especialmente relevante cuando el colesterol forma parte de los complejos de surfactante, un efecto que además depende de la palmitoilación de la proteína. Dado que el colesterol participa en los mecanismos adaptativos del surfactante en respuesta a diferentes condiciones respiratorias (como por ejemplo temperatura, presión o ejercicio), es necesaria la existencia de mecanismos que permitan detectar sus niveles así como otros implicados en su rápida movilización. Esto está directamente relacionado con él carácter modulador del colesterol sobre las propiedades del surfactante. Además, incrementos en la relación colesterol/fosfolípido, dan lugar a una inapropiada función biofísica que puede desembocar en patologías respiratorias. De acuerdo con estudios recientes, la proteína SP-C parece ser un candidato prometedor en los mecanismos reguladores del colesterol, lo cual podría explicar la estabilización pulmonar a largo plazo asociada a la actividad de esta proteína.

Teniendo en cuenta los factores anteriormente descritos, el objetivo principal de esta Tesis ha sido caracterizar las propiedades de la proteína SP-C a nivel molecular en contextos de membrana de surfactante pulmonar. Particularmente, se ha hecho énfasis en la actividad de la proteína sobre la estructura y propiedades de membranas de surfactante en ausencia y presencia de colesterol. Enmarcados en este objetivo general, se han establecido los siguientes objetivos específicos:

1. Estudio del papel de la palmitoilación en la estructura de la SP-C e interacciones lípido-proteína en películas de membranas multilamelares.

2. Análisis de la actividad de la SP-C sobre la dinámica del colesterol en membranas surfactante-miméticas y derivadas de surfactante nativo.
3. Evaluación del efecto del SP-C y del colesterol sobre la estructura de membranas y segregación lateral de fases.
4. Validación de interacciones selectivas SP-C/lípido en membranas considerando la palmitoilación de la proteína.
5. Estudio del efecto de la SP-C y el colesterol sobre la homeostasis del surfactante en relación con la endocitosis y el metabolismo de lípidos por macrófagos alveolares.

RESULTADOS Y CONCLUSIONES

El trabajo experimental presentado en esta Tesis revela actividades moduladoras de la SP-C sobre la estructura y dinámica de membranas de surfactante. Junto con los efectos del colesterol, estos resultados contribuyen a la comprensión de la relevancia fisiológica de la SP-C en el marco del surfactante y la homeostasis pulmonar. A continuación se presenta un resumen de los principales resultados y conclusiones.

Inicialmente, se investigó el papel de la palmitoilación de la SP-C en la estructura de la proteína y las interacciones lípido/SP-C. Para ello, se generaron películas de membranas multilamelares empleando diferentes composiciones lipídicas: DPPC/POPC/POPG 50:25:15 p/p/p, DPPC/POPC 50:40 p/p y POPC/POPG 75:15 p/p. De esta forma, se compararon membranas de lípido puro con membranas lipoproteicas que incorporaban una forma de SP-C nativa palmitoilada o una versión recombinante no palmitoilada, rSP-C mediante espectroscopia infrarroja con transformada de Fourier por reflexión total atenuada (ATR-FTIR). Se observó que la palmitoilación SP-C no afectaba la estructura de la proteína en ninguno de los sistemas lipídicos analizados. Sin embargo, en términos generales, la acilación del segmento N-terminal de la SP-C daba lugar a un mayor grado de inclinación con respecto a la normal de la bicapa. Esto además se relacionaba con un incremento en la polaridad de las membranas a nivel de los grupos fosfato, lo cual maximizaba las interacciones SP-C-lípido. Por lo tanto, se podría concluir que la palmitoilación de la SP-C es un elemento importante para definir una configuración funcionalmente óptima en bicapas lipídicas y monocapas.

Para analizar la posible interacción SP-C/colesterol, incluyendo efectos de la proteína sobre la dinámica del colesterol, se generaron vesículas con diferentes composiciones y se estudiaron empleando un ensayo de partición. Esta metodología se basa en la extracción de un análogo fluorescente de colesterol, el colestatrienol (CTL), desde membranas lipídicas. Para ello se empleó metil-β-ciclodextrina, un polisacárido en forma de anillo capaz de albergar moléculas hidrófobas en su cavidad interna. A partir de medidas de anisotropía de fluorescencia del CTL, es posible calcular el coeficiente de reparto (K_X) entre la ciclodextrina y las vesículas lipídicas, determinando así la afinidad del esterol (CTL o colesterol) por membranas de una determinada composición. Nuestros resultados demostraron que tanto la SP-C nativa como la fracción nativa de proteínas hidrófobas del surfactante, SP-B y SP-C, incrementaban de forma específica la

movilización de colesterol en bicapas lipídicas, lo cual se traducía en menores valores de K_X. El análisis de membranas de diferentes composiciones, incluyendo las generadas a partir de POPC, la fracción lipídica del surfactante o sistemas surfactante-miméticos (DPPC/POPC/POPG 50:25:15 p/p/p), demostró que el efecto de la SP-C no dependía de la composición lipídica. Estos resultados sugieren que la SP-C puede tener un papel específico en la movilización del colesterol y su regulación en el sistema surfactante, un efecto que podría estar relacionado con la homeostasis pulmonar.

En este mismo estudio, se observó que la SP-C daba lugar a la fragmentación de membranas, generando vesículas pequeñas (~ 30 nm) y con una curvatura pronunciada a partir de liposomas de mayor tamaño. Este efecto, además, no parecía depender de la composición lipídica ni de la palmitoilación de la proteína. Asimismo, la movilización de colesterol inducida por SP-C parecía estar relacionada con la fragmentación de membranas o inducción de curvatura, dado que vesículas pequeñas generadas a partir de lípidos sintéticos también se asociaban a menores coeficientes de partición en ausencia de la proteína. Cabe destacar que en presencia de SP-B no se observaba el efecto de fragmentación de membranas inducido por SP-C, lo cual indica que la actividad de ambas proteínas está relacionada, bien a nivel de interacción proteína/proteína o por inducción de efectos que se equilibran en el contexto del surfactante.

Para caracterizar las consecuencias de la incorporación de SP-C en bicapas lipídicas a nivel estructural, se llevó a cabo un estudio espectroscópico mediante resonancia magnética nuclear de deuterio (^{2}H-NMR, del inglés *deuterium-nuclear magnetic resonace*) y resonancia de espín electrónico (ESR, del inglés *electron spin resonance*). Los resultados obtenidos a partir de ^{2}H-NMR demostraron que, en ausencia de colesterol, la SP-C inducía segregación de fases en membranas surfactante-miméticas (DPPC/POPC/POPG 50:25:15 p/p/p) a 37^{o}C. Una de las fases generadas presentaba propiedades espectrales características de fases líquido cristalinas. Además, esta no mostraba cambios apreciables tras la incorporación de SP-C en comparación con sistemas lipídicos puros. Por otro lado, la fase ordenada presentaba características consistentes con la formación de una fase interdigitada, donde los lípidos aparecen altamente ordenados y con movilidad restringida. Para validar esos resultados, se llevaron a cabo experimentos de ESR, los cuales permitieron confirmar la restricción en movilidad mediada por la SP-C. El análisis en detalle de los datos de ^{2}H-NMR permitió concluir que los diferentes lípidos que formaban parte del sistema, DPPC, POPC y POPG, estaban implicados en diferente medida en la fase ordenada o "interdigitada" propiciada por la SP-C. Además, la palmitoilación de la proteína parece ser un factor implicado en la selectividad de las diferentes especies lipídicas por la fase ordenada, lo cual apoya los resultados mostrados por ATR-FTIR. La participación diferencial de determinados lípidos en la fase ordenada podría estar implicada en las transformaciones estructurales entre diferentes formas de surfactante, tales como las que tienen lugar durante la exclusión de ciertas especies lipídicas de la película interfacial durante su compresión y la generación del reservorio por parte de la SP-C.

La adición de colesterol a este sistema daba lugar a membranas que exhibían una segregación de fase a 30^{o}C, la cual también parecía implicar ciertas especies lipídicas

preferentemente. Esto podría ser indicativo de la contribución de la SP-C sobre la actividad moduladora del colesterol en las membranas de surfactante.

Con el objetivo de describir interacciones específicas SP-C/lípido que pudieran participar particularmente en las modificaciones estructurales de la membrana introducidas por la proteína, se realizó un análisis mediante cromatografía de capa fina (TLC del inglés *thin layer chromatography*). Suspensiones acuosas de surfactante nativo y vesículas de diferente composición fueron aplicadas sobre la placa de sílice, y tras la evaporación del disolvente, se desarrolló la cromatografía empleando una fase móvil orgánica optimizada para la separación de lípidos polares. Sorprendentemente, se observó que determinadas interacciones selectivas lípido/lípido y lípido/SP-C eran preservadas a pesar del tratamiento con disolvente orgánico. Tales interacciones se identificaron como bandas características en la placa, dando lugar a un patrón de migración definido para la SP-C que describimos en esta Tesis por primera vez. Por lo tanto, podemos concluir que los efectos sobre la estructura de la membrana inducida por SP-C están asociados a fuertes interacciones proteína/lípido que resisten a la solubilización por disolventes orgánicos. Como hemos visto, esta metodología podría aplicarse a diversos sistemas de membranas biológicas, ya que permite la identificación de interacciones lípido/lípido y lípido/proteína tales como las descritas para la SP-C.

Por último, quisimos determinar la importancia fisiológica de la acción combinada de la SP-C y colesterol sobre las membranas de surfactante. Con ese fin, analizamos el efecto de un surfactante clínico y vesículas de diferente composición sobre macrófagos alveolares, un tipo celular implicado en la homeostasis pulmonar. La combinación de SP-C y colesterol propiciaba la incorporación de lípidos por parte de células MH-S, una línea celular de macrófagos alveolares de ratón. Sin embargo, el tratamiento de dichas células con diferentes inhibidores de endocitosis o un anticuerpo bloqueante de CD14, dio lugar a índices de incorporación lipídica menores. Esto apunta a que no hay un único mecanismo de entrada en las células, donde tanto vías independientes como dependientes de receptor pueden estar implicadas. Tras el tratamiento con lípidos, se observó que la proteína SP-C marcada fluorescentemente aparecía en regiones definidas de la membrana plasmática. Esto indica que esta proteína podría participar en la captación de lípidos y/o en el procesamiento endocítico de los mismos. Los lípidos, sin embargo, aparecían acumulados intracelularmente en los denominados *lipid droplets* tal y como se observó mediante microscopía electrónica de transmisión.

Por otro lado, observamos que el tratamiento con lípidos provocaba alteraciones a nivel transcripcional en células MH-S. Dichos efectos parecían depender de la composición lipídica y proteica de las preparaciones utilizadas. Entre los genes afectados encontramos diversos transportadores de lípidos y colesterol, enzimas implicadas en el metabolismo lipídico y diferentes factores de transcripción.

En conclusión, los resultados presentados en esta Tesis ilustran los efectos de la proteína SP-C sobre la estructura y dinámica de membranas de surfactante, los cuales contribuyen al comportamiento dinámico global de este complejo lipoproteico. Además, los resultados obtenidos sugieren un posible papel fisiológico de las relaciones SP-C/colesterol en la

homeostasis pulmonar llevado a cabo a través de los macrófagos alveolares. De esta forma, la proteína SP-C podría considerarse como una molécula central entre la biofísica del surfactante y la homeostasis pulmonar, dando respuesta a sus características particulares, su localización específica pulmonar y su alto grado de conservación a lo largo de la evolución.

3. Introduction

Lung physiology

The respiratory function allows organisms to retrieve oxygen, an essential element required for aerobic functions. Depletion of vital compounds such as water or nutrients is lethal in a time lapse ranging from one to several weeks, whereas without oxygen, survival would be unmanageable over 5-6 minutes.

Oxygen is required for multiple metabolic processes, and more importantly, it powers the production of energy (ATP) through mitochondrial respiration. The amount of oxygen needed to sustain vital functions at rest equals 3.5 ml O_2/ min^{-1} kg of body $weigth^{-1}$ in humans (1), meaning that for an average human of 75 kg at atmospheric pressure, approximately 16 liters of O_2 would be consumed per hour just to maintain the organism alive.

For such an amount of oxygen to be delivered to the body per time unit, evolution has developed the lungs, highly specialized organs in charge of gas exchange. The lungs provide one of the largest surfaces in contact with the air from the human body, around 70 m^2 (2), maximizing oxygen intake and CO_2 elimination. This is possible thanks to lungs branched structure, which from top to bottom includes trachea, bronchi, bronchioles and **alveoli**. The functional unit of the lung is precisely the latter, alveoli, which consist in small sacs with a mean diameter of 200 µm (3).

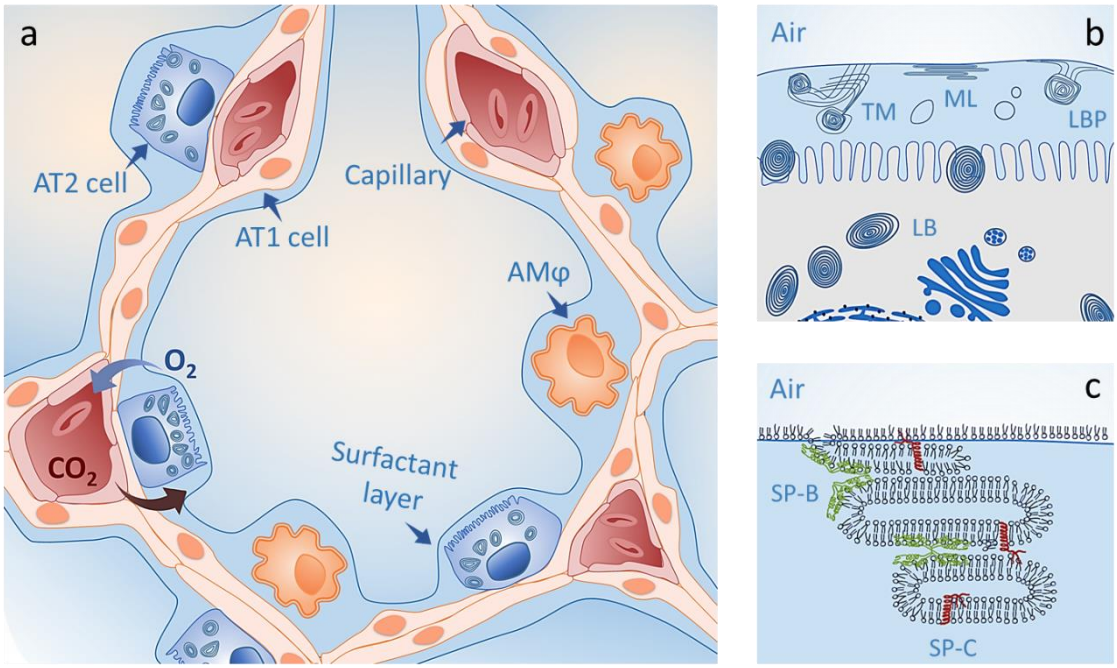

Figure 1. (a) Schematic representation of the alveolar structure including type I and II pneumocytes (AT1 and AT2) and alveolar macrophages (AMφ). (b) Amplification of the air liquid interface, where different surfactant structures are found, such as lamellar bodies (LB), lamellar body like particles (LBPs), tubular myelin (TM) and surfactant multilayers (ML). (c) Zoom in of a surfactant multilayer stabilized by surfactant proteins SP-B and SP-C.

Gas exchange takes place by passive diffusion, reason why origin and destination, namely air and blood and *viceversa*, need to be spatially close. The thickness O_2 and CO_2 needs to go through is roughly that of two thin cells, approximately 500 nm (4), which constitutes the air capillary barrier. From alveoli to erythrocytes, oxygen would encounter the liquid film lining the alveolus, alveolar epithelial cells, the interstitial layer, endothelial cells in capillary and finally erythrocytes (Fig. 1).

The delicate structure alveoli possess must sustain those physical forces originated by respiratory muscles to allow moving air in and out of the lungs, during inhalation and exhalation. Those processes involve great changes in alveolar volume, and for that reason, connective tissue supports alveolar cells providing elasticity and consistency to the alveolar structure (5).

In a healthy subject, three types of cells can be found in alveoli: **alveolar type I** and **type II epithelial cells** (AT1 and AT2 cells), also termed type I and II pneumocytes, and **alveolar macrophages** (AMφ). Most of the gas exchange surface (>95%) is covered by the thin AT1 cells (<0.1 µm) or squamous cells (6), whereas AT2 cells represent the 15% parenchymal lung cells and cover the 5% of the alveolar surface (7). AT2 cells are able of self-renewing and differentiate into AT1 cells in response to injury and replenishing the cell alveolar cell pool (7, 8). Alveolar macrophages constitute the first barrier against pathogenic agents by regulating the immune response in the lung, and they have an important role in lung homeostasis (9).

One of the most important functions of AT2 cell is the synthesis and secretion of **lung surfactant**. This lipid-protein complex is rapidly adsorbed and spread all over the alveolar air-liquid interface upon secretion. There, it minimizes surface tension to the extremely low values required upon exhalation, avoiding alveolar collapse and sustaining breathing.

Lung Surfactant: composition, structure and function

The need of lung surfactant

In the lung, the fluid lining alveolar cells faces the air establishing the air-liquid interface through which gas exchange occurs. Molecules deep into the fluid experience cohesive forces with surrounding molecules that are balanced, resulting in a null net force. However, molecules at the surface establish much less interactions with the diffuse molecules in gas state (air) and consequently, they experience a net attractive force towards the bulk of the fluid (Fig. 2a). This tendency to reduce the exposed surface is termed **surface tension (γ)**, and it is defined as the energy required to increment the surface of a fluid per area or length unit. In the context of alveoli, surface tension at the air-liquid interface would promote alveoli to shrink and collapse, greatly increasing the energy demands to open the respiratory surface upon inhalation. In the case of water, hydrogen bonding makes interactions between molecules stronger, and consequently surface tension can reach values as high as 72 mN/m.

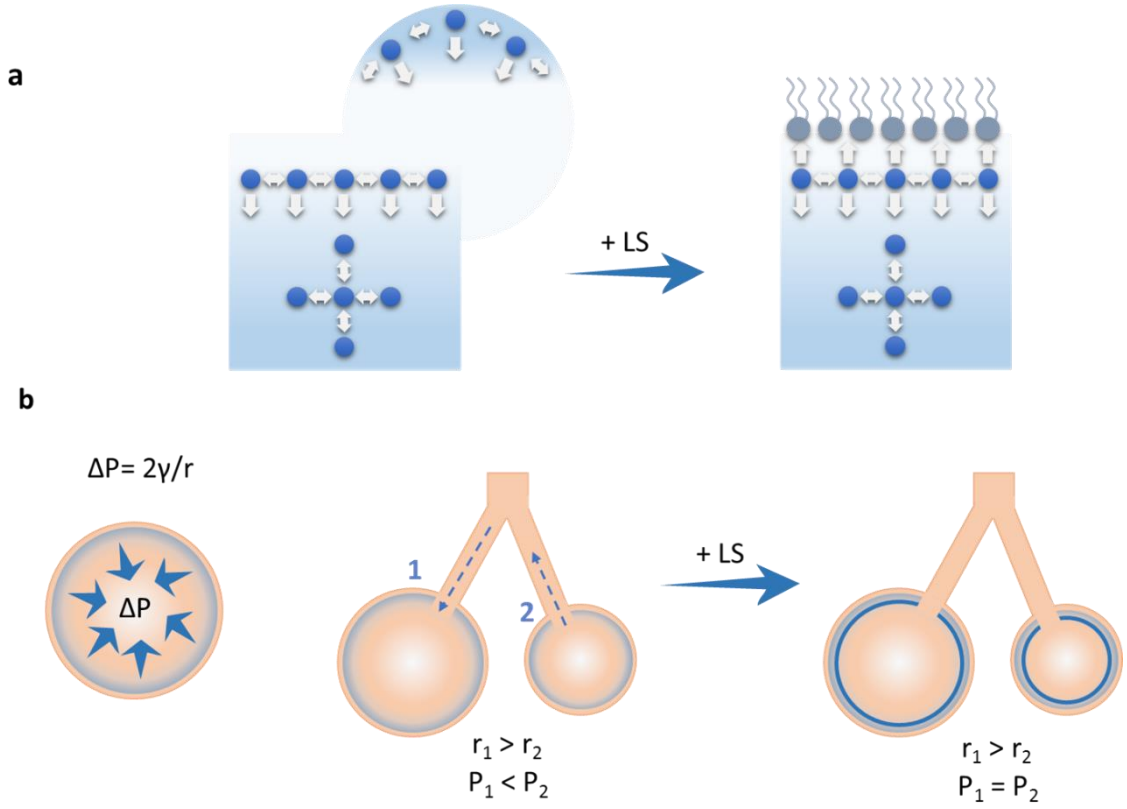

Figure 2. (a) Schematic representation of the surface tension (γ) concept. Molecules at the air-liquid interface experience a net force toward the bulk of the fluid. The surface of the liquid bends to minimize the exposed area. When lung surfactant is present, forces are balanced and surface tension is reduced. (b) Representation of the Young-Laplace law for ideally spherical alveoli. With no surfactant, the inner pressure (P) experienced by alveoli with different radius (r) would lead to collapse of small alveoli toward larger ones.

The alveolar shape could be approximated to spherical chambers diameters ranging from 185 to 210 µm (3). Because of the difference in size, in the absence of any surfactant the pressure experienced by the air in each alveolus would differ according to the **Young-Laplace law** (P= 2 γ/r) (10) .This pressure (P), also termed Laplace pressure, results from surface tension of a liquid lining the inner surface of a curved structure. Lateral interactions between water molecules exert a net force towards the center of the curved structure that translates in pressure, which inversely correlates with the radius of the structures (Fig. 2b). Therefore, for two interconnected alveoli with different sizes and a given surface tension, the smaller ones would tend to collapse toward those of larger size in the absence of surfactant, resulting in the progressive collapse of the lung (Fig. 2b).

Lung surfactant (surface-active agent) provides an efficient way to reduce surface tension by occupying the alveolar air-liquid interface and minimizing water exposure to air at the interface. Furthermore, the lung surfactant system reduces surface tension in a proportional way to area reduction, therefore compensating differences in pressure and thus, stabilizing alveoli of different sizes preventing collapse. Surface tension reduction is achieved by surfactant lipids, which are transferred from the aqueous subphase into the air-liquid interface generating a monolayer with

the polar headgroup facing the water and the hydrophobic part toward the air. Surfactant is able to provide a surface tension reduction to less than 2 mN/m when exhalation takes place (lowest alveolar area) thanks to its high content in dipalmitoyl phosphatidyl choline (DPPC) (11). This saturated phospholipid can attain an extremely high packing density because of the saturated nature of its two hydrocarbon chains.

Lung surfactant composition

Lung surfactant consists of a complex network of lipid assemblies, in lamellar and non-lamellar forms, modulated by **surfactant-associated proteins (SP)**: **SP-A**, **SP-B**, **SP-C** and **SP-D**. It is produced and secreted by AT2 cells in the form of highly packed organelles termed lamellar bodies.

The properties of this lipid-protein complex are due to its particular composition (Fig. 3). In most mammals, lipids represent approximately 90% of surfactant mass, from which phosphatidyl choline (PC) is the predominant specie (60-70%). **DPPC**, a lipid rarely found in most biological membranes, accounts for a 40%, whereas unsaturated PCs represent around 25%. Anionic phospholipids, mainly phosphatidyl glycerol (**PG**) and phosphatidyl inositol (**PI**), also form part of surfactant (8-15%) (12), together with other less abundant phospholipids, such as phosphadityl ethanolamine (**PE**), phosphatidyl serine (**PS**) or plasmalogens. Neutral lipids, predominantly **cholesterol**, represent an important fraction (5-10% by mass) and they are crucial regulators of surfactant properties adapting surfactant in response to diverse stimuli (13). The remaining 10% of surfactant mass is represented by the four specific surfactant proteins, which constitute essential elements for surfactant biophysical function and immune-protective role.

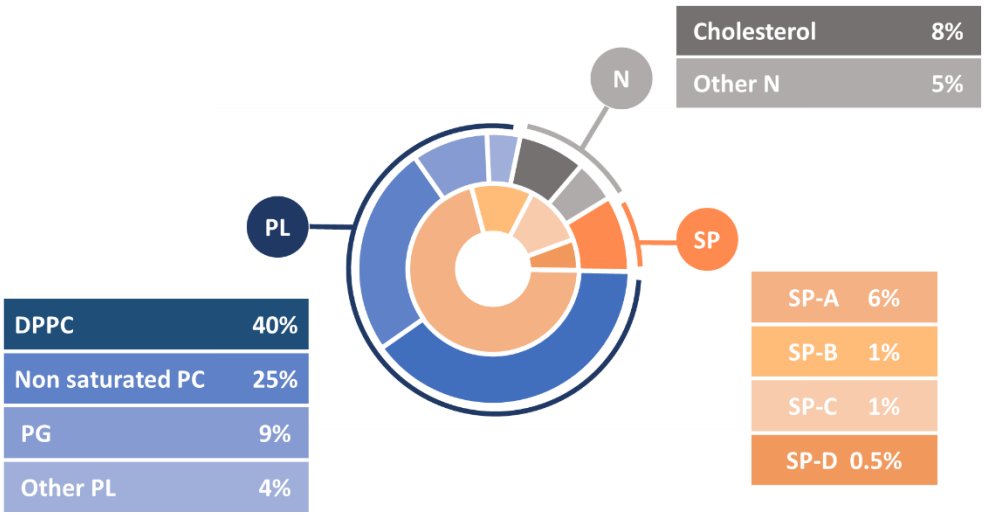

Figure 3. Representation of lung surfactant composition showing its main fractions: phospholipids (PL), neutral lipids (N) and surfactant associated proteins (SP). The inner circle represents the proportion of each lung surfactant protein.

Surfactant composition is finely tuned to sustain respiratory demands depending on lung architecture. For instance, significant differences in terms of lipids and proteins are found between lung surfactant composition in mammals and birds, demonstrating how surfactant adapts either to a alveolar, branched structure that suffers volume changes during breathing (mammals) or to a static tubular lung (birds) (10). Besides, mammals cope with different situations based on their way of living such as high pressures (e.g. sea lions, dolphins) (14), sustained changes in body temperature (e.g. heterothermic mammals) (10) or diet (15); differences that are also reflected in modifications in surfactant composition.

Lipid fraction

As mentioned earlier, from all lipids forming part of surfactant, phospholipids represent the most abundant molecules. They are responsible for the surface tension reduction properties of surfactant given their amphipathic character as they are constituted by two moieties, a polar "headgroup", and a hydrophobic part constituted by two hydrocarbon chains (Fig. 4). A **glycero-phosphate group** is the central piece in to which the **two acyl chains** and a **variable polar group** are attached. Phospholipids are usually named after the polar group, which can provide the molecule a net charge (zwitterionic phospholipids), as occurs with phosphatidylcholine (PC), or a negative charge (acidic or anionic phospholipids), as in the case of phosphatidylglycerol (PG) or phosphatidylinositol (PI). The two fatty acids esterifying the glycerol molecule define important properties of the lipid depending on their chain length and saturation.

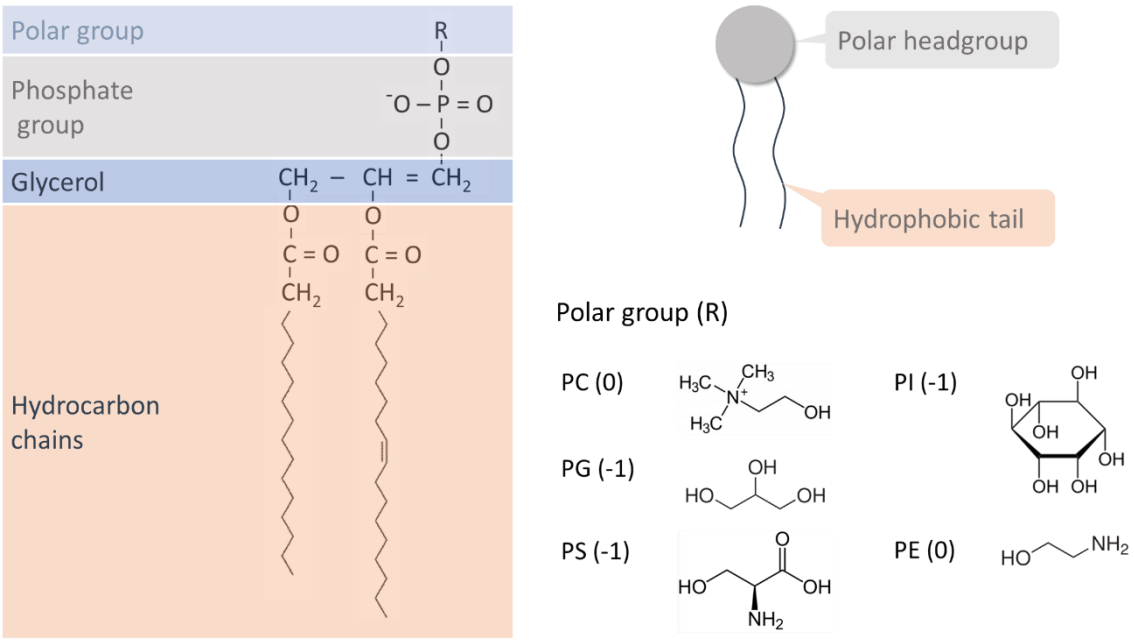

Figure 4. Amphipathic structure of glycerophospholipids. Phospholipids are named according to their polar group (R), which also confer a defined electrostatic charge to the molecule. The most common in surfactant are choline (PC), glycerol (PG), serine (PS), inositol (PI) and ethanolamine (PE) with a charges of 0, -1,-1,-1 and 0 respectively.

Lipid polimorfism

In order to minimize the exposure of hydrophobic groups to a polar environment (i.e. water), lipids are able to self-assemble into different supramolecular organizations. Depending on their **molecular shape**, they preferentially organize into certain structures as a consequence of the hydrophobic effect giving rise to the so-called lipid polymorphism. Phosphatidyl cholines (PC), for instance, keep an almost constant cross-sectional area from the headgroup to the acyl chains, reason why there are considered as **cylindrical phospholipids** (Fig. 5a). This molecular shape favors the generation of lamellar structures, in which the spontaneous curvature is virtually zero. Those species incorporating a small polar headgroup compared to the cross-sectional area of the acyl chains adopt a **conical shape** (Fig. 5b) such as phosphatidyl ethanolamines (PE), and promote the generation of non-lamellar negatively-curved structures like the hexagonal type II phase. The opposite situation gives rise to positively-curved structures such as the hexagonal phase I or different aggregation states such as micelles (Fig. 5c).

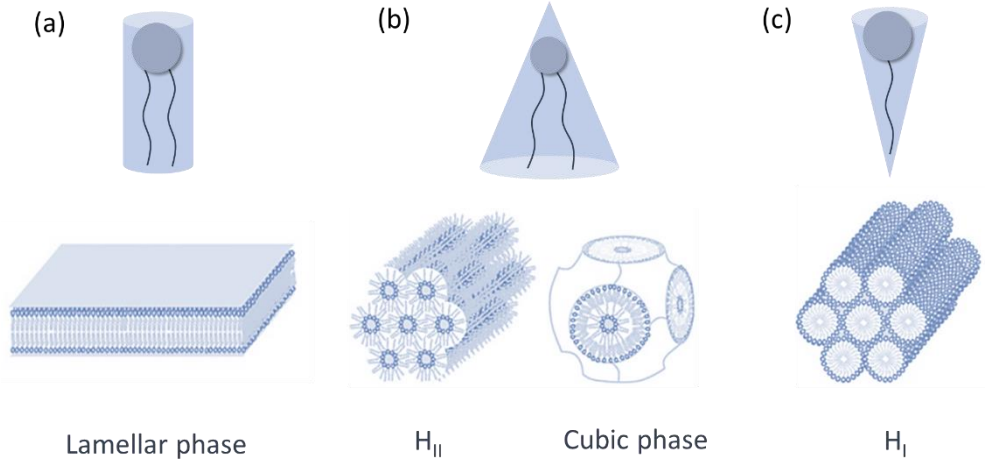

Figure 5. Shape adopted by phospholipids according to their molecular structure. (a) Cylindrical phospholipids, such as PC, preferentially assemble into lamellar phases generating membrane bilayers. (b) Conical phospholipids organize into type II hexagonal phases or bicontinuos cubic phases by inducing negative curvature, as occurs with PE. (c) Inverted conical phospholipids, such as lysophospholipids, induce positive curvature leading to the generation of micelles or hexagonal I phases. Figure adapted from (16).

In lung surfactant, lipid composition defines the local structure of the lipid network, which is able to adopt different configurations in order to fulfil an efficient surfactant function. The structure of those lipid assemblies is also subjected to the modulation by surfactant proteins, which have extensively proved their capacity to modify and adapt lipid organizations. Many other factors including temperature, lateral pressure, pH and hydration state among others, control transitions between lipid organizations resulting in optimized structures that respond to specific physiological demands.

Lateral organization and phase behavior

Phospholipids arranged in lamellar forms establish molecular interactions between them, leading to the generation of thermodynamic phases. In a bilayer, highly packed phospholipids suffer motional constraints that are relieved upon an increase in thermal energy, which influence lipid mobility and order. Thus, an ordered phase such as the gel phase or L_β, transforms into a more disordered phase, liquid-crystalline or L_α, at a temperature defined as **melting** or **transition temperature (T_m)**, which is characteristic of every system and depends on chain saturation and length and the polar headgroup (17). At that temperature, the entropy of the system changes leading to the release of latent heat while the temperature of the system remains constant. The two phases (L_β and L_α) coexist in equilibrium at the melting temperature. This occurs at higher values for saturated phospholipids, such as DPPC (T_m=41^{0}C), than for non-saturated phospholipids, such as POPC or POPG (T_m=-2^{0}C).

For monolayers, temperature also defines lipid packing and order but **lateral pressure** becomes an important factor responsible for the transition between phases. Those lipids exhibiting high lateral mobility and conformational freedom are considered as forming part of a liquid expanded (L_e) phase, which would be equivalent to a L_α phase in bilayers in terms of lipid mobility. However, when area per lipid molecule is reduced as a result of lateral compression, phospholipids shift to a liquid-condensed (L_c) state, somehow analogous to a L_α phase in bilayers, in which lipid packing and order increases and the exposure of water to the air is minimized (18). High lateral pressures can result in films adopting a two-dimensional solid state (S_0) that may even lead to collapse and material loss if the pressure is further increased (19).

Besides temperature and lateral pressure, **cholesterol** plays a pivotal role in phospholipid phase behavior. This small amphipathic molecule inserts into the bilayer positioning its polar headgroup (OH) close to the polar region of the membrane, whereas the four rings and the isoprenoid tail remain in the hydrophobic region. When cholesterol forms part of a given lipid membrane, phospholipid retain a considerable mobility even at the most packed states and phases are re-defined being considered as liquid-ordered (L_o) and liquid-disordered (L_d) (20). For fluid membranes, the addition of cholesterol results in a condensing effect in such a way that phospholipids translational mobility and diffusion is restricted and order increments. For ordered states though, cholesterol alters molecular interactions of phospholipids with their surrounding neighbors leading to a reduction in order and that high mobility.

A complex mixture of phospholipids responds to temperature depending on its composition, with those lipids with similar T_m and properties clustering together. This is further complicated by the presence of cholesterol, which finely modulates the phase behavior of a lipid mixture. The consequence is that lipids are not distributed uniformly throughout the membrane and clustering results in **phase coexistence** and the appearance of **lipid domains**, which affect membrane properties such as bending, permeability, compressibility and membrane protein distribution (20, 21).

Because of its specific lipid composition, lung surfactant seems to exhibit phase coexistence at physiological temperatures (T_m=37ºC) as observed in Fig. 6a (22, 23). Membranes made of the organic extract of surfactant (depleted of hydrophilic components), with or without the hydrophobic proteins SP-B and SP-C, display the same phase behavior when compared to native membranes, which confirms that lipid composition is the main responsible for surfactant phase segregation(23). Both hydrophobic proteins, SP-B and SP-C, have been shown to preferentially partition in disordered domains (23), frequently associated with membrane folds that may lead to 3D-structural reorganizations (23, 24). Besides, SP-C has been demonstrated to localize at the boundary between phases in membranes (25), and monolayers (26). In the context of the interfacial film, both proteins are excluded from condensed DPPC enriched domains upon compression, concentrating in those regions connecting condensed and expanded phases (27).

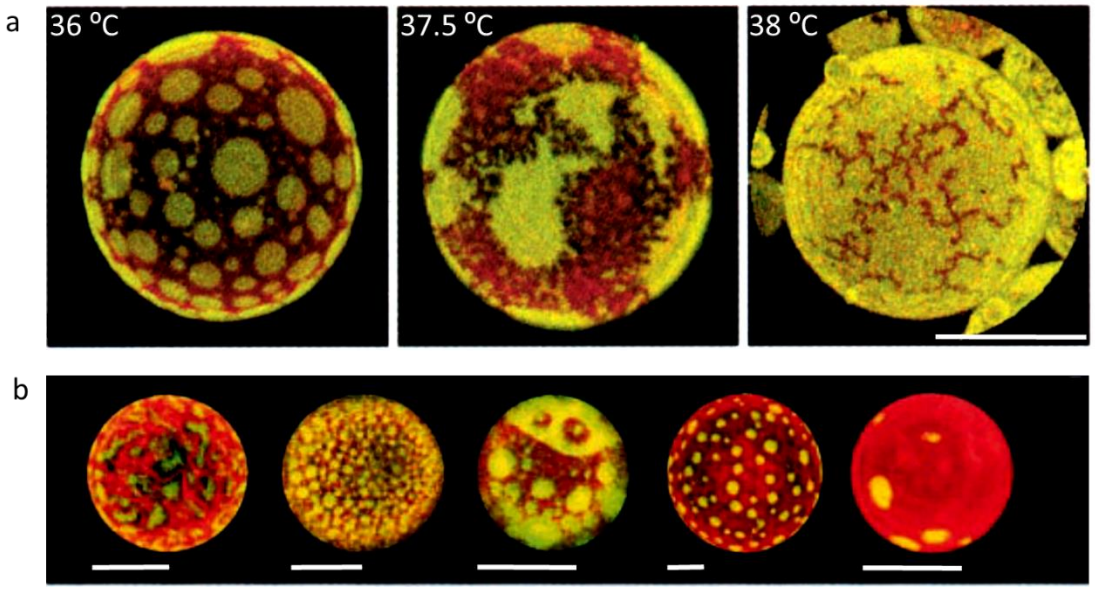

Figure 6. Phase behavior of giant unilamellar vesicles made of lung surfactant. (a) Domains observed in yellow (labelled with the fluorophore Bodipy-PC) correspond to disordered regions, whereas those marked in red ($DiIC_{18}$) match ordered regions, likely enriched in DPPC. Domain coexistence depends on the melting temperature of the mixture as observed (T_m surfactant ≈ 37^0C). Scale bar = 20 µm. (b) From left to right, surfactant membranes exhibit different domain coexistence depending on cholesterol content (10, 15, 18, 21 and 30 mol %). Scale bar = 10 µm. Adapted from (23).

Cholesterol depletion leads to the generation of markedly different lipid phases in comparison to native surfactant (Fig. 6b), highlighting cholesterol as a crucial element to modulate lipid domain segregation at the micron- and nano-scale (23). Lipid composition is therefore critical to promote a high dynamic character to surfactant membranes, right at the edge of physiological temperatures. This could be important in the context of lungs, where the large fluctuations in area can require the interplay of surfactant fluid states to adapt surfactant structures and properly fulfil surfactant function.

Surfactant proteins

Surfactant associated proteins (SP-A, SP-B, SP-C and SP-D) represent an important fraction of lung surfactant mass and are crucial actors sustaining surfactant biophysical and immunological roles. Typically, they can be divided in two groups based on protein nature, solubility and associated function.

Surfactant and lung immunity: hydrophilic proteins SP-A and SP-D

SP-A and **SP-D** belong to a family of proteins related to **innate immunity**, termed **collectins** (1). SP-A is the most abundant protein in surfactant (6% by mass), and as in the case of SP-D (0.5%), can adopt different oligomeric states as illustrated in Fig. 7 (28). SP-A (monomers of 28-36 kDa) is typically found in bronchoalveolar fluid (BALF) forming part of a bouquet-like structure formed by six trimers (630 kDa) (29), whereas SP-D (monomers of 43 kDa) is usually present in a trimeric form that can further oligomerize generating dodecamers (520 kDa) and even larger structures (8x12, ~4,2 MDa) (30, 31).

Surfactant SP-A and D are produced both by alveolar type II cells (32) and club cells, previously known as Clara cells (33, 34), and their biosynthesis and secretion seem to be independent of pathways involving lamellar bodies (35). However, newly synthesized SP-A can ultimately be targeted to lamellar bodies (36), suggesting that SP-A association to surfactant does not depend on a unique mechanism.

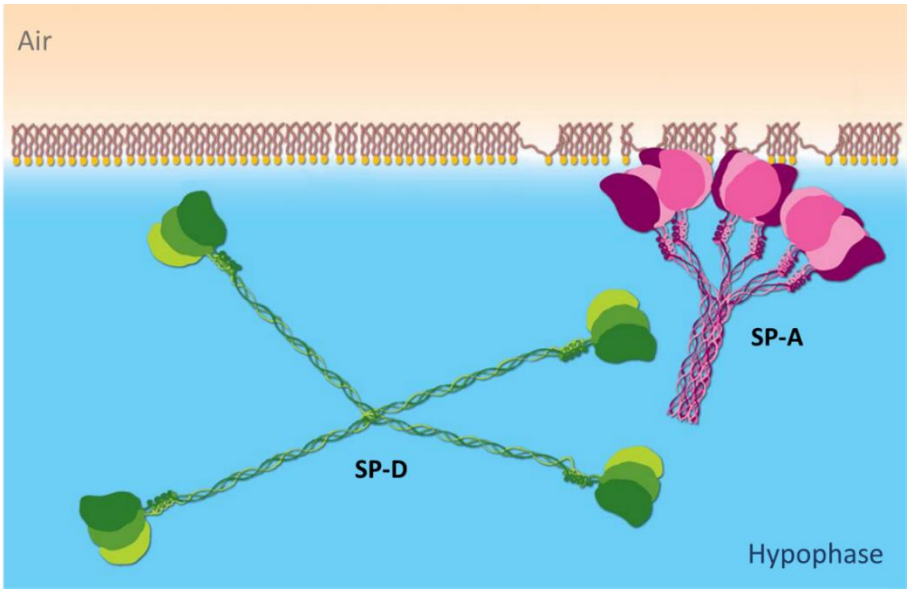

Figure 7. Lung collectins at the air-liquid interface. SP-D dodecamers (green) and SP-A octadecamers (pink) associated to DPPC are shown in the hypophase (modified from (37)).

SP-A and SP-D provide surfactant with a **protective role against infection**. They act as antimicrobial proteins by recognizing non-host oligosaccharides through their carbohydrate

recognition domain (CRD). Upon recognition, they opsonize and agglutinate pathogens in a process that facilitates their phagocytosis by macrophages and monocytes (28). They also show an intrinsic antimicrobial activity by increasing pathogen membrane permeability (38). These collectins act as immunomodulators by controlling the inflammatory response thought their interaction with immune cells such as macrophages (28, 39).

Besides, they are also involved in **surfactant homeostasis** and possess a structural function shaping surfactant membranes and multilayers. SP-A avidly binds DPPC (40, 41), reason why it is co-isolated with surfactant complexes (42). It is essential for the generation of **tubular myelin** in a calcium dependent manner (43, 44) and contributes to the surface activity of surfactant, enhancing the adsorption of lipids into the interface (45) and generating surface-associated surfactant structures with optimal biophysical properties (46). SP-D binds to certain lipid species such as PI and glucosylceramide, both minor components of surfactant (47, 48), but it is not strongly associated to surfactant membranes (42). Both proteins are involved in surfactant homeostasis and recycling (49), being SP-D important to modulate surfactant pools (50, 51).

Surfactant biophysics: Hydrophobic proteins SP-B and SP-C

In contrast to lung collectins, **SP-B** and **SP-C** are small hydrophobic proteins strictly required for the air-breathing mode of life in mammals (Fig. 8) (52). They are mainly responsible for the **biophysical function** of lung surfactant including the efficient stabilization of an open air-liquid interface.

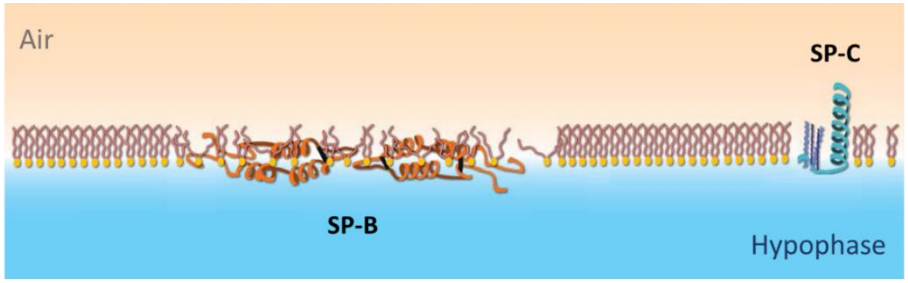

Figure 8. Hydrophobic surfactant proteins associated to a surfactant interfacial monolayer. SP-B is shown in a dimeric form (orange) while SP-C appears as a monomer (blue) (modified from (37)).

It has been already pointed out that lipids provide the tension reduction properties required for ensuring breathing, but hydrophobic surfactant proteins are the key to understand the mechanisms sustaining respiratory mechanics. For surfactant films to achieve the **surface tension reduction**, especially upon compression (exhalation), the surfactant active species must first experiment a **fast interfacial adsorption** into the air-liquid interface and, during expansion (inhalation), they have efficiently **re-spread** (53, 54). Those dynamic properties mobilizing surfactant lipids along respiratory mechanics are critically dependent on the presence of SP-B and SP-C, whose perturbations on lipid assemblies allow for the generation of an extremely dynamic lipid matrix able to adapt to the continuously changing alveolar context (Fig. 9).

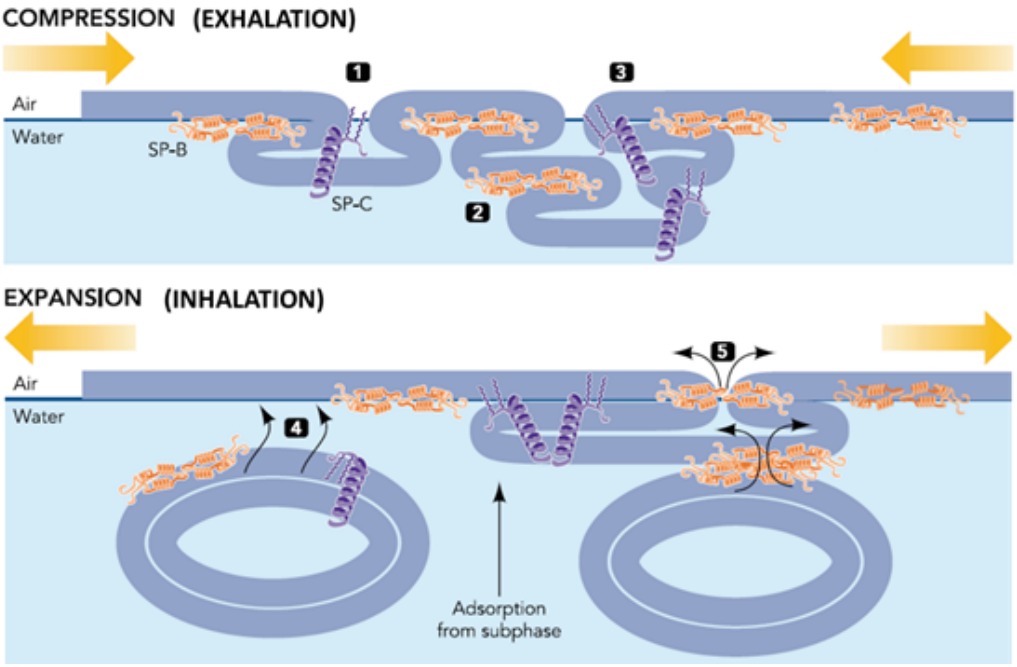

Figure 9. Proposed model of how SP-B and SP-C could sustain the generation of a surfactant reservoir during compression and assist surfactant spreading upon expansion. SP-B and SP-C promote compression-driven membrane protrusions (1) that would be stabilized by SP-B-induced bilayer-bilayer contacts (3) and SP-C-promoted anchoring by its palmitic chains (4). Both SP-B and SP-C could facilitate membrane insertion (5) and re-spreading of lipid assemblies from the aqueous hypophase to the interface upon expansion (adapted from (55)).

In order to understand how these proteins function, it is important to consider the current models proposed for the lung surfactant system. Experiments performed during the late 60s and 70s leaded to the proposal of the "**squeeze-out model**" (56–58), which estates that upon compression, the composition of the interfacial film would be selectively refined to a pure DPPC monolayer, which is the only lipid competent to achieve a solid state leading to the low surface tension required for breathing (< 2 mN/m). Thus, other lipid species that would be required to fluidize DPPC and facilitate its adsorption, would be excluded from the interface at the time it must reach the lowest tensions. Years later, it was proposed that material excluded from the interface during compression would constitute a surfactant reservoir, promoted by the action of the hydrophobic proteins. From this reservoir, surfactant could be re-spread during expansion by transferring lipids into the interface. The proteins could be responsible of establishing the bilayer-bilayer and monolayer-bilayer contacts through which the lipids could be mobilized in and out of the interface. The presence of stacked multilayers is supported by *in vitro* observations (59, 60), but in which direction they form (air or hypophase) or whether they occur also *in vivo* is still under discussion (61). Another model propose that no reservoir is required since surfactant could behave as a **super-compressed monolayer**. This means that surfactant can possess the high fluidity required for adsorption and still reach the high rigidity that avoids alveolar collapse when it is compressed to the high rate imposed by breathing dynamics (62, 63). Technical limitations have prevented the validation of this model to date.

According to bibliography, the "squeeze-out" theory is still widely accepted and the following sections will refer to this model as the one ruling surfactant function. SP-B and SP-C are thus important to define the mechanical properties of surfactant membranes, which must display proper behavior in terms of elasticity, stability and remodeling. The relevance of SP-B and SP-C is highlighted by what occurs when protein levels are reduced or absent. SP-B deficiency is life threatening; the complete lack of the protein results in respiratory failure leading to death after birth (64–66). SP-C effects though, seem to be more subtle, and although early in life does not seem to be so critical, SP-C deficiency results in unstable lungs that ultimately develop interstitial lung disease.

Both proteins seem to act in a coordinate manner to sustain breathing and sometimes they apparently exhibit redundant functions. However, they also display characteristic and independent actions that are addressed in the following section.

SP-B

SP-B (8,7 kDa) is usually purified from BALF as a covalent **homodimer** (17,4 kDa) and belongs to the saposine-like protein family (SAPLIP), a group of amphipathic polypeptides involved in the mobilization of lipids (67). Approximately half of the SP-B sequence is constituted by hydrophobic amino acids and a fair number of residues are remarkably conserved along evolution. Seven cysteines are essential to maintain protein structure and dimerization ability (through 3 intramolecular and 1 intermolecular disulfide bonds) and 9 charged residues, 8 cationic and 1 anionic, confer the protein a net positive charge (67, 68). Despite widespread efforts, the high resolution 3D structure of SP-B has remained elusive so far. Some information has been inferred from circular dichroism and infrared spectroscopy experiments, which showed results consistent with an average of 40-50% α-helical content (69, 70).

SP-B adopts a **superficial orientation** in phospholipid membranes, with the protein oriented in-plane with the bilayer (71–75). This configuration is supported by the interactions of amphipathic helical segments of the protein and the headgroup region of membranes. Besides, electrostatic interactions involving acidic phospholipids present in surfactant and the positive charges of SP-B play an important role.

SP-B on its own is able to provide to surfactant phospholipids the most important properties of surfactant surface activity, **facilitating lipid adsorption** and **re-spreading of the lipid films** during inhalation (76–78). SP-B causes extensive **membrane rearrangements** with marked changes in **membrane curvature** leading to membrane fusion and lysis (79–81). These effects could be the basis sustaining SP-B-promoted connection and transfer of lipids from the surfactant reservoir into the interfacial film (82, 83). Together with SP-A, SP-B shapes surfactant membranes into **tubular myelin**, a highly ordered network of membranes, in the presence of calcium (43, 44) and it has been observed to generate highly cohesive multilamellar arrays (22). SP-B activity also results in an increase in membrane permeability through the generation of **proteolipid pores** and

supramolecular complexes (84–86), an effect that can be somehow connected with the SP-B-mediated increase in oxygen diffusion through surfactant multilayers (87).

SP-B is involved in **surfactant biogenesis**, participating in SP-C processing and in promoting the lipid packing to generate lamellar bodies (88, 89). SP-B has been also proposed as the key anchor triggering the unraveling of secreted surfactant into extracellular forms in a process that seems to involve a coordinate action of SP-B and SP-C (90).

SP-C

SP-C is the smallest (4,2 kDa) and most hydrophobic protein forming part of surfactant. It accounts for ~1% of surfactant mass, becoming the most abundant protein in molar terms. SP-C appeared relatively late in evolution and its sequence has remained highly conserved among species (Fig. 10a) (91). This, coupled to the lack of any known homologous protein and its confined expression (92), transforms it into a **specific marker** associated with the differentiation of **lung tissue**.

SP-C exists as a 35 amino acid **transmembrane protein** expressed as a larger precursor (21 kDa) in AT2 cells, where it follows several proteolytic cleavages and some posttranslational modifications (detailed in following sections). Structurally, it adopts a metastable **α-helical structure** comprising residues 9-34 (Fig. 10b) (93), although its high proportion of branched residues (valine, leucine and isoleucine) are typically associated to β-sheet structures (94). For this reason, under certain pathologic circumstances SP-C turns into β-sheet strands ultimately leading to the formation of fibrillogenic amyloid-like aggregates (95, 96). SP-C misfolded forms are cytotoxic and they are associated to several interstitial lung diseases including pulmonary fibrosis and pulmonary alveolar Proteinosis (97). The N-terminal segment of SP-C (residues 1-8) is the only region of the protein that projects out from the membrane and does not have a reported defined structure. Predictive studies, though, have suggested that it adopts β-turn configuration giving rise to a hairpin-like amphipathic structure allowing it to strongly perturb phospholipid bi- and monolayers (98, 99).

Figure 10. Sequence and structure surfactant protein SP-C. (a) A sequence aligment (Clustal Omega) is shown highlighting conserved residues (*), cysteines in the palmitoylation site (orange), and positively charged amino acids (blue) at physiological pH. (b) Structure of porcine SP-C determined by NMR (PDB 1SPF) in organic solvents without displaying the palmitoyl chains.

In vitro, SP-C displays several functions related to the biophysical behavior of surfactant. SP-C greatly **alters lipid packing** in membranes influencing lipid motion and lateral distribution (100, 101). It also increases **membrane permeability** (84, 85, 99) and promotes **interfacial lipid adsorption** and **lipid transfer** among different lipid structures (102–104). SP-C is responsible for the reversible formation of **multilayered stacks** connected to the interfacial monolayer (60, 103). Doing so, it allows for the capture of surfactant material presumably squeezed out during exhalation (area compression) and surfactant re-spreading upon inhalation (area expansion). In this process protein palmitoylation seems to be relevant in order to sustain protein association to the highly compressed interfacial films reached during exhalation (105, 106). The activity of SP-C mainly relies on its rigid transmembrane helix, which mediates protein-induced lipid alterations through hydrophobic interactions. The N-terminal segment, though, has been also reported to interact with membranes inducing packing defects that lead to vesicle aggregation and leakage *in vitro* (99). The **cationic charges** of the N-terminal segment establish electrostatic interactions with acidic phospholipids such as phosphatidyl glycerol (99). Besides, it has been proposed that palmitic chains couple protein motion to those occurring in the membrane (107).

Mice models for SP-C deficiency exhibit different phenotypes depending on the genetic background. This seems to be consistent with patients suffering from SP-C deficiency either caused by the complete absence of the protein and its precursor, or due to mutations that prevent a proper protein processing and maturation (97, 108, 109). In some cases, no pathology is apparently associated to SP-C absence in SP-C KO mice, although surfactant is observed to be less stable at low volumes (110). In other genetic backgrounds, SP-C deficiency results in an increase in phospholipid pools and significant lung remodeling (111). These lungs displayed an increased susceptibility to challenging conditions such as infection (112, 113), inflammation (114) and fibrosis inducting elements (115). Nonetheless, mutations in SP-C exhibit a dominant effect when inherited in heterozygosity, and they lead to much severe phenotypes than SP-C genetic ablation resulting in several forms of interstitial lung disease as a consequence of accumulation of aberrantly processed precursors (97). Thus, SP-C seems to be important for **stabilizing the lungs**, especially when they are exposed to challenging conditions.

The particular **relationship** between **SP-C** and **cholesterol**, both constituting important surfactant modulators, is an important feature that has attracted the attention of researchers over the last years. As discussed previously, cholesterol modulates membrane properties, and depending on its proportion and the overall composition of lipid films and membranes, both beneficial and adverse effects on surfactant behavior have been reported (23, 116–119). However, *in vitro* studies have demonstrated that in cases in which cholesterol impaired the function of surfactant mimicking mixtures, SP-C restored surfactant properties depending on SP-C palmitoylation state (120, 121). Besides, cholesterol miscibility in surfactant-mimicking membranes improves upon addition of SP-C (120) and SP-C configuration in bilayers has been reported to be affected by the presence of cholesterol (122). This evidence strongly suggests that SP-C and cholesterol functions are connected in the lung and could somehow cooperate to modulate

surfactant activity, although the molecular mechanisms sustaining their relationship are still unknown.

Finally, SP-C is not only important for the biophysical function of surfactant, but also possesses **immunomodulatory properties** in the lung (123). SP-C binds bacterial lipopolysaccharide, mediating its interaction with the membrane receptor CD14 (124).

Homeostasis in the lung

Lung surfactant synthesis and secretion

Lipid synthesis

AT2 cells are in charge of synthetizing and secreting surfactant to the alveolar hypophase. Phospholipids and proteins follow different biosynthesis pathways that converge into lamellar bodies, the highly packed lysosomal-derived organelles in which surfactant is stored until secretion.

De novo synthesis in the **endoplasmic reticulum** or **recycling/remodeling** are the two possible sources for surfactant phospholipids (125). In the case of DPPC, the major surfactant phospholipid, both pathways contribute significantly, with a 45% newly synthetized DPPC (via the Kennedy pathway) and the rest from the remodeling pathway (126). PCs are synthetized *de novo* in several steps that combine the action of a choline kinase (CK), a CTP:phosphocholine cytidyl transferase (CCT) and a phosphotransferase (CPT). A tight regulation of these enzymes, especially CCT, modulates the amount of lipid synthesis in order to keep lung homeostasis. In the remodeling pathway phospholipase A2 (PLA2) and lysophosphatidylcholine acyltransferase 1 (LPCAT1) are crucial enzymes (127).

Other phospholipids, such as PG, can also be produced either way, with some species being reported as coming from *de novo* synthesis, and others such as DPPG, from the remodeling pathway (125). In any case, to maintain surfactant pools and functionality, a cross-talk between pathways that responds to surfactant demands is necessary. In the case of DPPC, LPCAT1 is the enzyme responsible for coupling both pathways (127), whereas it also plays a role in the production of surfactant PG (128).

Surfactant cholesterol represents a **paradox** regarding its origin (129). Some works have suggested that it is supplied by the low and high-density lipoproteins present in blood circulation (125). However, other studies have failed to prove that circulating cholesterol ends up forming part of surfactant complexes (129, 130), suggesting that other possible sources must be taken into account. It is remarkable that cholesterol levels in surfactant are tightly regulated to ensure a proper breathing function, and they are able to increase and decrease extremely fast in response to changes in temperature or breathing rate (13, 131). This seems to imply that a **cholesterol reservoir** might exist in order to provide cholesterol at fast rates when an increase is required. A

specific cell type, the lipofibroblast, has been suggested as a reservoir of cholesterol (132, 133), although further validation is required to confirm whether it is present in all organisms and if it really constitutes a cholesterol storage. AT2 cells are able of producing cholesterol in peroxisomes (134), but also alveolar macrophages exhibit enzymes involved in cholesterol synthesis (135). Even though it is not known how cholesterol incorporates into lamellar bodies, the Niemann-Pick C pathway appears as a suitable candidate, through the cholesterol transporters Niemann-Pick C1 and C2 (NPC1 and C2) present in the lamellar body proteome (136). Elucidating how cholesterol levels are regulated in the context of surfactant physiology is key to understand responses associated with several respiratory pathologies characterized by the incorporation in surfactant of abnormal cholesterol amounts such as the acute respiratory distress syndrome (ARDS) (137) or pulmonary alveolar proteinosis (PAP).

Protein synthesis

Synthesis and processing of **SP-A** and **SP-D** is not specific of AT2 cells and their secretion has been observed to occur through pathways not involving lamellar bodies. In the case of SP-A, a small protein fraction seems to be secreted actually associated to lamellar bodies (36) although the molecular mechanisms guiding this process are still unknown.

In contrast, **SP-B** is essential for surfactant biogenesis participating in the maturation of lamellar bodies (138) and the processing of SP-C (89). SP-B is produced as a **381 amino acid precursor** (40-42 kDa) in which N-terminal (proSP-$B_{1\text{-}200}$) and C-terminal (proSP-$B_{280\text{-}381}$) propeptides flank mature SP-B domain (proSP-$B_{201\text{-}279}$) protecting it from the polar cellular environment until it is assembled into lamellar bodies (139–141). proSP-B is translocated to the endoplasmic reticulum via a signal peptide and it is subsequently cleaved in different steps along the trafficking pathway (Fig. 11). The first proteolytic cleavage is mediated by **napsin A**, an aspartil protease, which removes most of the N-terminal propeptide of the protein (142). The resulting intermediate proSP-B travels through the Golgi apparatus reaching the acidic multivesicular bodies and composites bodies.

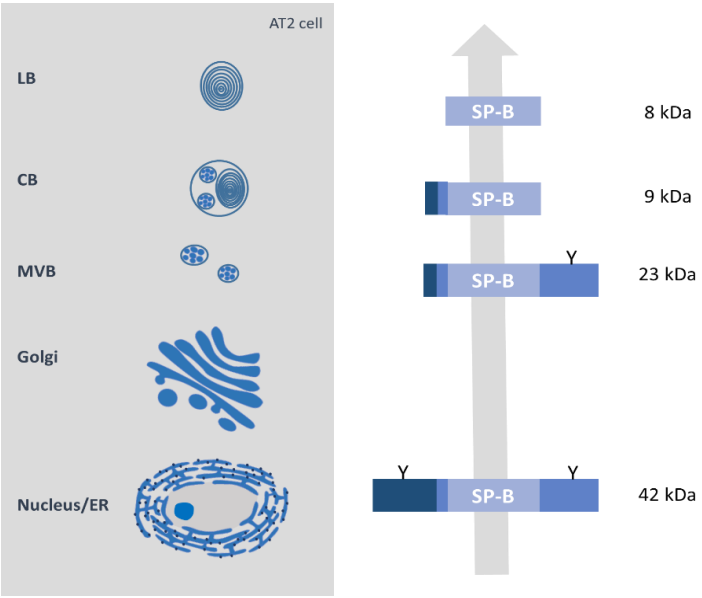

Figure 11. Schematic representation of proSP-B processing in a type II pneumocyte. proSP-B is sequentially cleaved along the exocytic pathway (ER, endoplasmic reticulum; MVB, multivesicular bodies; CB, composite bodies; LB, lamellar bodies) until it is assembled into lamellar bodies for its secretion. Figure adapted from (42).

Along trafficking, the remaining N-terminal residues of the propeptide and the whole C-terminal region is cleaved and removed by the action of **cathepsin H** (cystin protease) and **pepsinogen C** (aspartil protease), resulting in the 79 amino acid mature protein (143) that is finally transferred to lamellar bodies.

SP-C processing converges with SP-B in lamellar bodies. The gene encoding SP-C is structured into 6 exons and 5 introns located in the short arm of chromosome 8 (8p21) and its expression is orchestrated by **TTF1** (thyroid transcription factor 1), as well as that of SP-B and SP-A (144). Human SP-C mRNA is translated into a proprotein consisting of 191 or 197 amino acid residues depending on alternate splicing in AT2 cells. Most studies have reported that proSP-C (21 kDa) is inserted in the endoplasmic reticulum (ER) with a type II configuration, with the C-terminal end facing the ER luminal cavity (145, 146), although a type III configuration has also been suggested (147).

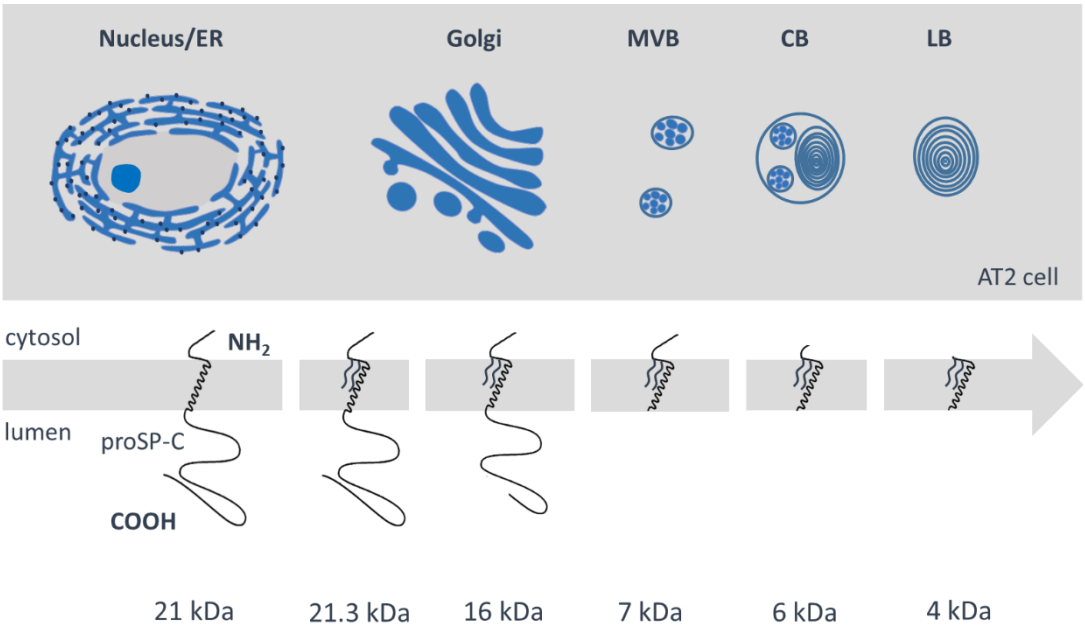

Figure 12. Schematic representation of proSP-C processing in type II pneumocytes. proSP-C is sequentially cleaved along the exocytic pathway (ER, endoplasmic reticulum; MVB, multivesicular bodies; CB, composite bodies; LB, lamellar bodies) until it is assembled into lamellar bodies for its secretion. Figure adapted from (42, 146, 151).

The sequence corresponding to mature SP-C (Phe_{24}-Leu_{58}) acts as a membrane anchor and comprises the only transmembrane segment (148). This region also serves as a **dimerization motif** required for SP-C sorting along the regulated secretory pathway (149). proSP-C is **dually palmitoylated** after its insertion in the ER (150) by a yet unknown palmitoyl transferase. The two palmitoylcysteines correspond to positions 5 and 6 in the mature SP-C sequence, and in some mammals, a phenylalanine substitutes one of those residues (91). For the acylation to occur, not only the N-terminal segment must be close to the membrane but also lysine and arginine residues occupying positions 11 and 12 in the mature protein are essential (146, 151, 152), since their mutation leads to defects in protein sorting preventing SP-C palmitoylation (150). After acylation,

proSP-C leaves the ER toward the trans-Golgi to initiate the proteolytic process (153, 154). Both the N-terminal and C-terminal segments are removed sequentially completing **four proteolytic steps** (Fig. 12). The C-terminal region (proSP-C_{59-197}) contains a **chaperone domain** termed **BRICHOS** (from Bri protein associated with familial British dementia, chondromodulin, and proSP-C; residues 94-197) (155), which facilitates the formation of SP-C α-helix (156) and stabilizes it until palmitoylation occurs (157). A 30-residue C-terminal segment is firstly removed in the medial Golgi resulting in a 16 kDa protein. This step is followed by the subsequent cleavage of the remaining C-terminal propeptide occurring along proSP-C trafficking through multivesicular and composite bodies (158). The N-terminal segment (proSP-C_{1-23}) is essential for protein sorting, and it is also processed and removed in two steps (159). From the 7 kDa proprotein generated after C-terminal cleavage, a 6 kDa peptide corresponding to proSP-C_{10-58} is produced in multivesicular bodies by the action of **cathepsin H** (160). This peptide has been observed both in composite bodies and lamellar bodies, whereas mature SP-C is mainly present in lamellar bodies (159, 160). This suggest that the **last step of processing** takes place in the lumen of those lysosome-related organelles right before secretion, in a process that has been shown to be **dependent on SP-B** presence (88, 89).

Lamellar bodies assembly and secretion

Once synthetized, lipids and proteins have to be transferred to lamellar bodies in order to be secreted. How hydrophobic proteins reach these organelles coupled to their maturation has been detailed before. On the contrary, lipid transport is not completely understood and may involve vesicular and non-vesicular transport (125). Lipids coming from the recycling pathway reach lamellar bodies through the multivesicular bodies (MVB), but newly synthetized lipids seem to bypass those organelles. Non-vesicular transport of PC is supported by the finding that a dysfunctional Golgi do not affect lipid secretion (127, 161) and experimental observations suggest that DPPC and PG can be transferred directly from ER to MVB together with the ATP-binding cassette A3 (ABCA3) (162, 163), a protein absolutely required for lamellar bodies generation.

ABCA3 is localized at the limiting membrane of lamellar bodies and is responsible for the transfer of lipids to the lumen of those organelles with ATP cost. Thus, the energy provided by ATP could be used to assemble the extremely highly packed lipid-protein organizations in which surfactant is stored (11). Due to the high packing state achieved, structural transitions can lead to the generation of highly dehydrated states and non-lamellar phases (164, 165). Upon secretion and depacking once at the air liquid interface, this accumulated energy may constitute the driving force for achieving an efficient and fast spreading of the interfacial film.

The AT2 cell secretes surfactant in the form of lamellar bodies by **exocytosis**. **Stretching forces** are the most physiologically relevant inducer of surfactant exocytosis as observed experimentally, but many other agents are able to stimulate exocytosis such as ATP and other purinergic receptor agonists and β2-mimetic drugs (166). Secretion starts with the fusion of the limiting membrane of the lamellar body with the plasma membrane in order to release surfactant to the medium, a process in which Ca^{2+} is the major second messenger triggering the fusion event (166).

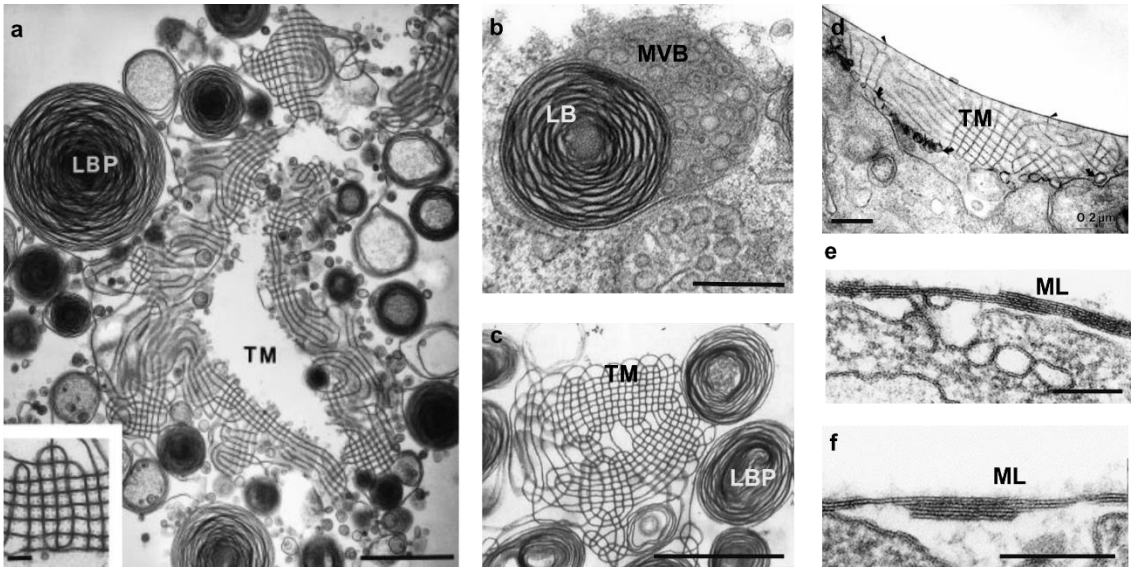

Figure 13. Electron transmission micrographs of surfactant extracellular and intracellular forms. Once secreted, surfactant is observed as lamellar body like particles (LBPs) (a,c), tubular myelin (TM) (a,c,d) and membrane multilayers (ML), which presumably are associated to the interfacial film (e,f). A lamellar body (LB) is also shown in the process of fusing to a multivesicular body (MVB) within a type II pneumocyte (b). Figures taken from (7, 12, 88, 167, 168). Scale bars correspond to (a) 0.1 µm (lower left), 1 µm (lower right); (b) 1 µm; (c) 1 µm; (d) 0.2 µm; (e) 0.3 µm; (f) 0.1 µm.

When lamellar bodies are released, they maintain a packed state in the alveolar fluid as **lamellar body like particles**. These organizations retain characteristics of lamellar bodies and, by the coordinate action of SP-B and SP-C (90), unravel in a cooperative and efficient manner once touching the air-liquid interface. In some cases, unraveling of the LBPs leads to the generation of different structures including a lattice-like ordered network of membranes defined as tubular myelin (Fig. 13) (166). **Tubular myelin** has been considered as an intermediate state between the lamellar bodies and the interfacial film, being associated with, but not strictly necessary for, a proper biophysical surfactant function *in vivo* (166). For tubular myelin to form, SP-A, SP-B and Ca^{+2} are essential elements (43). Although its specific function is still unknown, it has been proposed that it can serve a defensive purpose functioning as a scaffold for SP-A, SP-C, lysozyme and other molecules with a role in host-defense (169). Several studies have reported that tubular myelin is not essential for producing the interfacial film, suggesting that other mechanisms are responsible for triggering the adsorption of surfactant material to the air-liquid interface. Those mechanisms would rely either on the direct adsorption of the lamellar body like particles or on the formation of other intermediate structures (large vesicles or lipid aggregates) which could also promote surfactant adsorption.

Lung surfactant degradation and recycling

Once surfactant is secreted, its constituents, both lipid and proteins, are long-lived molecules with a half-life going from 10 to several tens of hours. This is consequence of a slow clearance from alveoli to upper airways and from continuous recycling/re-secretion of material by AT2 cells (166). Surfactant turnover then becomes the most informative parameter, which measures the time required for surfactant pools to be replenished by newly secreted surfactant. In alveolar fluid, the turnover rate goes from 4 to 11h (32).

When surfactant reaches the interface, it suffers several compression/expansion cycles along breathing leading to compositional and structural reorganizations, after which it is considered "used" surfactant (170). This material is released from the interfacial film in the form of small aggregates and cleared by AT2 cells and alveolar macrophages.

AT2 cells

AT2 cells are responsible for a **65% of surfactant clearance** (171), leading to lipid catabolism and recycling. The recycling pathway depends on the protein SP-A (127), which upon interaction with a specific receptor on the AT2 cell plasma membrane (172), promotes the combined internalization of lipids and SP-A by a clathrin-dependent pathway (172, 173). Lipids are sorted to early endosomes and transferred to lamellar bodies in a calmodulin-dependent mechanism (49). However, not all SP-A is rapidly recycled and secreted again to the alveolar space, with a protein fraction following an actin-dependent degradation route (127). Clathrin-dependent endocytosis is not the only pathway guiding surfactant recycling but it becomes the main recycling mechanism in the absence of SP-A (173).

SP-D deficiency results in the accumulation of lipids in the alveolar spaces (174, 175). However, rather than a direct activity on surfactant uptake and degradation (174), SP-D effect seems to be caused by the structural transformation of large surfactant aggregates into small, less functional, ones, which are preferentially taken up by AT2 cells (51, 176).

Non-recycled phospholipids are mainly degraded by the action of PLA2 in both AT2 cells and macrophages (125). Besides, AT2 cells have mechanisms to eliminate excess PC such as the basolateral transport of lipids via the ATP-binding cassette transporter A1, ABCA1 (177, 178).

Alveolar macrophages

Although surfactant clearance mainly occurs through AT2 cells activity, **alveolar macrophages** metabolize a significant fraction **(20%-30%)** (9, 32, 125, 171). This cell type is critical to maintain alveolar homeostasis as illustrated by the pathologies derived from a deficient alveolar macrophage (AMφ) function, such as pulmonary alveolar proteinosis (PAP) (179).

Alveolar macrophages are equipped with a set of enzymes and regulators of lipid catabolism and transport whose alteration results in impaired lipid degradation and accumulation in the alveolar fluid (135, 180–183), leading in some instances to the generation of "foamy macrophages" showing lipid accumulation in "lipid droplets". **GMCSF (granulocyte-macrophage colony stimulating factor)** is the master modulator of surfactant clearance by AMφ (179). This growth factor mediates the differentiation of monocytes into macrophages and is crucial for the activation of the lipid degradation and transport machinery (179). Neutralizing GMCSF autoantibodies (184, 185) and defective GMCSF receptor versions (186) result in PAP phenotype, which can be relieved upon macrophage lentiviral transduction and expression of genes downstream GMCSF such as *pparγ* (peroxisome proliferator-activated receptor gamma) or *abcg1* (ATP-binding cassette transporter G1) (181, 187). GMCSF regulates the transcription of the transcription factor PU.1 through the JAK/STAT signaling pathway, and therefore, PU.1 dependent genes (179). Among them, scavenger receptors class II (CD36 and SR-BI) and lysosomal enzymes (lysozyme or lysosomal phospholipase A2; LPLA2; (188)) can be associated to lipid homeostasis in the lung (179).

PPARγ, a central piece in lipid catabolism, is also under the regulation of GMCSF, and its deficiency leads to lipid accumulation in the lung. It controls the expression of ABC transporters, such as ABCG1 and scavenger receptors class II, such as CD36 (135). Additionally, it directly regulates the levels of lysosomal acid lipase (LAL or LIPA), sterol-27-hydrolase (CYP27A1 and CYP27A6) (135, 189) and acylcholesterol acyltransferase 1 (ACAT1), all enzymes involved in lipid and cholesterol metabolism linked to PAP (190).

The role of **ABCA1** and **ABCG1** seems to be especially important. Both proteins participate in cholesterol efflux to LDL and HDL respectively (191), and mice models have proved that their deficiency in the lung is sufficient to lead to the PAP phenotype (192–194). Both transporters are regulated by LXR (nuclear oxysterol receptors) (195, 196) and their expression responds to cholesterol uptake (135). AMφ also possess other cholesterol transporters, NPC1 and C2, in some instances related to patients suffering from PAP (197).

Lipid clearance by AMφ is also influenced by surfactant proteins since deficiency in SP-C (110–113) and SP-D (50, 174) leads to the accumulation of lipids in the alveolar fluid. SP-D for instance is able to regulate alveolar macrophage number and therefore surfactant pool size (51), although in general, the mechanisms by which surfactant proteins influence lipid homeostasis are still a matter of study. It seems particularly interesting how the small lipopeptide SP-C is able of interfering with AMφ function especially concerning cholesterol metabolism (198). It has been previously mentioned that SP-C establishes a relationship with cholesterol that seems to be relevant in the regulation of surfactant function. Animals deficient in SP-C exhibit foamy alveolar macrophages, in which crystals with similar characteristics to those generated in atherosclerosis accumulate (111). This suggests that SP-C might somehow be involved in surfactant homeostasis regarding cholesterol regulation. Besides, SP-C is an immunomodulator (123), as it interacts with the AMφ CD14 regulating the recognition of lipopolysaccharide (124) by binding LPS itself, thus regulating the immune response in the lung. Hence, SP-C could play a pivotal role linking surfactant homeostasis and immunity in alveoli, a potential integrative role that requires further exploration.

Surfactant associated diseases

Impairment in surfactant homeostasis

Surfactant homeostasis is tightly regulated at several levels in order to maintain surfactant pools without altering film composition at the alveolar air-liquid interface. This is crucial for a proper respiratory function, and any imbalance in surfactant secretion/uptake or alterations in surfactant composition, results in severe respiratory disorders.

Surfactant absence was the first cause of neonatal mortality in premature babies until the achievemnt of surfactant replacement therapy (199). These newborns developed **neonatal respiratory distress syndrome (NRDS)** at birth as a consequence of having immature lungs, unable of secreting surfactant since the first inhalation (200). Nowadays, intratracheal administration of surfactant clinical preparations aid to support the first breathing cycles, stabilizing the lungs and promoting surfactant secretion by the baby.

The **acute respiratory distress syndrome (ARDS)** in adults is a far more complex pathology. It is characterized by an exacerbated inflammatory process that damages alveolar structure and causes severe hypoxemia (201). One of ARDS hallmarks is the leakage of serum proteins to the alveolar spaces as a consequence of the alteration of the alveolar-capillary barrier. Leaked proteins compete with surfactant complexes for the air-liquid interface, leading to surfactant inhibition. Besides, compositional and structural alterations of surfactant as a consequence of lung injury, result in a decrease in DPPC content and an increment in surfactant inactive forms (202), which coupled to the deficiency in surfactant proteins, such as SP-A and SP-B, contributes to an impaired biophysical function. This situation is accentuated by an abnormal increase in neutral lipids, mainly cholesterol (203), promoting surfactant dysfunction and leading to cellular damage.

Pulmonary alveolar Proteinosis (PAP) is a good example of a respiratory pathology caused by an impaired surfactant homeostasis (204). As previously described, PAP is characterized by a pathological accumulation of surfactant complexes in alveolar spaces due to alterations in surfactant clearance by AMφ. To date, the treatment is purely symptomatic and involves bronchoalveolar lavage to eliminate lipid excess from alveoli (205). However, cell therapy is emerging as a promising alternative for PAP patients and so far, AMφ transplantation has been successful to revert the PAP phenotype in mice models (206) .

Congenital alterations in surfactant proteins can also lead to several pathologies. **Mutations** in the **SP-B, SP-C** or **ABCA3 genes** disturb surfactant homeostasis causing different interstitial lung diseases (204). SP-B deficiency impairs lamellar body formation and SP-C processing causing respiratory failure (88). In the case of SP-C, 14 different mutations in its precursor have been associated with the development of diffuse parenchymal lung disease (97). Heterozygous mutations of SP-C are sufficient to cause lung pathologies as it occurs in some neurodegenerative disorders such as Alzheimer's or Huntington's disease. Typically, proSP-C mutations generate aberrant protein isoforms that are misfolded or abnormally trafficked leading to conformational

disease. Aggregated protein forms trigger the unfolded protein response which ultimately cause endoplasmic reticulum stress and apoptosis (97). SP-C-induced cellular stress has been related to several pathologies including interstitial lung diseases such as **pulmonary fibrosis**.

Mutations in ABCA3 result in AT2 cells failing to properly produce and secrete lamellar bodies. As a result, SP-B and SP-C processing are also altered and the phenotype of these mutations results in lethal respiratory failure (204).

Many other mutations and disorders can affect surfactant homeostasis leading to respiratory associated diseases, highlighting the central role of surfactant in lung health and disease.

4. Objectives

Lung surfactant biophysical function critically depends of the activity of the hydrophobic surfactant proteins SP-B and SP-C. Nevertheless, whereas SP-B absence is life-threatening, supporting its essential role for the breathing function, the specific role of SP-C is still a matter of debate. SP-C becomes functionally relevant when cholesterol is incorporated into surfactant mimicking preparations, and the presence of cholesterol modulates SP-C orientation in membranes. In addition, SP-C palmitoylation appears as an essential element to sustain the dynamic behavior of surfactant membranes and films. Considering the role of cholesterol in rapidly adapting surfactant structures to different environmental conditions, and the long-term stabilization of the lung associated to the presence of SP-C, it could be suggested that SP-C and cholesterol are somehow related in the modulation of surfactant structures to sustain respiratory dynamics. Indeed, according to previous evidence, SP-C activity could depend on the palmitoylation of its N-terminal segment, which might play a role in defining SP-C-induced effects on membrane structure. Taking this into consideration, the general objective of the present Thesis has been the **characterization in detail of the behavior of surfactant protein SP-C in lung surfactant membrane contexts**, with particular interest in its **potential role to modulate the structure and properties of surfactant membranes in the presence of cholesterol**. This general objective has been approached through the following specific objectives:

1. ***Examination of the role of SP-C palmitoylation on SP-C structure and lipid-protein interactions in membrane multilayers***.
   To identify lipid components specifically involved in defining SP-C configuration in lipid bilayers, SP-C orientation has been analyzed in membranes with different composition by Attenuated Total Reflectance- Fourier Transformed Infrared spectroscopy (ATR-FTIR). (Results. Chapter 1).

2. ***Analysis of the effect of SP-C on cholesterol dynamics in native surfactant-derived and surfactant-mimicking membranes***.
   SP-B and SP-C combined activities have been assessed with respect to protein-induced membrane reorganization activities and their effect on cholesterol distribution. (Results. Chapter 2).

3. ***Evaluation of the effect of SP-C and cholesterol on membrane structure and lateral phase segregation***.
   Each lipid component of model surfactant membranes (DPPC, POPC, POPG and cholesterol) has been assessed independently to analyze specific SP-C/lipid interactions. The effect of SP-C palmitoylation has been also investigated concerning the generation of lipid phase segregation. (Results. Chapter 3).

4. ***Validation of selective SP-C/lipid interactions in membranes concerning SP-C/phospholipid, SP-C/cholesterol and protein palmitoylation***.
   A new method to assess specific protein/lipid interactions based on Thin Layer Chromatography (TLC) has been described. (Results. Chapter 4)

5. ***Study of the effect of SP-C and cholesterol on surfactant homeostasis regarding lipid endocytosis and metabolism by alveolar macrophages***. (Results. Chapter 5).

5. Results

Chapter 1

Role of palmitoylation in SP-C protein-lipid interactions in membrane multilayers

The experiments included in the present chapter were done in collaboration with Prof. Erik Goormaghtigh from the Laboratory for the Structure and Function of Biological Membranes (Center for Structural Biology and Bioinformatics, Université Libre de Bruxelles, Belgium) and published in the following article:

Roldan, N; Goormaghtigh, E; Perez-Gil, J. and Garcia-Alvarez, B. "**Palmitoylation as a key factor to modulate SP-C-lipid interactions in lung surfactant membrane multilayers**"

Biochimica et Biophysica Acta 1848 (2015), 184–191. Doi:10.1016/j.bbamem.2014.10.0090005-2736.

EBSA
Biophysics in Europe

ULB
UNIVERSITÉ
LIBRE
DE BRUXELLES

Introduction

In the context of lung surfactant bilayers, SP-C adopts a transmembrane configuration with its N-terminal segment closely associated with the membrane by cysteine-attached palmitic chains (207, 208). However, SP-C N-terminal segment has proven its ability to perturb and interact with membranes regardless of its acylation state (99), suggesting that palmitoylation may have other role in SP-C function than merely anchoring the N-terminal segment to the membrane.

Palmitoylation seems to be involved in stabilizing SP-C α-helical conformation (208–210), although some studies have suggested that the presence of palmitoylated cysteines does not affect protein structure (211, 212). Besides, SP-C is known to promote the formation and stabilization of an interconnected multilayer meshwork associated to interfacial films (60, 213), a function that is thought to depend on protein palmitoylation. According to surfactant most accepted models (42, 54, 214), SP-C palmitic chains would facilitate the establishment of monolayer/bilayer and bilayer/bilayer contacts by inserting into lipid structures ahead of those in which the α-helical region is embedded. This mechanism could also explain how SP-C palmitoylation sustains proper surfactant dynamics, especially in the presence of cholesterol (215). Therefore, palmitoylation appears as a key factor modulating SP-C function, although the limited experimental information available so far has prevented the elucidation of its specific role in SP-C-associated activities.

The aim of the research summarized in this chapter is to analyze the nature of palmitoylation-mediated effects on SP-C-lipid interactions in the lung surfactant context, also considering effects on protein structure. With this purpose, Attenuated Total Reflectance-Fourier Transform Infrared (ATR-FTIR) spectroscopy has been employed, since it allows the simultaneous analysis of lipid and protein characteristic absorption bands. One of the most powerful applications of this technique is the study of oriented lipid-protein multilayers, providing information not only on the state of lipids and proteins regarding structure and hydration, but also on the average configurational orientation of molecules by using polarized infrared light (for a review see (216)). This is particularly interesting in the case of surfactant, since the oriented multilayers studied here resemble the structure of those stacked membranes occurring naturally as part of the so-called surfactant reservoir, and thus, our approximation allows the study of SP-C simulating the environment close to the air-liquid interface.

Here we describe the analysis by ATR-FTIR of lipid-protein films containing either native palmitoylated SP-C or a recombinant non-palmitoylated SP-C version (rSP-C), in lipid systems designed to mimic the different properties of lung surfactant membranes. Our results suggest that palmitoylation is involved in defining SP-C configuration in membranes, and also in modulating lipid-protein interactions at the polar region of lipid bilayers. Nevertheless, protein acylation did not seem to affect protein structure. This information is relevant from a structural point of view, considering that SP-C palmitoylation could favor certain protein-lipid interactions promoting lipid structures optimized for an efficient surfactant interfacial activity.

Results

Protein structure

To analyze whether protein structure was altered by the lipid environment or palmitoylation, the ATR-FTIR spectra of palmitoylated and non-palmitoylated SP-C were obtained in films prepared from suspensions of the proteins in different phospholipid mixtures. Membranes composed of DPPC/POPC/POPG (50:25:15, w/w/w) were used as a model capturing the main features of lung surfactant in terms of the combination of saturated/unsaturated and zwitterionic/anionic phospholipid species. The other two lipid systems tested were DPPC/POPC (50:40, w/w) and POPC:POPG (75:15, w/w) in order to define the importance of electrostatic charge and lipid phase coexistence on protein-lipid interactions, respectively.

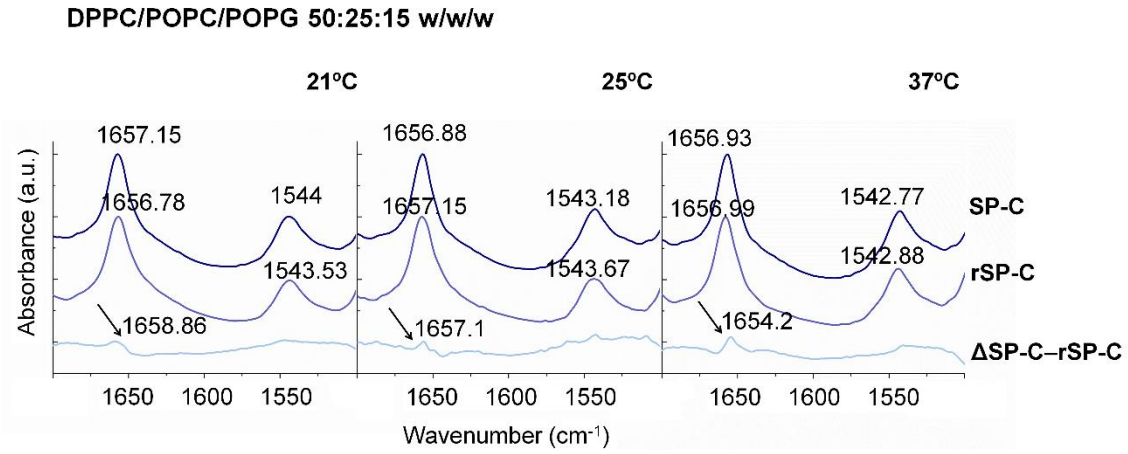

Figure 1.1. SP-C and rSPC structure in DPPC/POPC/POPG membranes. ATR-FTIR spectra of SP-C and rSP-C reconstituted in DPPC/POPC/POPG (50:25:15, w/w/w) multilayers, at 21^{0}C, 25^{0}C and 37^{0}C. Frequency maxima for amide I (1700-1600 cm^{-1}) and amide II (1600-1500 cm^{-1}) bands are shown. Differences between the two proteins are illustrated in the subtraction spectra SP-C – rSP-C below, with the main difference marked by an arrow. Both spectra were scaled to the same intensity for the amide I band (1700-1600 cm^{-1}).

The ATR-FTIR spectra of SP-C and rSP-C inserted into DPPC/POPC/POPG membranes are illustrated in Fig. 1.1. The difference spectrum, ΔSP-C-rSP-C, reveals an apparent shift of the amide I contribution of native SP-C with respect to the non-palmitoylated form. Amide I and II bands of SP-C and rSP-C appeared centered around 1657 cm^{-1} and 1543 cm^{-1}, respectively. The narrow shape of these bands and their frequencies are consistent with a predominantly α-helical structure, as previously described for these proteins (93, 217). Secondary structure determinations for the two proteins estimated more than 80% α-helical content with no significant differences between them. However, the SP-C – rSP-C difference spectrum revealed an upward band deviation in the amide I wavenumbers, which increased in intensity and decreased in frequency with temperature.

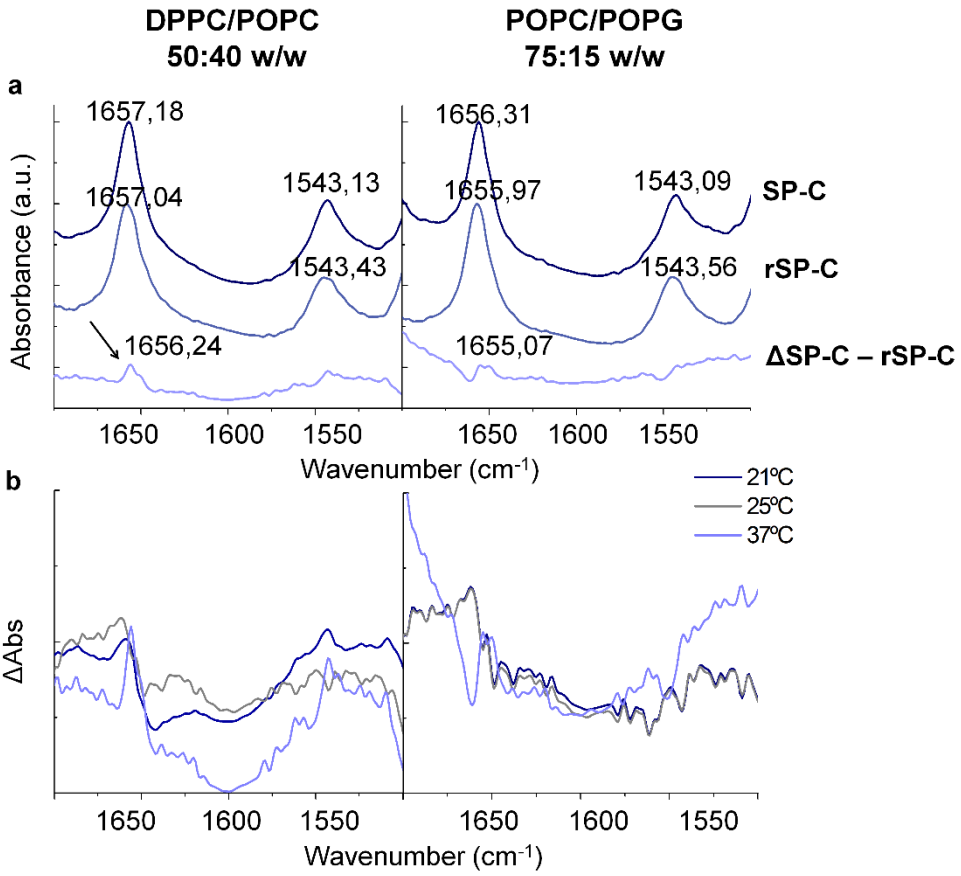

Figure 1.2. Structure of SP-C and rSPC in different lipid environments. (a) ATR-FTIR spectra of proteins SP-C and rSP-C reconstituted in DPPC/POPC (50:40, w/w) or POPC/POPG (75:15, w/w) membrane multilayers, at 37^{0}C. Frequency maxima for amide I (1700-1600 cm^{-1}) and amide II (1600-1500 cm^{-1}) bands are shown. ΔSP-C – rSP-C represents the subtraction spectra. (b) Subtraction spectra ΔSP-C – rSP-C at 21^{0}C (blue), 25^{0}C (grey) and 37^{0}C (light blue), for each of the two lipid compositions. All spectra were scaled to the same intensity.

The amide I contribution in the other two lipid environments assessed, DPPC/POPC and POPC/POPG, at three different temperatures is illustrated in Fig. 1.2. The shift in amide I wavenumber in palmitoylated vs. non-palmitoylated protein was also apparent in DPPC/POPC multilayers but not so much in the purely unsaturated phospholipid films. The consistent finding of this feature could be explained by slightly lower vibration frequencies for amides corresponding to the palmitoylated protein.

As it will be discussed later, our results indicate that palmitoylation increased SP-C tilt-angle resulting in a more pronounced perturbation on membrane polar region. Thus, palmitoylation indirectly promotes water penetration at the membrane surface by influencing protein embedment in lipid bilayers. Higher penetration of atmospheric water, and thus higher polarity, could result in a reduction of SP-C amide I stretching frequency as a consequence of hydrogen-bonding (218), an effect consistent with our findings.

Lipid-protein interactions

To assess whether SP-C and rSP-C could perturb the lipid systems studied in a different manner, we have monitored the thermotropic profile of phospholipids by following the shift of the frequency associated with CH_2 stretching vibrations. These bands are sensitive to the lipid chain trans/gauche isomerizations leading to temperature-dependent frequency changes. An increase in temperature generates vibrational bands towards higher wavenumbers, which can be used to compare the thermotropic profiles of phospholipid layers in the absence or presence of either palmitoylated or non-palmitoylated protein.

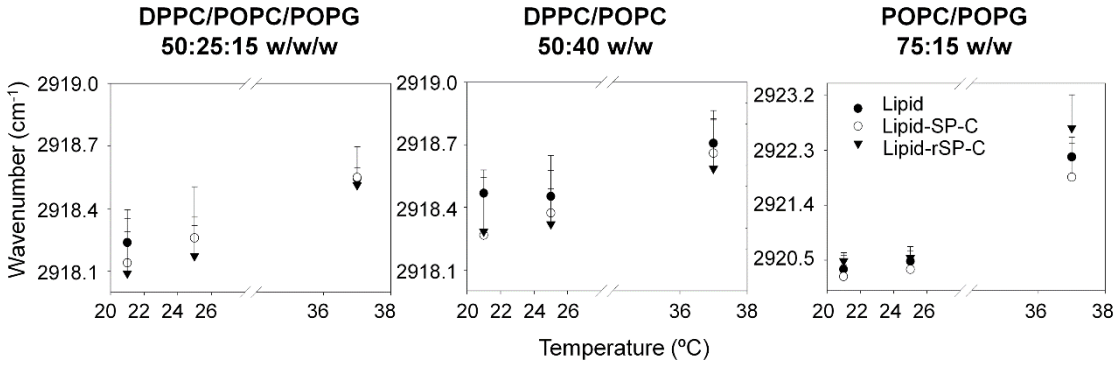

Figure 1.3. Effect of SP-C and rSP-C on the thermotropic profile of different membrane multilayer systems. Thermotropic profiles of the three different lipid systems assessed, in the absence or in the presence of proteins SP-C or rSP-C, as monitored by the position of the CH_2-asymmetric vibration absorption band. The profiles show the effect attributable to protein insertion into the membrane for each temperature studied.

The thermotropic behavior of the three lipid systems studied, in the absence and in the presence of the native or the recombinant SP-C variants, is shown in Fig. 1.3. In none of the lipid compositions studied there is a clear effect attributable to the protein insertion into membranes in the range of temperatures analyzed. Methylene asymmetric stretching frequencies (2900-2950 cm^{-1}) overlap for samples containing or not SP-C or rSP-C at the temperatures tested, suggesting that neither lipid composition nor palmitoylation are critical factors to modulate lipid-protein interactions at the multilayer membrane films, at least as sensed by acyl chain vibrations under the conditions used for this study.

To gain further insight into the characterization of SP-C-lipid interactions, we focused on the differences observed in the polar region of lipid spectra. Phosphate-associated vibration bands can provide information about superficial interactions in the membrane that modulate both their intensity and frequency (219). Fig. 1.4a illustrates the effect of the palmitoylated and non-palmitoylated SP-C on the phosphate-associated vibration bands for the three different lipid systems studied. The largest differences are observed in the phosphate asymmetric and symmetric stretching region in the presence of the palmitoylated SP-C protein compared to non-palmitoylated SP-C. For the surfactant mimicking synthetic mixture, DPPC/POPC/POPG 50:25:15 w/w/w, the differences are mainly observed on peak intensity, which decreases when the

incorporated protein is non-palmitoylated SP-C. For the other two lipid systems, differences are also more conspicuous in the presence of the palmitoylated protein, although there are also some variations on the frequency of the vibrations. These alterations could be associated with a different extent of perturbation of the headgroup region of the membrane multilayers by the N-terminal segment of the protein.

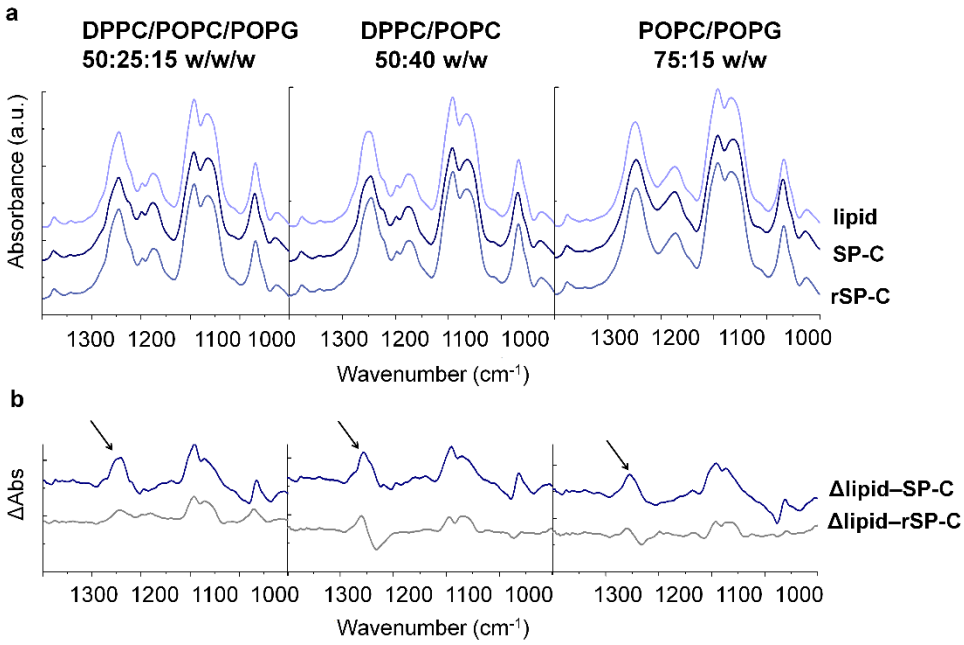

Figure 1.4. Effect of SP-C on phosphate vibrations in different lipid systems. (a) Spectra corresponding to the phosphate vibration region (1400-900 cm^{-1}) are shown for the three different lipid systems assessed, in the absence or in the presence of proteins SP-C or rSP-C, at 37°C. (b) Subtraction spectra of pure lipid – lipid-SP-C (black line) and lipid – lipid/rSP-C (dashed line). The main difference, introduced mainly by palmitoylated SP-C, is marked with a black arrow.

Molecular orientation

The molecular orientation of SP-C and rSP-C in the three lipid systems studied, as estimated by the dichroic absorption ratio of polarized IR, is summarized in Table 4.1. Different effects can be observed on protein tilting depending on temperature, palmitoylation or lipid composition. A slight increase in the tilt angle was found at higher temperatures for both proteins and all compositions tested, consistent with the assumption that disordering on lipid membranes at higher temperatures decreases membrane thickness, and thus results in hydrophobic mismatch that is resolved by the tilting of the helix.

Table 4.1. Tilting angles for SP-C and rSP-C proteins in the different lipid environments.

Temperature	Protein	Lipid system		
		DPPC/POPC/POPG	DPPC/POPC	POPC/POPG
21°C	SP-C	25° ± 5°	20° ± 5°	25° ± 5°
	rSP-C	20° ± 5°	17.5° ± 2.5°	22.5° ± 2.5°
25°C	SP-C	25° ± 5°	20° ± 5°	25° ± 5°
	rSP-C	20° ± 5°	17.5° ± 2.5°	27.5° ± 5°
37°C	SP-C	30° ± 5°	22.5° ± 2.5°	37.5° ± 2.5°
	rSP-C	22.5° ± 2.5°	32.5° ± 2.5°	37.5° ± 2.5°

On the other hand, palmitoylation seems to induce a consistent trend towards higher protein tilt angles in most of the cases analyzed. Palmitoylation-induced anchoring of SP-C to the membrane may induce a deeper embedment of the N-terminal end of the protein into the polar region of the bilayer, thus pulling out the helix that would form a wider angle with respect to the membrane normal. This is consistent with the fact that depalmitoylation induced a more perpendicular orientation of the protein when it is reconstituted in lipid bilayers as reviewed in (220). Nevertheless, the effect of palmitoylation cannot be analyzed independently of lipid composition. POPG-containing systems induced a more tilted protein configuration for both SP-C and rSP-C at 21°C than estimated for the purely zwitterionic system. This could indicate again a closer association of the N-terminal segment with the membrane, in this case due to electrostatic interactions, as it has been previously described (99). The positively charged N-terminal end of both proteins would be then interacting with the negative charge of POPG forcing again the helix to adopt a less perpendicular orientation.

Discussion

Palmitoylation is thought to be one of the main features associated with the functional activity of surfactant protein SP-C (209, 215), contributing to define the optimal conditions for the re-spreading ability of lung surfactant during inspiration (221, 222). In the current study, we have studied the structure, lipid-protein interactions and orientation of palmitoylated and non-palmitoylated versions of SP-C in partly dehydrated multilayer films, which could somehow mimic the organization of lipids and proteins at the multilayer reservoir of surfactant. Our results suggest that palmitoylation is important to modulate the proper configuration of the protein in these lung surfactant-mimicking multilayers, however, how this configuration could be related to the function of the protein has to be analyzed carefully.

In terms of protein structure, several studies have previously addressed the effect of SP-C palmitoylation with controversial results. Some of them have suggested that depalmitoylation

induce a loss of alpha helical structure increasing the chance of protein aggregation (208–210), whereas others have pointed out that lack of acylation does not alter protein α-helical structure and even may favor it, at least with respect to the length of the helical segment (211, 212). SP-C has a strong tendency to aggregate even in non-polar solvents (223), particularly when it is free of lipids. For this reason, some of the chemical treatments used in those previous studies to add or remove the acyl chains could be the indirect or direct cause of the alteration in the protein structure, rather than the absence or presence of the chains themselves. Our study suggests that palmitoylation does not affect much the secondary structure of the protein as the infrared difference spectrum do not show large variations in amide I and II line shape and frequencies between SP-C and rSP-C proteins in the different lipid systems analyzed, which is consistent with the results found in a previous study (211). It could well be that the structure of the protein is particularly stabilized at its maximal α-helical conformation in the partly dehydrated, possibly highly packed, multilayered films, and this could be the reason why our estimations of that secondary structure yield at least 80% α–helical content, for the two proteins in all the lipid environments. However, a subtle but consistent difference was revealed as a shift of the α-helical wavenumbers from the difference spectra in the amide I region of palmitoylated and non-palmitoylated SP-C. Stretching vibrations are influenced by the polarity of the environment of any defined IR chromophore. Thus, differences in the presence of water molecules that could form hydrogen bonds with our molecule of study could explain such a decrease of the frequency of stretching vibrations. Taking into account that the energy of amide I band comes principally from vibrations of the C=O bond (224), a change of environmental polarity could be behind the shift in the vibration frequency.

Protein-promoted perturbations may be also important to facilitate intermembrane topological connections and efficient transfer of surface-active lipid molecules through the whole surface film. From our results, we speculate that palmitoylation could generate a deeper insertion of the N-terminal segment of SP-C into the headgroup region of the lipid layers, producing larger packing defects and a local polarity increase in the membrane. In this sense, and considering that palmitoylated SP-C is also on average more tilted into membranes than the non-palmitoylated form, the more external N-terminal end of the α-helix would sense this change of polarity varying its frequency of vibration to lower wavenumbers. This effect is particularly observed when the lipid composition includes saturated phospholipids, suggesting a modulating effect of membrane composition. SP-C has been found to locate preferentially into liquid-disordered phases in membranes (23) and liquid-expanded regions in interfacial films (27, 225), but accumulating at the boundaries between ordered and disordered regions in membranes and monolayers exhibiting phase coexistence (25, 226). We propose that SP-C, or at least its palmitoylated N-terminal segment, could be located at the edge of the domains formed by DPPC, where SP-C-induced perturbation could be maximal. In our experiments the difference in the amide I spectra of palmitoylated and non-palmitoylated SP-C increase while approaching to 37oC in those systems whose melting temperature is in the range of physiological temperatures. With increasing temperature, membranes reach a higher dynamic character, including more frequent and larger molecular fluctuations, deeper water penetration

and a possibly larger difference in water accessibility of the N-terminal end of SP-C helix. If palmitoylation were at least in part responsible for the association of SP-C with the boundaries of DPPC-enriched ordered lipid domains, differences in perturbations induced between palmitoylated and non-palmitoylated SP-C would be further accentuated, as observed in our experiments.

The stronger effect of the palmitoylated protein to perturb the contribution of phosphates to the IR spectra would be consistent with changes promoted by the acylated segment of the protein on the organization, packing and polarity of the headgroup region of the lipid/protein multilayers. This is also consistent with the thermotropic profiles registered for these samples, which suggest that the effect of the proteins (both palmitoylated and non-palmitoylated) is limited as sensed by the acyl chains. Altogether these results indicate that the effect of palmitoylation is somehow focused to that headgroup level, in agreement with previous studies such as the one by Morrow et al (100).

The study of SP-C orientation in membranes has been addressed before (122, 207, 208). Most of these studies have indicated an orientation for the alpha helix almost parallel to the acyl chains. In the present work we have observed differences on protein tilting depending on the lipid system studied and palmitoylation state. Discrepancies between previous values and those obtained in the current study could come from the assumption of an order parameter (S) of 1 for our determinations, which was compatible with our results and theoretical values. Therefore, the angles discussed here correspond to maximum tilts, although it is not possible to discard the existence of disorder sources that could shift the values to more perpendicular orientations.

Temperature seemed to have some effect on protein orientation, increasing slightly tilt angles toward higher values. This effect could be originated in a more pronounced hydrophobic mismatch when membrane thickness decreases at higher temperature, particularly when values above the melting temperature are reached and the phase transition occurs, as it may be the case for the lipid mixtures containing DPPC.

The results presented here have shown that palmitoylated SP-C may alter the polar region of the membranes to larger extent than rSP-C. Consequently, for the acylated protein, the α-helix may be suffering the effect of a more polar environment caused by a deeper embedment of the N-terminal segment into the headgroup region of the phospholipid layers. These observations are consistent with our findings on protein orientation. When SP-C is inserted into multilayered films made of DPPC/POPC/POPG, palmitoylation seems to roughly induce a 5o more pronounced tilting angle with respect to the membrane normal. We are aware that the magnitude of this increase in the tilting angle is close to the limit of significance defined by the calculation method, but we still see it as relevant considering that in most experiments this trend is maintained in the same direction. Such palmitoylation-promoted increase on helical tilting is not so clear in the system containing no DPPC, suggesting that for palmitoylation to cause a more pronounced tilt a context of thicker membranes or membranes sustaining phase coexistence could be required. It is important to mention that for systems containing POPG, the

calculated tilt angles were higher for both proteins when compared to those in the purely zwitterionic DPPC/POPC system, supporting the idea that electrostatic interactions between the N-terminal segment of the proteins and the anionic phospholipid also contribute to restrict SP-C mobility and modulate its orientation.

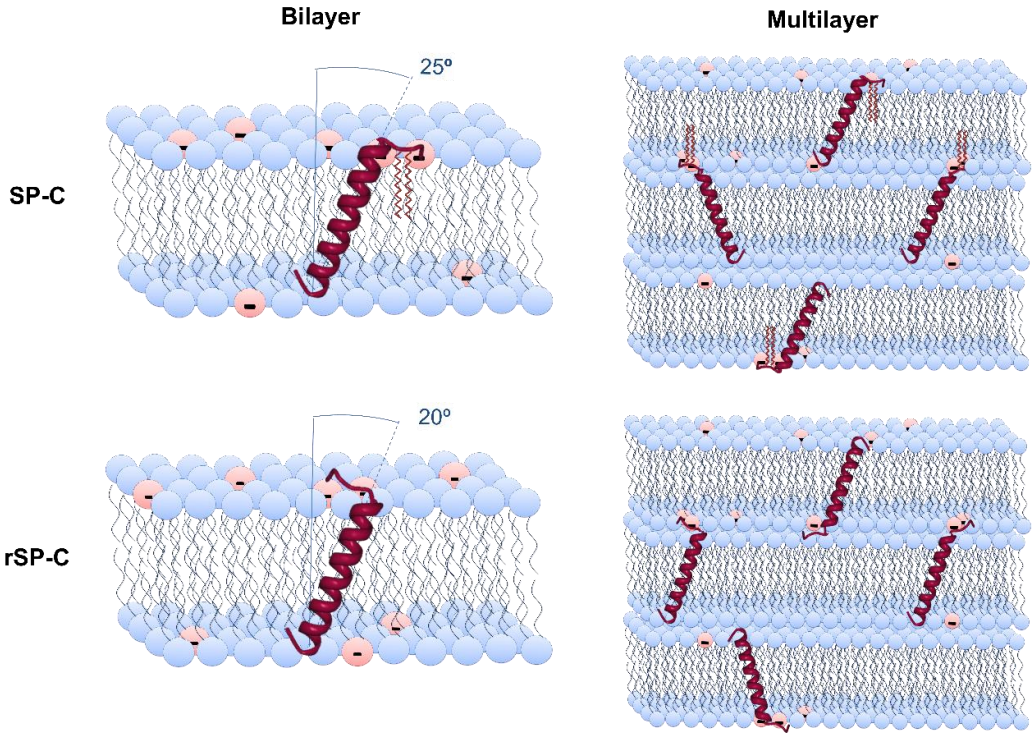

Figure 1.5. Model for the role of palmitoylation of SP-C and the presence of anionic phospholipids in lipid bilayers and multilayers.

Finally, one has to consider the particular context imposed by the insertion of the protein into the partly dehydrated multilayer phospholipid films studied here. The cartoon in Fig. 1.5 presents a model illustrating how selective protein-lipid interactions and differential tilting could define the configuration of SP-C in single membrane and in multilayer membrane arrangements. That configuration could be relevant for the efficient generation of the surface-associated surfactant reservoir, in which palmitoylation-promoted intermembrane contacts might facilitate re-spreading of surfactant membranes during inspiration.

As a whole, the results obtained in this chapter allow to delimit the effects of protein palmitoylation to the membrane polar region, barely affecting lipid hydrophobic core as noticed by acyl chain motion over a range of temperatures. Palmitoylation has also been shown to be important to maintain a close association of SP-C N-terminal segment with the membrane, affecting protein tilting and polarity. Our results suggest that, together with SP-C palmitoylation, lipid composition is involved in modulating SP-C orientation in bilayers, promoting certain configurations that could be related to defined surfactant structures optimized for an efficient interfacial activity.

5. Results

Chapter 2

Cholesterol distribution in the lung surfactant system: a role for SP-C

Most of the experiments included in the present chapter were performed during a short-term stay (EMBO; ASTF 241-2014) in the Laboratory of Lipid and Membrane Biochemistry (Biochemistry, Faculty of Science and Engineering, Åbo Akademi University, Turku, Finland) assisted and supervised by Prof. Peter Slotte and PhD. Thomas Nyhom. Cryo-TEM samples were obtained and imaged in the Electron Microscopy Facility (EMF) at the Biological Research Center (CIB-CSIC, Madrid). The results of this study were published in the article:

Roldan, N; Nyholm, T.K.; Slotte, P.; Pérez-Gil, J; García-Álvarez, B. "**Effect of Lung Surfactant Protein SP-C and SP-C-Promoted Membrane Fragmentation on Cholesterol Dynamics**" Biophysical Journal 111 (2016), 1703–1713. Doi: 10.1016/j.bpj.2016.09.016.

Introduction

Cholesterol is a controversial molecule in the context of lung surfactant function. Although its presence in surfactant complexes has been extensively demonstrated, little is known about its origin or regulation (129, 227). Cholesterol defines the complex lateral structure of surfactant membranes and monolayers, including the segregation into ordered (L_o) and disordered (L_d) fluid phases (23). This was confirmed by cholesterol depletion experiments, which revealed a markedly different phase segregation upon cholesterol removal by the solubilizing agent methyl-β-cyclodextrin (mβCD) (23). Proteins SP-B and SP-C do not appear to contribute to lateral phase segregation (23) but rather to the formation of highly cohesive multilayer assemblies (228); whereas cholesterol has been shown to be essential especially at the edge of physiological temperatures (23, 227).

From a functional point of view, the incorporation of cholesterol above a certain threshold has been reported to be deleterious for the proper surface activity of clinical surfactant preparations (199), and abnormally high cholesterol levels are associated to surfactant dysfunction in some respiratory disorders (203, 229). However, it has also been shown that cholesterol improves the spreading capability of model surfactant lipids (116) and as mentioned before, cholesterol is critical to maintain surfactant lateral structure especially at physiological temperatures (23). These contradictory findings suggest that the role of cholesterol is subtly related to the architecture and properties of lung surfactant at the air-water interface, and that it could critically depend on the presence of other surfactant components and/or structures as assembled in native complexes.

To sustain the presence of cholesterol in surfactant without functional impairment, protein SP-C has been suggested as an essential element (120, 121). Besides, SP-C has been shown to modulate cholesterol miscibility in surfactant-mimicking membranes (120), whereas protein configuration in bilayers is affected by the presence of cholesterol in a way that suggests it is not merely an consequence of the general effects derived from cholesterol incorporation into lipid bilayers (122). SP-C might therefore be an important factor regarding cholesterol modulation in the surfactant context, although the molecular mechanisms connecting SP-C and cholesterol remain unclear.

The aim of the work presented in this chapter was to obtain further information about the role of the hydrophobic surfactant proteins, and particularly SP-C, in cholesterol distribution in surfactant membranes. With that purpose, a recently developed fluorescent sterol-partitioning assay was employed (230). With this technique, the partitioning of a fluorescent analogue of cholesterol (cholesta-5,7,9(11)-trien-3-β-ol, CTL) between membranes and a solubilizing agent, such as cyclodextrin, can be followed by measuring the anisotropy of the fluorophore. These measurements yield the determination of a partition coefficient, K_x, which indicates the affinity of the sterol for a given membrane. Thus, using the CTL partitioning assay, model and native surfactant membranes were assessed to detect whether the proteins SP-C and/or SP-B are involved in regulating cholesterol distribution in the surfactant context.

Results

CTL partitioning between mβCD and Lung Surfactant-derived Membranes

As an indirect measurement of CTL distribution in lung surfactant membranes, we measured CTL affinity for lung surfactant-derived membranes using large unilamellar vesicles (LUVs) made of the most physiologically relevant lipid mixtures. The organic extract (OE) of surfactant constituted the most representative surfactant sample, since it contained all the hydrophobic components of surfactant in their native proportion. These components were first separated into protein (Prot), phospholipid (PL) and neutral lipid fraction (N) and later recombined for testing by the CTL partitioning assay. In this assay, the concentration of CTL can be calculated from its anisotropy for each sample (see Materials and Methods). Those values are plotted against the concentration of mβCD, allowing the determination of the partitioning coefficient into membranes, K_x, as observed in Fig. 2.1.

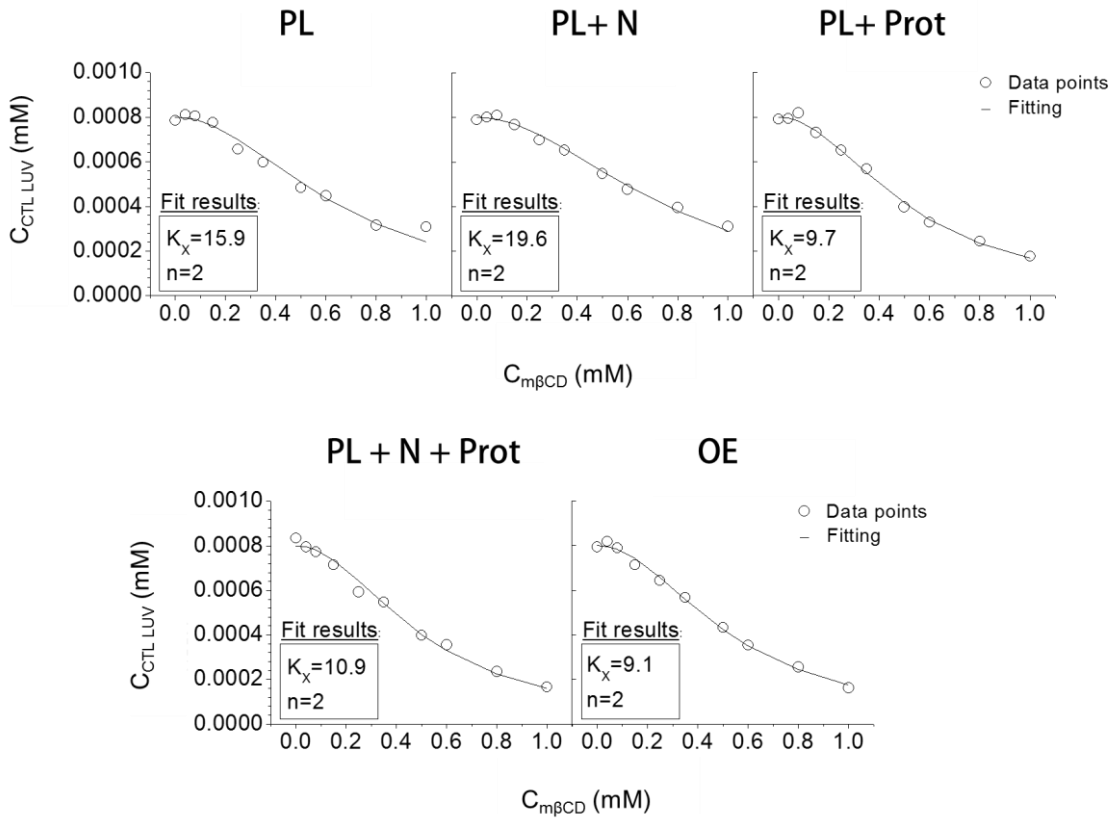

Figure 2.1. Representative fittings of calculated CTL concentrations for surfactant-derived membranes to equation (2) allows the calculation of K_x (see Materials and Methods). Experimental data points are represented by empty circles and the fitting, by a solid line.

Fig. 2.2a shows CTL anisotropy for each combination as a function of the concentration of mβCD, and Fig.5.2b, the corresponding partitioning coefficient K_x. Higher anisotropy values indicate less motion for CTL, meaning it is in a more rigid environment, whereas higher K_x values indicate higher affinity of CTL for that particular membrane. For no mβCD and every mβCD concentration

added, the anisotropy achieved in the presence of the hydrophobic surfactant proteins (PL+Prot) was below the anisotropy reached for samples containing only surfactant phospholipids (PL). This tendency was maintained when the neutral lipid fraction was added (PL+Prot+N versus PL+N). Lastly, the organic extract (OE) behaved similarly to those samples containing all the components of surfactant (PL+Prot+N) as expected. Thus, the anisotropy data suggest an alteration on CTL distribution to a more fluid environment (lower anisotropy) depending on the presence of the proteins.

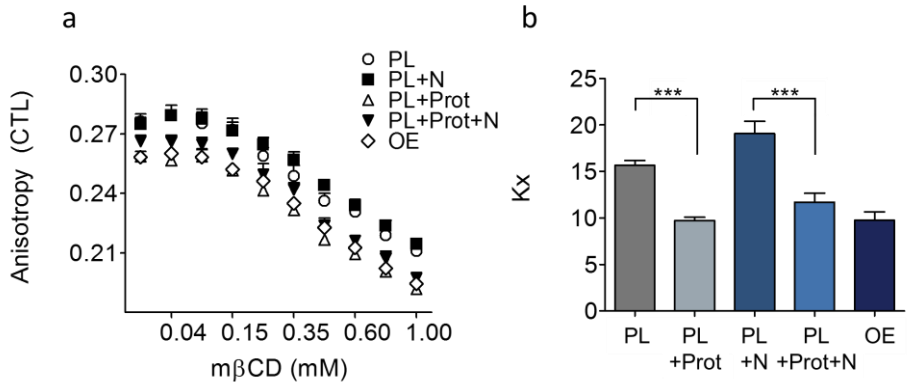

Figure 2.2. CTL anisotropy and partitioning into lung surfactant-derived membranes incorporating surfactant phospholipids (PL) to which either surfactant neutral lipid fraction (PL+N), protein fraction (PL+Prot) or both (PL+Prot+N) was added. OE represents the organic extract of native lung surfactant membranes. (a) CTL anisotropy is shown as a function of mβCD concentration at 37°C. (b) The partition coefficients are computed from the CTL anisotropy values for each lung surfactant combination. Average ± s.d. of n=3, *p < 0.05, **p < 0.01, ***p <0.001.

A significant decrease in K_x values was also observed in the presence of the proteins (PL+Prot versus PL and PL+Prot+N versus PL+N), suggesting that the proteins increase cholesterol susceptibility to be removed from the membrane by mβCD (Fig. 2.2b).

From these results, it is clear that in the presence of surfactant proteins, CTL acquires increased motion and a decreased affinity for lung surfactant-derived membranes. SP-B and SP-C have been widely reported to perturb lipid membranes (85, 231, 232), and their effect on cholesterol-induced membrane phases has been also assessed (23, 233). The effect we observed could be explained by an indirect consequence of the membrane perturbation induced by SP-B and SP-C, or by a direct alteration of the sterol partitioning mediated by the proteins.

Regarding the effect of the neutral lipid fraction, slightly higher anisotropy values were found when it was included in the vesicle composition (PL+N versus PL) even in the presence of the proteins (PL+Prot+N versus PL+Prot), especially for mβCD concentrations beyond 0.15 mM (Fig 5.2a). This is reflected by the observed increase in K_x for samples including the neutral lipid fraction (PL+N versus PL) (Fig. 2.2b). As can be deduced from the graph in Fig. 2.1a, the same thing occurred when K_x was calculated in the presence of the proteins (PL+Prot+N versus

PL+Prot). It is important to note that CTL and cholesterol compete for mβCD, and that could be the reason for these apparently higher K_x values.

Cholesterol apparently partitions into ordered domains in lung surfactant membranes at physiological temperatures (23). We assumed that CTL partitions analogously as cholesterol in different lipid environments within the membrane given previous evidence (234, 235), although its lateral distribution is difficult to predict in these complex membranes. To better picture the effect of proteins or cholesterol (N) addition to each lipid system regarding CTL motions, we analyzed CTL anisotropy in the absence of cyclodextrin (Fig. 2.3a). Again, our results indicate that the effect of the proteins is to increase CTL motion, as detected by the decrease in anisotropy (PL+Prot vs PL, Fig 5.3a), which could be accomplished by favoring CTL distribution to a more fluid environment. The addition of neutral lipids (PL+N) did not significantly change the apparent anisotropy of CTL in the pure lipid system (PL), as seen from the anisotropy data (Fig. 2.3). This could be interpreted as indicating that CTL environment was not disturbed by solely cholesterol addition. In membranes perturbed by the action of SP-B and SP-C (PL+Prot), the presence of cholesterol partially counteracted the decrease on CTL anisotropy induced by the proteins (PL+Prot+N). A possible explanation for this could be a cholesterol-induced membrane reorganization, which could modify proteins' density and distribution. In this sense, the motion of CTL would be more restricted, as indicated by its higher anisotropy.

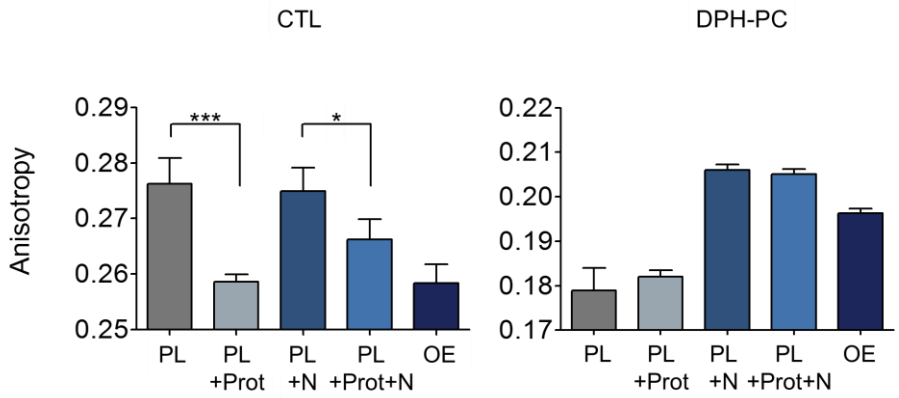

Figure 2.3. CTL and DPH-PC anisotropy in LS-derived membranes. Anisotropy measurements are shown for CTL (left panel) and DPH-PC (right panel) in membranes prepared from each indicated combination of LS fractions including LS organic extract, in the absence of mβCD, and measured at 37°C. Average ± s.d. of n=3, *p < 0.05, **p < 0.01, ***p <0.001.

To determine whether the effect on CTL anisotropy was mediated directly by the proteins, the anisotropy of another fluorescent lipid probe, DPH-PC, was measured in the same samples. The measurements were conducted at 37°C, a temperature at the end of native surfactant phase transition (23, 236), where surfactant membranes are extremely dynamic. DPH-PC partitions preferentially into liquid-disordered phases (237), where both SP-B and SP-C are also preferentially located, while CTL would be likely distributed into Lo domains. It is expected that a non-selective perturbation of the membrane by the proteins would affect both probes in a similar magnitude, and therefore, the changes observed for CTL anisotropy could be mirrored by the effects on DPH-PC. Fig. 2.3 compares the anisotropy of DPH-PC with that of CTL in the

same samples. We observed that there were no significant differences in the anisotropy of DPH-PC in lipid systems alone compared with the same combinations in the presence of the proteins (PL versus PL+Prot, PL+N versus PL+Prot+N). However, as described above, the presence of the proteins caused a significant decrease in CTL anisotropy. This supports the idea that the presence of SP-B and SP-C alters the behavior of CTL in a yet unknown specific manner. Thus, we can conclude that the combined action of SP-B and SP-C results in an increase in CTL motion and a decrease in CTL affinity for lung surfactant-derived membranes.

Effect of SP-C and SP-B on CTL distribution

Once we confirmed that the hydrophobic protein fraction could be directly responsible for the alteration in CTL motion and its affinity for lung surfactant-derived membranes, the effect of SP-C on CTL distribution became of special interest because of previous evidence connecting SP-C with the structure and activity of surfactant preparations in the presence of cholesterol (120–122). To assess the specific action of SP-C on CTL affinity for membranes, we tested 200 nm LUVs of different compositions in the absence or presence of equimolar proportions of SP-C and CTL. Fig. 2.4 summarizes the effect of SP-C on CTL anisotropy in the pure lipid system (in the absence of mβCD) and K_x for two of the lipid systems analyzed.

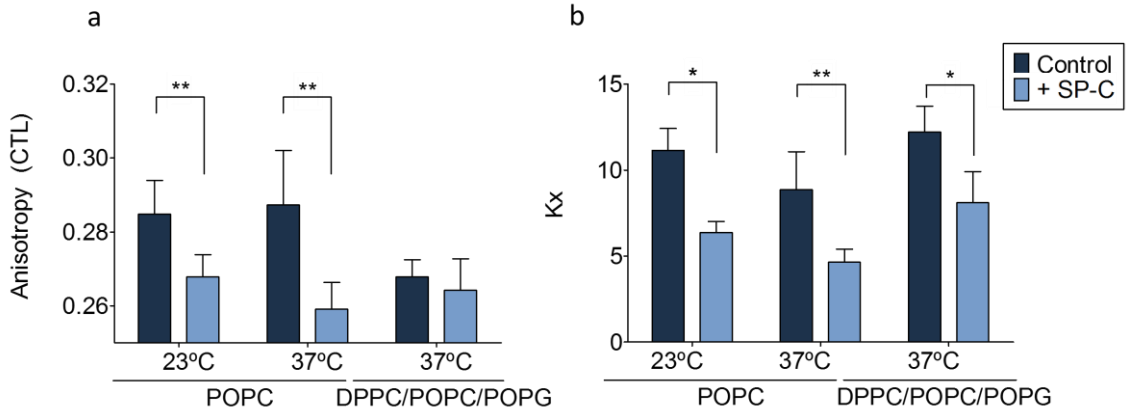

Figure 2.4. CTL anisotropy and partitioning into SP-C-containing membranes.(a) Comparison of CTL anisotropy in 200 nm vesicles made of POPC or DPPC/POPC/POPG (50:25:15 w/w/w), in the absence (control) or presence of SP-C, with no mβCD in the medium. (b) K_x calculated from the anisotropy values applied to the model explained in Methods. Average ± s.d. of n=3, *p < 0.05, **p < 0.01, ***p <0.001.

The protein caused a substantial reduction in CTL anisotropy for POPC membranes, suggesting again an increase in CTL motion. No significant differences were found for CTL anisotropy in the surfactant-mimicking mixture DPPC/POPC/POPG (50:25:15 w/w/w) in the presence of SP-C. A significant decrease in K_x for both POPC and DPPC/POPC/POPG membranes was observed, suggesting that CTL had a reduced affinity for the two types of membranes in the presence of SP-C.

It was previously reported that SP-C could cause membrane blebbing in giant unilamellar POPC vesicles (GUVs) (85). The increase in the dynamic character of those vesicles caused by the protein, with membranes showing more frequent undulations of higher amplitude, occasionally resulted in the formation of smaller liposomes. Taking into account this previous observation, we checked the size of the vesicles including SP-C by dynamic light scattering (DLS). Remarkably, the diameters obtained for the population of liposomes were greatly reduced compared to the 200 nm pore vesicles that were originally formed by extrusion (Fig. 2.5). This SP-C-induced fragmenting effect was also confirmed by cryo-electron microscopy (Cryo-EM). A high proportion of very small and highly curved vesicles was observed in the presence of the protein (Fig. 2.6a) whereas vesicles with no protein showed a size distribution centered around 130 nm, which followed the typical Gaussian distribution obtained upon vesicle extrusion (Fig. 2.6b). This effect was comparable in the two lipid systems studied.

Lipid composition	Protein	Vesicle diameter (nm)
	-	106 ± 25
POPC	**+SP-C**	24 ± 2
	+SP-B/C	83 ± 11
	-	114 ± 9
DPPC/POPC/POPG	**+SP-C**	29 ± 3
	+SP-B/C	101 ± 8
POPC PSM	**+SP-C**	27 ± 2
POPC Chol	**+SP-C**	24 ± 1

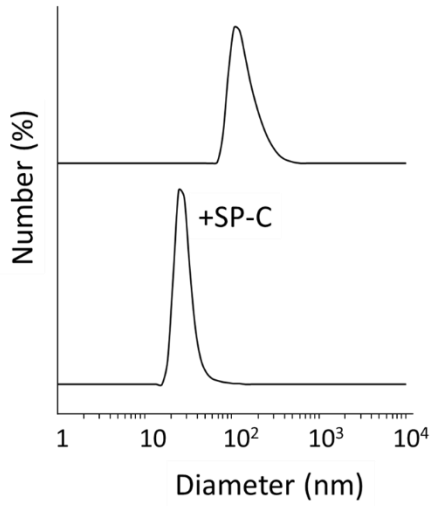

Figure 2.5. Effect of surfactant proteins on the size of lipid vesicles as measured by DLS. Right panel displays a representative DLS measurement from POPC and POPC+SP-C LUVs extruded through 200 nm pores. Left panel shows a table summarizing DLS measurements for vesicles with different compositions. Values are presented as means ± s.d. of n=3.

In an attempt to prevent the breaking effect of SP-C, we assayed stiffer membranes. Interestingly, POPC/PSM (80:20 mol/mol) vesicles showed the same fragmentation as those prepared from POPC and 30 mol% cholesterol (Fig. 2.5). These results suggest that, under the conditions tested, the high ability of SP-C to fragment large membranes into small nanovesicles is independent on the lipid composition.

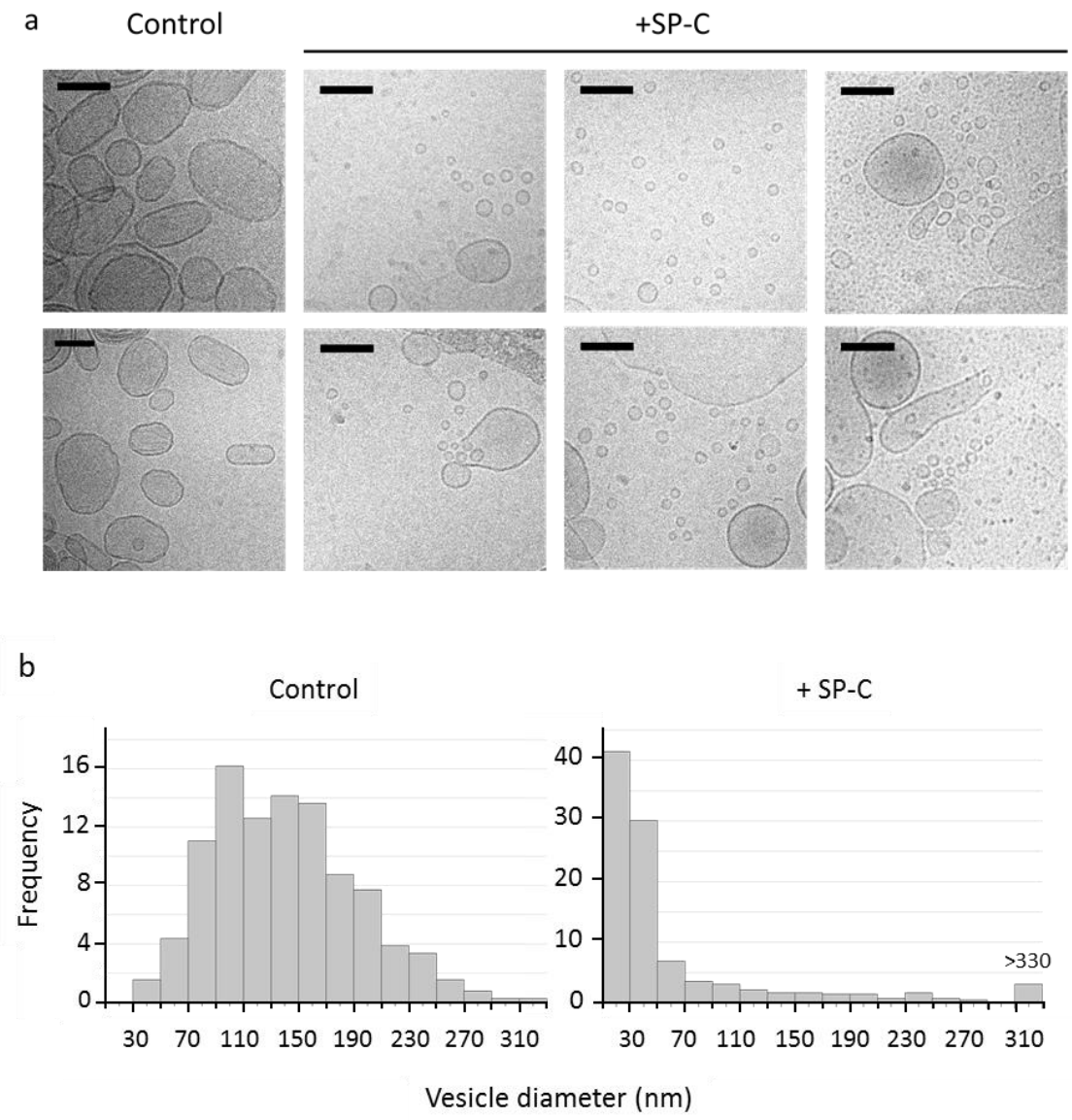

Figure 2.6. Effect of the presence of SP-C on the fragmentation of LUVs as observed by Cryo-EM. (a) Representative Cryo-EM micrographs illustrating differences in vesicle sizes in samples of LUVs reconstituted in the absence (left panels) or presence (right panels) of SP-C. Scale bars are 100nm. (b) Size distribution of vesicles obtained by quantification of the diameter of the vesicles in the absence (left panel) or presence (lower panel) of SP-C. n= 389 for pure lipid LUVs and n= 422 for SP-C-containing LUVs.

A recombinant version of SP-C lacking the two palmitic chains at the N-terminal segment was also incorporated into POPC vesicles. Preliminary results showed that this recombinant version of the protein also produced the conversion of large membranes into small vesicles (~40 nm diameter). Consequently, it seems that the fission activity of SP-C was independent of the palmitoylation state.

The effect of SP-B on membranes was different to that observed for SP-C. DLS measurements indicated an extremely high polydispersity index for the samples. For this reason, although CTL anisotropy seemed to be reduced when compared to pure POPC membranes (from 0.28 to 0.24 both at 23^{o}C and 37^{o}C in the absence of cyclodextrin), data could not be fitted to obtain a K_x

within an acceptable error caused by sample scattering. This result is consistent with previous studies that reported a fusogenic activity of SP-B (79, 238), which could generate different vesicle entities in the sample.

Lastly, we wanted to analyze the effect of the simultaneous presence of the two hydrophobic surfactant proteins, SP-B and SP-C. The hydrophobic protein fraction isolated from lung surfactant, includes the precise relative proportion SP-B/SP-C encountered in native surfactant membranes (~1:1 by weight). For this reason, samples including this fraction were assayed. The simultaneous presence of the two proteins reduced both the anisotropy and the calculated K_x (Fig. 2.7). However, the size of these vesicles was maintained at the same diameter of the extrusion membrane pores, as confirmed by DLS measurements (Fig. 2.5). This indicates that the fission/fusion activities of both proteins are canceled out when they are together.

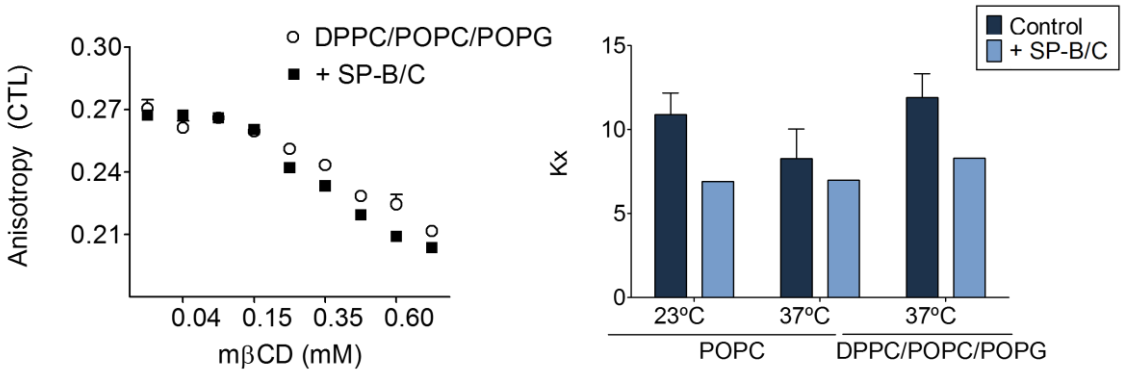

Figure 2.7. CTL anisotropy and partitioning into DPPC/POPC/POPG membranes incorporating the native fraction of surfactant hydrophobic proteins (+SP-B/C). (a) CTL anisotropy at 37ºC of vesicles made of DPPC/POPC/POPG. (b) Partition coefficients calculated for the two lipid systems at 23ºC and 37ºC. Error bars represent the standard deviation of three independent experiments.

There is evidence supporting that in highly curved vesicles, the looser packing of lipids increases cholesterol exchange from SUVs towards other SUVs or LUVs (239). Thus, it is very likely that CTL experiences a similar effect; however, the influence of membrane curvature in CTL partitioning has not been reported. Taking this into account, we cannot discard the possibility that the observed effect of SP-C on CTL partitioning could be due to the formation of highly curved membranes. For this reason, we also analyzed the influence of membrane curvature in CTL partitioning.

Effect of membrane curvature in CTL partitioning

To gain insights into how cholesterol distribution is affected by membrane curvature, we performed a CTL partitioning assay using vesicles of increasing diameters (30, 50, 100, 200 nm), and two different lipid systems. As shown in Fig. 2.8a, the lowest anisotropy values were found for the smallest vesicles. This was observed for the two lipid systems tested at the temperatures

measured. The K_x values also correlated with the anisotropy decrease for the more curved membranes (Fig. 2.8b). A more pronounced membrane curvature seemed to facilitate CTL extraction from the membrane by mβCD. This might be explained by an increase in CTL exposure to the media, which would improve its accessibility to mβCD, or by a weakening in CTL interactions with surrounding lipids, resulting in higher off-rates. Thus, it is possible that the conformational freedom of this molecule is intrinsically increased in more curved membrane environments.

Taken together, our results suggest that membrane curvature significantly alters the distribution and diffusion of CTL in model membranes. This finding could be extrapolated to cholesterol, with important physiological consequences.

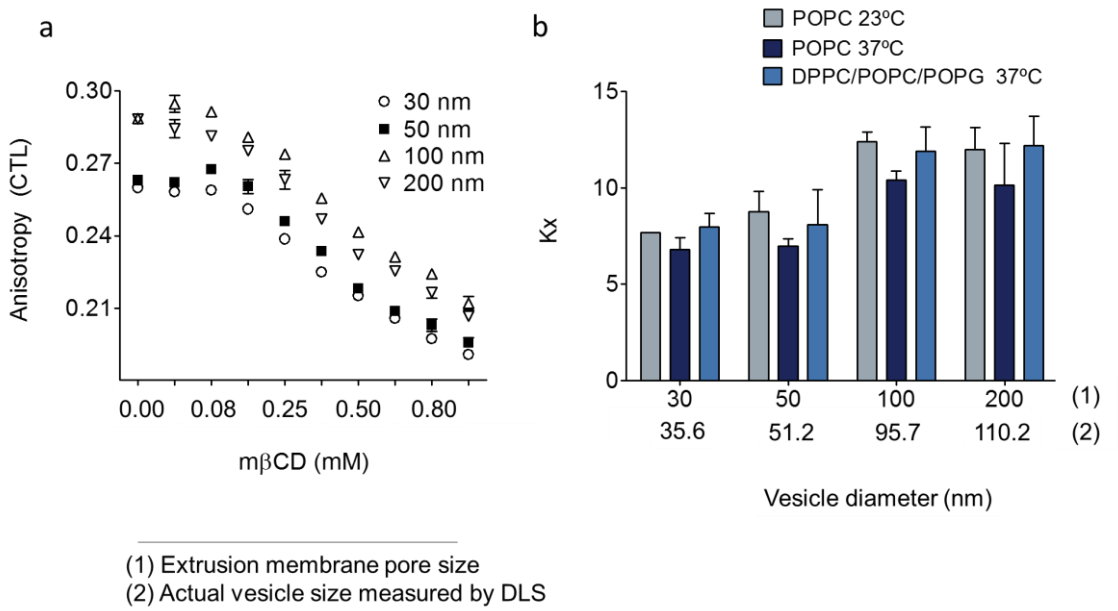

(1) Extrusion membrane pore size
(2) Actual vesicle size measured by DLS

Figure 2.8. CTL anisotropy and partition coefficient as a function of membrane curvature. (a) CTL anisotropy in POPC membrane vesicles of increasing diameters measured at 23°C. (b) Partition coefficients calculated for the two lipid systems in vesicles of different diameters. Actual vesicle size values are presented as means (n=3). Standard deviations were 5.8, 6.9, 18.4 and 29.7 respectively.

Discussion

In this chapter, we used a cholesterol fluorescent analog, CTL, to examine how the hydrophobic proteins of lung surfactant influence cholesterol distribution in membranes. According to our results, the hydrophobic proteins SP-B and SP-C increased CTL mobility in surfactant-derived membranes as detected by a decrease in anisotropy, which suggests a protein-induced change in CTL distribution toward more fluid phases. We are aware that the application of the CTL mβCD-partitioning model to membranes with phase coexistence might be controversial if CTL is segregated differently between phases. However, we think that our observation that proteins SP-B and SP-C alter mobility and partitioning of CTL is consistent because: 1) it was previously

reported that the proteins do not alter the lateral structure of surfactant membranes (23), and 2) the proteins caused a consistent reduction in anisotropy and CTL partition coefficient both in simple membrane systems and in the complex lung surfactant-derived membranes, which could exhibit marginal segregation of ordered and disordered phases.

We have observed that SP-B and SP-C are efficient in facilitating the CTL mobility within the membrane, a property that was also exhibited for other lipid probes such as spin-labelled lipids (231). The increase in motion for CTL seems to be related to lower K_x values, reflecting a higher susceptibility of CTL to be removed from the membrane. This increment in mobility could be particularly important at the interfacial film, where cholesterol has to be squeezed-out during compression for the film to reach the minimum tension required to sustain breathing (58, 59). The protein-promoted increase in CTL motion and diminished affinity for the membrane support the notion that SP-B and SP-C play a major role in modulating the dynamic properties of surfactant lipids. Given the similarities between CTL and cholesterol (234), our findings could be extrapolated to the behavior of cholesterol in the presence of the proteins.

Considering vesicle size, SP-C presence leaded to vesicle fragmentation, whereas SP-B incorporation resulted in the generation of a diverse population of vesicles with different diameters, an effect consistent with SP-B-induced membrane fusion (79, 238). However, when both proteins were included together in the native hydrophobic protein fraction, vesicle behavior differed greatly to that of each independent protein, resulting in vesicles that were stable in size. This study confirms that SP-B and SP-C have a carefully balanced combined action that can be relevant in the regulation of surfactant dynamic structure.

In the absence of any surfactant protein, we observed that in small and highly curved vesicles, CTL anisotropy was decreased and the partitioning towards cyclodextrin was favored (reduced K_x) when compared to larger vesicles. The SP-C-fragmenting effect leaded to the formation of very small and highly curved vesicles, also resulting in lower anisotropy and K_x values. These data suggests that CTL formed part of the SP-C-generated vesicles, and thus, a possible mechanism guiding the selective CTL mobilization observed here might be SP-C-induced membrane curvature.

At a molecular level, the effect of SP-C to promote surfactant membrane curvature, and ultimately membrane fission, should be related with the simple but particular structure of this lipopeptide. Here, we observed a membrane-fragmenting effect that seems to be independent of the lipid composition or palmitoylation state of SP-C.

In Chapter 1, we have observed that both palmitoylated and non-palmitoylated SP-C forms are tilted in membranes. It has also been proposed that SP-C contains a dimerization motif (212, 240, 241), and there is some evidence supporting the importance of SP-C oligomerization along intracellular pathways of SP-C sorting and trafficking (149). The dimerization of SP-C through its AxxxG motif at its C-terminal segment could generate a dimer with a conical configuration as illustrated in Fig. 2.9, which is consistent with the findings for SP-C tilting.

Transmembrane proteins with conical shape have been shown to generate membrane stress that can be relieved upon induction of curvature (242). Such a process would be consistent with our results for SP-C and the non-palmitoylated recombinant version, which share the same rigid α-helical structure supported by an unusual and highly conserved polyVal-like sequence (243). That particular rigidity might be required to force changes in membrane curvature, explaining why an α-helical protein such as SP-C is constituted by amino acids prone to generate β–sheet structures.

It was previously proposed that the N-terminal segment of SP-C is also able to promote protein-protein interactions (99, 244), which could progressively induce the accumulation of SP-C at high densities, an increase in curvature, and ultimately the segregation of small fissioned vesicles. The invariant size of small vesicles induced by SP-C in all the lipid systems assayed in this work could be a mere consequence of the geometry imposed by protein-lipid segregation. Furthermore, our results support that CTL/cholesterol formed part of these SP-C-promoted highly curved structures. This could be the basis for a selective refinement of surfactant; however, the functional or regulatory role played by SP-C in this process remains to be explored.

Here, we observed that when SP-B is present in membranes, the SP-C membrane fragmentation activity was no longer detected, at least with the same efficiency. This could be explained by differences in membrane curvature. The effects of SP-B and SP-C (fusion and budding respectively) would involve the concurrence of opposite curvatures, which would balance out in the membrane. SP-B may therefore counteract the SP-C effect, such that an increase in SP-C levels could be needed, at least locally, to achieve the same behavior as observed when no SP-B is present. Alternatively, it could be possible that a direct SP-B/SP-C interaction is required to prevent fusion/fission activities, a possibility that should be investigated.

In this study, we used an amount of SP-C that is beyond its natural abundance in surfactant. On average, SP-C represents 1 wt% of surfactant mass. However, SP-C is not distributed uniformly along the lung surfactant structure. SP-C has been shown to be located at the boundaries of liquid-ordered regions (25) and liquid-condensed phases in DPPC monolayers (105, 226), although it is also present throughout the liquid-disordered and liquid-expanded phases (23, 105). Our experimental conditions would therefore resemble what happens in membrane regions where SP-C is locally confined. In such situation, the association of several dimers could end up with the formation of highly curved structures, which might bud from the membranes or interfacial films with different consequences (Fig. 2.9). A possible trigger for this local increase in SP-C levels is the compression of the interfacial film during exhalation. In this scenario, SP-C could be transiently concentrated until it becomes excluded from the monolayer, when it would transfer either to the bilayers forming part of the surfactant reservoir or to the subphase, where small SP-C-containing vesicles would be prone to recapture by pneumocytes or macrophages. The ability of SP-C to mobilize lipids out from the compressed interfaces has been reported (105).

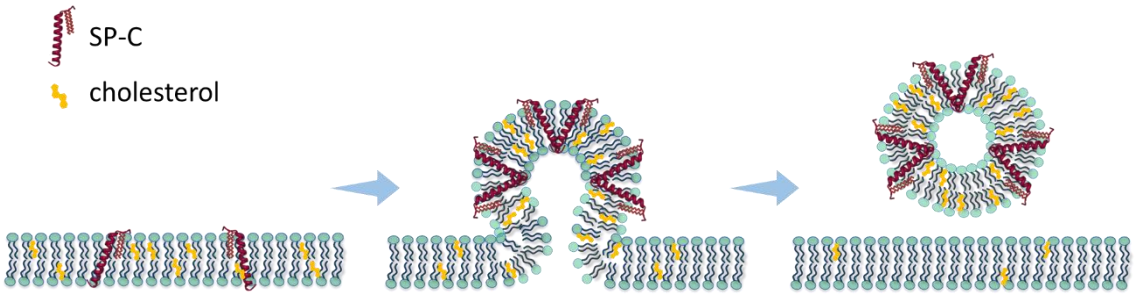

Figure 2.9. Model of the potential mechanism of membrane curvature and budding induced by SP-C in lipid bilayers.

Our results also highlight the importance of membrane curvature for CTL, and by extension, cholesterol distribution and diffusion. This has implications that go beyond the lung surfactant system, being especially relevant for membrane trafficking and mechanical events in which marked changes in curvature take place, such as those occurring during membrane fission and fusion (endo- and exocytosis), lamellipodia formation and cell migration. In this sense, membrane curvature may constitute a factor that is capable of modulating cholesterol distribution and mobilization, and consequently membrane viscoelastic behavior, with potential significance for the different mechanisms that regulate crucial cell processes.

Taken altogether, our data suggest that in the lung surfactant context, the combined action of SP-B and SP-C appears to facilitate cholesterol dynamics through protein-mediated changes in membrane curvature. Sterol partition was observed to be sensitive to the bending of bilayers, indicating that the effect of SP-C to mobilize cholesterol could be indirectly associated with SP-C-mediated membrane remodeling. Our results suggest a potential role for SP-C in generating small surfactant structures that may participate in cholesterol mobilization and pulmonary surfactant homeostasis at the alveolar interfaces.

5. Results

Chapter 3

SP-C effects on membrane structure: phase segregation and cholesterol

Most of the experiments included in the present chapter were performed in the Department of Physics and Physical Oceanography (Memorial University of Newfoundland, St. John's, Newfoundland, Canada) assisted and supervised by Prof. Michael Morrow. ESR measurements were performed in the Research Support Center (Resonance facility) at Complutense University, Madrid. The results of this study have been submitted for its publication in Biophysical Journal (2017BIOPHYSJ307428) and are currently under revision with the title:

"**Divide and conquer: Phase segregation in Lung Surfactant is modulated by Surfactant Protein SP-C and Cholesterol**"

Introduction

The role of cholesterol in lung surfactant has been addressed in previous sections. Both beneficial and impairing effects have been attributed to its presence regarding surfactant function (116, 117, 120, 121), in which SP-C appears as a modulating molecule (120, 215, 245). Cholesterol presence defines surfactant lateral structure, and as previously discussed, hydrophobic surfactant proteins have been excluded from playing a role in surfactant phase segregation (23). However, there is evidence suggesting that SP-C influences the size of ordered domains in a surfactant-mimicking model (25). This, together with the membrane structural changes attributed to the N-terminal segment of SP-C (244), the effects of SP-C on membrane permeability (84, 85) and the SP-C membrane-fragmenting behavior observed in Chapter 2, highlights the ability of this protein to cause deep membrane alterations, which likely reflect how SP-C adapts lipid assemblies in response to different physiological demands.

In the previous chapter, we have also demonstrated that the effect of SP-C on cholesterol distribution seemed to be mediated by the generation of highly curved structures, and therefore, that alterations in membrane architecture could constitute the missing link between SP-C and cholesterol in lung surfactant.

Hence, the objective of the work presented in this chapter was to analyze the combined effect of SP-C and cholesterol on a lung surfactant-mimicking system in terms of membrane structure and dynamics. The effects of SP-C palmitoylation have been also considered, given that this feature appears to be key in the SP-C/Cholesterol relationship (215). To investigate membrane structure, lipid vesicles were examined by means of two powerful techniques, ^{2}H-NMR (Deuterium Nuclear Magnetic Resonance) and ESR (Electron Spin Resonance). These two spectroscopic methods have been extensively used to evaluate SP-C effect on membranes (100, 244, 246–248), although SP-C behavior was always assessed in lipid systems with disaturated phospholipids as only constituents. For this reason, to better simulate lung surfactant composition, we have used here membranes incorporating saturated and unsaturated phospholipids, with cholesterol amounts resembling those occurring in surfactant. Independent labeling of lipids allowed the determination of direct effects of SP-C on each membrane constituent (DPPC, POPC, POPG or cholesterol) by ^{2}H-NMR, whereas average effects on membrane structure were determined by ESR.

This work provides proof of SP-C-induced alterations in membrane structure, which can be relevant to explain SP-C-related functions to sustain lung surfactant functionality at the air-liquid interface.

Results

^{2}H-NMR spectroscopy

As a lung surfactant model system, membranes of DPPC/POPC/POPG (50:25:15 w/w/w) were employed. For ^{2}H-NMR experiments, deuterated lipids were used to label three equivalent lipid systems: DPPC-d_{62}/POPC/POPG, DPPC/POPC-d_{31}/POPG and DPPC/POPC/POPG-d_{31}. Comparing observations on these systems allowed us to analyze the behavior of each component independently either in the pure lipid system or in the presence of SP-C or rSP-C and/or cholesterol.

Powder spectra obtained at 37°C from samples with different deuterated lipid components are shown in Fig. 3.1. Each deuteron contributes a doublet with prominent edges arising from molecules reorienting about symmetry axes that are perpendicular to the applied magnetic field. The splitting (Δν) of the prominent edges for a given deuteron is proportional to the orientational order parameter for that CD bond, $S_{\mathrm{CD}} = \langle 3\cos^2\theta_{\mathrm{CD}} - 1\rangle/2$, where θ_{CD} is the angle between the CD bond and the symmetry axis and the average is over motions that modulate the orientation-dependent quadrupole interaction on the time scale of the NMR experiment. Thus, for a perdeuterated phospholipid chain, the resulting spectrum is a superposition of doublets reflecting the orientational order for every position along the chain. A less restricted, more isotropic reorientation correlates with smaller splittings, as occurs for those deuterons located at the highly mobile methyl end of the acyl chain. More restricted motions, such as those of acyl chain methylene groups closer to the phospholipid polar headgroup, result in larger quadrupole splittings.

In the absence of cholesterol, spectra corresponding to pure lipid systems exhibit sharp Pake doublet features (bottom spectra in Fig. 3.1a, b and c) with splittings characteristic of perdeuterated acyl chains undergoing axially symmetric reorientation about randomly oriented lipid bilayer normals. Thus, these spectra represent multilamellar membrane suspensions in the liquid-crystalline phase. The prominent edges at about +/- 15 kHz reflect the existence of a plateau in the orientational order parameter profile of the saturated acyl chain on each deuterated lipid species (249). For DPPC-d_{62}/POPC/POPG (Fig. 3.1a), the addition of 5 wt% SP-C resulted in a relative decrease in the intensity of the Pake doublet spectral components corresponding to liquid crystalline phase bilayers. The appearance of broad spectral wings with peak intensities at ~±24 kHz, can be associated to highly ordered lipid chains undergoing reorientation that is not axially symmetric over the NMR timescale (~10^{-5} s). The superposition of spectral components corresponding to a liquid crystalline phase and a highly ordered phase for this sample, is indicative of a SP-C-induced phase separation. Spectra similar to the highly ordered phase component have been attributed to interdigitated lipid bilayers at high pressures (250–252), but the interpretation of the broad spectral component should be approached cautiously since other bilayer phases can produce a comparably high orientational order.

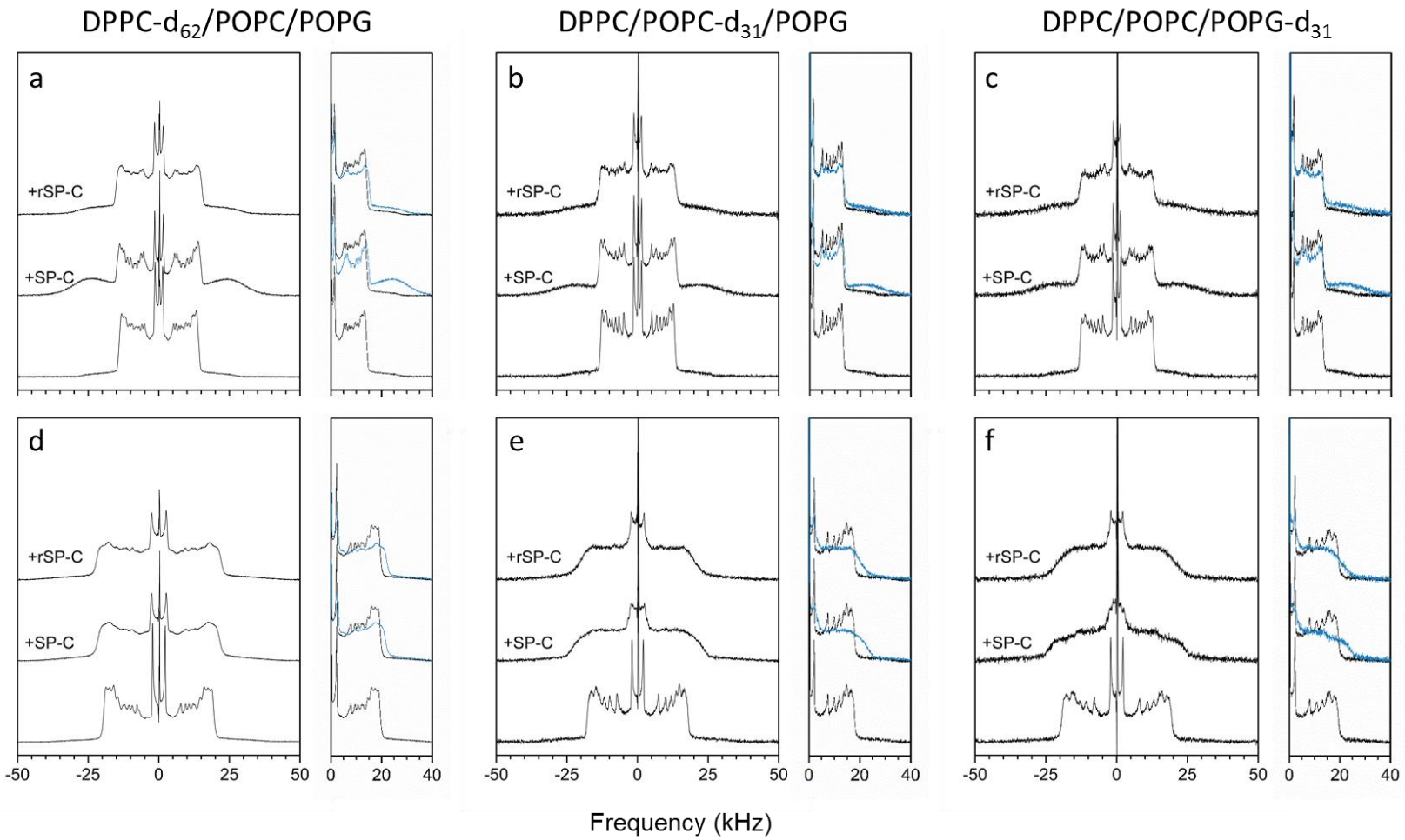

Figure 3.1. ^{2}H-NMR powder spectra measured at 37ºC for (a, d) DPPC-d_{62}/POPC/POPG, (b, e) DPPC/POPC-d_{31}/POPG and (c, f) DPPC/POPC/POPG-d_{31}. (d, e, f) correspond to samples incorporating 10 wt% cholesterol. 5 wt% SP-C and 5 wt% rSP-C addition resulted in an increase in orientational order for all the combinations tested. For simple visual comparisons, the right panel for each lipid combination represents the lipid-only spectrum (bottom), and an overlay of the lipid/SP-C (middle) and lipid/rSP-C (top) with the protein-containing spectra represented as a blue line.

DPPC-d_{62} was not the only lipid involved in the SP-C-induced ordered phase, since the analysis of POPC-d_{31} and POPG-d_{31}-containing vesicles demonstrated that these lipids were also affected by the ordering capacity of SP-C (Fig. 3.1b and c). Thus, the comparisons illustrated in Figs. 3.1a, b, and c indicated that at 37°C, the addition of SP-C to DPPC/POPC/POPG mixed lipid bilayers induced separation into a highly ordered, possibly interdigitated, phase enriched in SP-C and a liquid crystalline phase. However, the latter appeared to differ only slightly from the corresponding lipid-only DPPC/POPC/POPG phase in terms of average chain order and dynamics.

Incorporation of rSP-C also promoted the appearance of a component corresponding to highly ordered lipid in the spectra for all three deuterated lipids, but the fraction of each lipid in the highly ordered phase was smaller. However, a DPPC-d_{62} labeled lipid preparation incorporating another batch of rSP-C, showed a behavior similar to SP-C-containing samples (Fig. 3.2). SP-C palmitoylation stabilizes protein α-helical structure preventing its aggregation (157), thus, non-acylated SP-C versions are more prone to aggregate and that can result in significant differences from stock to stock in terms of protein structure. The effect observed here (Fig.6. 1a) could then be an indirect consequence of protein acylation state. A non-acylated, partially aggregated stock would result in a less effective protein, given that aggregated rSP-C could not incorporate completely into membranes. Thus, the absence of SP-C palmitoylation may not preclude the formation of a highly ordered phase, but did indirectly reduce the fraction of lipid that partitions into that ordered phase.

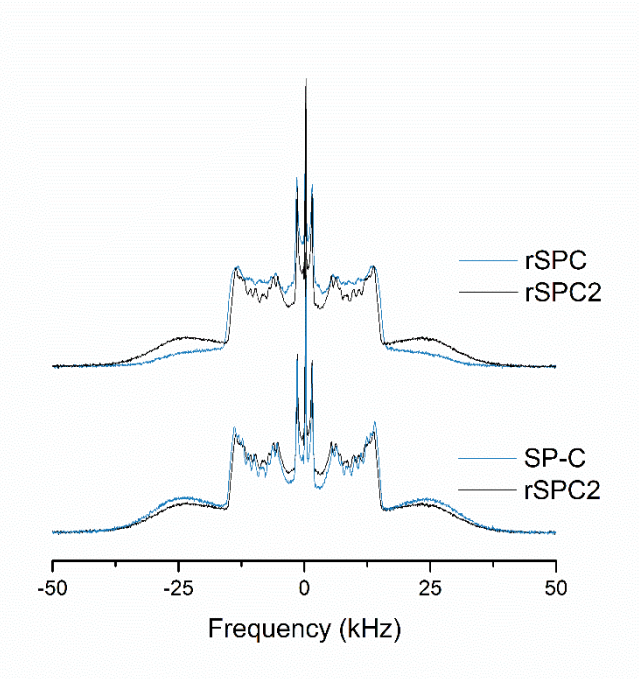

Figure 3.2. Powder spectra of DPPC-d62/POPC/POPG at 37°C incorporating different protein stocks. Top spectra represent the difference between two rSP-C batches, in particular the one presented in Fig. 3.1 (rSP-C, blue line), and an alternative one (rSP-C2, black line). Bottom spectra illustrate the similarities between the spectra containing native SP-C presented in Fig. 3.1 (SP-C, blue line) and the second batch of rSP-C tested (rSP-C2, black line).

The partitioning of deuterated lipids between different phases can be quantified; however, possible differences in quadrupole echo decay time between phases have to be considered. Using the same number of scans, unnormalized spectra registered for the lipid-only and lipid/SP-C samples both containing nominally identical amounts of DPPC-d_{62}, integrated to areas that

differed by only 4%. This suggests that quadrupole echo decay times for the two phases were similar and thus, spectral subtraction could provide an estimate of DPPC-d_{62} partitioning between the coexisting liquid crystal and highly ordered phases. For the DPPC-d_{62} spectra in Fig. 3.1a, it was found that subtracting 0.65 times the lipid-only spectrum from the lipid/SP-C spectrum eliminated most of the liquid crystalline spectral intensity from the lipid/SP-C spectrum. Even though the difference spectrum still contained some sharp features, due to slight differences in liquid crystal phase splittings between the two phases, these results suggest that about 35% of the DPPC-d_{62} was in the highly ordered phase in the lipid/SP-C sample. The same procedure was applied to samples containing POPC-d_{31} and POPG-d_{31}, indicating that 20%-25% of the POPC-d_{31} and about 25%-30% of the POPG-d_{31} in lipid/SP-C samples, partition into the highly ordered phase. Therefore, according to these estimates the SP-C-induced ordered phase would be slightly enriched in DPPC-d_{62} and POPG-d_{31}, and slightly depleted in POPC-d_{31}. When the non-palmitoylated protein was added, the partitioning of the three lipids into the small fraction of ordered phase was not as differentiated, suggesting that palmitoylation might amplify differences in the capacity of the SP-C-induced ordered phase to accommodate different lipids.

The spectra in Figs. 3.1d, e and f show that when cholesterol is incorporated into the lipid phase, the effect of SP-C on the mixture exhibited different features. Addition of 10 wt% cholesterol to the DPPC/POPC/POPG lipid mixtures resulted in an increase in quadrupole splittings for deuterons on each of the deuterated lipids (Fig. 3.1d, e, f, bottom spectra). Such cholesterol-induced ordering of lipid acyl chains is typical of the liquid-ordered phase observed in a number of lipid-cholesterol mixtures (21, 253, 254). In contrast to the situation in the absence of cholesterol, where SP-C induced the separation of a highly ordered phase from a largely unperturbed lipid phase at 37^{o}C, the effects of adding SP-C to the cholesterol-containing lipid mixtures appeared to be more subtle, possibly because of the high degree of orientational order already imposed by the presence of the sterol.

The middle spectra of Figs. 3.1d, e and f show how the combination of cholesterol and SP-C affect each lipid component in the mixture. The DPPC-d_{62} spectrum for lipid/cholesterol/SP-C (Fig. 3.1d, middle spectrum) still displays a clear vertical edge, corresponding to the orientational order parameter plateau at ~ +/- 20 kHz. This suggests that the DPPC-d_{62} acyl chain reorientation in the mixture with cholesterol and SP-C is still axially symmetric. Pake doublets corresponding to individual methylene deuterons, however, are less sharply resolved in this spectrum. This broadening indicates that the correlation time for reorientation is larger than in the absence of SP-C, and is approaching the upper threshold for fast motions on the ^{2}H-NMR timescale. In the spectra for POPC-d_{31} and POPG-d_{31} for the corresponding mixtures (middle spectra in Figs. 3.1e and f), methylene doublets are unresolved.

The loss of resolution in the POPC-d_{31} and POPG-d_{31} spectra for the lipid/cholesterol/SP-C mixtures could reflect two situations, either acyl chain reorientation is too slow to be axially symmetric on the ^{2}H- NMR time scale, or an intermediate rate exchange between domains with slightly different acyl chain order occurred (21). In the POPG-d_{31} spectrum for this mixture (Fig.

3.1.f, middle spectrum), there is a small spectral edge with a splitting similar to the one observed for the plateau in the corresponding lipid-only spectrum (bottom spectrum of Fig. 3.1e), and evidence of a narrower methyl doublet. At 30°C, the POPC-d_{31} spectrum for the lipid/cholesterol/SP-C mixture is a superposition of two components, indicating separation into a more ordered and a liquid crystalline phase (Fig. 3.3 a, b). For the corresponding mixture containing DPPC-d_{62}, however, the spectrum at 30°C (Fig. 3.3c) shows no evidence of phase separation and is characteristic of reorientation that is not axially symmetric on the ^{2}H NMR timescale.

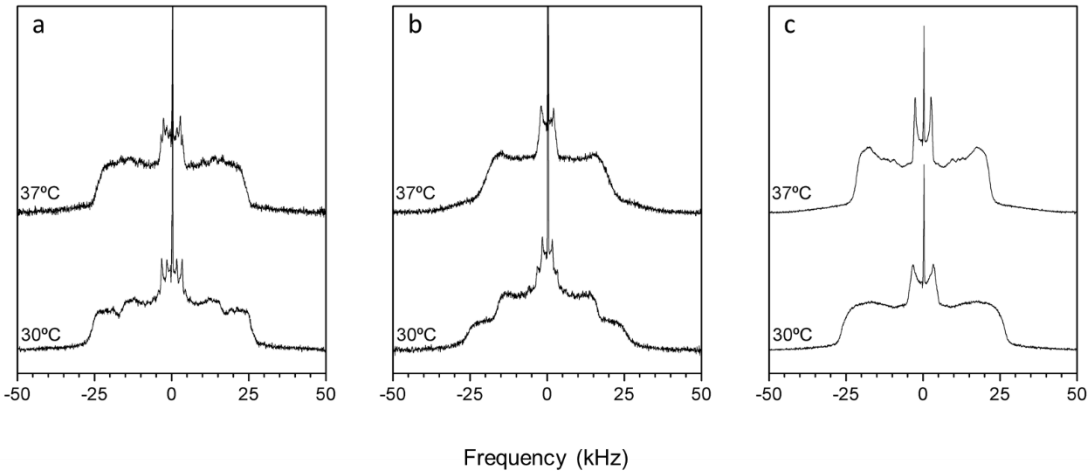

Figure 3.3. (a, b) ^{2}H-NMR spectra of multilamellar vesicles made of DPPC/POPC-d_{31}/POPG + 10 wt% Cholesterol and 5 wt% SP-C. Each panel represents an independent experiment performed with a newly prepared sample incorporating different stocks of SP-C. Spectra at 30°C are characteristic of a two-component phase segregation that is not observed in the same manner in spectra at 37°C. Differences found between replicates are likely due to slight different cholesterol concentrations found between the lipid batches used to prepare these samples. (c) Powder spectra of DPPC-d_{62}/POPC/POPG incorporating 10 wt% cholesterol and 5 wt% SP-C at 30°C. The spectra show lipid reorientations too slow to be axially symmetric on the experiment timescale. No phase separation is observed. This sample was prepared with different lipid stocks compared to the one presented in Fig. 3.1a.

The spectra shown in Figs. 3.1d, e and f suggest that in DPPC/POPC/POPG (50:25:15 w/w/w) mixtures containing 10 wt% cholesterol, addition of 5 wt% SP-C affects the dynamics of all three lipid components but not necessarily in the same ways. In order to gain more insight into the dynamics of bilayer components in the lipid/cholesterol/SP-C bilayers, ^{2}H-NMR spectra were obtained from a series of bilayer mixtures containing cholesterol-d_6. Fig. 3.4a shows the structure of cholesterol including the deuteron locations. The bottom spectrum of Fig. 3.4b is obtained from DPPC/POPC/POPG (50:25:15 w/w/w) containing 10 wt% cholesterol-d_6 at 37°C. By comparison with previously reported spectra for cholesterol-d_6 in DMPC membranes (255), the doublet with the largest splitting can be assigned to the deuteron on carbon 3 and to the axial deuterons on carbons 2 and 4. The doublet with a splitting of ~ +/-15 kHz can be assigned

to the equatorial deuterons on carbons 2 and 4, and the central doublet with a very small splitting, to the deuteron on carbon 6 (Fig. 3.4a).

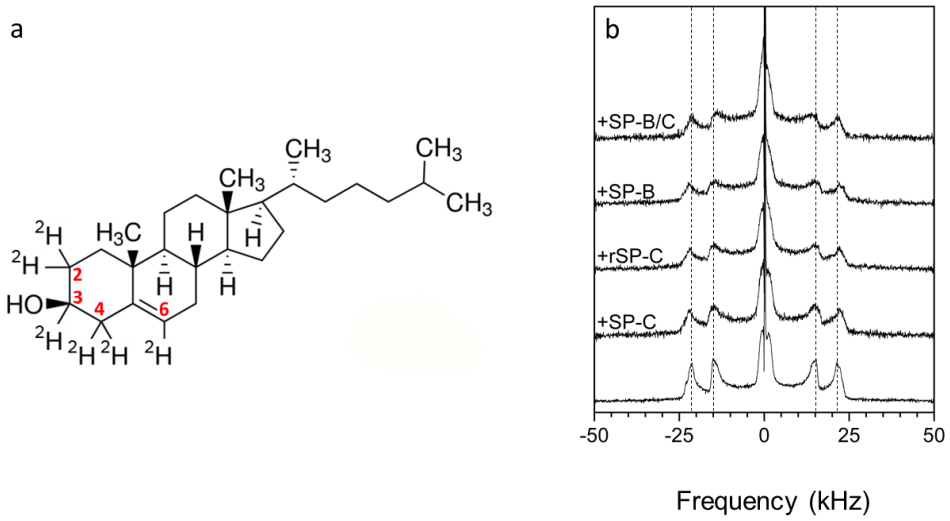

Figure 3.4. (a) Structure of Chol-d_6. Deuterated positions are numbered. (b) Powder spectra of DPPC/POPC/POPG (50:25:15 w/w/w) +10 wt% Chol-d_6 measured at 37^{o}C. The different proteins incorporated (5 wt%) did not alter the spectra substantially.

The addition of SP-C had little effect on the doublet splittings; however, it leaded to some broadening of the lineshape and an overall reduction in area of the unnormalized spectrum by about a half. This appeared as a decrease in the signal-to-noise ratio of the normalized spectra shown in Fig. 3.4. Addition of rSP-C, SP-B, or the hydrophobic protein fraction of native lung surfactant, SP-B/SP-C, had a similar effect on the cholesterol-d_6 spectrum. Comparison of the lipid/cholesterol-d_6 and lipid/cholesterol-d_6/protein spectra indicated that the orientational order of the rigid portion of cholesterol-d_6 was not affected by the addition of SP-C or any of the proteins. The insensitivity of the observed splittings to the addition of SP-C suggests that the observed line broadening and loss of intensity cannot be due to intermediate rate exchange between environments in which the deuterons have different splittings. It would thus appear that the addition of SP-C to the lipid/cholesterol-d_6 mixture resulted in an increase in the correlation time for reorientation of the rigid portion of the cholesterol-d_6.

ESR spectroscopy

To confirm our results on SP-C-induced increase in lipid order, we performed ESR experiments using the lipid system previously mentioned. Spin-labelled lipids can be incorporated into lipid bilayers in a low proportion without perturbing membrane behavior. Besides, different positions along the acyl chain and the phospholipid headgroup can be labeled, and thus it is possible to obtain information on the dynamics and conformational order of lipids at different levels within the membrane. Measurements were carried out at different temperatures and two different amounts of SP-C were tested, 5 wt% and 10 wt%.

Two spin-probes, 12PSCL and 5PCSL, were incorporated in multilamellar vesicles of DPPC/POPC/POPG 50:25:15 (w/w/w). Results for 12PCSL-containing samples are shown in Fig. 3.5a . 12PCSL is labelled in n12 position, and therefore represents acyl chain mobility close to the hydrophobic core of the membrane. The increase in temperature resulted in line narrowing correlating with an increase in membrane fluidity. Samples incorporating SP-C showed broader spectra when compared with the lipid-alone one, especially above 25°C. Greater differences were observed in the range from 30-37°C, where the pure lipid exhibited a spectrum characteristic of a more fluid character than the SP-C-associated ones. The two amounts of SP-C tested generated very similar spectra, although 10 wt% protein restricted lipid motion to a slightly higher extent. This is reflected in an increased outer hyperfine splitting, $2A_{max}$, which was significantly higher for samples incorporating SP-C (Fig. 3.5b).

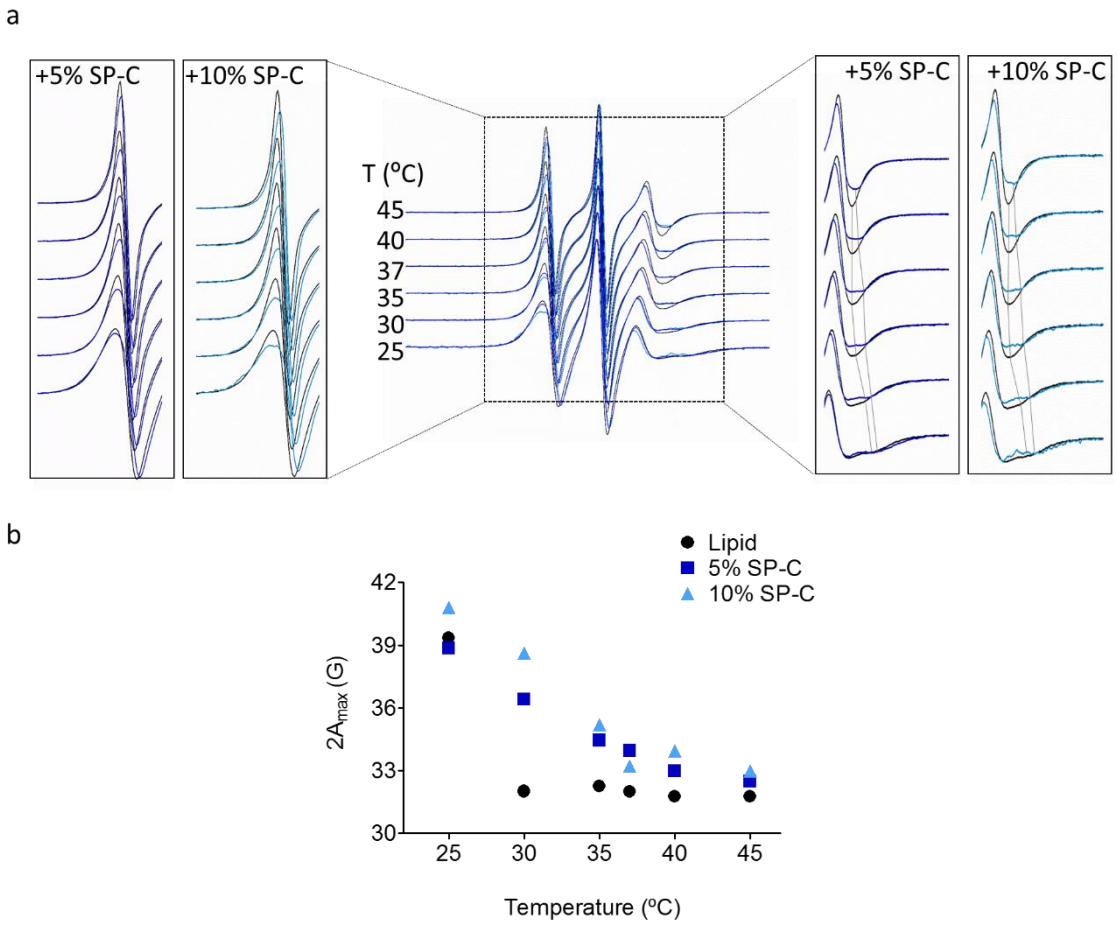

Figure 3.5. (a) ESR spectra of DPPC/POPC/POPG membranes incorporating no protein (dotted line), 5 wt% (dark blue line) or 10 wt% SP-C (light blue line) labelled with 1 mol% of the probe 12PSCL at different temperatures. The spectra to the left and right correspond to magnifications showing a detailed view of the low and high-field spectra for membranes containing no protein (black line), and samples containing either 5 wt% SP-C or 10 wt% SP-C (dark and light blue lines respectively). In the right panels, lines connecting consequent minimums have been added as a visual guide. The total scan range was 100G. (b) Outer hyperfine splittings ($2A_{max}$) of 12PCSL-labeled samples containing no protein (full circles), 5 wt% SP-C (dark blue squares) or 10 wt% SP-C (light blue triangles) as a function of temperature.

However, even though SP-C induces restriction in lipid motion as observed for the "bulk" fluid phase, we cannot distinguish a second immobilized component, which is consistent with what was previously reported for this protein (231). These results are in agreement with our previously observed SP-C-induced immobilizing effect in the lipid system, and could support the proposed interdigitated structure. Furthermore, the induction of such structure would require that all positions along the acyl chain showed a restricted motion under the presence of SP-C. Our results for samples incorporating a probe positioned closer to the lipid headgroup, 5PCSL, suggest that SP-C also induced a trend towards higher splittings at this level (Fig 6.6). Taken together, these results support the SP-C-induced restriction in the average lipid motion of the lipid system studied that could be mediated by the generation of an interdigitated structure.

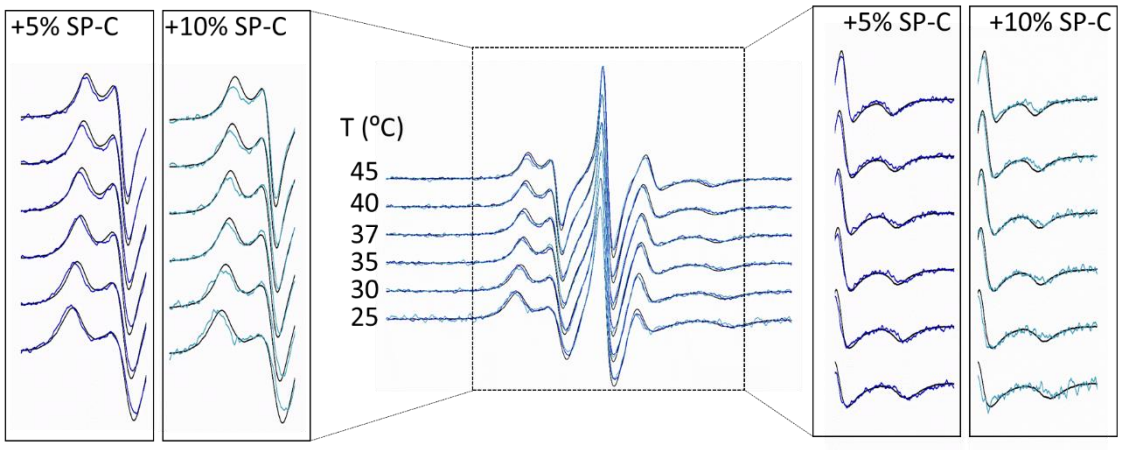

Figure 3.6. ESR spectra of DPPC/POPC/POPG vesicles incorporating no protein (black line), 5 wt% or 10 wt% SP-C (dark and light blue lines respectively) labelled with 1 mol% of the probe 5PSCL at different temperatures. Spectra to the left and right correspond to magnifications showing a detailed view of the low and high-field spectra for vesicles with no protein (black line), and samples containing either 5 wt% SP-C or 10 wt% SP-C (dark and light blue lines respectively). The total scan range was 100G.

Discussion

As in previous chapters, in this work lung surfactant-mimicking membranes comprising the most representative lipid components of surfactant, DPPC/POPC/POPG (50:25:15 w/w/w) were studied. According to our results, SP-C is able to induce lateral phase segregation in the absence of cholesterol in that lipid environment. Such phase segregation occurred at near-physiological conditions (37ºC, pH 7) and resulted in an immobilized lipid fraction involving the three phospholipids analyzed here. These results agree with those of other works, in which the generation of lipid nanodomains (25) or even immobilized lipid phases (244) have been observed upon addition of SP-C or SP-C N-terminal peptides, stressing SP-C efficiency to alter lipid packing.

Similar studies, though, reported little effect of SP-C observed on other lipid assemblies. This can be explained by differences in the lipid composition, since ^{2}H-NMR and ESR studies of SP-C

have been classically approached employing membranes made of disaturated phospholipids (100, 244, 246–248), given that DPPC is the major surfactant lipid. However, under some circumstances, even in those environments SP-C has proven to increment lipid order substantially, resulting in the appearance of ordered striated domains (256) or immobilized phases (244). In these studies, effects associated with hydrophobic mismatch or SP-C/lipid electrostatic interactions have to be taken into account, which highlights the importance of providing a native-like lipid environment for SP-C to fulfil membrane rearrangements. The lipid system employed in this chapter incorporates an additional level of membrane complexity compared to the previous works, resembling more closely the native protein environment.

In our experimental approach, the liquid crystalline phase observed in lipid/SP-C spectra (Fig. 3.1a, b and c, middle) remained essentially unaltered compared to the lipid-only system, suggesting that either SP-C was concentrated in the ordered regions or its presence in the fluid regions caused no effect. SP-C could be locally concentrated through the establishment of protein-protein interactions (212, 240, 241), such as those occurring in protein dimerization. SP-C dimers could precede a larger extent of oligomerization or clustering, a possibility already suggested as the cause of SP-C-induced packing defects or pores in membranes (84, 85). We propose a model in which an increased protein density in localized regions of the membrane could amplify the extent of those interactions, triggering the lateral segregation observed in our experiments (Fig. 3.7). This is supported by previous evidence showing SP-C confined localization, either at the boundaries of ordered/disordered domains in bilayers or condensed/expanded regions in monolayers (25–27). However, it must be noted that SP-C partitioning amongst domains cannot be directly deduced from the results shown in this chapter.

In the absence of cholesterol, the SP-C-induced ordered phase exhibited spectral features consistent with interdigitated structures (250–252). Nevertheless, as previously mentioned, we cannot discard other lipid organizations that could result in spectra of similar characteristics. ESR experiments showed an average decrease in lipid mobility at levels close to the phospholipid headgroup (5PCSL, Fig. 3.6) but also at the hydrophobic core of the membrane (12PCSL, Fig. 3.5), supporting an SP-C-induced ordering effect that could be also related to an interdigitated phase, an activity previously attributed to the SP-C N-terminal segment (244). ESR spectra, though, do not show any features characteristic of a strongly immobilized lipid phase, in agreement with a previous study (231). It must be considered that upon phase separation, spin probes can partition unevenly among domains providing only partial information on the system. The probes used in our approach were PC-based nitroxide-labeled molecules and consequently, their behavior and partitioning might be more similar to that of POPC, a lipid that although was more ordered upon SP-C presence, seems to be the least SP-C-influenced one according to ^{2}H-NMR results.

In DPPC/POPC/POPG membranes, we have observed that the SP-C-induced ordered phase was slightly enriched in DPPC and POPG, and partially depleted in POPC. In the ordered phase, the stronger accommodation of POPG-d_{31} relative to POPC-d_{31} may reflect a balance between an

electrostatically favored compatibility with the positively charged SP-C-rich phase, and the mechanical mismatch between unsaturated chains and the SP-C-induced ordered environment. Thus, in line with ^{2}H-NMR results, SP-C creates packing defects promoting phase segregation, which might facilitate the sorting of unsaturated phospholipids out of DPPC-enriched regions as proposed in the model in Fig. 3.7. Given that DPPC can be packed more tightly than unsaturated lipids, this could be relevant for reaching low surface tensions during exhalation. Another possible implication of the potential SP-C-induced interdigitated phase would be promoting the generation of curved structures. The interdigitated phase could then represent a possible intermediate state between the interfacial monolayer and the underlying bilayered reservoir. This would facilitate both adsorption and re-spreading of lung surfactant material, a function already related to SP-C-induced interdigitation (244). Lipid interdigitation combines a high degree of tail ordering and a high level of hydration of the head groups, providing membrane characteristics between liquid crystalline and gel phases. Shifting that to the lung surfactant context, a potential SP-C-induced membrane-interdigitation could also generate highly condensed lipid patches to provide stability to the multilayered interfacial film.

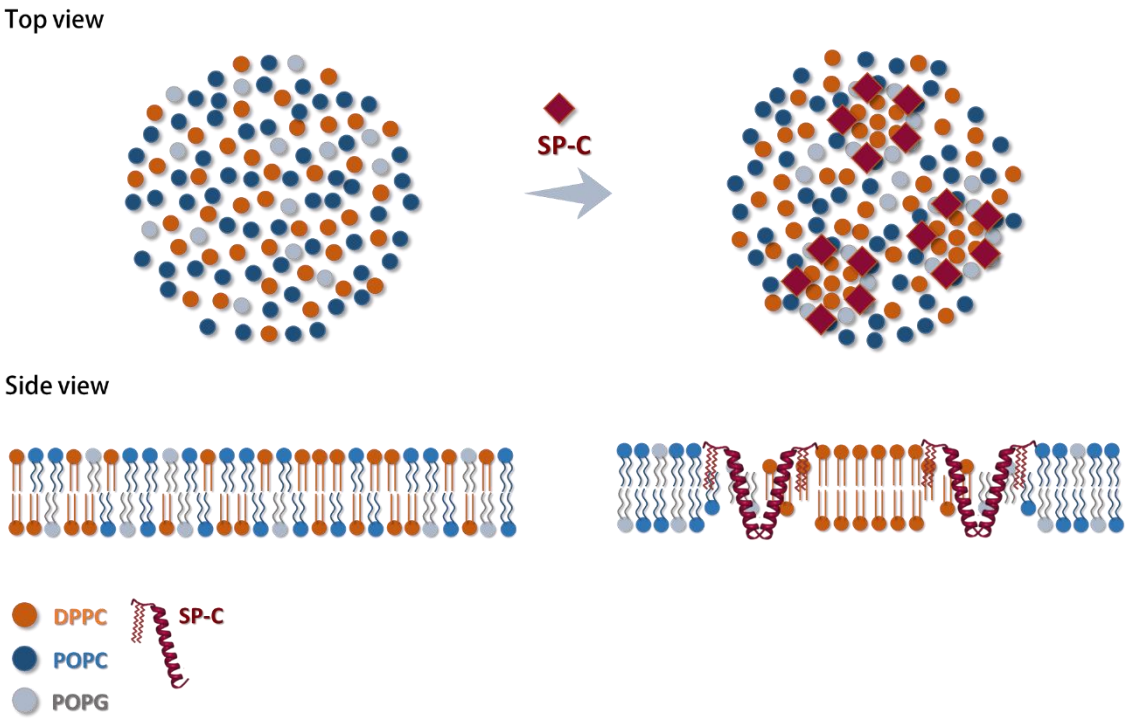

Figure 3.7. Model of the potential mechanism of SP-C-induced selective lipid interdigitation.

The molecular basis supporting SP-C-promoted interdigitation is an intriguing matter. SP-C is reported to cause changes in the polarity of the membrane through its N-terminal segment, which alters the disposition of the phosphate moiety in DPPC membranes causing a “pulling” effect towards the aqueous medium (100, 231). Additional perturbations in lipid packing include those derived from the potential SP-C oligomerizing capacity (212, 240, 241) and its tilted orientation in membranes (Chapter 1). Therefore, SP-C could nucleate packing defects that could

be relieved upon the adoption of a new lipid configuration, possibly representing the first steps towards protein-promoted interdigitation.

Regarding the effects of protein acylation, SP-C palmitoylation seemed to enhance the extent of lipid perturbations. Conversely, non-palmitoylated SP-C showed a somewhat heterogeneous behavior depending on protein batches, some of them equaling the effects of the palmitoylated protein (Fig. 3.2). This highlights the importance of protein acylation in stabilizing protein structure and accordingly, protein functionality. Palmitoylation of SP-C N-terminal peptides appeared to be determinant for promoting the membrane-ordering effect interpreted as interdigitation (244), however, those peptides bound and disturbed phospholipid packing independently of their acylation state (99, 257). Considering that full-length SP-C anchors the N-terminal segment to the membrane through the transmembrane α-helix, acylation of the full-length protein might not be so critical compared to its importance for N-terminal peptides as already reported (25). Thus, according to our results, the main role of SP-C palmitoylation seems to be the magnification of differences between the lipids involved in SP-C-induced phase separation, suggesting that a non-palmitoylated protein could be less effective in sorting out lipids properly.

To provide further insight into the cholesterol/SP-C relationship, the combined effect of SP-C and cholesterol on membranes mimicking surfactant composition was assessed. In DPPC/POPC/POPG membranes, cholesterol increased lipid order as described for many other lipid-cholesterol combinations. However, the presence of SP-C resulted in a more subtle effect when compared to the cholesterol-free system, where there was a marked phase separation into a highly immobilized phase and a liquid crystalline phase. For lipid/chol/SP-C samples, all phospholipids seemed to be more immobilized than in lipid/chol membranes, displaying slower reorientations especially in the case of POPC and POPG (Fig. 3.1e, f). Their broadened spectra were indicative of reorientations that were too slow to be axially symmetric on the ^{2}H-NMR time scale or an intermediate rate exchange between domains with slightly different chain order (21). Cholesterol was oriented along the bilayer normal in all samples with an almost unaltered motion (Fig. 3.4b). For a rigid and planar structure such as cholesterol, only motion involving the whole molecule with respect to the bilayer normal could modify its order parameter and consequently, its splittings. Different proteins were tested in an attempt to detect any protein/cholesterol specific interaction. Cholesterol deuteron splittings did not change substantially in the presence of SP-C, rSP-C or SP-B, nor when the native hydrophobic protein fraction of surfactant (SP-B+SP-C) was included, so specific perturbations on cholesterol behavior could be discarded. The presence of the proteins, though, slowed slightly cholesterol reorientation about its molecular axis, likely resulting from the overall increase in lipid order.

Even though in the presence of cholesterol no phase segregation was clearly evident at 37^{o}C for any of the preparations tested, DPPC/POPC-d_{31}/POPG exhibited phase separation at 30^{o}C when SP-C and cholesterol were combined (Fig. 3.3a, b). DPPC did not show any signs of phase separation in those conditions (Fig. 3.3c), although possible differences in membrane fluidity between systems due to deuteration could explain this difference. Nonetheless, the effects

observed here suggest that SP-C and cholesterol are subtly related in modulating membrane architecture, also responding to changes in temperature in a coordinate manner. Besides, the higher ordering induced by cholesterol/SP-C for POPC and POPG compared to DPPC, together with the phase separation observed for POPC at 30^{o}C could suggest that cholesterol might be unequally distributed, with a higher proportion being localized together with unsaturated phospholipids. Such an effect might be in line with SP-C promoting a compositional refinement in the lung surfactant system as previously proposed in Chapter 2.

Taken altogether, ^{2}H-NMR and ESR results support that SP-C restricts lipid mobility as previously reported (231, 233), both in the absence and in the presence of cholesterol. SP-C is able to induce a highly ordered, possibly interdigitated, phase, which provides some insights into how SP-C-induced membrane rearrangements could participate in processes such as lipid adsorption or DPPC enrichment at the interfacial film.

The combination of SP-C and cholesterol resulted in an increase in lipid chain order compared to cholesterol alone, suggesting that although SP-C induces an ordering effect in both cases, it also depended on the presence of the sterol. These results complement the information obtained in Chapter 2, highlighting the importance of the SP-C/cholesterol relationship in modulating surfactant architecture with potential functional consequences.

5. Results

Chapter 4

Study of SP-C-lipid interactions through TLC fingerprinting

The study presented in this chapter started as a continuation of the experiments performed by Dr. Elena Lopez-Rodriguez, who developed the approach described here. Part of the experiments included in this chapter were carried out by Dr. Lopez-Rodriguez

Introduction

From all surfactant-associated proteins, SP-C is regarded as a lipopeptide because of its high hydrophobicity and its "hybrid" protein and lipid character conferred by palmitoylation. In some instances, SP-C has been considered as the most hydrophobic protein in the global proteome (258, 259). Very frequently, this protein exhibits lipid-like characteristics resulting from this extremely hydrophobic character. Because of these characteristics, as we have observed through previous chapters, SP-C establishes strong lipid-protein interactions mainly mediated by its hydrophobic α-helical transmembrane segment, although in terms of lipid selectivity, additional efforts are required to define SP-C affinity for certain type of lipids.

We have previously observed how SP-C modulates membrane structure by inducing curvature and perturbing lipid packing (Chapters 1, 2 and 3). From these results, specific lipid-protein interactions could be inferred, since DPPC and POPG, for instance, seemed to be altered by SP-C to a higher extent than POPC. Nevertheless, whether those interactions rely directly on SP-C features or they are a consequence of specific membrane structural constraints, requires further study. This makes necessary alternative approximations to assess SP-C-lipid interactions. From a lipid point of view, thin layer chromatography (TLC) emerges as a simple and fast technique to analyze lipid behavior in terms of partition between polar and non-polar phases and the resulting migration through the silica plate.

TLC is a classical procedure employed to analyze the lipid composition of a complex mixture, and has been broadly used to assess the lipid profile of different tissues (260–264) and membrane complexes such as lung surfactant (265–272). Since one of the main purposes of TLC has been phospholipid characterization, native samples of membranes or lipids have been typically subjected to organic extraction and then applied as organic solutions. Thus, water-soluble molecules such as hydrophilic proteins and polar interactions between lipids and proteins were systematically skipped.

Given the particular behavior of SP-C in membranes, in this chapter we aimed to further characterize protein-lipid interactions established in lung surfactant, particularly those concerning SP-C. In a TLC, we hypothesize that tight lipid-protein interactions might influence the running pattern of different phospholipid species, so these lipids interacting closely with proteins might be identified by altered lipid migration profiles. To identify these potential interactions, in this study native surfactant membranes were applied on TLC plates avoiding organic extraction procedures and thus, preserving polar interactions. To have a closer look on SP-C-specific effects, we made use of surfactant-mimicking membranes configuring different lipid systems to which SP-C might preferentially bind. The role of cholesterol was also analyzed and the possible contribution of SP-C palmitoylation was taken into account.

The results derived from this study stress the strong character of SP-C-lipid interactions and the highly hydrophobic nature of this protein, which are important characteristics to define SP-C function at the air-liquid interface. These features need to be further explored and

undoubtedly considered for the development of SP-C mimicking peptides with application in lung surfactant replacement therapy.

Results

Analysis of surfactant membranes

Lung surfactant was isolated from porcine lungs and applied as a whole aqueous suspension on a TLC plate. The developing phase employed, Chl/MeOH/water 65:25:4 v/v/v, has been classically used for resolving polar lipids such as phospholipids, which run along the plate generating differentiated bands depending on their headgroup. Molecules with a higher polarity interact strongly with the silica-plate over the organic solvent, so that their migration is delayed and appear as bands located closer to the application point (AP). In contrast, more hydrophobic and less polar molecules interact preferentially with the developing phase, being observed at the top of the plate with larger distances from the application point (larger Rfs).

To differentiate bands occurring in native surfactant (NS) potentially associated to specific lipid-protein interactions, organic extracted surfactant (OE) was applied in organic solvent for comparison. Fig. 4.1 illustrates iodine-stained lipid bands of a TLC run with native and organic extracted surfactant as well as lipid references: phosphatidylcholine (PC), phosphatidylethanolamine (PE), phosphatidylinositol (PI), phosphatidylserine (PS), sphingomyelin (SM), lysophosphatidylcholine (LPC) and cholesterol (Chol). Lipid bands did not show appreciable differences between native and organic extracted complexes, which mainly comprised PC, and less abundantly, PG, PE and neutral lipids such as cholesterol (NL). Nevertheless, given their polarity, surfactant-associated proteins presumably remained at the application point, so that strong-lipid protein interactions might retain interacting phospholipid molecules within protein bands. Organic phosphorus determination assays yielded no phospholipid detection in the application point, but interestingly, the analysis of the protein profile shed interesting results (Fig. 4.2).

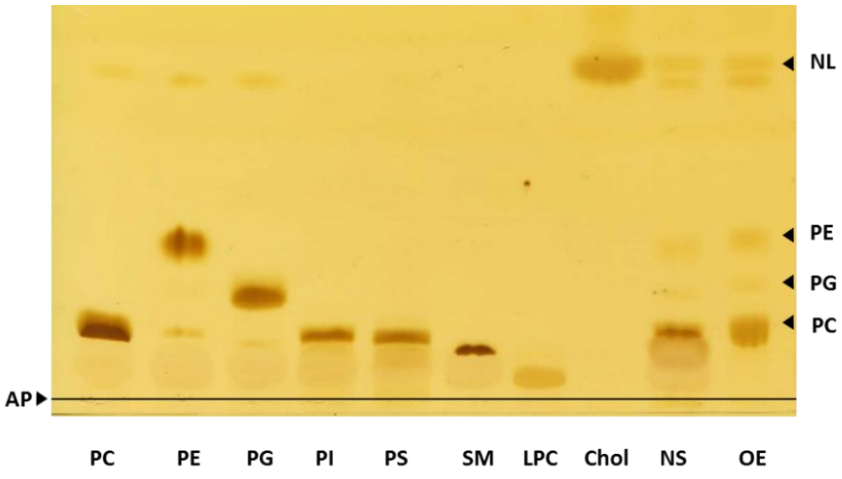

Figure 4.1. Iodine-stained TLC of surfactant complexes applied as native membranes (NS) or organic extracted (OE). Specific lipid bands can be identified by comparison with lipid references: PC, PE, PI, PS, SM, LPC and Chol, and the application point (AP) is indicated.

Specific bands were scratched out from the silica and subjected to SDS-PAGE and western blot analysis (Fig. 4.2). SP-A was exclusively found in native surfactant membranes, since the organic extraction procedure removes hydrophilic components from surfactant (Fig. 4.2). As expected, upon examination of the organic extract the only proteins observed were SP-B and SP-C as previously reported (273), which remained at the application point. Nevertheless, a parallel analysis for native surfactant membranes revealed several protein bands in the application but total absence of SP-C (Fig. 4.2a). A thorough analysis of the TLC plate revealed that, far from staying at the application point like most proteins, SP-C run along with lipids localizing close to the PC band. This particular behavior was only exhibited when membranes were applied as aqueous suspensions, and therefore when polar interactions were somehow preserved on the silica plate. The migration pattern of SP-C might be interpreted as a result of strong SP-C-lipid interactions that pull the protein within the developing organic phase. This unexpected finding suggests that this technique could be useful for the study of specific lipid-protein interactions.

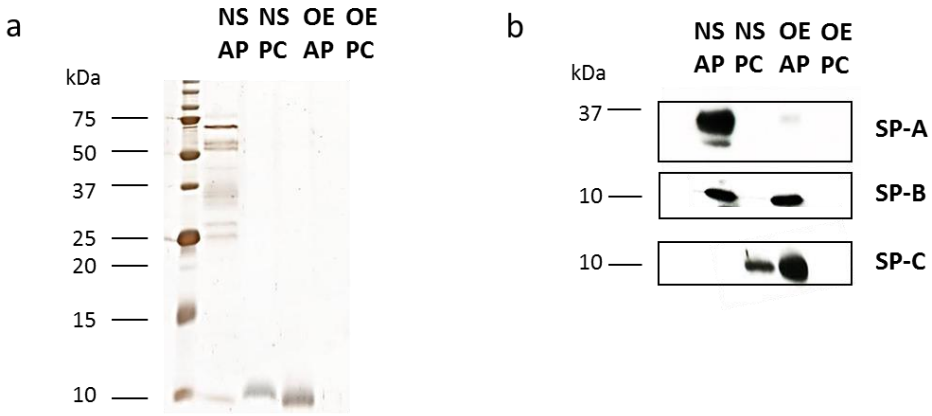

Figure 4.2. (a) Silver staining of a 13% polyacrylamide gel with the material scratched from AP (application point) and PC (phosphatidylcholine) TLC-bands from NS or OE. (b) Immunodetection of surfactant associated proteins in the different TLC regions and samples by western blot.

Effect of SP-C palmitoylation and membrane composition in SP-C-lipid interactions

Several features of SP-C structure could be crucial for the particular behavior exhibited by the protein in the TLCs. The particular sequence of SP-C and its dually palmitoylated cysteines contribute to its hydrophobic character, which together with SP-C small size (35 amino acids, 4.2 kDa), might explain why a peptide is competent to migrate in a phospholipid TLC. To test if protein acylation could be a factor worth considering, both native SP-C (palmitoylated) and recombinant SP-C (rSP-C, non-palmitoylated) were assembled into membranes of different compositions and analyzed. This experimental design allowed us to test simultaneously whether membrane composition and protein palmitoylation defined SP-C migration pattern. As observed in Fig. 4.3, iodine-stained lipid bands could be unequivocally associated to each lipid component in the different mixtures, whereas SP-C was localized in a unique fluorescent band detected by fluorescamine staining. Fluorescamine binds covalently to the amine groups present in the

protein but not to the lipid components of these samples. No differences in the protein migration pattern were observed associated to SP-C palmitoylation state nor lipid composition. It is remarkable that both SP-C and rSP-C migrated exactly to the same region, generating a band located below the one displayed by PC species (DPPC or POPC). No protein was observed in association to POPG as revealed by fluorescamine staining. Nevertheless, POPG only represented a minor portion of the membranes employed here, so that possible SP-C-POPG migrating complexes might pass unnoticed in this type of lipid samples.

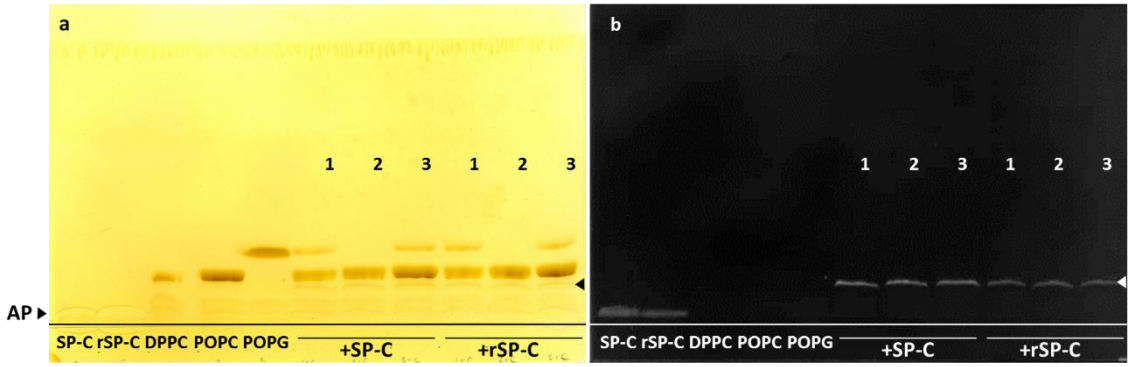

Figure 4.3. Migration pattern in a TLC of SP-C and rSP-C incorporated in membranes of different compositions. (a) Iodine staining of a TLC showing lipid bands corresponding to DPPC, POPC, POPG and a small SP-C-associated lipid band (black arrow). The application point is marked as AP. (b) Fluorescamine staining showing protein localization in the TLC plate. It is possible to observe how the protein is concentrated in the small band beneath the PC band observed in (a) (white arrow). 1,2 and 3 correspond to samples with different lipid compositions: DPPC/POPC/POPG (50:25:15 w/w/w); DPPC/POPC (50:40 w/w) and POPC/POPG (75:15 w/w).

Once observed that SP-C palmitoylation did not affect the SP-C-lipid interaction detected in TLCs, we wanted to examine whether PG could influence protein migration. Given that lung surfactant is mainly composed of PC species and a fair proportion of anionic phospholipids, mainly PG, for the next set of experiments, lipid vesicles included a higher amount of PG to detect specific PG-SP-C interactions. Membranes of pure POPG and POPC/POPG (1:1 w/w) were used as illustrated in Fig. 4.4.

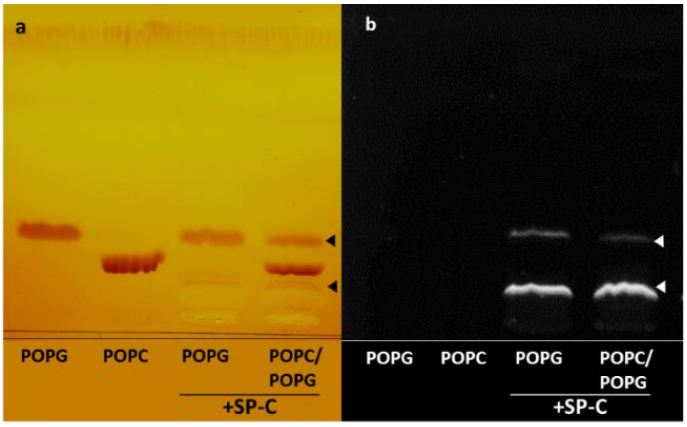

Figure 4.4. TLC of PG containing vesicles in the presence of SP-C. (a) Iodine staining showing lipid bands corresponding to POPC, POPG and SP-C-associated bands (black arrows). (b) Fluorescamine staining showing protein localization in the TLC plate (white arrows). Membrane composition was POPG and POPC/POPG (1:1 w/w).

Even in pure POPG membranes, the SP-C-associated band was positioned close to the one configured by PC, revealing that this position was protein-specific and not due to the lipid used to generate the membranes. However, in those samples, besides the PC-like band, a small fraction of the protein was pulled up with POPG, reflecting a balance between specific and non-specific interactions.

SP-C- cholesterol interaction

We have observed that SP-C behavior seemed to be independent on protein palmitoylation and depended only to some extent on lipid composition. POPG displayed a specific interaction with the protein, and thus, it seemed feasible to detect other specific SP-C-lipid interactions occurring in membranes. Due to the evidences connecting SP-C and cholesterol in lung surfactant (120, 121, 245), we extended our analysis to detect possible SP-C-cholesterol interactions. With this purpose, different membrane compositions with increasing amounts of cholesterol were used. Using this approach, if direct SP-C-cholesterol interactions are stablished, we would expect to detect SP-C associated to cholesterol bands. Membranes including POPC and POPG were assayed as observed in Fig. 4.5.

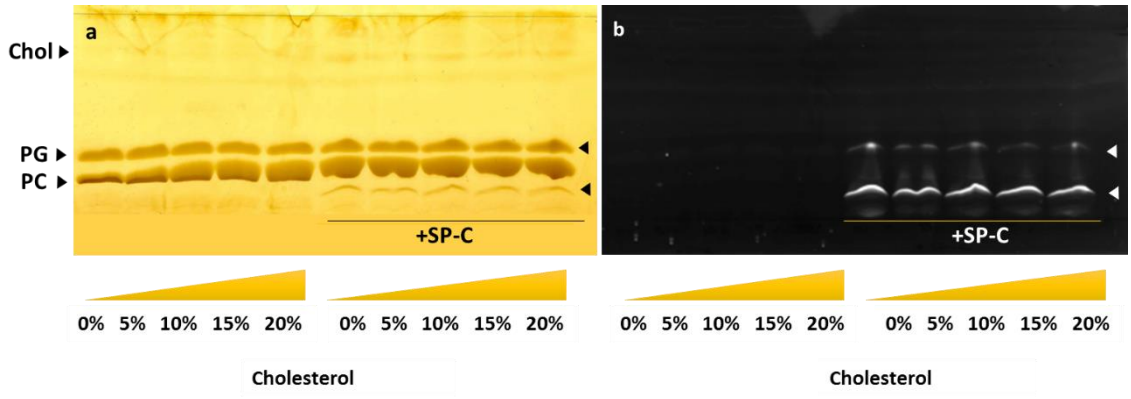

Figure 4.5. TLC of POPC/POPG (7:3 w/w) membranes containing increasing amounts of cholesterol and SP-C. (Left panel) Iodine staining showing lipid bands corresponding to POPC, POPG, cholesterol. SP-C-associated bands are marked with black arrows. (Right panel) Fluorescamine staining showing protein localization in the TLC plate (white arrows).

The results observed in Fig.4.5. show how SP-C preferentially located under the POPC band, although a slight proportion of the protein remained with POPG. Remarkably, no cholesterol-associated protein band was observed, suggesting that if an interaction exists, it is not preserved under this conditions or it is not strong enough to be revealed by the TLC protein-fingerprinting assay. It is interesting to note, however, how the narrow POPC bands become more diffuse with increasing amounts of cholesterol in the absence of SP-C. When SP-C is added though, bands are diffuse even when no cholesterol was present, and no changes in shape are observed while cholesterol amount increased. This fact could mean that not only certain lipid-protein interactions observed in membranes are preserved, but also lipid-lipid interactions such as those

exhibited between phospholipids and cholesterol. Besides, the fact that the lipid mixture behaved invariably for membranes containing SP-C with and without cholesterol, suggests that the phospholipid-SP-C interactions detected here do not seem to be affected by the presence of cholesterol.

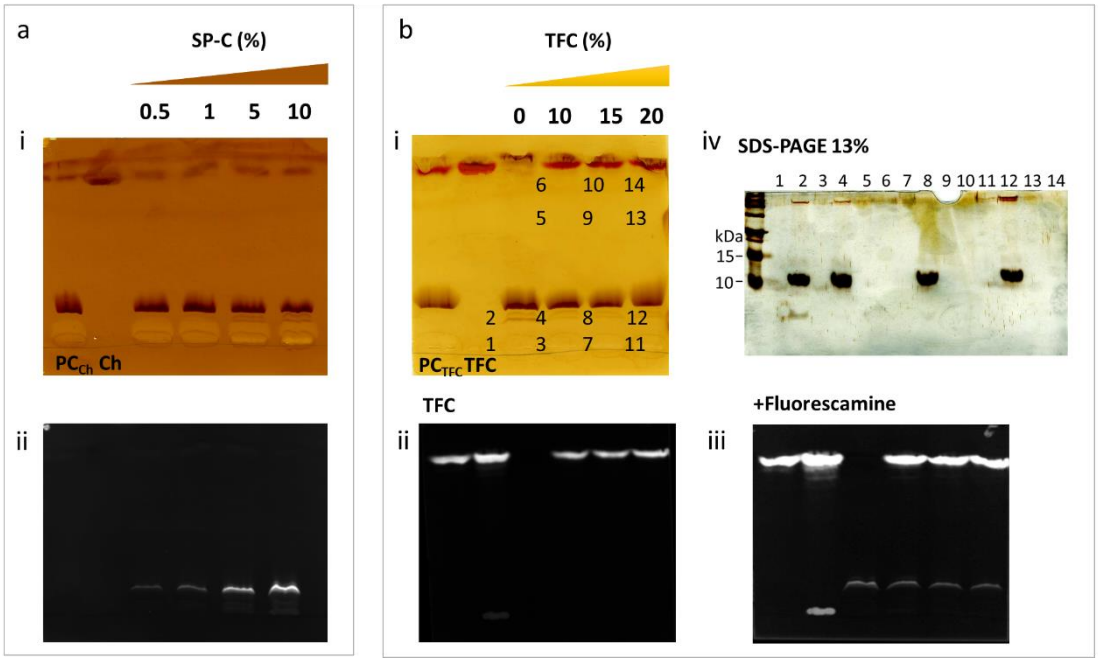

Figure 4.6. (a) (i) Iodine-stained TLC of POPC vesicles incorporating 5 wt% cholesterol and increasing amounts of SP-C. PC_{Ch} and Ch correspond to lipid references, PC-cholesterol and cholesterol respectively. (ii) Fluorescamine-stained TLC showing bands corresponding to SP-C. (b) (i) Iodine-stained TLC of POPC vesicles including 5 wt% SP-C and different amounts of TFC (TopFluor-Cholesterol). PC_{TFC} and TFC correspond to lipid references, PC-TFC and TFC respectively. (ii) Visualization of fluorescent TFC corresponding bands. After fluorescamine staining, both TFC and SP-C-containing bands are observable (iii).(iv) SDS-PAGE and silver staining from silica-scraped-bands numbered in (i).

To discard that the interaction SP-C-cholesterol was not observed by an effect of detection limit, two different approaches were used. Firstly, the proportion of SP-C was incremented to observe if some of it appeared with cholesterol in the upper TLC band. As observed in Fig. 4.6a, the SP-C-associated band increased in intensity for higher protein concentrations, whereas no protein fluorescent band was again detected associated to cholesterol. In a second approach, a cholesterol fluorescent analog, TopFluor-cholesterol (TFC), was incorporated in PC membranes containing a fixed proportion of SP-C. As illustrated in Fig. 4.6b, before fluorescamine staining, fluorescent bands correlated with the migration pattern of cholesterol, but no fluorescence was detected for lower bands that could correlate with the one associated to SP-C. In order to observe if any protein remained in bands other than the SP-C-associated one, different regions of the TLC plate were scrapped from the silica for a SDS-PAGE analysis. Silver stained bands confirmed that the protein was only present at the TLC band stained with fluorescamine, thus discarding again any SP-C-cholesterol interaction.

Finally, since no cholesterol/SP-C interaction was detected in phospholipid systems, cholesterol/SP-C particles were generated to test whether they could be solubilized when they were combined in the absence of phospholipids. The particles obtained were non-soluble in an aqueous system as observed in Fig. 4.7. Upon centrifugation, they were detected in the pellet as demonstrated by the Coomassie staining of SP-C bands subjected to SDS-PAGE (Fig. 4.7a). Interestingly, the presence of increasing amounts of cholesterol resulted in deformed bands, indicating that cholesterol run though the gel disrupting SP-C running pattern. A TLC of these insoluble particles showed that SP-C migrated again in the TLC configuring a band comparable to those observed previously as SP-C-associated bands (Fig 4.7b). Besides, increasing amounts of cholesterol were translated into more protein detected in those bands, demonstrating that in aqueous solution, SP-C and cholesterol associate generating non-soluble particles.

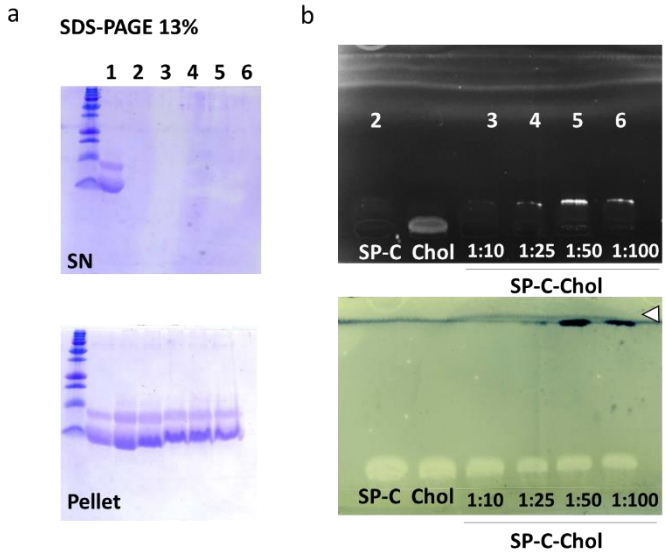

Figure 4.7. (a) 13% SDS-PAGE of Chol-SP-C samples. Numbered lanes correspond to particle composition shown in (b). Lane 1 corresponds to a SP-C reference. (b) Top panel, fluorescamine staining of a TLC of insoluble Chol-SP-C particles. SP-C and Chol references were also treated with aqueous buffer and applied. Particles contained 5 μg of SP-C and the amount of cholesterol indicated in molar proportions. Bottom panel. Phosphomolibdic acid staining of the TLC shown in top panel. Cholesterol bands are marked by a white arrow.

Discussion

SP-C is a transmembrane protein which strongly interacts with surrounding lipids modifying membrane properties. In this study, we have detected that from all SP-C-lipid interactions established in a membrane environment, some are resistant to organic solvents after being mostly depleted of water. Since the TLC developing phase is mainly composed of organic solvents (chloroform/MeOH/water 65:25:4, v/v/v), it is unlikely that intact membranes could be found, meaning that SP-C-lipid complexes in organic solvents exhibit this characteristic running pattern.

SP-C alters lipid packing and mobility restricting lipid motion, effects that have been typically associated to hydrophobic SP-C-lipid interactions mediated by the α-helix. In Chapter 3 we have detected an immobilizing effect of SP-C towards DPPC, POPC and POPG that leaded to phase segregation and could involve an interdigitated-like state. Alternatively, SP-C N-terminal segment is also known to disturb lipid bilayers even in the absence of palmitoylation (99, 244)

and at high densities, it even restricts lipid motion generating packed structures such as those involved in the interdigitated phase (244). These findings imply that in a physiological context, SP-C establishes different types of protein-lipid interactions: labile interactions with surrounding lipids that might be exchanged with other lipids in a longer length-scale, and stronger interactions that lead possibly to the tight immobilization of certain lipids (231).

In a bilayer, lipids can interact with a transmembrane protein either acting as a "hydrophobic solvent" forming rings around it (annular shell) or positioning in defined protein regions, such as those located in the middle of oligomeric structures, or protein clefts (non-annular sites) (274). Typically, lipids forming part of the annular shell are not very specific and adapt to match the protein surface. However, lipids forming part of non-annular sites exhibit a higher specificity as observed in crystallized proteins (274). Shifting this information to SP-C, we would expect that lipids interacting strongly with the protein would be the ones revealed by TLCs. According to previous evidence (231), the possibility that this protein is enclosed by an annular shell of lipids tightly interacting with it seemed unlikely. Conversely, considering the experiments shown in Chapter 3 and the confined localization of SP-C in membranes and monolayers (25, 27), specific protein-lipid interactions cannot be ruled out. According to our results though, SP-C displayed an almost invariable migrating pattern when embedded in either POPC or POPG membranes, although specific SP-C-POPG interactions were also detected. This indicates that although most of the interactions detected did not exhibit a strong specificity, this methodology could be useful to discriminate those less populated specific cases. This is consistent with previous results (231), which suggested that SP-C interacts with lipids in a very dynamic way, promoting fast and continuous lipid exchange.

To understand SP-C/lipid interactions, it is necessary to consider SP-C amino acid composition and sequence. SP-C α-helix contains mainly Val, Leu and Ile, non-polar residues that preferentially interact with the hydrocarbon chains of phospholipids fatty acids. SP-C α-helical segment is well embedded in the lipid bilayer leaving unpaired charged residues (Arg and Lys) located close to the polar lipid headgroup. These amino acids are extremely conserved and required for the proper processing and trafficking of SP-C precursor (146, 150). Their long and flexible non-polar side chains keep them buried in the hydrophobic core of the membrane, whereas their charged groups lead to the "snorkeling" effect on the membrane surface (275, 276). These groups could then be involved in hydrogen bonding to a phosphate and/or ester oxygen of the phospholipid molecule, or establish electrostatic interactions with the negatively charged phosphatidyl glycerol. However, for all those interactions to occur, a polar environment is required. Interestingly, the C-terminal end of SP-C is nearly depleted of polar groups, in which only the C-terminal carboxyl could be charged depending on its protonation state. Upon protonation, the C-terminal end of SP-C could easily dive into the hydrophobic core of the membrane. Therefore, it seems that the sequence and structure of SP-C could be particularly well suited for its function at the respiratory air-liquid interface. The hydrophobic C-terminal side of the protein can be projected towards the air while the N-terminal polar segment of SP-C

would remain anchored at the surface of the surface-active film that pulmonary surfactant establishes at the alveolar spaces.

In a TLC performed as described here, membrane suspensions are applied and left to dryness, so that original polar interactions could be preserved thanks to residual solvation molecules. However, the contact with the developing phase would disrupt those membranes and most of these polar interactions. SP-C exhibits a deep membrane-disturbing character, and we have observed how it modulates membrane structure. We propose here that those membrane regions already disturbed by SP-C could be prone to adopt lipid configurations that resist the development with organic solvent. A suitable explanation is the transient generation of inverse micelles such as the subunits of a H_{II} structure. In that way, lipid polar headgroups would keep the solvation water in the inner part of the micelle, whereas acyl chains and the hydrophobic SP-C helix could be exposed to the organic solvent from the TLC developing phase (Fig. 4.8). This would explain why protein palmitoylation does not affect SP-C migration pattern (Fig. 4.3). Thus, the interactions dominating here would be mainly those established by the α-helical region of the protein with little contribution of the N-terminal segment.

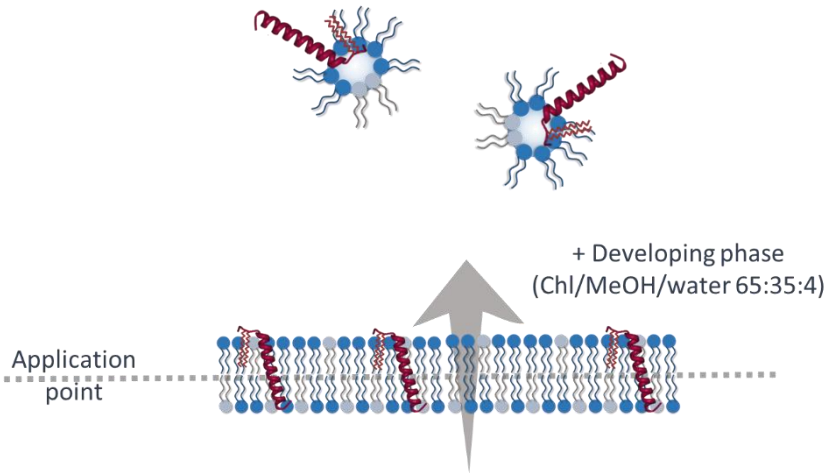

Figure 4.8. Model for SP-C-lipid complexes migrating thought the TLC plate. Membranes in the form of vesicles are deposited as aqueous solutions in the application point and air-dried. When the developing phase reaches samples, membranes are dissolved forming inverse micelles with a core of water in which the hydrophobic regions would be exposed to the organic solvent.

Regarding the SP-C/cholesterol relationship, the evidence provided by this work does not support the establishment of a direct specific interaction, in agreement with the results described in Chapters 2 and 3. The SP-C/phospholipid interaction observed here remained unaltered under the presence of cholesterol, and apparently, no SP-C-cholesterol association was detected in the TLCs. This was deduced from the experiments with increasing SP-C-content, in which no protein was detected in association with the sterol-containing band. Similarly, when the fluorescent cholesterol analog TFC was incorporated into SP-C-containing membranes, no TFC fluorescence was observed in association to SP-C. Thus, to explain how cholesterol and SP-C participate in the modulation of surfactant properties, a membrane environment seems to be

required. Whether cholesterol could interact differently with phospholipids due to the presence of SP-C or whether minor amounts (not detected by the TLC-fingerprinting assay) are present at the SP-C-associated band, needs further exploration.

Surprisingly, the preparation of Chol/SP-C particles resulted in non-soluble complexes in which cholesterol altered the apparent electrophoretic mobility of SP-C. Moreover, the application of these insoluble particles on a TLC demonstrated that SP-C was also able of migrating through the plate associated to cholesterol. However, in this case, since both components are non-soluble in water, a certain type of complex might self-associate to prevent exposure to the aqueous environment, but this does not necessary involve the establishment of specific cholesterol/SP-C interactions. This hypothetical complex could also retain some solvation molecules and develop in the TLC plate in a similar way to the one proposed here.

To conclude, the migration pattern of SP-C through a TLC seems to be a combination of SP-C properties: small size, extreme hydrophobicity and strong membrane association. All of this, together with residual solvation water coming from membrane assemblies, could promote the generation of small lipid/SP-C particles under organic solubilization, which might be the clue to understand how this protein interacts with lipids. This technique is therefore useful to identify those lipids interacting with SP-C, and thus provides a way to infer the local lipid composition in SP-C partitioning regions in surfactant membranes.

5. Results

Chapter 5

SP-C-mediated lipid endocytosis and cholesterol metabolism in alveolar macrophages

The study presented in this Chapter comprises preliminary evidence acquired during an internship at the Institute for Functional and Applied Anatomy at the Hannover Medical School, directed and supervised by Dr. Elena Lopez Rodriguez and MD. Matthias Ochs and funded by a fellowship from the Spanish Ministry of Education, Culture and Sport (EST15/00594).

Introduction

Lung surfactant synthesis and degradation are critical processes with a direct impact on lung homeostasis. Alveolar type 2 cells (AT2) play a central role in these processes, constituting the only cell type capable of producing and secreting surfactant (9, 125). These cells are also involved in surfactant uptake, recycling and degradation, and despite the fact that they have been considered as the main actor in charge of these functions, the implication of alveolar macrophages (AMφ) has been gaining relevance during the last years (135, 180, 181). The importance of AMφ in surfactant catabolism becomes especially apparent in patients of pulmonary alveolar proteinosis, a disease characterized by the accumulation of abnormally high amounts of surfactant material in the alveolar spaces due to AMφ dysfunction (179, 184). Therefore, a balanced action of AT2 cells and AMφ is crucial, in which crosstalk mechanisms might be key to maintain lung homeostasis (9).

Recent studies have linked AMφ with cholesterol degradation in surfactant, a mechanism that seems to rely on GM-CSF and PPARγ dependent genes (135, 179–181). Some of the proteins are transporters involved in cholesterol efflux, such as the ATP-binding cassette ABCA1 and ABCG1, and influx, as the LDL receptor (LDL-R), scavenger receptors as SR-AI and CD36, enzymes involved in cholesterol synthesis and metabolism, such as the hydroxymethyl-glutaryl-coenzyme A reductase (HMGCR) and the sterol 27-hydroxylase (CYP27A1), and nuclear receptors as the liver X receptors LXRα and β, which in turn regulate several other mediators and proteins (135, 180, 181). This illustrate the complexity of AMφ response to lipid uptake and degradation and definitely prove that AMφ constitute an active agent in surfactant catabolism and homeostasis. This is particularly interesting considering the controversy in the regulation of cholesterol levels in surfactant membranes and films (116, 118, 129, 137, 227, 277), which must be compositionally optimized to support breathing according to different respiratory demands. To date, the origin of surfactant cholesterol and the molecular mechanisms by which it is sensed by alveolar cells remain unknown, but current models have started to consider AMφ as a suitable switch involved in cholesterol regulatory mechanisms.

In different pulmonary diseases, such as the Hermansky-Pudlack syndrome or different forms of pulmonary fibrosis, and animal models of respiratory pathologies, AMφ develop dysfunctional phenotypes leading to the appearance of lipid, and particularly cholesterol accumulation in the so-called lipid droplets (278–280). In certain pathological conditions, due to this accumulation, these macrophages acquire an increased granularity and a peculiar shape, reason why they are also are termed lipid laden or “foamy” macrophages (281, 282). In some instances, highly ordered cytoplasmic structures have been observed (283, 284), resembling cholesterol crystals reported in atherosclerosis (282, 285). Remarkably, SP-C deficiency has also been reported to alter AMφ function and lead to lipid accumulation, and in a study, crystalline structures were also detected in AMφ cytoplasm of SP-C KO mice (111). Thus, taking into account the role of AMφ, and considering the combined effects of SP-C and cholesterol on lung surfactant structure and dynamics, we could speculate that the SP-C-cholesterol relationship could contribute to a homeostatic purpose.

In this chapter, we have assessed the possible physiological consequences of SP-C/cholesterol combinations regarding cellular surfactant homeostasis. To explore the effect of SP-C and cholesterol on lipid uptake by AMφ, a flow cytometry-based engulfment assay was performed in a murine alveolar macrophage cell line, MH-S. MH-S treated with vesicles of different composition were also analyzed by fluorescence and transmission electron microscopy and the effects of SP-C and cholesterol on lipid metabolism and transport were studied using RT-PCR.

Our results suggest that surfactant-derived vesicles containing certain SP-C/cholesterol proportions increase lipid uptake in AMφ and regulate the expression of several genes involved in lipid metabolism and transport. These results provide the first proof of the implication of SP-C in surfactant lipid engulfment depending on cholesterol, representing a possible mechanism involved in cholesterol regulation to maintain compositionally optimized lung surfactant membranes and films fully competent to sustain the respiratory function.

Results

Lipid engulfment in AMφ

Lung surfactant engulfment by MH-S cells was evaluated by means of flow cytometry. A clinical surfactant preparation (Curosurf; Chiesi Farmaceutici, Parma, IT), was labelled with a 5 wt% fluorescent cholesterol analog, TopFluorCholesterol (TFC). This surfactant preparation consists in an organic extraction of porcine lung surfactant depleted of neutral lipids and thus, cholesterol. Therefore, Curosurf comprises surfactant phospholipids and the hydrophobic surfactant proteins SP-B and SP-C in a near-physiological proportion (199). To determine the most effective times and lipid concentration for assessing effects on lipid engulfment, a time-course experiment adding different surfactant concentrations to MH-S cells was performed. Results are expressed in terms of %engulfment, defined as the percentage of positive cells for TFC fluorescence (Fig. 5.1a,b).

According to our results, lipid uptake consists in a very fast process at the temperatures assessed here (23^{o}C), resulting in lipid incorporation even at the shortest times (t<5min) (Fig. 5.1c). Regarding lipid concentration, surfactant administered above 0.5 µg /10^5 cells leaded to a saturation in the engulfment index reaching values close to 100% of positive events after 5 min of treatment. Thus, in order to detect differences based on cholesterol or SP-C concentration, 0.25 µg /10^5 cells and times ranging from 30 min to 1 hour were selected for subsequent assays. The fluorophore used for labelling lipid vesicles was a cholesterol fluorescent analog, hence, to account for cholesterol effects on lipid uptake, a validation of its possible interference with the engulfment assay was required. A fluorescent lipid molecule also detected with the FITC filters (Bodipy PC, BPC), was selected to discard any particular effects of TFC on lipid uptake. Our results suggest that no significant increment in the engulfment index was due to the use of TFC, confirming that TFC could be reliably used to analyze the effect of cholesterol on lipid engulfment by AMφ (Fig. 5.1d). Additionally, to discriminate between the engulfment of

surfactant vesicles and possible unspecific interactions that could lead to the association of labelled vesicles to the plasma membrane, experiments quenching the external cell fluorescence with Trypan Blue confirmed that fluorescence was unaltered upon quenching, confirming that the detected signal was specific to lipid engulfment.

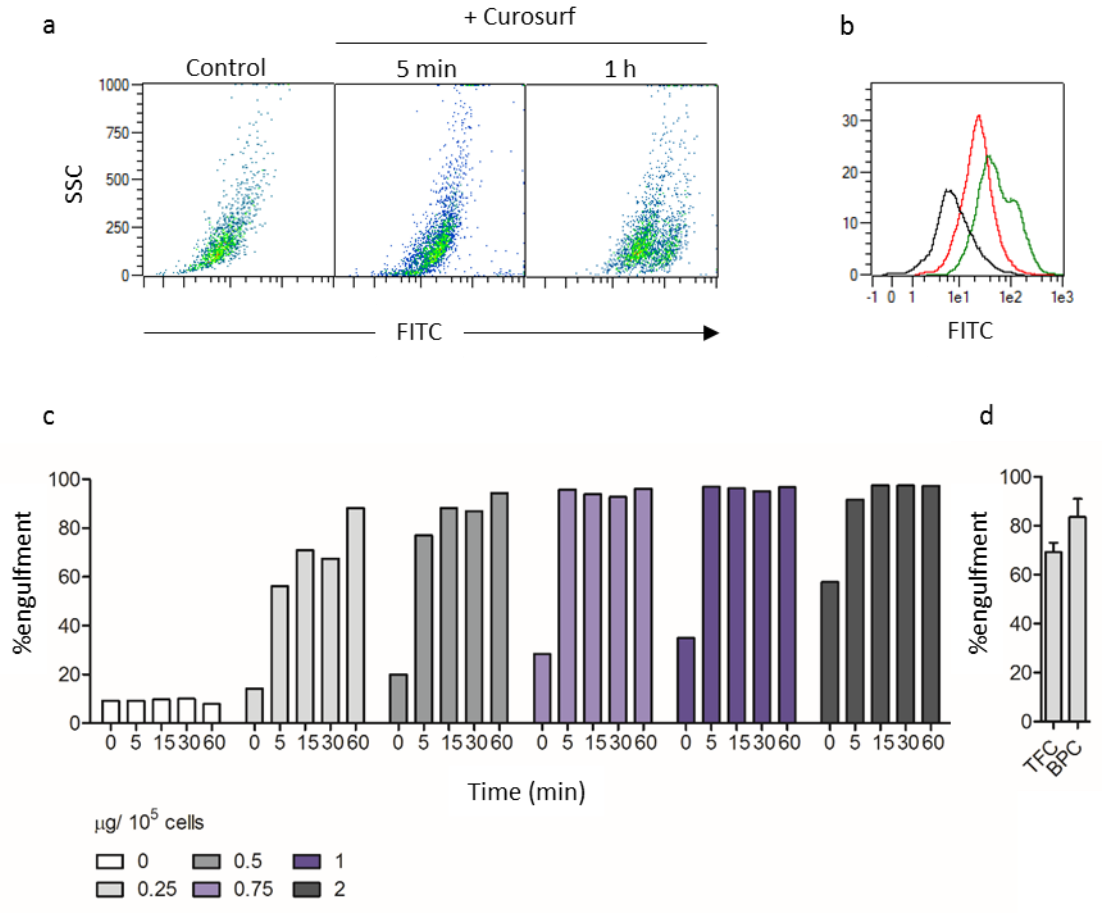

Figure 5.1. (a) Density plots illustrating cells in the FITC channel (TFC). Upon the addition of 0.25 µg /10^5 cells of Curosurf, cells incorporating the fluorescent lipids shifted towards higher fluorescence intensities increasing along time. (b) Representative histogram showing an overlay of the FITC (TFC) fluorescence intensity reached for no lipid (black), 0.25 µg /10^5 cells at 5 min (red) and 1h (green). (c) Time-course engulfment of different lung surfactant concentrations by MH-S cells. (d) Lipid engulfment assessed by BPC-labelled Curosurf. Cell viability was above 80%.

MH-S cells treated with 0.25 µg /10^5 of Curosurf for 1 hour were centrifuged and cytospin slides were stained using the Diff-Quik kit to assess cell morphology. MH-S cells remained apparently unaltered after lipid engulfment under the bright field microscope (Fig. 5.2). However, a detailed characterization by TEM resulted in the detection of cytoplasmic lipid inclusions consistent with the appearance of lipid droplets that were larger and more abundant in treated cells compared to the control.

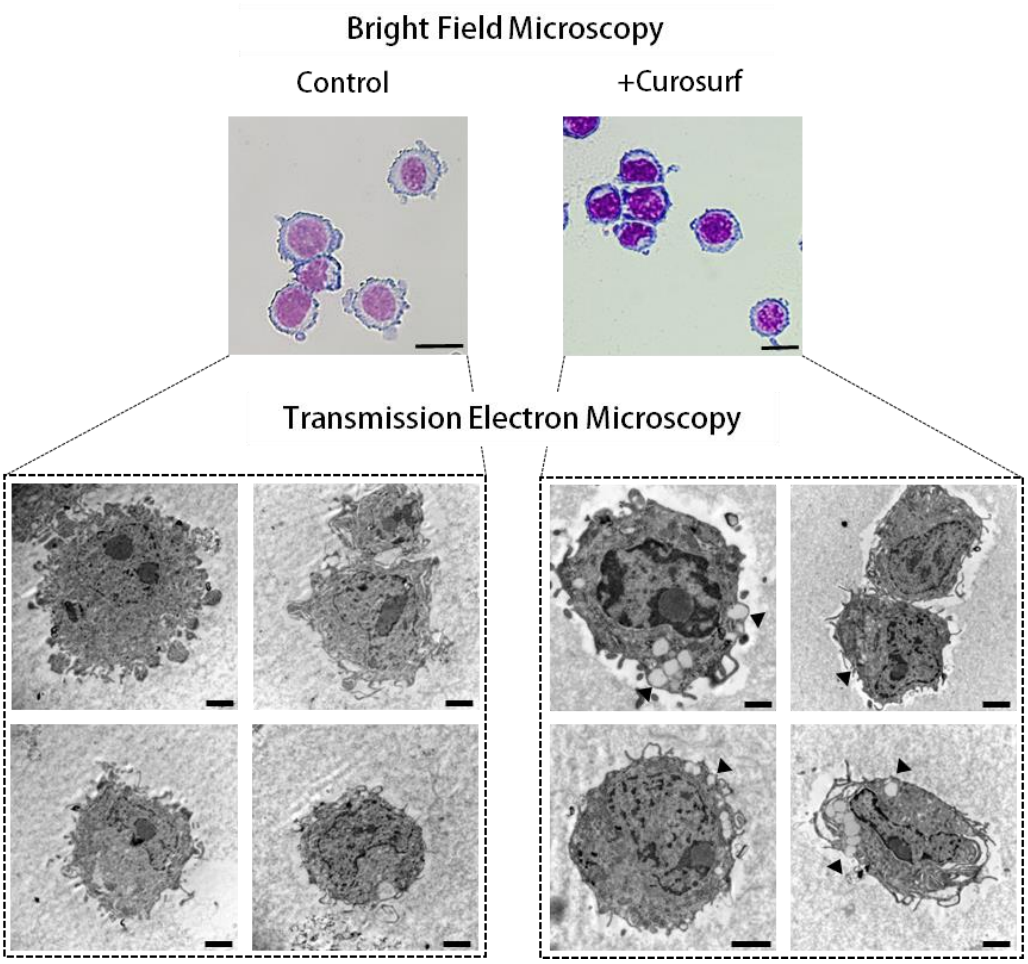

Figure 5.2. Diff-quik staining of untreated MH-S cells (top left) and treated with 0.25 µg /10^5 cells of Curosurf for 1h (top right). Scale bar=10 µm. TEM micrographs of sections from non-treated MH-S cells (left, bottom panels) and treated with Curosurf (right, bottom panels). Lipid inclusions are marked with arrows. Scale bar=2 µm.

Engulfment mechanism

Macrophages exhibit a broad capacity of endocytosis being capable of engulfing bacteria, apoptotic cells or nanoparticles by different mechanisms. Some of them are receptor-dependent, whereas others, as in the case of lipid vesicles, have been explored to less detail. To investigate the possible mechanisms ruling surfactant engulfment, inhibitors of different endocytic pathways were used and MH-S cells were treated with Curosurf (Fig. 5.3).

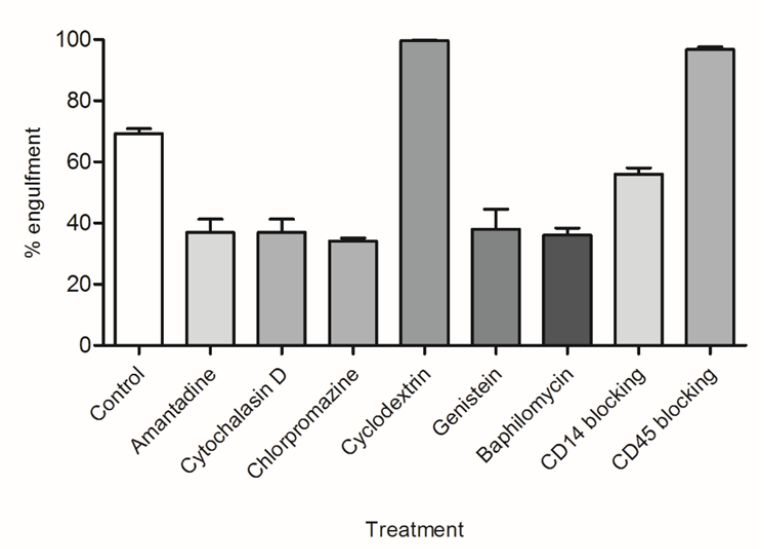

Figure 5.3. Inhibition of endocytic pathways in MH-S cells. All the inhibitors were incubated for 30 min and washed prior the engulfment assay. Cells were treated with 0.25 µg /10^5 cells TFC-labelled Curosurf for 1h. Data are presented as means ± SEM. Cell viability was above 70% for every treatment.

Most of the treatments analyzed reduced lipid engulfment to some extent in comparison to untreated control cells, which reached 70% of positive events. Amantadine (2.5 mM, (286)), cytochalasine D (2 µM, (287)) and chlorpromazine (10 µM, (288)) are considered as inhibitors of the clathrin-dependent endocytosis. Cytochalasine D disrupts actin polimerization whereas chlorpromazine avoids chlatrin coating of the endocytic vesicle. Amantadine acts at a different level, stabilizing chlatrin-coated vesicles hindering its dissociation. Despite the different acting mechanisms, all inhibitors reduce engulfment to a 30%. Cholesterol depletion caused by cyclodextrin treatment (2 mM, (289)) resulted in a surprisingly high %engulfment index, which was above the control. This could be interpreted as an increment of cell avidity for the sterol in order to replace cholesterol levels at the plasma membrane, although there is no evidence of similar results for comparable treatments in alternative cell lines. This could also be an effect not directly related to endocytosis, by which the cell could transfer directly lipids from the vesicle to the plasma membrane.

Genistein (15 µM, (287)) is a tyrosine kinase inhibitor that destabilizes the actin network avoiding the recruitment of dynamin II, which is indispensable for caveolae-mediated endocytosis. Baphylomicin (0.1 µM, (290)), however, perturbs the H^+ gradient by blocking H^+-ATPases avoiding acidification of endocytic vesicles. Both treatments leaded to an engulfment inhibition similar to those related to chlatrin-mediated endocytosis.

CD14 is a membrane receptor involved in the recognition of bacteria lipopolysaccharide (LPS) and its endocytosis. There is evidence relating SP-C with CD14, demonstrating that not only it is able to bind LPS in a competitive manner (291, 292), but also interacts with CD14 modulating LPS recognition (124). Given these observations, we analyzed whether surfactant engulfment

could be related to an SP-C/CD14 interaction. CD14 blocking with a specific antibody also reduced slightly surfactant engulfment, possibly representing a minor specific pathway.

Lastly, as negative control we blocked CD45, a membrane phosphatase expressed by macrophages with no reported implication in endocytosis. As expected, CD45 blocking did not reduce lipid endocytosis when compared with the control.

Effect of cholesterol in surfactant lipid engulfment

AMφ have been specifically related to cholesterol metabolism in the lung. Thus, to analyze whether cholesterol could play a role in lipid engulfment, Curosurf preparations were incubated with different cholesterol amounts and lipid uptake was validated in MH-S cells (Fig. 5.4).

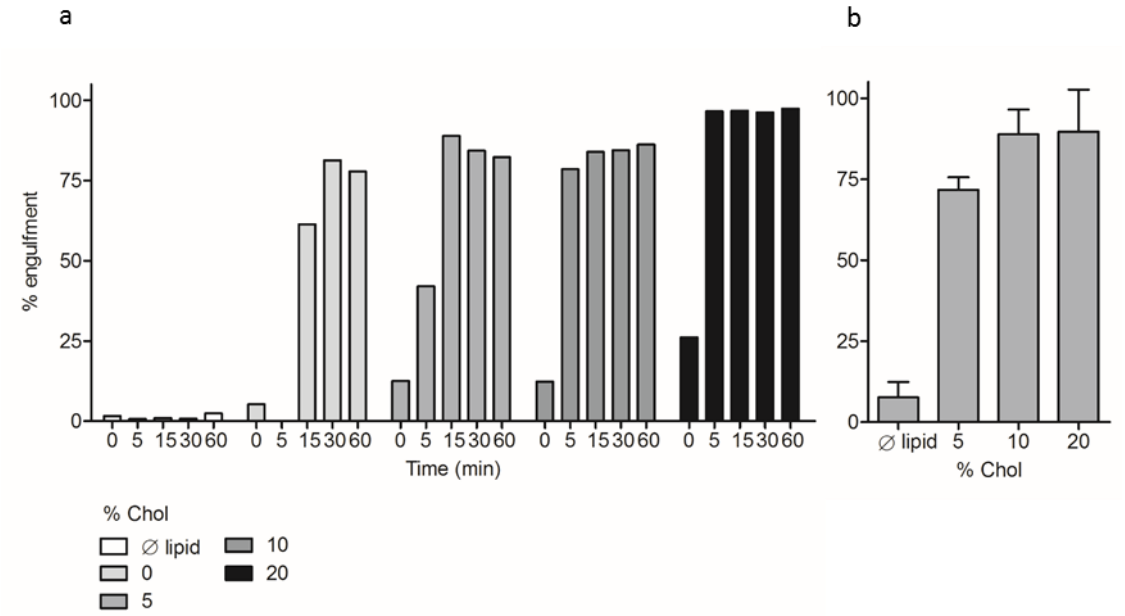

Figure 5.4. Effect of cholesterol in lipid engulfment of a lung surfactant preparation by MH-S cells. (a) Time-course of lipid engulfment using 0.25 μg /10^5 cells of Curosurf labelled with 5 wt% TFC incorporating different amounts of cholesterol. (b) Lipid engulfment assay performed for 1h and 0.25 μg/10^5 cells of Curosurf vesicles labelled with 5 wt% BPC incorporating increasing cholesterol content.

Cholesterol content seemed to increase lipid uptake, revealing higher %engulfment indexes for larger cholesterol proportions using two types of labelling, TFC or BPC. Besides, for the highest amount of cholesterol tested, saturation was rapidly reached, suggesting that cells had a larger affinity for cholesterol-containing vesicles.

Effect of SP-C on lipid engulfment

Cholesterol seemed to have an effect on lung surfactant uptake by alveolar macrophages. However, how SP-C could additionally modulate this engulfment cannot be directly inferred from these experiments. To properly evaluate SP-C effects, lung surfactant phospholipids were isolated and combined with different amounts of SP-C and cholesterol. Time-course experiments were performed to assess lipid uptake in response to different SP-C (0, 1%, 5%, 10%) and cholesterol (0%, 5%, 10%, 20%) concentrations over time. Our results displayed a high variability depending on the experiment and batch of SP-C employed. To reduce disparity and combine all data in a same analysis, data were normalized according to the saturation point in every plate, which was reached after 30 min treatment (Fig. 5.5). Despite the variability, vesicles incorporating the lowest amounts of SP-C seemed to have a slight tendency towards higher engulfment indexes in comparison to the pure lipid, although the effect of cholesterol in SP-C containing vesicles was not that clear. In the absence of SP-C, cholesterol leaded to an increase in lipid uptake, whereas for 1% and 5% SP-C, its effect was somehow balanced by the presence of the protein. Apparently, the incorporation of 10% SP-C resulted in larger engulfment indexes, both in the absence and presence of cholesterol, yielding a maximum lipid uptake value when cholesterol was incorporated (5-20%). This reveals that the proper combination of SP-C and cholesterol might influence macrophage endocytic activity, with possible implications in surfactant compositional refinement and lung homeostasis.

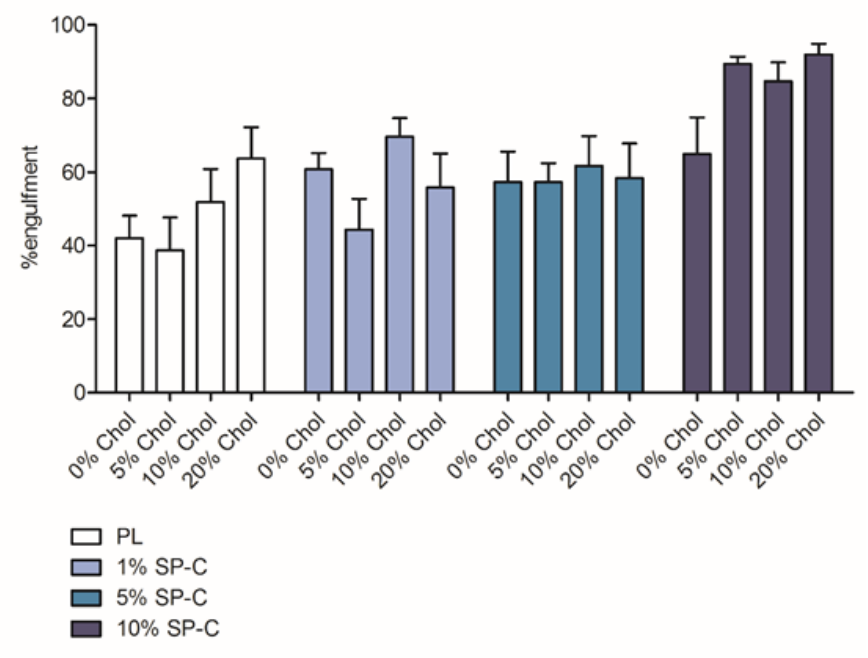

Figure 5.5. Effect of SP-C and cholesterol on lipid engulfment by MH-S cells. Lipid vesicles containing the phospholipid fraction of surfactant (PL) were supplemented with different SP-C and cholesterol amounts. The results presented here represent the exposure of cells to a lipid concentration of 0.25 μg/10^5 cells for 30 min.

To further evaluate SP-C effects, we hypothesized that when excess cholesterol needs to be depleted from surfactant to achieve a proper biophysical activity, SP-C/cholesterol-enriched vesicles might be released from the surface-active material and follow degradation routes that might involve AMφ. Thus, the effect of the larger SP-C and cholesterol amounts employed, 10 wt% SP-C and 20 wt% cholesterol, was analyzed in subsequent experiments. Results from separate engulfment assays showed that although the increase in lipid uptake associated to SP-C and cholesterol independent effects was not significant, the combination of both elements (10 wt% SP-C and 20 wt% cholesterol) ended up into a significant increase in lipid engulfment (Fig. 5.6a). These results are in agreement with our hypothesis, which involves the modulation of lipid uptake by SP-C and cholesterol enriched vesicles in AMφ.

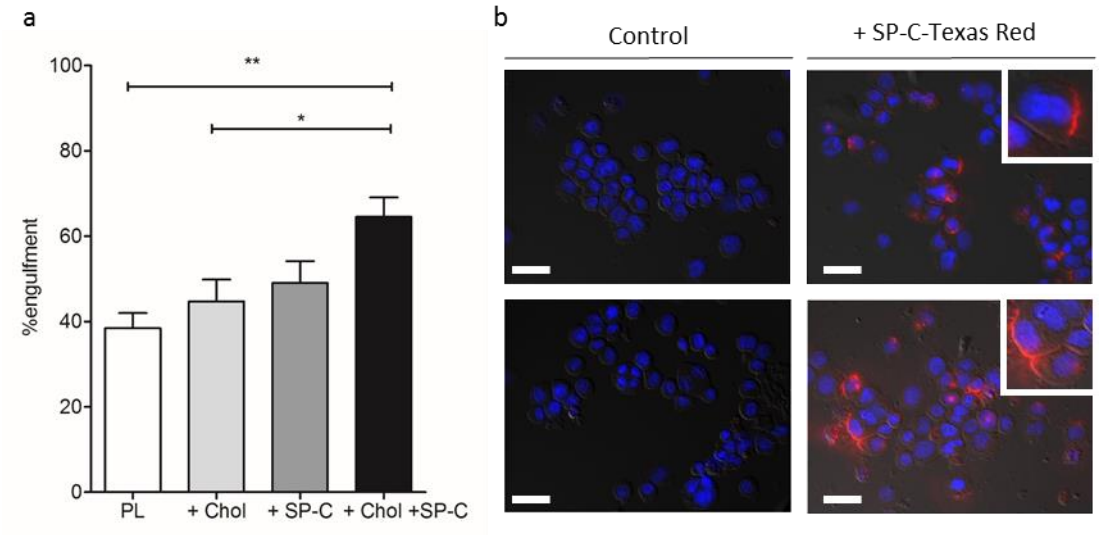

Fig 5.6. Effect of SP-C and cholesterol-enriched vesicles on lipid engulfment by MH-S cells. (a) Lipid vesicles containing the phospholipid fraction of surfactant (PL) including either 10 wt% SP-C and/or 20 wt% chol were added at a final lipid concentration of 0.25 μg/10^5 cells and assessed for 30 min. Data are presented as means ± SEM. Differences between groups were evaluated by one-way ANOVA with a post-hoc Tukey test (*p< 0.05, **p<0.001). (b) Epifluorescence micrographs of MH-S cells treated with surfactant-derived lipid vesicles (PL) or vesicles incorporating 10 wt% TxR-SP-C. DAPI-stained nuclei are observed in blue and TxR-SP-C in red. Scale bar= 50 μm.

To narrow down the possible mechanisms ruling SP-C and cholesterol combined action, the subcellular localization of SP-C was analyzed upon the engulfment assay. Texas Red was used to label SP-C molecules at the N-terminal end, generating fluorescently labelled SP-C (TxR-SP-C). To avoid problems of detection limit, the amount of lipid employed in the engulfment assay was increased substantially. SP-C seemed to be restricted to the plasma membrane, where the fluorescence was localized in defined regions. However, whether SP-C does not enter the cells or whether it is redirected to the plasma membrane after the engulfment process are questions yet to answer.

Metabolism and lipid transport

We have observed how SP-C in combination with cholesterol is able to modulate lipid uptake by an alveolar macrophage cell line. However, we were also interested in analyzing how these cells would respond to the engulfment of lipid vesicles with different compositions. With this purpose, MH-S cells were treated with surfactant-derived liposomes and the expression of several genes related to lipid transport and metabolism was analyzed by real-time PCR.

MH-S cells were treated for 1h with liposomes with different compositions. In one group, cells were administrated 0.25 μg/10^5 cell of Curosurf or Curosurf supplemented with 20% cholesterol for 1h (Fig. 5.7 and 5.8).

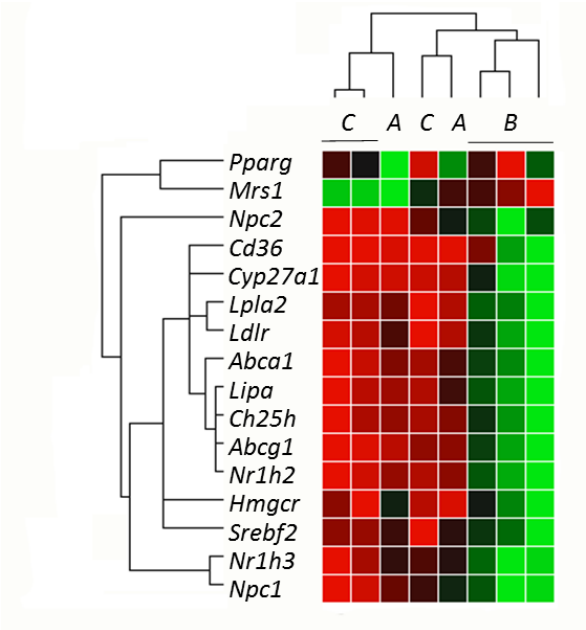

A: Control
B: +Curosurf
C: +Curosurf+Chol

Figure 5.7. Clustergram showing the expression of genes related with lipid transport and metabolism in response to Curosurf treatment with or without 20 wt% cholesterol. Minimum expression levels are shown in red whereas maximum levels are represented in green. Samples and target genes are clustered according to similitudes in the expression profile.

In these preliminary experiments, Curosurf treatment altered gene expression in MH-S incrementing expression of most of the analyzed genes, except for *Msr1*, coding for the scavenger receptor SRAI, and *Pparγ*. Genes coding for several enzymes involved in lipid metabolism such as the lysosomal acid lipase (*Lipa*) or the lysosomal phospholipase 2 (*Lpla2*) and those participating in cholesterol metabolism, including the cholesterol hydroxylase CH25H, or the sterol 27 hydroxylase, CYP27A1, were overexpressed in Curosurf-treated cells in the absence of cholesterol. This indicates that upon lipid uptake, MH-S cells apparently upregulate genes involved in lipid metabolism, promoting the degradation of newly incorporated lipid material. *Nr1h2*, coding for the nuclear receptor LXRβ (an sterol sensor), also appears overexpressed, and similarly, targets of the LXR/Retinoid X receptor heterodimer were increased, including genes for cholesterol efflux transporters such as *Abca1* or *Abcg1* (Fig.5.8).

Other lipid transporters such as Niemann Pick type C 1 and 2 proteins (*Npc1* and *Npc2*) appear increased at the mRNA level (293). There is a trend towards higher expression of genes coding for receptors involved in cholesterol/lipid uptake, such as the LDL receptor (LDL-R) or CD36, which could facilitate lipid uptake for its degradation.

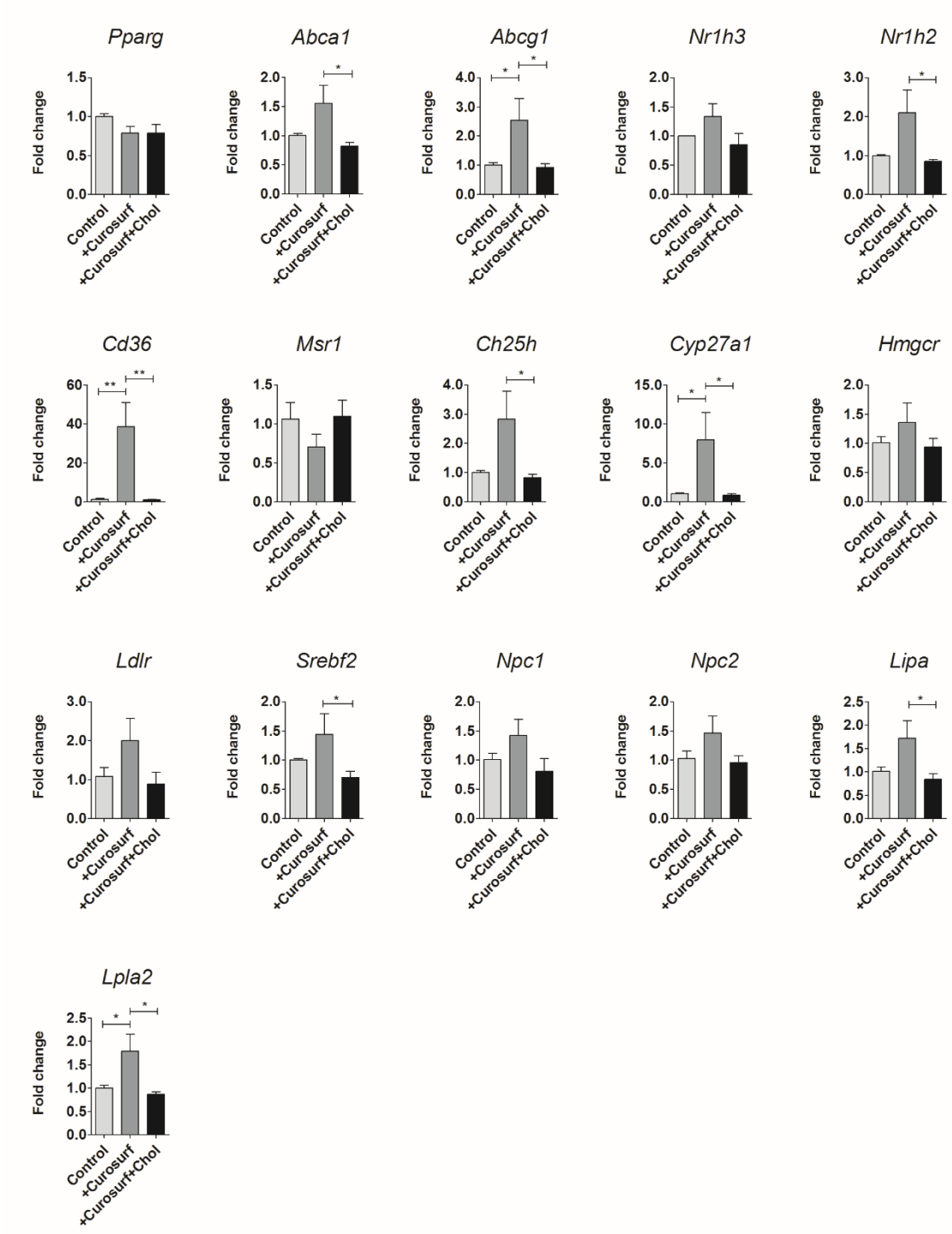

Figure 5.8. Gene expression of lipid metabolism and transport genes induced in MH-S cells treated with Curosurf or Curosurf/20% cholesterol measured 1h after treatment. Results are expressed as fold change with respect to the control (untreated cells). Data are presented as means ± SEM. Differences between groups were evaluated by one-way ANOVA with a post-hoc Tukey test (*p< 0.05, **p<0.001).

Cd36 and *Abcg1* expression are known to be regulated by Pparγ in macrophages (135, 182, 294), but in our case, Pparγ mRNA levels remain unaltered in Curosurf-treated cells, suggesting that alternative mechanisms might be involved. It is remarkable, however, the trend observed for the hydroxymethyl-glutaryl-coenzyme A reductase (HMGCR) expression, an enzyme implicated in cholesterol *de novo* synthesis. How lipid uptake could increase HMGCR mRNA levels seems contradictory, which reveals the complexity of pathways connecting lipid engulfment and gene expression in AMφ. Strikingly, the engulfment of Curosurf supplemented with 20 wt% cholesterol resulted in gene expression levels similar to control cells. It might be then possible that supraphysiological amounts of cholesterol (~20 wt%) could alter lipid metabolism in AMφ leading to lipid accumulation.

Curosurf includes physiological proportions of proteins SP-B and SP-C. However, it does not allow the evaluation of possible effects associated specifically to SP-C. In the previous section, treatment with surfactant-derived vesicles incorporating 10 wt% SP-C and 20 wt% cholesterol leaded to an increased lipid uptake by MH-S cells. Thus, gene expression was evaluated for cells treated with the deproteinized phospholipid surfactant fraction (PL) or lipids supplemented with 20 wt% cholesterol, 10 wt% SP-C or both (Fig. 5.9 and 5.10). As can be deduced from Fig. 5.9, there are considerable variations from sample to sample, specially concerning those incorporating SP-C. In the previous section, we described how the engulfment assay showed variability issues, which could be related to several factors going from SP-C batches to a differential response of MH-S cells depending on cell passage or cell state. Despite this variability, it is still interesting how the enzymes associated to cholesterol metabolism, CH25H and CYP27A1, exhibited an increased gene expression upon lipid treatment with any of the preparations used, as occurred in genes coding for the scavenger receptors SRAI and CD36. ABCA1 levels were slightly decreased for samples not including cholesterol, suggesting that cholesterol efflux in these cases might be regulated depending on the lipid composition of engulfed vesicles.

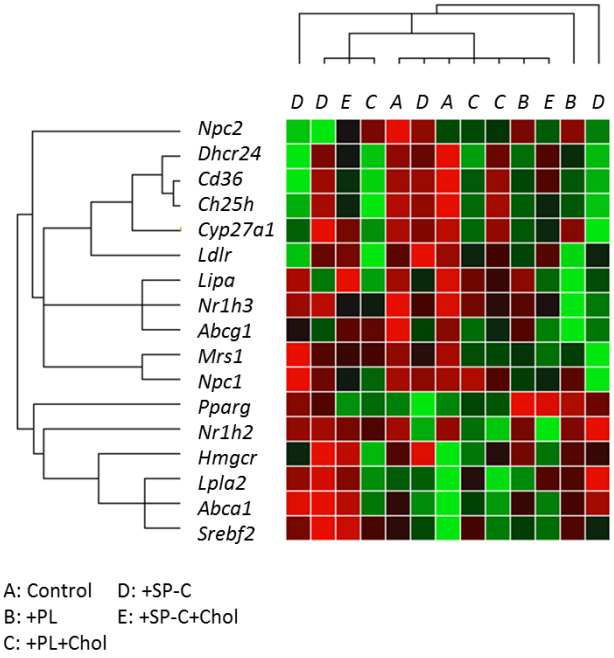

Figure 5.9. Clustergram showing the expression of genes related with lipid transport and metabolism in response to the administration of lipid vesicles incorporating lung surfactant phospholipids (PL) supplemented with 10 wt% SP-C, 20 wt% chol or both. Minimum expression levels are shown in red whereas maximum levels are represented in green. Samples and target genes are clustered according to similitudes in the expression profile. Some samples have been removed from the scheme for clarity.

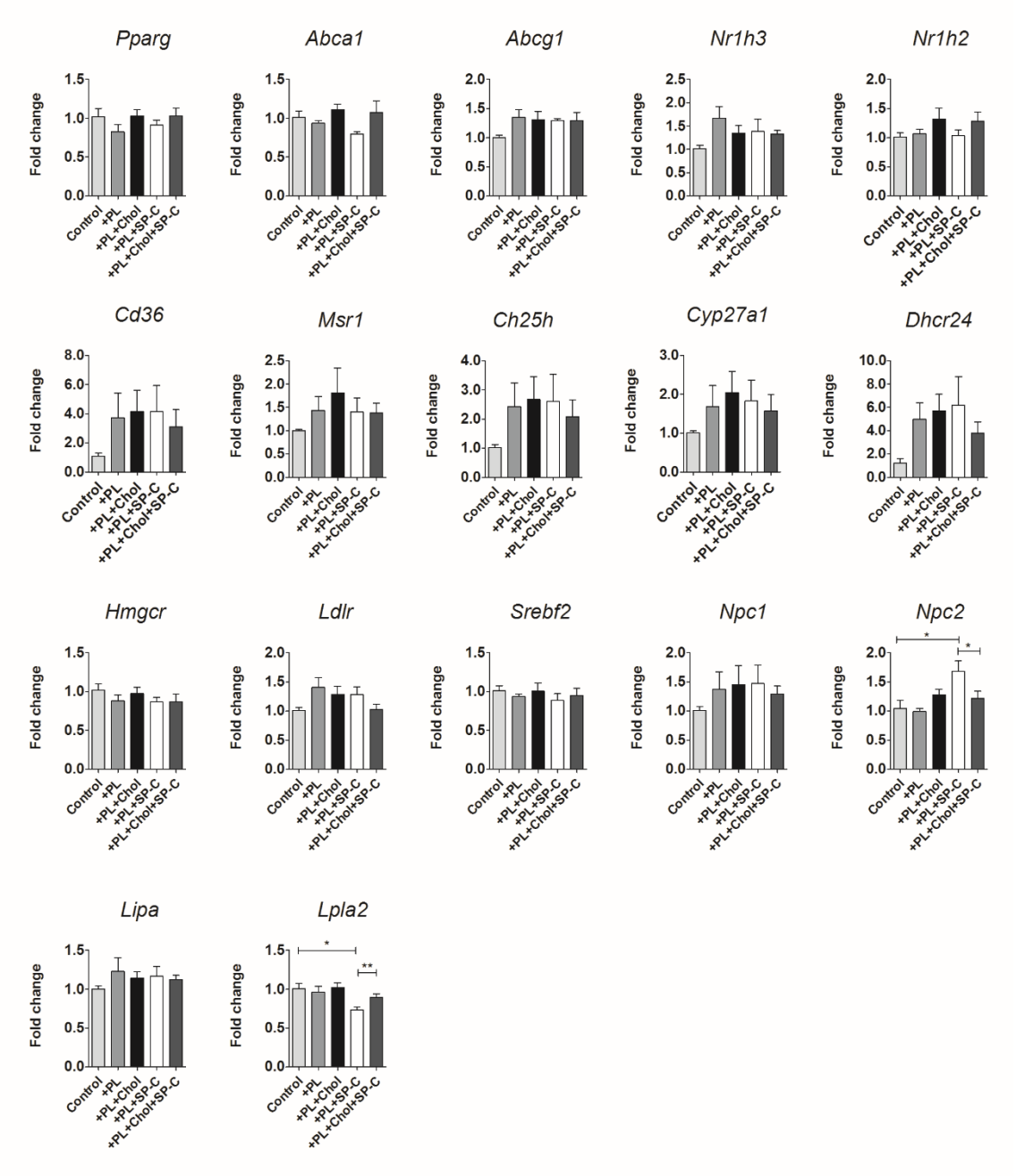

Figure 5.10. Gene expression of lipid metabolism and transport genes in MH-S cells treated with lung surfactant-derived vesicles measured 1h after treatment. Lipid suspensions used included the phospholipid fraction (PL), and PL supplemented with either 10 wt% SP-C, 20wt% Chol or a combination of both. Results are expressed as fold change with respect to the control (untreated cells). Data are presented as means ± SEM. Differences between groups were evaluated by one-way ANOVA with a post-hoc Tukey test (*p< 0.05,**p<0.001).

However, in general terms, nor SP-C or cholesterol presence modified gene expression significantly, with levels remaining in the range of control cells. Two genes appeared to be significantly altered by SP-C presence, *Lpla2* and *Npc2*, both encoding lysosomal-produced proteins. This suggests that SP-C may directly or indirectly act through the endosomal/lysosomal system once the engulfment event has taken place. NPC2 is involved in the intracellular

mobilization of exogenous cholesterol, transferring non-esterified cholesterol from the lumen of late endosomes/lysosomes to NPC1, located in the limiting membrane. From there, cholesterol is exported to reach different cellular compartments, such as the endoplasmic reticulum and plasma membrane, although the molecular mechanism has not been defined yet (295, 296). Lysosomal phospholipase A2 (LPLA2) is highly expressed in AMφ, and it is involved in surfactant catabolism (188, 297). Deficiency in this enzyme results in phospholipidosis, leading to lipid accumulation in the alveolar spaces (188, 297). According to our results, *Npc2* mRNA was substantially incremented when SP-C-containing vesicles were used in the absence of cholesterol, whereas *Lpla2* expression was decreased both compared to the control and to vesicles incorporating SP-C/Chol. Again, these results seem to be contradictory, since they suggest that SP-C could be involved in promoting cholesterol mobilization from the endocytic vesicle to other cells compartments when no cholesterol is being incorporated, an effect that is no longer observed when SP-C is combined with 20 wt% cholesterol. Similarly to Curosurf/cholesterol treatment, it is possible that the use of such a high concentration of cholesterol render cells insensitive to it, resulting in cholesterol accumulation in AMφ. However, how SP-C could reduce LPLA2 expression is an intriguing matter. One would think that upon lipid uptake, LPLA2 levels would be increased to facilitate lipid catabolism, although it is possible that SP-C might somehow regulate this process favouring lipid degradation through alternative mechanisms.

Discussion

The relevance of cholesterol and SP-C in lung surfactant dynamics and structure has been described in the previous chapters. To highlight the importance of the cholesterol/SP-C relationship in surfactant lipid membranes physiologically, we have analyzed the effect of the different lipid, cholesterol and protein composition in a model of one of the cells involved in lung homeostasis. With the aim to establish a connection with the biophysical properties of cholesterol and SP-C lipid mixtures, we propose here a cellular mechanism with potential relevance *in vivo*.

Lung homeostasis results from the balance between surfactant synthesis and degradation/recycling, but specific mechanisms are still being explored. AMφ play an important role in surfactant catabolism, and although they might not account for most of surfactant degradation (30%), AMφ dysfunction give rise to lipid/cholesterol accumulation resulting in severe pathologies. These findings suggests that AMφ could modulate cholesterol metabolism in the lung and participate in the regulation of surfactant cholesterol levels. To test this hypothesis, we have conducted experiments evaluating vesicle engulfment of a clinical surfactant preparation, Curosurf, and of samples with different compositions including surfactant phospholipids supplemented with variable amounts of SP-C and cholesterol. We considered SP-C as an interesting element to assess given its reported involvement in lung homeostasis (97, 123), its interaction with the AMφ receptor, CD14 (124), and the particular

relationship stablished with cholesterol in surfactant membranes (25, 120, 121, 245). Besides, SP-C has been proposed before to increment lipid uptake by alveolar cells (298). Our results show that MH-S cells, an AMφ-like cell line, are capable of engulfing Curosurf complexes extremely fast below physiological temperatures, showing lipid incorporation at the shortest times tested. This effect was dose and time-dependent, which is consistent with a previous study (299). This reveals the high efficiency of AMφ in uptaking lipid assemblies from the environment, a property that could be likely related to their ability in regulating lung surfactant pools at the alveolar spaces. In addition, although MH-S can exhibit some lipid droplets in the absence of any treatment, incubation with the lower lipid concentrations resulted in a qualitatively apparent increment in the number of droplets, which also occurred with higher frequency. This further supports the role of AMφ in both uptaking and metabolizing lipids, stressing their importance for surfactant clearance and metabolism.

The engulfment of lipid vesicles by AMφ seems to be related with membrane properties such as charge and fluidity (300–302). Furthermore, it has been suggested that membrane lateral structure could be involved in a preferential engulfment by macrophages without the need of specific recognition by a cellular receptor (302). Cholesterol modulation of membrane fluidity and lipid packing has been studied thoroughly, and in previous chapters we have described how SP-C and cholesterol modulate membrane properties altering membrane lateral structure and lipid dynamics. Thus, the preferential engulfment of vesicles with a certain SP-C/Chol ratio observed here could be explained by the adoption of certain membrane properties, although possible receptor-mediated recognition cannot be ruled out. Similarly, cholesterol incorporation into Curosurf could enhance lipid engulfment by a similar process, since cholesterol incorporation in surfactant is reported to modulate membrane fluidity. Interestingly, although there is some controversy, some reports have pointed to preferential lipid uptake in the form of small vesicles rather than larger liposomes by macrophages (303, 304), an effect that translated to AMφ, could be related to the degradation/recycling of surfactant in the form of the less surface-active *small aggregates* (SA), lipid assemblies derived from "exhausted" surfactant (305). Then, SP-C activity could influence macrophage engulfment by generating small vesicles that might be enriched in less active surfactant components, a feature we described in Results Chapter 2.

Inhibition of clathrin-mediated (amantadine, cytochalasine D and chlorpromazine) and caveolae-dependent endocytosis (genistein) as well as the disruption of endocytic vesicle acidification process (baphylomycin) resulted in a similar reduction of the engulfment index, suggesting that lipid uptake does not occur through a single pathway and several mechanisms might be involved. Cholesterol depletion of the cell plasma membrane induced by cyclodextrin treatment resulted in a higher lipid uptake measured as %engulfment. This could result from a compensatory mechanism, by which the cell could transfer directly lipids from the vesicles to the plasma membrane to quickly replace cholesterol levels. Surprisingly, CD14-blocking also resulted in a slight decrease in lipid uptake (~18%). Given SP-C/CD14 reported interaction (124), we could hypothesize that a minor part of surfactant vesicles could be engulfed in a CD14-

mediated manner. Besides, an specific SP-C/receptor interaction could explain the observed characteristic SP-C localization in the plasma membrane, where its seems to be confined in defined regions. Nevertheless, studies specifically assessing the possible implication of CD14 in lipid endocytosis and whether SP-C could be involved are required to contrast this hypothesis.

In this study, lipid uptake by MH-S cells seemed to be influenced by lipid composition and SP-C content. To evaluate the effect of lipid engulfment, the expression of several genes involved in lipid transport and metabolism were analyzed. In AMφ, PPARγ is the master element regulating lipid metabolism (135, 180, 181). PPARγ has been related to GM-CSF-induced signaling, and it coordinates with the sterol regulatory-element binding proteins (SREBPs) and the liver X receptors (LXRs) to regulate lipid metabolism in AMφ. Several genes have been associated to PPARγ regulation in vivo, including ABCG1, SRA-I, CD36, LXRα, CYP27A1, SREBP2, HMGCR, and LDL-R (135). Therefore, we intended to analyze how these genes were altered by lipid engulfment specially observing effects focusing the effects on PPARγ mRNA levels. Our results suggest that lipid engulfment elicited a complex response according to changes in gene expression, in which both cholesterol and phospholipid metabolism genes seemed to be involved. Although no changes in PPARγ expression were observed in cells treated with Curosurf, they displayed an increased gene expression affecting cholesterol efflux transporters ABCA1 and ABCG1, enzymes implicated in cholesterol (CH25H and CYP27A1) and phospholipid metabolism (LAL, LPLA2). However, we have shown for the first time that receptors in charge or cholesterol uptake (CD36, LDL-R) and enzymes participating in cholesterol *de novo* synthesis (HMGCR) also showed increased expression levels. Hence, a possible explanation would be that macrophages could trigger a general response towards lipid degradation and efflux upon lipid engulfment and at the same time, they could sense cholesterol absence in the engulfed vesicles resulting in activation of cholesterol uptake and synthesis. Strikingly, the addition of supraphysiological cholesterol concentrations to Curosurf preparations resulted in gene expression levels similar to the control, indicating that high cholesterol concentrations might lead to cell desensitization after lipid engulfment resulting in lipid accumulation as occurs in some respiratory disorders. In the case of vesicles made of lung surfactant phospholipids (PL), results also showed some controversy. In general, there was a trend towards higher expression of the cholesterol metabolism enzymes CH25H and CYP27A1, as well as it occurs for scavenger receptors SRA-I and CD36, regardless of SP-C or cholesterol presence. SP-C incorporation seemed to increment specifically Npc2 and decrease LPLA2 mRNA levels in the absence of cholesterol. Thus, we show for the first time that SP-C could promote cholesterol intracellular mobilization from the endocytic vesicle to other compartments through Npc2, whereas it could reduce phospholipid metabolism by reducing LPLA2 mRNA levels. These effects seem to be contradictory, but pathways for cholesterol synthesis, degradation and mobilization in alveolar macrophages are still unknown. This means that further investigation is needed to understand lipid metabolism in these cells.

The results obtained from gene expression analysis suggest that lipid uptake/engulfment by MH-S cell lead to complex changes in gene expression associated to lipid metabolism and

transport. These effects seemed to depend on lipid composition, including the presence or absence of SP-C and/or cholesterol. Nevertheless, the information obtained from these experiments should be considered cautiously. To properly understand the response of AMφ to lipid uptake and interpret the implication of changes in gene expression, additional evidence concerning treatment time and lipid concentration must be collected. Besides, variability issues prevent us to clearly conclude the effects of SP-C and cholesterol, in which cell compensatory mechanisms might also be involved. The use of intermediate amounts of SP-C and cholesterol could provide important information concerning whether a threshold must be reached to trigger changes in gene expression.

We are aware that the use of an immortalized murine alveolar macrophage cell line, MH-S, presents some limitations. Although the phagocytic capacity of this cell line seems to resemble that of primary AMφ, they differ in some features as in the expression of certain surface markers (306). For this reason, the extrapolation of these results to the behavior of primary AMφ must be done carefully. The complementation of these results with experiments using primary AMφ would provide a wider overview of how AMφ respond to lipid engulfment validating the results obtained here.

The evidence obtained in this chapter contributes to support the important role of AMφ in lipid uptake and clearance, essential to maintain surfactant pools assuring a proper respiratory function. Lipid engulfment results in changes in gene expression with potential consequences in lipid mobilization and metabolism, and we have described a particular effect of SP-C and cholesterol on vesicle uptake. These encouraging results define a new line of research based on SP-C and cholesterol effects on lung homeostasis. Besides, plenty of different molecular metabolic pathways in macrophages need to be investigated in detail. Additional aspects, such as differential macrophage polarization, should be considered in the future experiments. This would contribute to the elucidation of the AMφ role in integrating the immune response and the regulation of lung surfactant homeostasis, in which SP-C and cholesterol are promising candidates.

6. General discussion

A proper respiratory function depends on the activity of lung surfactant, a lipid protein complex compositionally optimized to support breathing. From all surfactant components, the relevance of the hydrophobic surfactant proteins SP-B and SP-C becomes evident from respiratory pathologies resulting from their deficiency. SP-B absence renders surfactant dysfunctional, leading to respiratory failure upon birth (64–66). However, SP-C has been associated to the long-term stabilization of the lung (110). The lack of SP-C is related to pulmonary pathologies developed progressively with age and whose severity strongly depends on the genetic background (111–115). SP-C-related disorders are more often caused by mutant forms of the protein that fold improperly (307), generating protein structures that are cytotoxic for alveolar cells and result in conformational lung disease (97). SP-C-associated functions overlap in many cases with SP-B activity, at least when assayed in different in vitro models. This includes facilitating lipid adsorption (102–104) into the air-liquid interface or generating 3D structures that serve as a surfactant reservoir (60, 103), which stores newly secreted surfactant complexes and surfactant molecules squeezed out from the interface upon compression. In this context, SP-C could be figured as a supporting molecule for SP-B function rather than an element competent by itself to assist specific features of the complex and dynamic surfactant functionality. Nevertheless, considering the extensive processing of SP-C to its mature form, its extremely conserved sequence and tissue-specific localization, and the difficulties that a cell must overcome to produce and store such a hydrophobic molecule, it is unlikely that this peptide appeared evolutionarily just as an alternative strategy to assist SP-B activities.

With this in mind, in this Thesis we aimed to shed light on SP-C specific activities considering a relevant structure-function determinant, the palmitoylation of the protein. This covalent modification takes place early during SP-C processing (150), and it has been considered as an important element stabilizing SP-C α-helical structure (157, 210, 213). One of the main roles associated to SP-C acylation is its participation in monolayer/bilayer and bilayer/bilayer contacts, which could explain how such a small protein can lead to the generation of bilayer stacks associated to the interfacial surfactant film (60, 121). Thus, to deduce palmitoylation-dependent SP-C features, we carried out an ATR-FTIR study on lipid-protein multilayered membranes in which protein structure, orientation and lipid-protein interactions could be analyzed (Chapter 1). According to our results, acylation did not affect α-helical content, since both native SP-C and non-palmitoylated rSP-C were determined as ~80% α-helical. However, although palmitoylation itself might not be involved in promoting the adoption of a certain protein structure, it could contribute to stabilize the SP-C α-helix (157, 210, 213). This effect is manifested in Chapter 3, in which the effects of different rSP-C variants could be explained in terms of protein structure, suggesting that non-palmitoylated protein forms are more prone to aggregation. SP-C structure was neither dependent on the composition of the lipid systems used in Chapter 1, which were systematically varied to assess effects on lipid-protein interactions. In these lipid systems, SP-C showed little effect on packing or mobility of lipid acyl chains as detected by the degree of *trans-gauche* isomerizations, which in average, were not indicative of any specific effects derived either of protein incorporation, or protein palmitoylation. In Chapter 3, however, ^{2}H-NMR experiments revealed that SP-C induced segregation into a highly ordered,

possibly interdigitated, phase and a liquid crystalline phase. Besides, according to our estimations, lipid species contributed unevenly to ordered domains, which were enriched in DPPC and POPG and partly depleted in POPC. In average, an increase in lipid order was also detected by ESR, involving acyl chains positions (n=12) close to the hydrophobic core of the membrane, and the polar headgroup (n=5). The discrepancy regarding lipid fluidity and order between ATR-FTIR results (Chapter 1) and the results obtained by ^{2}H-NMR and ESR (Chapter 3), can be explained in terms of sample hydration. For ATR-FTIR experiments, lipid and lipid/protein films are prepared by deposition and partial drying on the ATR crystal, resulting in films retaining just solvation water molecules. ^{2}H-NMR and ESR, though, require highly concentrated lipid suspensions in which the level of membrane hydration is substantially higher than for ATR-FTIR films. Therefore, partly dehydrated films such as those examined by ATR-FTIR would possibly remain in a more packed state, in which the ordering induced by SP-C or by the non-palmitoylated rSP-C might pass undetected.

Protein palmitoylation has been shown to be important to define SP-C configuration into lipid membranes and modulates lipid-protein interactions (Chapter 1). Regarding ATR-FTIR results, we have described that palmitoylated SP-C suffered a higher tilting degree that non-palmitoylated rSP-C in the lipid systems studied. This is consistent with a deeper embedding in the membrane promoted by the palmitic chains, which could pull the protein towards more tilted configurations. In the same line of reasoning, we also observed that palmitoylation promoted a deeper water penetration on the membrane polar region, affecting phosphate vibrations to a wider extent. These effects can be related to the ability of the protein to induce lipid interdigitation (Chapter 3), characterized by a high hydration level at the polar headgroup and increased acyl chain order. We have proposed that SP-C mediated-lipid segregation could be triggered by the interaction of the N-terminal segment of the protein and the polar region of the membrane (Chapter 3), an effect that seems to depend on protein palmitoylation to maximize the differences between lipid species involved. In lung surfactant and surfactant-mimicking membranes, SP-C is not randomly distributed and localizes specially at the boundaries between liquid-ordered and disordered domains in bilayers (25) and between liquid-expanded and condensed phases in monolayers (105, 226). In addition, SP-C palmitoylation has been described to couple N-terminal acyl motion to those of DPPC (308), and it has been suggested as a relevant element to generate interdigitated phases (244). This evidence is in agreement with the results from Chapters 1 and 3, indicating that protein palmitoylation is important to define a proper SP-C configuration in surfactant membranes and films, which assists protein-induced interdigitation by maximizing the differences between the lipids species involved in SP-C-induced lipid domains (Chapter 3).

SP-C tilted configuration could be associated to the dimerization of the protein. As previously discussed, SP-C has been reported to dimerize during the processing of the proSP-C precursor along the exocytic pathway (149), and although proof of the functionality of SP-C dimers is still limited (240), some models have reported the potential dimerization of the protein though the AxxxG motif (212, 241). Besides, this motif is extremely conserved through evolution, suggesting

it could be an important structural factor to account for SP-C function. As illustrated in Chapter 2, for SP-C dimers to accommodate in a lipid bilayer, each monomer should be tilted with respect to membrane normal, adopting a conical configuration. Accordingly, the accumulation of several dimers in a certain region could alter membrane curvature, a process that could explain the SP-C-induced fragmenting effect into small and highly curved vesicles (Chapter 2). We have detected that the non-palmitoylated protein form, rSP-C, also induced membrane fragmentation. Preliminary experiments, however, suggested that the vesicles generated were slightly larger (~40 nm) than those generated by SP-C activity (~20-30 nm). Differences in tilting regarding SP-C acylation state could be the reason behind this difference; however, further research is required to define the role of SP-C palmitoylation in the membrane fragmenting effect.

We have discussed that the **membrane fragmenting effect** (Chapter 2) and lateral segregation (Chapter 3) induced by SP-C are consistent with SP-C tilted configuration (Chapter 1). These lipid reorganizations could be viewed as different intermediary states of a same process. First, SP-C could promote phase segregation separating DPPC-enriched regions from unsaturated phospholipids, as depicted in the model suggested in Chapter 3. The packing defects generated between domains could be the first step towards curved structures facilitating membrane budding, a process that could depend on a certain amount of SP-C to be accumulated. Thus, the interdigitated phase promoted by SP-C could be an intermediate state between the interfacial monolayer and the underlying multilayered reservoir, stressing the importance of SP-C induced membrane reorganizations in the dynamic structure of lung surfactant. SP-C induced interdigitation might also be involved in the final membrane fission producing the transformation of large membranes into small nanovesicles. These two SP-C effects, membrane-fragmenting and lipid interdigitation, could be somehow related to the selective protein/lipid interactions revealed by the TLC analysis performed in Chapter 4. Lipids enclosed by the SP-C or rSP-C dimeric configuration or those forming part of the protein-promoted interdigitated regions would be tightly immobilized. As a result of these strongly stablished protein/lipid interactions, SP-C/lipid complexes appear after organic solubilization as detected by the TLC-based method described in this Thesis (Chapter 4). We propose that inverse micelles could explain the behavior of these protein/lipid complexes, which somehow simulate the air-liquid interface (apolar organic phase: air, micelle polar core: aqueous subphase).

Shifting the individual observations based on SP-C analysis to surfactant behavior in the lung requires the consideration of additional important factors such as SP-B effects. SP-B presence counteracted the SP-C-induced membrane fragmentation, indicating a relevant **SP-B/SP-C relationship**. This has been manifested before, such as in the combined SP-B/SP-C effects on membrane permeability and stability (85) or even in lamellar bodies unfolding (90). It is also important to note that SP-B/SP-C complexes as assembled and secreted in lamellar bodies might differ from those established by the combination of independently isolated SP-B and SP-C. This suggests that SP-B/SP-C interactions could have a different nature depending on the particular stage of pulmonary surfactant metabolism, including surfactant biogenesis and secretion, the

generation of the different surfactant extracellular forms, surfactant interfacial activity and surfactant degradation and recycling. Whether this relationship occurs though specific protein/protein interactions o indirectly through protein-induced membrane alterations requires further study, but it remains clear that both proteins regulate lung surfactant structures in a coordinate manner to support surfactant function.

A second focus of this Thesis has been the analysis of **SP-C and cholesterol relationships in the lung surfactant context**. As we have extensively discussed, cholesterol is one of the most controversial elements of surfactant. Its origin has not been completely elucidated yet, even though several studies have been carried out to assess this issue (9). The presence of cholesterol establishes a marked segregation of fluid phases in surfactant (23, 119), and variations in cholesterol levels are known to adapt surfactant structures extremely fast to defined physiological situations (129, 131). This evidence highlights cholesterol as an structural modulator of surfactant membranes and films, and indicates that mechanisms involved in cholesterol sensing and mobilization may be evolutionary conserved to regulate cholesterol levels in surfactant. Considering this, recent evidences pointed to SP-C as a suitable molecule involved in cholesterol regulation (25, 120, 121, 245), which could also be linked to the role of SP-C in lung homeostasis. Therefore, we have analyzed the role of SP-C in cholesterol mobilization and dynamics considering also effects on membrane structure.

The effect of SP-C in cholesterol mobilization was described in Chapter 2, which seemed to depend on protein-induced alterations in membrane structure. Cholesterol motion was higher upon incorporation of SP-C into vesicles, an effect potentially associated to the SP-C-promoted membrane-fragmenting effect. The increase in cholesterol motion was also observed in the most physiological system tested (surfactant-derived membranes), in which the coordinated effect of the native hydrophobic protein fraction of surfactant (SP-B and SP-C) was resulted in a significant increase of cholesterol motion. In Chapter 3, it has been described how SP-C and cholesterol are related in modulating membrane architecture, responding in a coordinate manner to temperature changes. Together with the observations made in Chapter 2, this evidence suggest that SP-C is involved in cholesterol mobilization by altering membrane structure. In addition, taking into account that SP-C supplementation restores the functionality of cholesterol-containing films in a dynamic context (120, 121), these results support the hypothesis that SP-C could be related to the compositional refinement of lung surfactant films from less surface-active molecules, involving cholesterol and other unsaturated phospholipids. Interestingly, observations made by Leonenko et al. (277) could support this hypothesis. The incorporation of increasing amounts of cholesterol in a surfactant clinical preparation resulted in structurally and functionally different interfacial films (118, 277). Compression-expansion isotherms allowed the determination of lipid loss from the interfacial film upon compression, which were considerably low for physiological cholesterol amounts, permitting the re-establishment of a functional interfacial film (118, 277). Shifting that to SP-C function, lipid loss occurring for physiological cholesterol levels could be associated with an SP-C-dependent cholesterol depuration, in which SP-C-induced lipid reorganizations could be involved. However,

lipid loss increased substantially upon cholesterol increase beyond physiological levels, showing a markedly different film structure and impaired functionality (118, 277). For these supraphysiological cholesterol levels, the SP-C amount present in a clinical surfactant preparation like the one tested in this study (~1 wt%), is likely insufficient to overcome cholesterol impairing effects and the irreversible film collapse. Supplementation of these films with different SP-C amounts would provide valuable information to confirm SP-C effects on cholesterol mobilization.

To test the hypothesis that SP-C/Cholesterol relationships might be involved in **surfactant refinement with a homeostatic purpose** in the lung, we analyzed the effect of cholesterol- and SP-C-containing vesicles on one of the cell types involved in lung homeostasis, the alveolar macrophage (Chapter 5). Alveolar macrophages were chosen over type II epithelial cells given their implication in lipid and cholesterol transport and metabolism (135, 180, 181), which seemed to be altered in different respiratory pathologies due to macrophage dysfunction (179, 186, 229). As a model, the murine AMφ-like cell line MH-S was used. According to our results, although SP-C on its own did not elicited significant changes in lipid uptake, its combination with cholesterol apparently regulated lipid engulfment. Increased cholesterol content, however, seemed to increase lipid uptake by alveolar macrophages regardless of the presence of SP-C. Lipid engulfment did not seem to be restricted to a unique mechanism, and possible receptor-mediated processes cannot be discarded. Vesicle size and membrane fluidity can affect lipid uptake by alveolar macrophages, and thus, the combined effect of cholesterol and SP-C on membrane structure and fluidity analyzed in previous chapters (2 and 3) is a factor that must be taken into account. The study of the transcriptional response of MH-S cells to lipid administration revealed that genes associated to lipid metabolism and cholesterol transport were altered upon lipid uptake. Changes in gene expression appear to depend on lipid composition, including the presence or absence of SP-C and/or cholesterol. However, specific effects of cholesterol and SP-C require a thorough and extensive analysis, which also require a deeper exploration of the poorly studied pathways for cholesterol synthesis, degradation and mobilization in alveolar macrophages. It must be considered that MH-S cells share several properties with AMφ such as phagocytosis, although they differ in certain characteristics such as some surface markers (306, 309). For this reason, the complementation of these results with experiments using primary AMφ would provide a way of validating the results obtained here, and contribute to the understanding of how AMφ respond to lipid engulfment.

The evidence presented in this Thesis illustrates how specific SP-C-induced membrane reorganizations support the complex and dynamic behavior of lung surfactant structures, providing proof of SP-C-induced membrane fragmentation and revealing SP-C-promoted lipid segregation in surfactant-mimicking membranes. The results introduced here constitute robust arguments supporting a physiological role for SP-C and cholesterol relationships in lung homeostasis involving alveolar macrophages, a hypothesis tested for the first time in this Thesis. SP-C could then be considered as a pivotal molecule linking cholesterol and lipid homeostasis,

lung immunity and lung surfactant biophysics, which would explain its particular features, lung tissue specific localization and sequence conservation along evolution.

Several questions remain to be answered, including how SP-C effects are coordinated with SP-B function to modulate surfactant activity; which are the molecular mechanisms and SP-C structural determinants involved in membrane reorganizations; and how cholesterol levels in surfactant are sensed and regulated regarding SP-C function by both type II alveolar cells and alveolar macrophages. Future research assessing these questions would constitute an essential piece to understand the molecular mechanisms ruling lung surfactant behavior and its implication in respiratory pathologies, generating valuable information useful to improve the current clinical preparations applied for surfactant replacement therapy.

7. Conclusions

The experimental work presented in this Thesis has revealed specific SP-C effects on membrane structure and lipid dynamics, which in combination with the role played by cholesterol, are important to understand the relevance of SP-C in the framework of lung surfactant function and homeostasis. In general terms we may conclude:

1- SP-C palmitoylation does not affect protein structure incorporated in lipid membranes but contributes to SP-C α-helix stabilization. N-terminal acylation of SP-C leads to a greater protein tilting degree with respect to the membrane normal in most of the lipid systems studied, increasing the polarity at the phosphate region of the lipid bilayer and promoting SP-C-lipid interactions at this level. Thus, it is confirmed that palmitoylation is an important feature to define a functionally optimal SP-C configuration in lipid bilayers and monolayers.

2- SP-C and the native hydrophobic protein fraction of surfactant, incorporating SP-B and SP-C, affect specifically cholesterol mobilization in lipid bilayers. This was revealed by a decreased partition of the cholesterol fluorescent analog, cholestatrienol, in lipid membranes over the solubilizing agent methyl-β-cyclodextrin. The same behavior was observed for different lipid compositions including POPC model membranes, surfactant-derived lipid vesicles or surfactant mimicking systems such as DPPC/POPC/POPG 50:25:15 w/w/w. This effect suggests a role for SP-C in cholesterol mobilization and regulation in surfactant membranes with potential implications in lung homeostasis.

3- SP-C-induced structural modifications in lipid bilayers results in liposome fragmentation into highly curved and small vesicles. Membrane composition did not affect this SP-C-associated activity, which apparently was not dependent on SP-C palmitoylation. SP-B counteracted SP-C-induced effects, indicative of either a direct protein/protein interaction or balanced SP-B and SP-C modulating effects on membrane structure.

4- ^{2}H-NMR studies demonstrated that SP-C induces phase segregation in lung surfactant-mimicking membranes in a cholesterol and temperature-dependent manner as shown in DPPC/POPC/POPG (50:25:15 w/w/w) membranes. In the absence of cholesterol, SP-C leads to the segregation of a highly ordered and a liquid crystalline phase at physiological temperatures, whereas upon cholesterol addition phase segregation occurred at 30^{o}C. Cholesterol dynamics did not seem to be affected by SP-C, rSP-C, SP-B or the native SP-B/SP-C protein fraction, at least in the microsecond time scale sampled by ^{2}H-NMR experiments. However, SP-C and cholesterol combined effects on membrane structure and lateral segregation suggest a contribution of SP-C on cholesterol modulating activity on surfactant structures.

5- The lipid ordered phase induced by SP-C in the absence of cholesterol is consistent with an interdigitated structure that accommodates DPPC, POPC and POPG to different extents. This differential accommodation seems to depend on protein palmitoylation.

The restriction in lipid mobility related to SP-C incorporation was confirmed by ESR experiments.

6- The effects on membrane structure induced by SP-C are associated to strong protein/lipid interactions that can resist organic solvent solubilization. The TLC-based method developed here permits the identification of selective lipid/lipid and lipid/protein interactions such as those described for SP-C.

7- SP-C and cholesterol increased lipid uptake by a murine alveolar macrophage cell line, MH-S. Several mechanisms appeared to be involved in lipid engulfment, including receptor-unspecific and receptor-specific pathways. After the engulfment process, SP-C was confined at defined regions in the plasma membrane suggesting a role for SP-C in lipid uptake and/or vesicle endocytic processing. Lipids were accumulated intracellularly in the form of lipid droplets.

8- Lipid uptake elicits alterations in the transcriptional estate of alveolar macrophages. Genes coding lipid and cholesterol transporters, enzymes implicated in lipid metabolism or different transcription factors were affected depending on the composition of the vesicles engulfed. Additional experiments are required to define specific gene targets responding to SP-C and/or cholesterol incorporation.

8. Materials & Methods

Materials

Synthetic molecules and reagents

Synthetic lipids were purchased from Avanti Polar Lipids (Alabaster, AL) and chemicals and reagents were supplied by Sigma Aldrich (St. Louis, MO) unless otherwise stated. Chloroform (Chl) and methanol (MeOH) were from LabScan (Gliwice, POL).

Purification of PSM, DPH and CTL

Customized lipids and fluorescent probes were synthetized by Prof. Peter Slotte´s group in the department of Biosciences, Abo Akademi, Turku (Finland).

Palmitoyl sphingomyelin (PSM) was purified from egg yolk sphingomyelin by reverse-phase high-performance liquid chromatography (HPLC) using MeOH/water (95:5, v/v) as the eluent. $\Delta^{5,7,9}$Cholestatrien-3β-ol (CTL) was synthesized from 7-dehydrocholesterol as described (310). Purified CTL was aliquoted and stored dessicated under N_2 at -70^{0}C in light protected vials until used. 18:1-DPH-PC (1-oleoyl-2-propionyl-DPH-sn-glycero-3-phosphocholine) was prepared from 1-oleoyl-2-OH-sn-glycero-3-phosphocholine and DPH-propionic acid (Setareh Biotech, Eugene, OR) according to established methods (311, 312). The probe was purified by preparative HPLC (Discovery C18 column; Supelco, Bellefonte, PA) with methanol as the eluent. The purity and identity of DPH-PC were assessed by electrospray ionization mass spectrometry and analytical HPLC. The concentrations of the fluorophore stock solutions were determined based on their molar extinction coefficients (DPH-PC: 88,000 cm^{-1} M^{-1} at 350 nm in methanol; CTL: 11,250 cm^{-1} M^{-1} at 324 nm in ethanol).

Purification of lung surfactant and derived fractions

Lung surfactant was isolated from bronchoalveolar lavage fluid (BALF) of slaughtered porcine adult fresh lungs and purified as described (313). Approximately a total of 2.5L of cold 0.9% NaCl per complete respiratory apparatus (lungs and trachea) was used (2-3 lavages were performed). The recovered bronchoalveolar fluid (BALF) was filtered through a gauze and centrifuged (1000g 5min 4^{o}C) to eliminate cells and debris. Typically, BALF was stored at -20^{o}C until employed. To obtain the surfactant active fraction, constituted by surfactant large aggregates, BALF was thawed at 4^{o}C and centrifuged in a first step at 100000g for 1h at 4^{o}C. This step yielded the recovery of membranes in the pellet. A subsequent gradient centrifugation allowed the separation of lung surfactant complexes from other cell lipids and membranes based on their differential density. Pellets were thoroughly resuspended in a solution containing 16% NaBr 0.9% NaCl and the discontinuous gradient was formed by slowly adding 13% NaBr 0.9%NaBr and

0.9%NaCl on top of the heavy solution. Tubes were centrifuged in a swinging angle rotor (SW40 Ti, Beckman Coulter) at 120000g for 2h at 4°C. Surfactant complexes were concentrated between the lighter solution (0.9% NaCl) and the medium dense one, 13%NaCl 0.9%NaCl. After removing carefully the first solution, surfactant pellets were transferred to a homogenizer, diluted with 0.9% NaCl and aliquoted. This is the thereafter defined as native surfactant, and contained the lipid fraction of surfactant as well as surfactant associated proteins SP-A, SP-B and SP-C. Other proteins closely interacting with surfactant such as traces of immunoglobulins and hemoglobin are also co-isolated with surfactant complexes. Native surfactant was frozen in liquid N_2 and stored at -80°C until employed.

To obtain lung surfactant hydrophobic constituents, an organic extraction following the procedure established by Bligh and Dyer was performed (see Organic Extraction below) (314). The Chl/MeOH fraction was termed surfactant organic extract, called hereafter OE, and contained surfactant lipids and the hydrophobic proteins SP-B and SP-C. To allow the separation of lung surfactant constituents, the OE was concentrated using a rotary evaporator and chromatographed using a gel filtration resin (Sephadex LH-20, GE Healthcare; Little Chalfont, UK), with Chl/MeOH (1:1, v/v) acidified with 0.05% HCl (0.1N) as the eluent in a 1000mm-SR25 column (Ge Healthcare, Little Chalfont, UK). This column was operated by gravity and permitted the separation of proteins and lipids. Absorbance at 240 and 280 nm was measured to detect fractions containing either protein or lipids. The proteins eluted in the void volume given their large size compared to the lipids. Thus, the native hydrophobic protein fraction, containing SP-B and SP-C in their natural protein/protein ratio, was obtained in the first peak and termed Prot. The second fraction corresponded to surfactant phospholipids and was designated as PL, and the third fraction, containing the neutral lipids, was named N. All fractions were preserved at -20°C and recombined taking into account their volumetric proportions as eluted from the column.

SP-B and SP-C isolation

Native surfactant proteins SP-B and SP-C were isolated from porcine lungs as described (273). A complete respiratory apparatus was minced and lavaged with 1L 0.9% NaCl. Minced and lavaged lungs were extensively filtered and the resulting lavage was centrifuged in two steps. The first centrifugation (5min 1000g 4°C) yielded the elimination of cells and debris in the pellet. A second centrifugation (2h 3000g 4°C) allowed the recovery of protein-lipid complexes and membranes (pellet). Pellets corresponding to ~500 ml of lavage were transferred to B19 glass tubes and stored at -20°C until used. Because of their highly hydrophobic character, SP-B and SP-C were co-isolated with lipids after performing an organic extraction. The Chl/MeOH fraction, containing SP-B/C and lipids, was concentrated in a rotary evaporator and loaded onto a Sephadex LH-20 gel filtration column equilibrated with Chl/MeOH 2:1 v/v. This step allowed the delipidation of the protein fraction. Tubes corresponding to the SP-B/C fraction were pooled and concentrated again using the system previously mentioned. To obtain each protein separately,

the protein fraction was again loaded on a second Sephadex LH-60 (GE, Healthcare) chromatography column equilibrated with Chl/MeOH 1:1 v/v 0.05% HCl (0.1 N). The acidification with HCl minimized protein/resin interaction and allowed an easier protein recovery. SP-B eluted in the first fraction resolved from SP-C eluted. Given the lack of aromatic amino acids in SP-C, whereas SP-B registered absorbance at 240nm and 280 nm, SP-C only did at 240 nm. Each fraction was pooled independently and kept in glass containers at -20^{o}C.

Samples purity and identity was confirmed by SDS-PAGE and amino acid analysis (detailed below in “Amino acid analysis”).

Production and purification of rSP-C

Human recombinant rSP-C (sequence: GPFGIPCCPVHLKRLLIVVVVVVLIVVVIVGALLMGL) was purified according to the method of Lukovic and co-workers’ with modifications (217). Protein cloning and vector construction was conducted as described by Lukovic (217).

rSP-C was overexpressed as a fusion protein in *Escherichia Coli* B21 (DE3) pLys. The construction is detailed in Fig. 14. The 6-His-Staphylococcal nuclease and rSP-C sequences were connected by a glycine linker and a thrombin cleavage site (LVPR|GP). The two additional amino acids remaining in the rSP-C sequence after thrombin cleavage (GP) do not interfere with protein interfacial activity.

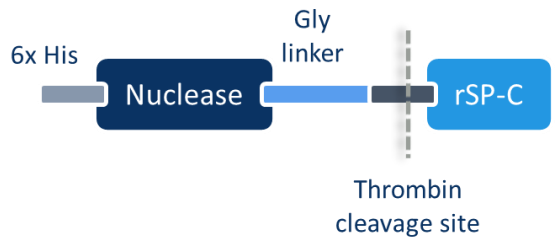

Figure 14. Schematic organization of the rSP-C-containing chimerical protein expressed in bacteria.

Fusion protein overexpression was induced with 1mM isopropyl β-D-1-thiogalactopyranoside at O.D.=0.4-0.5. After induction, the culture was grown for 3 h at 37 °C. Cells were recovered by centrifugation and the cell pellet was stored at -80^{o}C until used. Pellets were thawed on ice and re-suspended in lysis buffer (10 mM Tris pH 7.0 0.5% w/v N-lauroylsarcosine, DNAse (Roche, Basel, CH) and lysozyme). After 30min-incubation at 4^{o}C with stirring, 30s-sonication steps (0.5s on, 0.2s off) were performed on ice until the lysate was clear and non-viscous. A centrifugation step was carried out to eliminate the remaining membranes (18000g 30 min 4^{o}C) and the supernatant was collected. The lysate was filtered through 0.2 µm polyethersulfone filters. A 5ml pre-packed nickel affinity chromatography column (Hi-Trap, GE Healthcare; Little Chalfont, UK) was equilibrated in equilibration buffer (50 mM Tris pH 7.0 150 mM NaCl 0.5% N-lauroylsarcosine) using a peristaltic pump P1 (GE Healthcare; Little Chalfont,

UK). 10mM of imidazole was added to the lysate before loading to avoid nonspecific binding of proteins to the resin. 5-6 volumes of washing buffer (50 mM Tris pH 7.0 150 mM NaCl 0.2% N-lauroylsarcosine 30 mM imidazole) were employed to eliminate proteins nonspecifically attached to the column. rSP-C was recovered with elution buffer (50 mM Tris pH 7.0 150 mM NaCl 0.2% N-lauroylsarcosine 500 mM imidazole). 1 ml fractions were collected and the absorbance at 280 nm was recorded. Fractions containing eluted protein were pooled and dialyzed using SnakeSkin™ dyalisis membranes with a 10K molecular weight cut-off (Thermo Scientific, Waltham, MA) against dialysis buffer (50 mM Tris pH 7.0 150 mM NaCl 0.2% N-lauroylsarcosine). Dialysis was conducted o/n at 4°C to remove imidazole. To separate rSP-C from the nuclease, 0.5U of thrombin (Merck Millipore; Darmstad, DE) per mg of fusion protein were employed and incubated in cleavage buffer (20 mM Tris pH 8.4 150mM NaCl) at 4°C overnight. Cleavage was checked by SDS-PAGE and Coomassie-blue staining (detailed below). In order to obtain the cleaved SP-C polypeptide and to eliminate contaminant byproducts, an organic extract of the cleaved mixture was performed. During the organic extraction, the step of protein flocculation was avoided to increment the yield of the purification. The organic extract was concentrated in a rotary evaporator in the presence of lipid (PC 5:1 lipid/protein ratio w/w) to avoid irreversible protein precipitation and chromatographed through a gel-filtration LH-20 column (1.5 cm x 100 cm; SpectrumLabs, Breda, NL) eluted with Chl/MeOH 1:1 v/v HCl 0.05% (0.1N) v/v. rSP-C was obtained again free of lipid as it elutes from LH-20. Protein purity was assessed by SDS-PAGE and the concentration was determined by amino acid analysis.

SP-C labeling

Fluorescently labeled SP-C was obtained as described (27, 315). The preparation was slightly alkalinized (pH 7.8) with the appropriate amounts of 50 mM Tris in methanol to allow the N-terminal amine group of SP-C to be protonated. Texas Red (1 mg/ml) was added in methanol in a 3.5:1 molar probe/protein proportion.

The reaction took place overnight at 4°C. The sample was then acidified to pH 2.0 to stop the reaction and after the addition of egg phosphatidylcholine to prevent protein aggregation, it was concentrated using a rotary evaporator. To separate labeled protein from the free probe, the sample was chromatographed through a column with LH-20 resin and Chl/MeOH 1:1 v/v 0.05% HCl (0.1N) as the eluent. Protein identity was confirmed by SDS-PAGE, Western-Blotting and amino acid analysis.

Cell culture

In this Thesis, as a model of murine alveolar macrophages, the cell line MH-S was employed (309). This cell line was purchased from Sigma Aldrich (St. Louis, MO) and cultured in Roswell Park Memorial Institute (RPMI) 1640 medium (Merck Millipore; Darmstad, DE) supplemented

with 10% heat-inactivated fetal bovine serum (FBS) (Gibco, Thermo Fischer Scientific; Waltham, MS) at 37ºC under a humidified 5% CO_2 atmosphere. Cell passage was performed when confluence was 80-85% by trypsin treatment (Gibco, Thermo Fischer Scientific; Waltham, MS).

Methods

Organic extraction

To obtain hydrophobic constituents from different protein-lipid samples or lung tissue, the protocol of Bligh and Dyer was followed (314). A volume of sample in aqueous solution was mixed with two volumes of MeOH and one volume of Chl. This mixture was vortexed thoroughly for 30 s, and a single-phase solution was obtained. This mixture was incubated at 37-40°C for 30 min to allow the flocculation of water-soluble proteins. The addition of one more volume of Chl and water yielded the formation of a biphasic solution upon thorough mixing. This solution was centrifuged at ~600g for 5 min at 4ºC and the organic phase (lower fraction) was harvested carefully. Two volumes of Chl were added to the remaining aqueous fraction and vortexed, followed by another centrifugation step. This process increased the yield of hydrophobic material recovery. Again, the Chl/MeOH fraction was collected and the washing step was performed once more time. All hydrophobic fractions were pooled and kept at -20°C until used.

Phospholipid quantification

Phospholipid concentration was determined by phosphorus quantification (316). Samples were dried out in clean glass tubes and lipid hydrolysis and phosphorus mineralization was achieved by incubation at 260 ºC for 30 min in a sand bath in the presence of 0.65 ml of perchloric acid (70%). To avoid acid evaporation, tubes were capped with marbles or glass ampoules. The acid solution was then diluted with 3.5 ml or miliQ water and 0.5ml of 2.5 % molybdate and 0.5ml of 10% ascorbic acid were added. After each addition, samples were thoroughly vortexed. The incubation at 100°C in boiling water allowed the colorimetric reaction in which ascorbic acid reduced the phosphomolibdic complexes formed, resulting in a blueish color. Samples were measured in a spectrophotometer to obtain absorbance at 820 nm. A calibration curve made with known amounts of phosphate was included in each set of measurements to properly calculate the concentration of phospholipid phosphorus in the samples of interest.

Amino acid analysis

To determine protein concentration in SP-B, SP-C and rSP-C samples, the lack of aromatic amino acids (SP-C) and the highly hydrophobic character of these proteins (SP-B and SP-C) prevented the use of conventional techniques such as the Bradford or Lowry assay. For that reason, approximately 100-200 µl of isolated protein (typically 10-20 µg) was dried under a N_2 stream and subjected to an acid hydrolysis for 24h at 100°C under vacuum. The solution employed was HCl 6N 0.1% phenol w/v containing a known amount of *nor*-leucine as internal standard. After the hydrolysis, HCl was evaporated under a flow of N_2 followed by a wash with miliQ water and a evaporation step (SpeedVac Concentrator System, Thermo Fisher Scientific; Waltham, MS). Washing was performed twice to ensure the complete elimination of the acid. Finally, the hydrolyzed samples were resuspended in citrate buffer and subjected to ion exchange chromatography in a high performance amino acid analyzer. Knowing the amino acid sequence for each protein, amino acid quantification allowed the determination of protein concentration. Each concentration was corrected taking into account the internal standard.

SDS-PAGE

Gel electrophoresis under denaturing conditions was used for protein analysis. Polyacrylamide gels were made at 16% or 13% acrylamide (Bio-Rad; Hercules, CA) in the presence of SDS. Samples were prepared in loading buffer containing 0.03% bromophenol blue, 2% SDS, 10% glycerol containing 5% β-mercaptoethanol as reducing agent. Samples were boiled for 10 min (99°C) prior SDS-PAGE.

- **Coomassie staining**

  Gels were incubated in a solution of 1mg/ml Coomassie Brilliant Blue R-250, 50% MeOH, 10% acetic acid for 20 min. Staining of blue bands was visualized upon destaining with a 10% acetic acid, 45% MeOH solution.

- **Silver staining**

  Gels were fixed for 30 min in fixing solution (40% ethanol, 10% acetic acid) and incubated for 30 min in sensitizing solution (30% ethanol, 0.5% glutaraldehyde, 12.6 mM sodium thiosulphate, 0.8 M sodium acetate). To eliminate excess solution, gels were washed three times in miliQ water for 5 min. Gels were incubated with silver solution (0.6 mM silver nitrate, 0.04% formaldehyde) for 20 min, and after a quick wash with miliQ water, bands were developed with developing solution (0.2 M sodium carbonate, 0.02% formaldehyde). To stop the reaction, a 50 mM EDTA (pH 8.0) solution was used.

- **Western Blot**

Proteins were transferred to a PVDF membrane (Bio-Rad; Hercules, CA) using either a semidry system (1 h 2.3 mA/cm membrane) or a humid chamber (400 mA 1h 4^0C). Membrane was blocked with PBS-T 5% milk for 2h. The primary antibody was diluted in PBS-T and incubated overnight at 4°C. After extensive washing of the membrane to eliminate unbound antibody, a secondary antibody solution was incubated for 2h at room temperature. Washing allowed the elimination of excess of antibody and membranes were developed upon incubation with Millipore Immobilon® Western Chemiluminescent HRP Substrate (ECL). Images were recorded with ImageQuant LAS500 (GE Healthcare; Little Chalfont, UK).

The primary antibodies used were polyclonal rabbit anti-SP-C 1:1000 (WRAB-76696), and rabbit-anti-SP-B 1:1000 (WRAB-48604) from Seven Hills (Cincinnati, OH). The HRP-conjugated secondary antibody was a swain anti-rabbit 1:2000 (P0217) from Dako (Agilent technologies; Santa Clara, CA).

Thin Layer Chromatography (TLC)

Lipid-protein suspensions, including cholesterol/P-C particles, were prepared as in ATR-FTIR experiments (see sample preparation below). 10-40 µg of lipid standards in chloroform/methanol (2:1, v/v) and the different lipid-protein preparations were applied 1.5 cm from the bottom edge of a silica plate (Merck TLC Silica Gel 60; Merck Millipore; Darmstand, DE) and air-dried at room temperature. Lipid suspensions prepared to determine SP-C/Cholesterol interactions incorporated the fluorescent cholesterol analog TopFluor cholesterol (23-(dipyrrometheneboron difluoride)-24-norcholesterol; Avanti Polar Lipids, Alabaster, AL). In order to saturate the developing tank atmosphere with solvent vapors, the chamber was filled with the mobile phase 20 min before the development. The developing solvent used was chloroform/methanol/water (65:25:4, v/v/v) to allow phospholipids separation. To prevent drying of the solvent, the chamber was lined on three sides with Whatman No.1 paper (Whatman, Inc.) wetted with the mobile phase. TLC was developed at room temperature until the solvent front reached approximately 8-9 cm from the samples application point. Afterwards, the plate was removed from the chamber and air-dried to further analysis.

Sample detection

Two different methods of staining were used according to the detection of lipids or proteins:

- **Iodine staining**. A small amount of iodine crystals (Sigma Aldrich, St. Louis, MO) were deposited in a chromatographic chamber where the atmosphere saturates with iodine vapors upon sublimation. Iodine reacts with lipid C=C bonds resulting in yellowish spots appearing after 3-5 minutes incubation.

- **Phosphomolibdic acid staining**. A phosphomolibdic acid solution was employed to accurately detect neutral lipids, which are not properly observed upon iodine staining. Inorganic and organic molecules react generating intensely blue mixed oxides in which Mo (VI) is reduced to Mo (IV) (317). The solution was sprayed on the plate and spots were visualized upon incubation at 100ºC for at least 30 min.

- **Fluorescamine staining**. Fluorescamine reacts with primary amines yielding a fluorescent product visible under UV light. A 0.5% fluorescamine solution in acetone was sprayed on the plate and air dried. Proteins and amino lipids in our case were detected. The detection of fluorescence is possible under UV light. Images were recorded using a VersaDoc imaging system (Bio-Rad; Hercules, CA) in the epifluorescence mode. To confirm the presence of protein in the fluorescent bands revealed by fluorescamine staining, spots were scratched out from the silica plate and boiled in electrophoresis loading buffer with 5% β-mercaptoethanol 10 min at 99ºC. Then, protein bands were resolved by SDS-PAGE in a 13% acrylamide gel stained with silver and western blotting.

ATR-FTIR spectroscopy

Attenuated Total Reflectance Fourier Transform spectroscopy (ATR-FTIR) is a powerful technique based on the absorption of light in the medium infrared (MIR). The absorbed energy is translated into molecular vibrations with characteristic vibrational modes depending on the functional group. Thus, the ATR-FTIR spectrum represents a fingerprint of the molecule of interest.

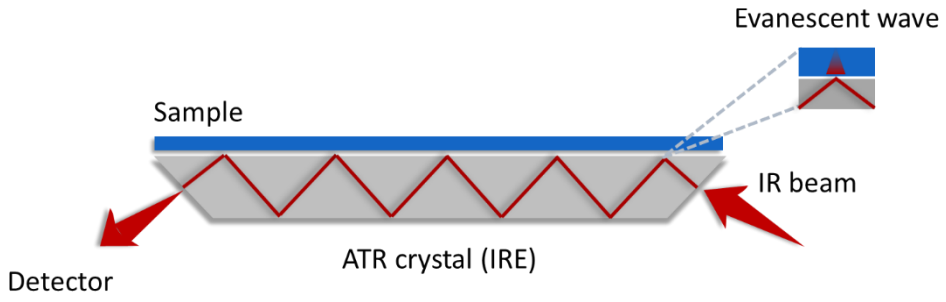

Figure 15. Schematic representation of the internal reflectance phenomenon. A sample film on a trapezoidal Internal Reflectance Element (IRE) absorbs energy from the evanescent wave generated by infrared light. The beam is reflected until it reaches the detector.

In an ATR-FTIR experiment, the sample is deposited on the surface of an internal reflectance element (IRE) made of a highly reflective material, a germanium crystal in this particular case. When the infrared beam enters the IRE, an evanescent wave is formed because of that internal reflectance (Fig. 15). The wave extends beyond the surface of the crystal into the sample (0.5-5 µm), and is attenuated by sample absorption. The remaining energy is passed back to the IR beam, which is reflected several times contacting the surface where the sample sits until it exits the IRE towards the detector.

ATR-FTIR is very useful to characterize lipid-protein samples, since the absorption bands associated to proteins and lipids present different frequencies in the spectrum and can be simultaneously analyzed (Fig. 16). In this Thesis, lipid-protein samples incorporating SP-C or rSP-C have been studied to assess the effect of palmitoylation on lipid-protein interactions in different lipid systems.

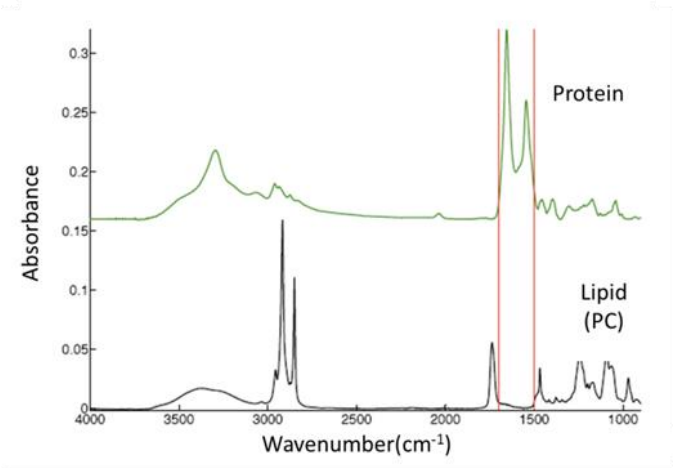

Figure 16. ATR-FTIR spectra of a protein (top) and lipid (bottom) film. Amide I and II bands (delimited between the red vertical lines) and lipid characteristic absorption bands appear in different wavenumbers.

- Sample preparation

Films were generated by mixing the appropriate amount of lipid or lipid and protein (7 wt%) in Chl/MeOH 2:1 v/v, and drying the samples under a stream of N_2. Solvent traces were eliminated by vacuum for 2 h in a SpeedVac Concentrator System (Thermo Scientific; Waltham, MS). Multilamellar vesicles were obtained by resuspending the dry lipid or lipid–protein films to a final phospholipid concentration of 10 mg/ml in 5 mM Tris pH 7.0 150 mM NaCl at 50°C for 1 h with intermittent shacking in a ThermoMixer (Eppendorf; Hamburg, DE). To increase sample concentration and eliminate salt excess, samples were centrifuged 1 h 21000g at 4°C and 4/5 of the supernatant was removed. The samples were kept at 4°C and resuspended prior measurements.

Acquisition of ATR-FTIR spectra

Oriented lipid multilayers were formed on the surface of the germanium crystal by slow evaporation of the lipid or lipid/protein aqueous suspensions under a nitrogen stream (318). Orientation of lipid multilayers was confirmed upon observation of the dichroic spectra.

ATR-FTIR spectra were recorded on a Bruker IFS66 FTIR spectrophotometer (Ettlingen, DE) equipped with a liquid nitrogen mercury cadmium telluride detector (MCT) in the double-sided, forward-backward mode at 2 cm^{-1} resolution and an aperture of 3.5 mm. The spectrometer was continuously purged with dry air. The internal reflection element was a germanium ATR plate with an aperture angle of 45^{o} yielding 25 internal reflections. To improve signal/noise ratio, 256 accumulations were collected per measurement. Measurements were carried out at 21, 25 and 37^{o}C. Temperature control was achieved by a thermostatized IRE support connected to a water bath Haake DC30 (Thermo Fisher Scientific Inc.; Waltham, MS).

Recorded spectra were corrected for the atmospheric water absorbance interferences by subtracting a reference atmospheric water spectrum. The subtraction coefficient was computed as the ratio of the atmospheric water band in the range 1562-1555 cm^{-1} on the sample spectrum with respect to the reference spectrum. Spectra were smoothed by apodization by a 4 cm^{-1} Gaussian line shape.

Secondary structure determination

The shape and intensity of the Amide I band is a sum of the contributions of all the secondary structure components of the protein or mixture of proteins present in the sample. To obtain the proportion of each particular secondary structure from the original spectrum, a deconvolution method is required (319). Using this method, the proportion of each structure is obtained by calculating the sum of all bands adjusted to a Lorentzian line (FWHH=30 cm^{-1}) and dividing by the total area of the amide I band.

Considering possible interferences due to the analysis method, spectral line shapes were directly compared. Subtraction spectra were obtained (SP-C – rSP-C) upon normalization with respect to amide I total intensity.

Molecular orientation

The determination of protein molecular orientation by infrared ATR spectroscopy has been reviewed by Goormaghtigh et al. (216). For these experiments, a thallium bromoiodiode wire grid polarizer KRS-5 (Specac; Kent, UK) was positioned between the IR beam and the IRE. Spectra were recorded with a parallel or perpendicular polarized incident light with respect to the plane defined by the ATR crystal. The dichroic ratio, R^{ATR}, is defined as the ratio of the absorption band recorded for the perpendicular polarization ($A^{\perp}$) with respect to the parallel polarization ($A^{\parallel}$):

$$R^{ATR}=A^{\perp}/\ A^{||}$$

In ATR, the dichroic ratio for an isotropic sample is different from the unity and is usually evaluated as the mean dichroism of the two lipid ester ν(C=O) bonds absorbing between 1762 and 1716 cm^{-1}. The mean orientation of the molecular axis with respect to the perpendicular of the ATR plate was estimated as described before (216). Although there is no consensus in the determination of an appropriate value for the orientation of amide I dipole in the α-helical structure; a value of 27^0 was used for the calculations (216).

- **Determination of band position**

Accurate band position (better than 0.1 cm^{-1}) were obtained by fitting a series of 11 data points, i.e. 5 cm^{-1} before the approximate maximum and 5 cm^{-1} after, by a third order polynomial and finding the roots of its derivative. It needs to be emphasized that this level of accuracy is much better than the nominal resolution of the spectrometer, which was set at 2 cm^{-1}, and the encoding of the data (every 1 cm^{-1}).

- **Data analysis**

Data were analysed with the subroutine Kinetics, (MATLAB R12), developed by Prof. Erik Goormatigh in the University of Brussels.

Fluorescence anisotropy

The phenomenon of fluorescence results from the emission of photons by molecules, termed fluorophores, in electronically exited states. This form of luminescence requires the previous excitation of those fluorophores from the ground state by providing energy in the form of light of a certain wavelength.

Fluorescence properties can be applied in several approaches to analyze molecular properties. In this Thesis, we made use of fluorescence anisotropy. The study of fluorescence anisotropy allows us to obtain information about the fluidity of a system by assessing the behavior of a fluorophore. A fluorophore is preferentially excited by those photons with electric vectors aligned parallel to its transition moment (photoselective excitation). When polarized light is applied, the selectively excited fluorophores emit photons in a certain direction, this is the polarized emission. Fluorescence anisotropy (r) is then calculated according to:

$$r = \frac{I_{II} - I_{\perp}}{I_{II} + 2I_{\perp}}$$

Where I_{II} is the fluorescence intensity recorded when the intensity of the emission polarizer is oriented parallel to the direction of the polarized excitation, and $I_{\perp}$ is that corresponding to the intensity with the emission polarizer oriented perpendicular to the polarized excitation. In the absence of artifacts, fluorescence anisotropy is not dependent on fluorophore concentration.

- CTL partitioning assay

The affinity of cholesterol for certain membranes can be assessed by measuring the amount of its fluorescent analog, CTL, remaining in lipid bilayers upon methyl-β-cyclodextrin (mβCD) extraction (230). The concentration of probe can be calculated from the anisotropy values considering that the mβCD-CTL complex moves isotropically (low anisotropy values) while within a lipid bilayer, CTL motions are restricted (higher anisotropy values). Using different mβCD concentrations it is possible to calculate a CTL molar fraction-partitioning coefficient (Kx) between the membrane and mβCD. Higher Kx values indicate a higher affinity of CTL for the bilayer as compared with mβCD.

The experiments conducted in this part of the Thesis were done at the laboratory directed by Prof. J. Peter Slotte in the Department of Biosciences in the Abo Akademi, Turku, Finland. Those experiments were supervised by PhD. Thomas Nyholm and Prof. J. Peter Slotte.

Lipid stocks were prepared in hexane/2-propanol 3:2 v/v and measured for phosphorus content. Vesicles were prepared by mixing phospholipids and CTL (2 mol%) in organic solvent. The solvent was evaporated under a stream of nitrogen at 40 ^{o}C. The dried films were thoroughly re-dissolved in Chl/MeOH (2:1, v/v) and the indicated amount of protein was added, typically 2 mol% (~10 wt% for SP-C). In the case of lung surfactant components, all were mixed in one single step and dried as described previously. Vesicles prepared for the experiments with synthetic phospholipids and the native protein fraction (SP-B+SP-C) included a 5-fold higher protein/phospholipid ratio compared to their native proportion in lung surfactant. After an additional solvent evaporation cycle, samples were maintained under vacuum overnight to eliminate solvent traces. Multilamellar suspensions were obtained by rehydrating lipid or lipid/protein films in 5 mM Tris pH 7.0 150 mM NaCl at a temperature above the gel-to-fluid transition temperature of phospholipids and vortexing. Large Unilamellar Vesicles (LUVs) were formed by extrusion through polycarbonate membranes with 200 nm pores. For vesicle curvature experiments, polycarbonate membranes with 30, 50, 100 and 200 nm pore size were used to generate unilamellar liposomes by extrusion.

For the partition assay, LUVs were dispensed into 100 nmol lipid fractions resulting in 10 tubes (final lipid concentration of 40 μM). One tube served to measure CTL anisotropy in each lipid system in the absence of mβCD, reflecting the motion state of CTL for each particular lipid composition. Increasing concentrations of mβCD were added to the remaining tubes (0.04 to 1 mM) to calculate the partition coefficient as detailed below.

For POPC and POPC/PSM vesicles, samples were saturated with argon to prevent oxidation, and incubated overnight at room temperature or 2h at 37ºC to allow the partitioning reach the equilibrium. For the rest of lipid systems tested, the incubation and measurements were carried out at 37ºC. After that, the steady-state anisotropy of CTL (at 23ºC or 37ºC) was measured using a PTI Quantamaster 1 (Photon Technology International; Edison, NJ) spectrofluorimeter operating in the T-format, with both the excitation and emission slits set to 5 nm. For CTL anisotropy, the samples were excited at 324 nm and the emission was measured at 390 nm. The molar concentration of CTL (C_{CTL}^{LUV}) for each sample was calculated from the measured anisotropies (230):

$$C_{CTL}^{LUV} = C_{CTL}\frac{(r_i - r_{m\beta CD})}{(r_{LUV} - r_{m\beta CD})} \qquad \text{(Eq.1)}$$

Where C_{CTL} is the total concentration of CTL in the samples, r_i is the anisotropy of CTL in the specific phospholipid bilayer in the absence of cyclodextrin, r_{LUV} is the CTL anisotropy in each measured sample, and $r_{m\beta CD}$ is the anisotropy of CTL in the CTL- mβCD complex. The anisotropy of the CTL- mβCD complex was 0.175 at room temperature and 0.170 at 37ºC. According to Eq. 1, the total concentration of CTL in the sample tube without mβCD, equals C_{CTL}^{LUV}.

The CTL concentrations calculated above were plotted against the mβCD concentration assuming a 2/1 CTL/cyclodextrin stoichiometry in the complexes as previously described (320). To calculate the molar fraction partition coefficient (K_x), those curves were fitted to Eq. 2 using the software Origin 7.5 (OriginLab corporation; Northampton, MA):

$$C_{CTL}^{LUV} = \frac{C_L - C_{CTL} + \frac{(C_{CD})^n}{K_X}}{2}\left(\sqrt{1 + 4\frac{C_L C_{CTL}}{\left[C_L - C_{CTL} + \frac{(C_{CD})^n}{K_X}\right]^2}} - 1\right) \qquad \text{(Eq. 2)}$$

Where C_L is the concentration of phospholipid; C_{CTL}, the concentration of CTL at the beginning of the assay; n, the stoichiometry of the complex CTL/mβCD; C_{CD}, the concentration of cyclodextrin and K_x, the partition coefficient. For the calculations, the phospholipid concentration was corrected after the CTL partitioning assay by phosphorus content determination.

▸ Determination of DPH-PC anisotropy in lung surfactant membranes

Hundred nmol lipid films were prepared by mixing the appropriate amount of the different lung surfactant fractions and DPH-PC (1 mol%). Films were dried as described in the previous section and maintained under vacuum overnight. The dried films were hydrated in 1 ml of 5 mM Tris pH 7.0 150 NaCl as described earlier, and extruded through 200 nm pores. An additional

milliliter of buffer was added and the steady-state anisotropy at 37°C was measured in the same instrument with the slits at 5 nm. All samples were excited at 358 nm and the fluorescence emission was measured at 430 nm.

Dynamic Light Scattering

Dynamic light scattering (DLS) is a well-stablished technique used to measure size and distribution of molecules in the submicron region. It is based on the principle of Brownian motion of molecules in a solution, which causes light to be dispersed at different intensities. By using the Stokes-Einstein relationship, it is possible to calculate particle size from the fluctuations in intensity.

In this Thesis, DLS measurements were performed to check the size of LUV dispersions using a Malvern Z-Sizer (Worcestershire, UK) with 5 mM Tris pH 7.0 150 mM NaCl as reference. Results are represented as sizes given by the number distribution.

Deuterium (^{2}H) - Nuclear Magnetic Resonance

^{2}H-NMR is a non-perturbing and very powerful technique employed to characterize lipid motion and structure in different environments. Replacement of hydrogen atoms by ^{2}H results in ^{2}H -labeled molecules suitable to study by ^{2}H-NMR.

^{2}H nuclei possess a nuclear spin of 1 (s=1), for that reason they are characterized by a quadrupolar interaction that governs the ^{2}H-NMR signal. For the resonance to occur, two principles must be fulfilled. First, a strong magnetic field needs to be applied in order to split the energy levels of the ^{2}H nucleus (Zeeman effect), and second, to induce a transition between those levels, the electromagnetic radiation applied has to match the ^{2}H nucleus resonance frequency or Larmor frequency. Because of the quadrupolar interaction, the energy levels of the ^{2}H nucleus lose their degeneracy, and therefore its associated spectrum is characterized by two peaks (a doublet). The distance between these two frequencies is termed the quadrupolar splitting ($\Delta\nu_Q$) and it is centered in the Larmor frequency (Fig. 3.4).

The quadrupolar splitting is related to the motion of each particular deuteron and to the orientational order parameter (S_{CD}):

$$S_{CD} = \frac{3\cos^2\theta - 1}{2} \qquad \text{(Eq. 3)}$$

Where θ is the angle between the C-^{2}H bond and the symmetry axis of the motion, that in the case of axially symmetric reorientations is the bilayer normal. These type of reorientations are very common in bilayers in the liquid crystalline phase. The quadrupolar splitting, and thus

the order parameter, reflects the average orientation of C-^{2}H bonds with respect to the direction of the magnetic field.

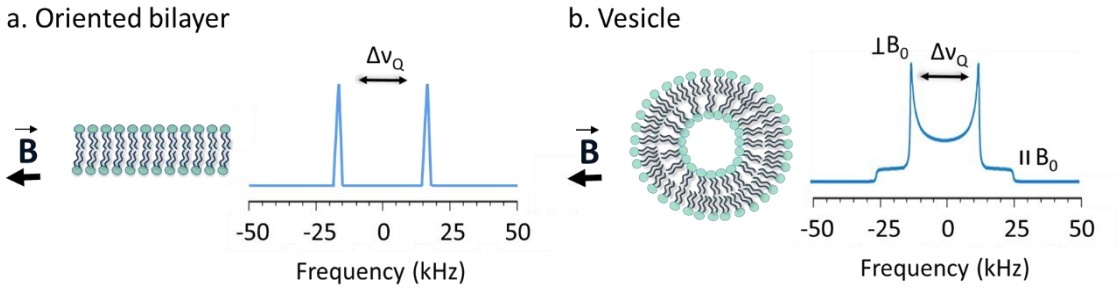

Figure 17. (a) ^{2}H-NMR spectrum for a molecule labeled with a single ^{2}H in membranes oriented with their normal perpendicular to the magnetic field. Two peaks are observed because of the quadrupolar interaction separated by the quadrupolar splitting. (b) In this case, the ^{2}H-labeled molecule forms part of a liposome. The highest signal is obtained for bilayer normals perpendicular to the magnetic field, and the lowest, for those in parallel.

For a deuterated lipid, every ^{2}H experience different conformational freedom depending on their position. In the case of perdeuterated phospholipids, ^{2}H motion along the acyl chain is more restricted for positions closer to the polar headgroup. The resulting spectrum will represent the contributions of each deuteron, characterized by doublets with particular quadrupolar splittings (Fig. 18 top and bottom).

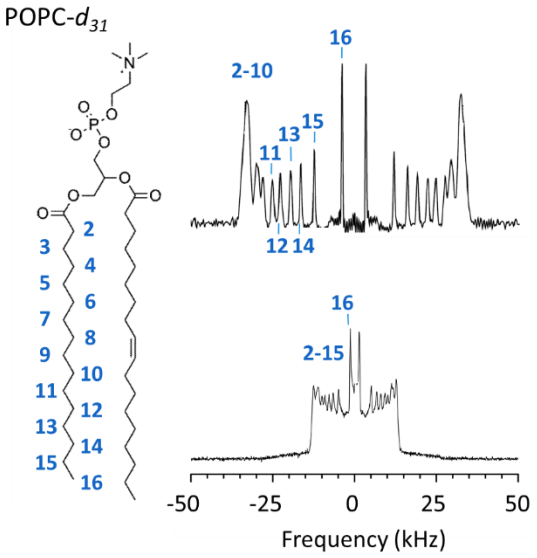

Figure 18. ^{2}H- spectra showing the contribution of ^{2}H placed in the indicated positions of the POPC molecule for an oriented membrane (top) and liposomes (bottom). More mobile positions (C16) appear with lower splittings whereas more restricted positions (C2) result in larger splittings.

For a multilamellar non-oriented sample, bilayer normal adopts all possible directions and the corresponding spectra is termed powder spectra. Higher intensities (represented by Pake doublets) are obtained when the bilayer normal is oriented perpendicular to magnetic field, whereas when it is located in parallel gives rise to the lowest intensities (Fig. 17b).

In the present Thesis, we aimed to characterize the effect of SP-C and cholesterol in lung surfactant mimicking membranes. Since SP-C palmitoylation has been observed as an important factor related to the SP-C/cholesterol relationship (215), the effects of a recombinant version of SP-C (rSP-C) lacking acylation was also analyzed.

The experiments described in this section were conducted in the laboratories of Dr. Valerie Booth and Dr. Michael M. Morrow at the Department of Biochemistry and Department of Physics and Physical Oceanography (Faculty of Science) in the Memorial University of Newfoundland, in Saint John's, Newfoundland, Canada.

For ^{2}H-NMR experiments, the deuterated lipids employed were: 1,2-dipalmitoyl-d62-sn-glycero-3-phosphocholine (DPPC-d_{62}), 1-palmitoyl-d31-2-oleoyl-sn-glycero-3-phosphocholine (POPC-d_{31}), 1-palmitoyl-d31-2-oleoyl-sn-glycero-3-[phospho-rac-(1-glycerol)] (POPG-d_{31}) and 5-Cholesten-3β-ol-2,2,3,4,4,5-d6 (Chol-d_6). Deuterated phospholipids were obtained from Avanti Polar Lipids (Alabaster, AL) and deuterated cholesterol were from Cambridge Isotope Laboratory (Tewksbury, MA). They were combined to configure three equivalent lipid systems: DPPC-d_{62}/POPC/POPG, DPPC/POPC-d_{31}/POPG and DPPC/POPC/POPG-d_{31} (50/25/15 w/w/w). To observe if cholesterol suffered any specific alteration in mobility, samples of DPPC/POPC/POPG + 10 wt% Chol-d_6 were also analyzed. All these systems allowed us to analyze the behavior of each component independently either in the pure lipid system or in the presence of SP-C or rSP-C and/or cholesterol.

Lipid and lipid-protein samples were prepared by mixing individual components in Chl/MeOH 2:1 v/v and drying by rotary evaporation at 50^{o}C. 12.6 mg of phospholipid were used per sample and 5 wt% protein and/or 10 wt% cholesterol were incorporated when indicated (see results section). Solvent traces were removed by vacuum for at least 6 hours and samples were kept at -20^{o}C until used. Multilamellar suspensions were obtained by the addition of 5 mM Tris pH 7.0 150 mM NaCl at 60^{o}C and vortexing yielding a final phospholipid concentration of 45 mg/ml. Samples were carefully transferred to 8-mm NMR tubes and sealed.

For samples containing Chol-d_6, the amount of material was increased to 25.5 mg of phospholipid. Samples were processed as previously mentioned and hydrated in 350 µl of 5 mM Tris pH 7.0 150 mM NaCl.

- NMR Spectra acquisition

Samples were positioned into a cylindrical coil and the probe was placed into the NMR spectrometer. Samples were allowed to equilibrate at the desired temperature for at least 15 min prior measurement. Temperature was measured and controlled to ±0.1 ^{o}C using a digital temperature controller (model 325, Lakeshore Cryotronics, Westerville, OH). ^{2}H-NMR spectra were collected in a 9.4 T superconducting solenoid operating at a resonance frequency of 61.42 mHz for ^{2}H nuclei.

Free-induction decay (FID) signals fades rapidly since ^{2}H-NMR line shapes are very broad. To collect those signals is thus problematic, since most of the FID signal is lost during the receiver

recovery time. A way to overcome this is to employ an echo pulse sequence (π/2− τ −π/ 2−acq) (321). The two pulses are separated by a time τ, delaying the echo formation a time 2τ, after which the receiver has already recovered and can start data collection. For these experiments, π/2 pulses were in a range of 5-6 µs separated by τ 35µs and acquired during 0.9 s as observed in the scheme in Fig. 19.

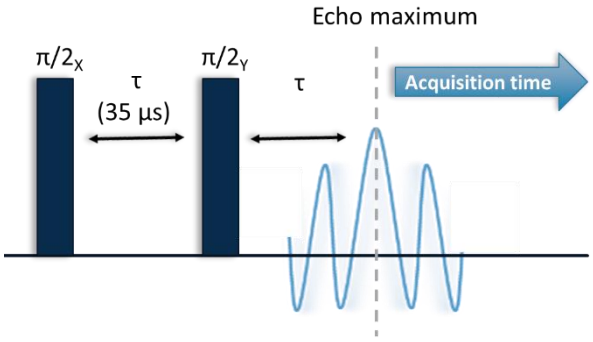

Figure 19. Schematic representation of the quadrupole echo sequence employed for the ^{2}H-NMR experiments carried out in this section.

A dwell time of 1 µs was employed and 8192 points were collected. Oversampling by a factor of 4 was applied to give an effective dwell time of 4 µs corresponding to a frequency of 250 kHz, appropriate for a liquid crystalline spectrum (322). The FID was left-shifted to place the echo maximum at the first point and Fourier transformed to obtain the spectra in the frequency domain. All the spectra presented here have been previously phase-corrected and normalized.

For each spectrum of samples containing DPPC-d_{62}, 40,000-48,000 transients were averaged. For samples containing POPC-d_{31}, 80,000 transients were averaged, and for POPG-d_{31}, 96000. In the case of samples with deuterated cholesterol, 176,000 transients were accumulated. Deuterium has a natural abundance of 0.016%, thus, the narrow peak obtained in the center of most spectra likely arises from isotropic reorientations of deuterium molecules present in the buffer.

Electron Spin Resonance (ESR)

ESR, also termed Electronic Paramagnetic Resonance (EPR), is a non-perturbing spectroscopic technique based on the properties of molecules possessing unpaired electrons. As well as ^{2}H-NMR, it has been widely employed to characterize membrane fluidity and order. Besides, it constitutes a very sensitive technique, since it allows the detection of amounts of probe in the order of ~0.05 pmol in 10-50 µl.

As occurs for ^{2}H nuclei in ^{2}H-NMR, under a magnetic field the energy levels of an unpaired electron split (Zeeman effect). A transition between those levels can take place by applying an electromagnetic radiation. Unlike ^{2}H-NMR frequency, for these experiments is fixed to 10 GHz and the magnetic field is varied until the resonance is registered, being that resonance the absorbance of frequency of a defined energy to perform a transition.

Since no unpaired electrons are usually present in biological membranes, spin-labels are employed to generate extrinsic spin-labeled probes. Different chemical groups, such as nitroxide

radicals, can be employed as spin-labels. These labels can be placed in different positions along the aliphatic chain of phospholipids, providing information on the degree of mobility at different depths in the membrane. For the studies performed here, the modified acyl chain is in the *sn*-2 position of a phosphatidylcholine. Because of that, these spin labels receive the name of *n*-PCSL, being *n* the position the nitroxide group occupies along the hydrocarbon chain.

In the nitroxide group, the spins of the oxygen electron and the nitrogen nucleus interact in what is designated as hyperfine coupling. Because of this phenomenon, the Zeeman energy levels are perturbed resulting in ESR spectra characterized by three lines (a typical ESR spectrum is represented in a first-derivate form). Depending on the rate and amplitude of the rotation of the spin-labeled position in the phospholipid, the spectral features of these lines differ. For fluid systems, a higher lipid mobility averages the orientational anisotropy of motion, resulting in narrower spectra. In contrast, for motionally restricted molecules, spectra are wider and exhibit shoulders as a consequence of their highly anisotropic movement.

Several spectral parameters can be used to characterize an ESR spectrum, but the more widely employed is the outer hyperfine splitting constant ($2A_{max}$). This is measured as the spectral width from the first maximum in the low-field wing of the spectrum and the last minimum of the high-field segment of the spectrum as illustrated in Fig. 20.

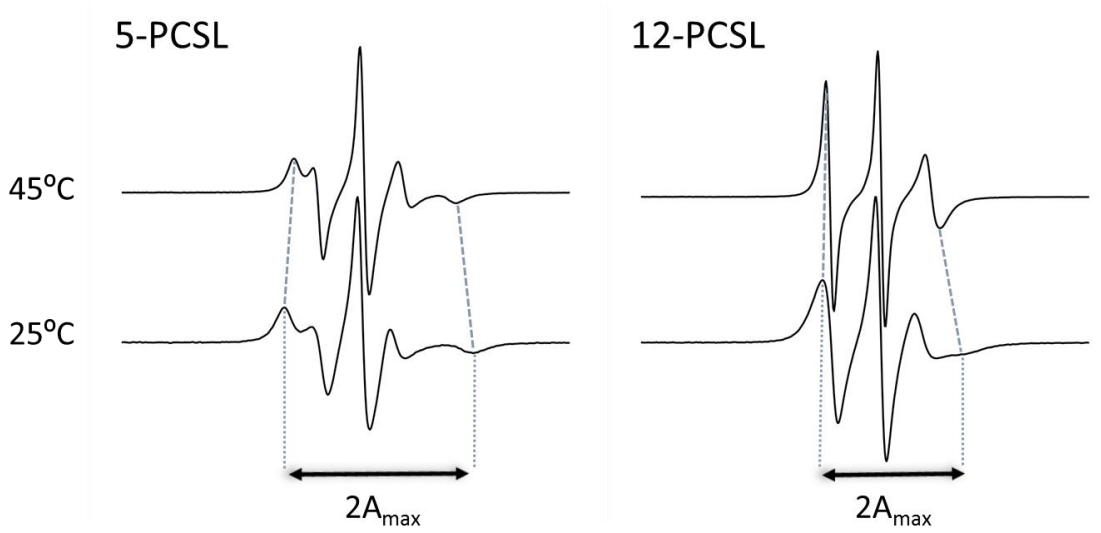

Figure 20. ESR spectra of 5-PCSL and 12-PCSL at 25ºC and 45ºC included in multilamellar vesicles of DPPC/POPC/POPG 50/25/15 (w/w/w). The outer hyperfine coupling constant ($2A_{max}$) is indicated below each set of spectra. $2A_{max}$ decreases with temperature as encounter a more fluid system. Depending on the n-position of the label along the acyl chain, $2A_{max}$ also adopts different values. Positions with a restricted mobility, such as those close to the polar headgroup, results in higher $2A_{max}$ values, as can be deduced from the comparison between 5-PCSL and 12-PCSL spectra.

In this Thesis, to sample motions close to the polar region and hydrophobic core of the membrane respectively, two spin-labeled lipids have been used, 5-PCSL and 12-PCSL. These modified lipids, 1-palmitoyl-2-stearoyl-(n-doxyl)-sn-glycero-3-phosphocholine, with n=5 or n=12

were purchased from Avanti Polar Lipids (Alabaster, AL). 1mg/ml stocks of each probe were prepared in Chl/MeOH 2:1 v/v and used without further analysis.

0.9 mg of lipid or lipid/protein samples were prepared by mixing individual components in Chl/MeOH 2:1 v/v. 1 mol% of probe was added in organic solvent. Samples were dried under a constant stream of nitrogen and solvent traces were vacuum-evaporated for 2 hours using an SpeedVac Concentrator System (Thermo Fisher Scientific; Waltham, MS). Until hydrated, samples were kept at -20^{o}C.

Hydration was carried out at 55^{o}C for 1h by addition of 5 mM Tris pH 7.0 150 mM NaCl to a final phospholipid concentration of 11.25 mg/ml in a ThermoMixer (Eppendorf; Hamburg, DE) with intermittent shacking. Samples were transferred to 1-mm capillaries and spun down at 21100g at 4^{o}C using a Sorvall microfuge equipped with a capillaries rotor. Excess of supernatant was removed and capillaries were flame-sealed before measurements.

- ESR Spectra acquisition

ESR experiments were performed in the Research Support Center (Resonance facility) in the Complutense University, Madrid. ESR spectra were recorded on a Bruker EMX 10/12 equipped with a nitrogen flow temperature regulation system. Sample capillaries were inserted into a quartz tube with silicone oil for thermal stability. Typically, 2 scans were accumulated to improve signal/noise ratio with 4-min scan time.

Spectra were collected using the WinEPR software with the following instrumental settings: 10 mW microwave power, 1.25-G modulation amplitude, 100 kHz modulation frequency, 0.33 s time constant, 100-G scan range and 3360-G center field.

Flow cytometry

Flow cytometry is a widely employed technique to characterize cell properties in a qualitative and quantitative manner. Cell size (measured by the Forward Scatter, FSC), internal complexity (measured with the Side Scatter, SSC) and other properties, including the presence of specific markers, can be investigated simultaneously by the use of cell optical properties and different fluorescent probes (Fig. 21).

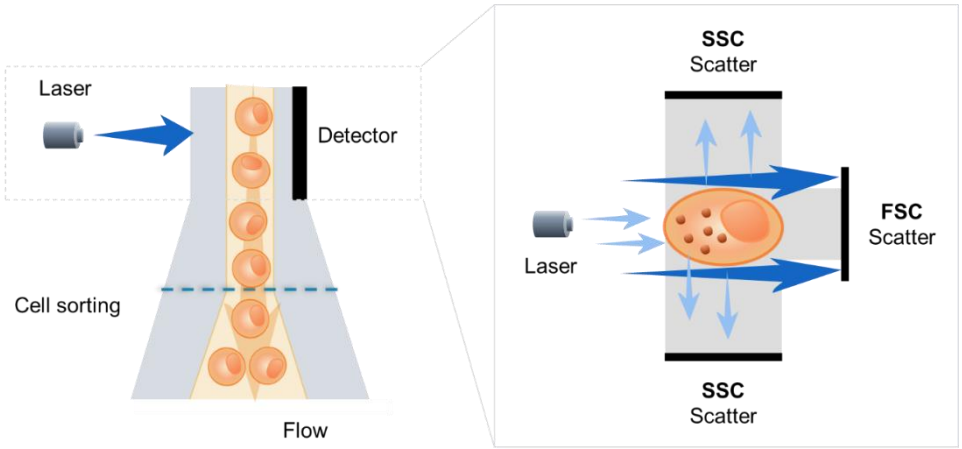

Figure 21. Schematic representation of a flow cytometry experiment.

The cytometer creates a laminar flow in which every single cell pass independently through a beam of monochromatic light (Fig. 21). At the intersection point, light is emitted in all directions and collected by the optical unit of the cytometer. The amplification of the signal (photomultiplier tubes) and the detection of concrete wavelengths (dichroic mirrors and detectors) allows the profiling of a particular sample in terms of fluorescence intensity for a defined fluorochrome, and relative proportion of positive events/cells with respect to measured events. Typically, results are presented as a histogram or a two-dimensional dot-plot graph.

To analyze the engulfment of lipid vesicles by alveolar macrophages, cells incubated with different types of fluorescently labeled vesicles were analyzed by flow cytometry using a MACSQuant 10 analyzer (Miltenyi Biotech, Cologne, DE). These experiments were done in collaboration with Prof. Matthias Ochs´s group (Department of Functional and Applied Anatomy, Hannover Medical School, Germany) under the supervision of Dr. Elena López-Rodríguez.

Engulfment assay

Lipids and proteins in Chl/MeOH were mixed in the indicated proportions and labeled with 5 wt% of TopFluor cholesterol (23-(dipyrromethene boron difluoride)-24-norcholesterol, Avanti Polar Lipids) in Chl/MeOH 2:1 v/v. When indicated, samples were labeled with 5wt% Bodipy PC (Bis-BODIPY® FL C11-PC; 1,2-Bis-(4,4-Difluoro-5,7-Dimethyl-4-Bora-3a,4a-Diaza-s-Indacene-3-Undecanoyl)-sn-Glycero-3-Phosphocholine); Thermo Fisher Scientific; Waltham, MS).Samples were protected from light to avoid fluorescence bleaching. Solvents were evaporated in a fume hood at 40ºC and samples maintained in a vacuum oven at 50ºC overnight. Lipid films were hydrated to 0.5 mg/ml with 50 mM Tris pH 7.0 150 mM NaCl at 60ºC for 1h at 1400 rpm in a Thermo–Shaker TS-100C (BioSan, Riga, LV).

5 wt% of TopFluor cholesterol (TFC) was also employed to label a clinical surfactant preparation (Curosurf, Chiesi Farmaceutici, Parma, IT). The calculated amount of probe was added to a tube as an organic solution and dried at room temperature. For cholesterol-

containing Curosuf samples, the required amount of cholesterol was also supplied as an organic solution and dried at the bottom of the tube. After drying, Curosurf was diluted to 0.5 mg/ml with 50 mM Tris pH 7.0 150 mM NaCl, and both labeling and cholesterol incorporation (when necessary) were performed at 50^0C for 1h in a Thermo-Shaker TS-100C (BioSan, Riga, LV).

The multilamellar lipid suspensions and Curosurf were diluted with 50 mM Tris pH 7.0 150 mM NaCl to add 10 µl per well of a p96 plate at the corresponding concentration (see Results).

For the cytometry experiments, 10^5 cells/well in 90 µl PBS were administrated 10 µl lipid suspensions and incubated at room temperature for the indicated times and lipid concentrations (see Results). Cells were re-suspended by pipetting before and after lipid addition and just prior flow cytometry measurements. At least 10.000 events were recorded per sample. Vesicle engulfment was detected in the FITC channel and quantified by stablishing a thershold according to the fluorescence detected from non-treated cells.

Data were analyzed with MacsQuant software (Miltenyi Biotec; Cologne, DE) and GraphPad Prism 5 (La Jolla, CA).

- **Engulfment inhibition**

Endocytosis inhibitors, amantadine, cytochalasin D, chlorpromazine, methyl-β-cyclodextrin, genistein and bafilomycin A1, were from Sigma Aldrich (St. Louis, MO). Blocking anti-mouse CD14 antibody was from Biolegend (Cambridge, UK) and anti-mouse CD45 antibody, from Miltenyi Biotech (Cologne, DE).

Inhibitors or antibodies were applied and incubated for 30 min at room temperature and 4^0C in darkness respectively. Cells were washed after treatment and resuspended in PBS for the engulfment assay.

Real time PCR (qPCR)

The transcriptional response of MH-S cells to lipid engulfment was analyzed by qPCR. 10^6 cells in 1ml of PBS were treated for 1h at room temperature with 2.5 µg of lipid suspension prepared as detailed above. After treatment, cells were washed with PBS and cell pellets were re-suspended in lysis buffer (RNA mini Kit; Bioline; Berlin, DE) and kept at -20^0C until employed. Total RNA was isolated from 10^6 cells with the RNA mini Kit (Bioline, Berlin, DE) and quantified by measuring the absorbance at 260 nm in a Nanodrop. 1 µg of total RNA was reversed transcripted in a thermocycler (MasterCycler, Eppendorf; Hamburg, DE) employing the iScript cDNA Synthesis Kit (Bio-Rad; Hercules, CA). Real-time PCR was performed with iQ SYBR Green Supermix (Bio-Rad; Hercules, CA) starting from 50 ng cDNA and a primer concentration of 100 nM. Antibody-mediated hotstart iTaq DNA polymerase was activated after an initial 3-min

denaturation step at 95°C. Denaturation of DNA was accomplished by holding further 95°C for 10 s. Annealing and extension temperature was set to 59°C (30 s) for 40 cycles in a Bio-Rad CFX96 Real Time PCR system (Bio-Rad; Hercules, CA).

qPCR data was analyzed using the Livak method (323) and represented as fold change with respect to the control sample (un-treated cells) and the gene for β-actin (*Actb*) as reference gene. Data was clustered according to target gene and type of sample using the corresponding tool in BioRad CFXManager (Bio-Rad; Hercules, CA.)

Primers were designed employing a NCBI tool (https://www.ncbi.nlm.nih.gov/tools/primer-blast/) and sequences are shown in Table 1.

Table 1. Sequence of the primers used of qPCR experiments.

Gene name	Forward	Reverse
Nr1h3	CAGGTTGGGTGTTTTCTGGC	GAAGAACCCTGCACAAAGTGG
Nr1h2	CTCGGTCCAGGAGATTGTGG	CTGTCTCGTGGTTGTAGCGT
Abca1	GCGACCATGAAAGTGACACG	CAGCACATAGGTCAGCTCGT
Abcg1	GGATTTCATCGTCCTGGGCA	TGGCTTGGAGGCGGTTTTTA
Cyp2711	GGTCGGAGGATTGCAGAACT	TCACCTTCTTGCTGGGAACC
Cd36	ATGAATGGTTGAGACCCCGTG	GATTGGCTTCAGGGAGACTGT
Msr1	CCTTTCACCTCTGGACAAGTCA	ATGTCAATGGAGGCCCCAAC
Srebf2	TGATGATCACCCCGACGTTC	GTCACGAGGCTTTGCACTTG
Hmgcr	TTGGAGTTGGCACCATGTCA	CTCTAGGACCAGCGACACAC
Ldl-r	TCAGTGCCAATCGACTCACG	GTCTCACACCAGTTCACCCC
Npc1	AAAGGCAACGTGTTCTTCACAG	GTTAAAACCCATGAGCGTTGTCT
Npc2	CATTGTCCCCCGAGATAGCC	CCATCCTGTCTGGTGGAACC
Lipa	CCACCAAGTAGGTGTAGGCAC	TGCATCTTCCGGGAGTGGT
Dhcr24	GATGAATGGTCAACGCGAGC	TTTGGGTGACACAGGTTGCT
Ch25h	CGTCCAGCTCCTAAGTCACG	AGGACGAGTTCTGGTGATGC
Lpla2	ACCCCAGCAAGAGGAATGTG	CCGTTTTCATTTGGGGCTCG
Pparg	CGGTGAACCACTGATATTCAGGA	CGGTGAACCACTGATATTCAGGA
Actb	ATCCTCTTCCTCCCTGGAGA	AGGATTCCATACCCAAGAAGGA

Bright field microscopy

Cell morphology was analyzed after staining with a Diff-Quik kit (Medion Grifols Diagnostics; Düdingen, CH), in a Zeiss microscope equipped with a Leica DM6000B camera (Leica; Weztlar, DE).

Fluorescence microscopy

Fluorescent microscopy allows visualizing specific fluorophores in a sample. The preparations were observed using a Leica DM-400B microscope (Weztlar, DE) illuminated with a mercury

lamp (LEICA EL6000) and equipped with L5 and TX2 fluorescence filter sets. Micrographs were recorded with a cooled digital camera (Model C10600-10B ORCA-R2, Hamamatsu).

Sample preparation

MH-S cells were treated with lipid suspensions (16 µg lipid/ 10^6 cells) prepared as detailed above (see Engulfment assay above) incorporating 10 wt% of fluorescently labelled SP-C (TxR-SP-C). Non-engulfed vesicles were removed by cell washing with PBS. Treated and non-treated cells were spun down on a slide using a Thermo Shandon cytospin 3 (Thermo Scientific; Waltham, MS). Cells were fixed with ice-cold acetone/MeOH 3:2 v/v for 5 min and washed extensively with PBS. DAPI (1:10000) was used to counterstain nuclei and excess was removed by washing with PBS. Finally, cell preparations were mounted with a fluorescence mounting medium (Leica; Weztlar, DE).

Transmission Electron Microscopy

Transmission Electron Microscopy (TEM) employs electrons as a light source, achieving resolutions at the amstrong (Å) scale. The electron beam goes through the sample of study and it is scattered depending on sample density. Unscattered electrons hit a fluorescent screen giving the final image. TEM micrographs were obtained in a Morgagni 268 microscope (Eindhoven, NL) equipped with a digital camera (Olympus Soft Imaging Systems; Münster, DE) at a final 9000x magnification.

Sample preparation for TEM

$5{\cdot}10^6$ MH-S cells were treated with 12.5 µg of lipid suspension (0.25 µg lipid/ 10^5 cells) for 1h at room temperature. Cells were centrifuged and fixed with 4% paraformaldehyde in PBS for at least 30 min. After that, cells were again concentrated by centrifugation and embedded in low melting point agarose (Sigma Aldrich, St. Louis, MO) previously dissolved in PBS at 40^0C. The agarose block was diced into small cubes and further fixed by immersion in 4% paraformaldehyde in PBS for 24 h at 4°C. Cubes were embedded in Epon (Serva, Heidelberg, DE), and contrasted with 1% osmium tetroxide (EMS, Hatfield, PA) and 4% uranyl acetate (Serva, Heidelberg, DE) for analysis by electron microscopy.

Cryo-TEM

Cryo-TEM is a high-resolution EM technique in which samples are studied at cryogenic temperatures without the need of staining. Cryogenized samples preserve their morphology and

ultrastructure, making this technique particularly useful to study membrane structure from vesicle solutions.

Freshly prepared LUVs made of DPPC/POPC/POPG (50:25:15, w/w/w), in the absence or presence of SP-C, were applied to holey carbon copper grids (R2/2; Quantifoil, Großlöbichau, DE) and vitrified using a Cryoplunge (Gatan, Pleasanton, CA). The grids were imaged in a JEM-1230 transmission electron microscope (JEOL; Tokyo, JP) operated at 100 kV and recorded at a final magnification of 5.68 Å/px using an F416 CMOS camera from TVIPS (Gauting, DE).

9. References

1. Jetté, M., K. Sidney, and G. Blümchen. 1990. Metabolic equivalents (METS) in exercise testing, exercise prescription, and evaluation of functional capacity. Clin. Cardiol. 13: 555–565.

2. Brown, E.S. 1957. Lung Area from Surface Tension Effects. Proc. Soc. Exp. Biol. Med. 95: 168–170.

3. Ochs, M., J.R. Nyengaard, A. Jung, L. Knudsen, M. Voigt, T. Wahlers, J. Richter, and H.J.G. Gundersen. 2004. The Number of Alveoli in the Human Lung. Am. J. Respir. Crit. Care Med. 169: 120–124.

4. Hogan, J., P. Smith, and D. Heath Peter Harris. 1986. The thickness of the alveolar capillary wall in the human lung at high and low altitude. Br. J. Dis. Chest. 80: 13–18.

5. Maina, J.N., and J.B. West. 2005. Thin and strong! The bioengineering dilemma in the structural and functional design of the blood-gas barrier. Physiol. Rev. 85: 811–844.

6. Mason, R.J. 2006. Biology of alveolar type II cells. Respirology. 11 Suppl: S12-5.

7. Fehrenbach, H. 2001. Alveolar epithelial type II cell: defender of the alveolus revisited. Respir. Res. 2: 33–46.

8. Barkauskas, C.E., M.J. Cronce, C.R. Rackley, E.J. Bowie, D.R. Keene, B.R. Stripp, S.H. Randell, P.W. Noble, and B.L.M. Hogan. 2013. Type 2 alveolar cells are stem cells in adult lung. J. Clin. Invest. 123: 3025–36.

9. Lopez-Rodriguez, E., G. Gay-Jordi, A. Mucci, N. Lachmann, and A. Serrano-Mollar. 2016. Lung surfactant metabolism: early in life, early in disease and target in cell therapy. Cell Tissue Res. : 1–15.

10. Orgeig, S., W. Bernhard, S.C. Biswas, C.B. Daniels, S.B. Hall, S.K. Hetz, C.J. Lang, J.N. Maina, A.K. Panda, J. Perez-Gil, F. Possmayer, R.A. Veldhuizen, and W. Yan. 2007. The anatomy, physics, and physiology of gas exchange surfaces: Is there a universal function for pulmonary surfactant in animal respiratory structures? Integr. Comp. Biol. 47: 610–627.

11. Pérez-Gil, J. 2008. Structure of pulmonary surfactant membranes and films: The role of proteins and lipid-protein interactions. Biochim. Biophys. Acta - Biomembr. 1778: 1676–1695.

12. Goerke, J. 1998. Pulmonary surfactant: functions and molecular composition. Biochim. Biophys. Acta - Mol. Basis Dis. 1408: 79–89.

13. Orgeig, S., J.L. Morrison, and C.B. Daniels. 2015. Evolution, Development, and Function of the Pulmonary Surfactant System in Normal and Perturbed Environments. Compr. Physiol. 6: 363–422.

14. Miller, N.J., A.D. Postle, S. Orgeig, G. Koster, and C.B. Daniels. 2006. The composition of pulmonary surfactant from diving mammals. Respir Physiol Neurobiol. 152: 152–168.

15. Pynn, C.J., M.V. Picardi, T. Nicholson, D. Wistuba, C.F. Poets, E. Schleicher, J. Perez-Gil, and W. Bernhard. 2010. Myristate is selectively incorporated into surfactant and decreases dipalmitoylphosphatidylcholine without functional impairment. Am. J. Physiol. Regul. Integr. Comp. Physiol. 299: R1306-16.

16. Jouhet, J. 2013. Importance of the hexagonal lipid phase in biological membrane organization. Front. Plant Sci. 4: 494.

17. Marsh, D. 2010. Structural and

thermodynamic determinants of chain-melting transition temperatures for phospholipid and glycolipids membranes. Biochim. Biophys. Acta - Biomembr. 1798: 40–51.

18. Cruz, A., and J. Perez-Gil. 2007. Langmuir films to determine lateral surface pressure on lipid segregation. Methods Mol. Biol. 400: 439–457.

19. Discher, B.M., K.M. Maloney, W.R. Schief Jr., D.W. Grainger, V. Vogel, and S.B. Hall. 1996. Lateral phase separation in interfacial films of pulmonary surfactant. Biophys J. 71: 2583–2590.

20. Mouritsen, O.G., and L.A. Bagatolli. 2015. Lipid domains in model membranes: a brief historical perspective. Essays Biochem. 57: 1–19.

21. Veatch, S.L., I. V Polozov, K. Gawrisch, and S.L. Keller. 2004. Liquid domains in vesicles investigated by NMR and fluorescence microscopy. Biophys. J. 86: 2910–22.

22. Bernardino de la Serna, J., R. Vargas, V. Picardi, A. Cruz, R. Arranz, J.M. Valpuesta, L. Mateu, and J. Perez-Gil. 2013. Segregated ordered lipid phases and protein-promoted membrane cohesivity are required for pulmonary surfactant films to stabilize and protect the respiratory surface. Faraday Discuss. 161: 535–589.

23. Bernardino de la Serna, J., J. Perez-Gil, A.C. Simonsen, and L.A. Bagatolli. 2004. Cholesterol rules: direct observation of the coexistence of two fluid phases in native pulmonary surfactant membranes at physiological temperatures. J Biol Chem. 279: 40715–40722.

24. Lopez-Rodriguez, E., A. Cruz, R.P. Richter, H.W. Taeusch, and J. Pérez-Gil. 2013. Transient exposure of pulmonary surfactant to hyaluronan promotes structural and compositional transformations into a highly active state. J. Biol. Chem. 288: 29872–29881.

25. Baumgart, F., L. Loura, M. Prieto, and J. Pérez-Gil. 2009. Pulmonary Surfactant Protein C Reduces the Size of Liquid Ordered Domains in a Ternary Membrane Model System. Biophys. J. 96: 608a–609a.

26. Wüstneck, R., J. Perez-Gil, N. Wüstneck, A. Cruz, V.B. Fainerman, and U. Pison. 2005. Interfacial properties of pulmonary surfactant layers. Adv. Colloid Interface Sci. 117: 33–58.

27. Nag, K., S.G. Taneva, J. Perez-Gil, A. Cruz, and K.M. Keough. 1997. Combinations of fluorescently labeled pulmonary surfactant proteins SP-B and SP-C in phospholipid films. Biophys. J. 72: 2638–50.

28. Wright, J.R. 2005. Immunoregulatory functions of surfactant proteins. Nat Rev Immunol. 5: 58–68.

29. Crouch, E., and J.R. Wright. 2001. Surfactant proteins a and d and pulmonary host defense. Annu. Rev. Physiol. 63: 521–54.

30. Crouch, E.C., A. Persson, D. Chang, and J. Heuser. 1994. Molecular structure of pulmonary surfactant protein D (SP-D). J. Biol. Chem. 269: 17311–17319.

31. Kishore, U., T.J. Greenhough, P. Waters, A.K. Shrive, R. Ghai, M.F. Kamran, A.L. Bernal, K.B.M. Reid, T. Madan, and T. Chakraborty. 2006. Surfactant proteins SP-A and SP-D: Structure, function and receptors. Mol. Immunol. 43: 1293–1315.

32. Wright, J.R., and J.A. Clements. 1987. Metabolism and Turnover of Lung Surfactant. Am. Rev. Respir. Dis. 136: 426–444.

33. Voorhout, W.F., T. Veenendaal, Y. Kuroki, Y. Ogasawara, L.M. van Golde, and H.J. Geuze. 1992. Immunocytochemical localization of surfactant protein D (SP-D) in type II cells, Clara cells, and alveolar macrophages of rat lung. J. Histochem. Cytochem. 40: 1589–1597.

34. Wang, J., P. Souza, M. Kuliszewski, A.K. Tanswell, and M. Post. 1994. Expression of surfactant proteins in embryonic rat lung. Am. J. Respir. Cell Mol. Biol. 10: 222–229.

35. Ochs, M., G. Johnen, K.M. Müller, T. Wahlers, S. Hawgood, J. Richter, and F. Brasch. 2002. Intracellular and intraalveolar localization of surfactant protein a (SP-A) in the parenchymal region of the human lung. Am. J. Respir. Cell Mol. Biol. 26: 91–98.

36. Fisher, A.B., C. Dodia, P. Ruckert, J.-Q. Tao, and S.R. Bates. 2010. Pathway to lamellar bodies for surfactant protein A. Am. J. Physiol. Lung Cell. Mol. Physiol. 299: L51-8.

37. Pérez-Gil, J. 2010. El sistema surfactante pulmonar. Investig. Cienc. 401.

38. Wu, H., A. Kuzmenko, S. Wan, L. Schaffer, A. Weiss, J.H. Fisher, K.S. Kim, and F.X. McCormack. 2003. Surfactant proteins A and D inhibit the growth of Gram-negative bacteria by increasing membrane permeability. J. Clin. Invest. 111: 1589–1602.

39. Minutti, C.M., B. García-Fojeda, A. Sáenz, M. de Las Casas-Engel, R. Guillamat-Prats, A. de Lorenzo, A. Serrano-Mollar, Á.L. Corbí, and C. Casals. 2016. Surfactant Protein A Prevents IFN-γ/IFN-γ Receptor Interaction and Attenuates Classical Activation of Human Alveolar Macrophages. J. Immunol. 197: 590–8.

40. Kuroki, Y., and T. Akino. 1991. Pulmonary surfactant protein A (SP-A) specifically binds dipalmitoylphosphatidylcholine. J. Biol. Chem. 266: 3068–3073.

41. Casals, C., E. Miguel, and J. Perez-Gil. 1993. Tryptophan fluorescence study on the interaction of pulmonary surfactant protein A with phospholipid vesicles. Biochem. J. 296 (Pt 3: 585–593.

42. Lopez-Rodriguez, E., and J. Perez-Gil. 2014. Structure-function relationships in pulmonary surfactant membranes: from biophysics to therapy. Biochim Biophys Acta. 1838: 1568–1585.

43. Suzuki, Y., Y. Fujita, and K. Kogishi. 1989. Reconstitution of tubular myelin from synthetic lipids and proteins associated with pig pulmonary surfactant. Am Rev Respir Dis. 140: 75–81.

44. Poulain, F.R., L. Allen, M.C. Williams, R.L. Hamilton, and S. Hawgood. 1992. Effects of surfactant apolipoproteins on liposome structure: implications for tubular myelin formation. Am J Physiol. 262: L730-9.

45. Saenz, A., O. Canadas, L.A. Bagatolli, F. Sanchez-Barbero, M.E. Johnson, and C. Casals. 2007. Effect of surfactant protein A on the physical properties and surface activity of KL4-surfactant. Biophys. J. 92: 482–492.

46. Lopez-Rodriguez, E., A. Pascual, R. Arroyo, J. Floros, and J. Perez-Gil. 2016. Human Pulmonary Surfactant Protein SP-A1 Provides Maximal Efficiency of Lung Interfacial Films.

Biophys. J. 111: 524–536.

47. Ogasawara, Y., Y. Kuroki, and T. Akino. 1992. Pulmonary surfactant protein D specifically binds to phosphatidylinositol. J. Biol. Chem. 267: 21244–21249.

48. Kuroki, Y., S. Gasa, Y. Ogasawara, M. Shiratori, A. Makita, and T. Akino. 1992. Binding specificity of lung surfactant protein SP-D for glucosylceramide. Biochem. Biophys. Res. Commun. 187: 963–969.

49. Wissel, H., A. Lehfeldt, P. Klein, T. Müller, and P.A. Stevens. 2001. Endocytosed SP-A and surfactant lipids are sorted to different organelles in rat type II pneumocytes. Am. J. Physiol. Lung Cell. Mol. Physiol. 281: L345-360.

50. Ikegami, M. 2000. Surfactant metabolism in SP-D deficient mice. Appl. Cardiopulm. Pathophysiol. 9: 251–253.

51. Ikegami, M., S. Grant, T. Korfhagen, R.K. Scheule, and J.A. Whitsett. 2009. Surfactant protein-D regulates the postnatal maturation of pulmonary surfactant lipid pool sizes. J Appl Physiol. 106: 1545–1552.

52. Nogee, L.M. 2004. Alterations in SP-B and SP-C expression in neonatal lung disease. Annu. Rev. Physiol. 66: 601–623.

53. Serrano, A.G., and J. Pérez-Gil. 2006. Protein-lipid interactions and surface activity in the pulmonary surfactant system. Chem. Phys. Lipids. 141: 105–118.

54. Parra, E., and J. Pérez-Gil. 2015. Composition, structure and mechanical properties define performance of pulmonary surfactant membranes and films. Chem. Phys. Lipids. 185: 153–175.

55. Perez-Gil, J., and T.E. Weaver. 2010. Pulmonary surfactant pathophysiology: current models and open questions. Physiol. 25: 132–141.

56. Clements, J.A. 1977. Functions of the alveolar lining. Am. Rev. Respir. Dis. 115: 67–71.

57. Watkins, J.C. 1968. The surface properties of pure phospholipids in relation to those of lung extracts. Biochim. Biophys. Acta - Lipids Lipid Metab. 152: 293–306.

58. Pastrana-Rios, B., C.R. Flach, J.W. Brauner, A.J. Mautone, and R. Mendelsohn. 1994. A direct test of the “squeeze-out” hypothesis of lung surfactant function. External reflection FT-IR at the air/water interface. Biochemistry. 33: 5121–5127.

59. Keating, E., Y.Y. Zuo, S.M. Tadayyon, N.O. Petersen, F. Possmayer, and R.A. Veldhuizen. 2012. A modified squeeze-out mechanism for generating high surface pressures with pulmonary surfactant. Biochim Biophys Acta. 1818: 1225–1234.

60. Amrein, M., a von Nahmen, and M. Sieber. 1997. A scanning force- and fluorescence light microscopy study of the structure and function of a model pulmonary surfactant. Eur. Biophys. J. 26: 349–57.

61. Sachan, A.K., and H.J. Galla. 2013. Bidirectional surface analysis of monomolecular membrane harboring nanoscale reversible collapse structures. Nano Lett. 13: 961–966.

62. Crane, J.M., and S.B. Hall. 2001. Rapid compression transforms interfacial monolayers of pulmonary surfactant. Biophys. J. 80: 1863–1872.

63. Smith, E.C., J.M. Crane, T.G. Laderas, and S.B. Hall. 2003.

Metastability of a supercompressed fluid monolayer. Biophys J. 85: 3048–3057.

64. Nogee, L.M., G. Garnier, H.C. Dietz, L. Singer, A.M. Murphy, D.E. deMello, and H.R. Colten. 1994. A mutation in the surfactant protein B gene responsible for fatal neonatal respiratory disease in multiple kindreds. J. Clin. Invest. 93: 1860–1863.

65. Clark, J.C., S.E. Wert, C.J. Bachurski, M.T. Stahlman, B.R. Stripp, T.E. Weaver, and J.A. Whitsett. 1995. Targeted disruption of the surfactant protein B gene disrupts surfactant homeostasis, causing respiratory failure in newborn mice. Proc Natl Acad Sci U S A. 92: 7794–7798.

66. Melton, K.R., L.L. Nesslein, M. Ikegami, J.W. Tichelaar, J.C. Clark, J. a Whitsett, and T.E. Weaver. 2003. SP-B deficiency causes respiratory failure in adult mice. Am. J. Physiol. Lung Cell. Mol. Physiol. 285: L543-9.

67. Olmeda, B., B. Garcia-Alvarez, and J. Perez-Gil. 2013. Structure-function correlations of pulmonary surfactant protein SP-B and the saposin-like family of proteins. Eur Biophys J. 42: 209–222.

68. Johansson, J., T. Curstedt, and H. Joernvall. 1991. Surfactant protein B: disulfide bridges, structural properties and kringle similarities. Biochemistry. 30: 6917–6921.

69. Andersson, M., T. Curstedt, H. Jörnvall, and J. Johansson. 1995. An amphipathic helical motif common to tumourolytic polypeptide NK-lysin and pulmonary surfactant polypeptide SP-B. FEBS Lett. 362: 328–332.

70. Serrano, A.G., A. Cruz, K. Rodríguez-Capote, F. Possmayer, and J. Pérez-Gil. 2005. Intrinsic structural and functional determinants within the amino acid sequence of mature pulmonary surfactant protein SP-B. Biochemistry. 44: 417–430.

71. Vandenbussche, G., a Clercx, M. Clercx, T. Curstedt, J. Johansson, H. Jörnvall, and J.M. Ruysschaert. 1992. Secondary structure and orientation of the surfactant protein SP-B in a lipid environment. A Fourier transform infrared spectroscopy study. Biochemistry. 31: 9169–76.

72. Cruz, A., C. Casals, I. Plasencia, D. Marsh, and J. Pérez-Gil. 1998. Depth profiles of pulmonary surfactant protein B in phosphatidylcholine bilayers, studied by fluorescence and electron spin resonance spectroscopy. Biochemistry. 37: 9488–9496.

73. Baatz, J.E., B. Elledge, and J.A. Whitsett. 1990. Surfactant protein SP-B induces ordering at the surface of model membrane bilayers. Biochemistry. 29: 6714–6720.

74. Gordon, L.M., S. Horvath, M.L. Longo, J. a Zasadzinski, H.W. Taeusch, K. Faull, C. Leung, and a J. Waring. 1996. Conformation and molecular topography of the N-terminal segment of surfactant protein B in structure-promoting environments. Protein Sci. 5: 1662–1675.

75. Morrow, M.R., J. Perez-Gil, G. Simatos, C. Boland, J. Stewart, D. Absolom, V. Sarin, and K.M. Keough. 1993. Pulmonary surfactant-associated protein SP-B has little effect on acyl chains in dipalmitoylphosphatidylcholine dispersions. Biochemistry. 32: 4397–4402.

76. Schurch, D., O.L. Ospina, A. Cruz, and J. Perez-Gil. 2010. Combined and independent action of proteins SP-B and SP-C in the surface

behavior and mechanical stability of pulmonary surfactant films. Biophys J. 99: 3290–3299.

77. Krol, S., M. Ross, M. Sieber, S. Künneke, H.-J. Galla, and A. Janshoff. 2000. Formation of three-dimensional protein-lipid aggregates in monolayer films induced by surfactant protein B. Biophys. J. 79: 904–918.

78. Rodriguez-Capote, K., K. Nag, S. Schürch, and F. Possmayer. 2001. Surfactant protein interactions with neutral and acidic phospholipid films. Am. J. Physiol. - Lung Cell. Mol. Physiol. 281: L231–L242.

79. Ryan, M.A., X. Qi, A.G. Serrano, M. Ikegami, J. Perez-Gil, J. Johansson, and T.E. Weaver. 2005. Mapping and analysis of the lytic and fusogenic domains of surfactant protein B. Biochemistry. 44: 861–872.

80. Chang, R., S. Nir, and F.R. Poulain. 1998. Analysis of binding and membrane destabilization of phospholipid membranes by surfactant apoprotein B. Biochim Biophys Acta. 1371: 254–264.

81. Baoukina, S., and D.P. Tieleman. 2010. Direct simulation of protein-mediated vesicle fusion: lung surfactant protein B. Biophys J. 99: 2134–2142.

82. Chavarha, M., H. Khoojlnlan, L.E. Schulwitz, S.C. Biswas, S.B. Rananavare, and S.B. Hall. 2010. Hydrophobic surfactant proteins induce a phosphatidylethanolamine to form cubic phases. Biophys. J. 98: 1549–1557.

83. Rugonyi, S., S.C. Biswas, and S.B. Hall. 2008. The biophysical function of pulmonary surfactant. Respir. Physiol. Neurobiol. 163: 244–55.

84. Parra, E., A. Alcaraz, A. Cruz, V.M. Aguilella, and J. Perez-Gil. 2013. Hydrophobic pulmonary surfactant proteins SP-B and SP-C induce pore formation in planar lipid membranes: evidence for proteolipid pores. Biophys J. 104: 146–155.

85. Parra, E., L.H. Moleiro, I. Lopez-Montero, A. Cruz, F. Monroy, and J. Perez-Gil. 2011. A combined action of pulmonary surfactant proteins SP-B and SP-C modulates permeability and dynamics of phospholipid membranes. Biochem J. 438: 555–564.

86. Olmeda, B., B. Garcia-Alvarez, M.J. Gomez, M. Martinez-Calle, A. Cruz, and J. Perez-Gil. 2015. A model for the structure and mechanism of action of pulmonary surfactant protein B. FASEB J. 29: 4236–4247.

87. Olmeda, B., L. Villén, A. Cruz, G. Orellana, and J. Perez-Gil. 2010. Pulmonary surfactant layers accelerate O2 diffusion through the air-water interface. Biochim. Biophys. Acta - Biomembr. 1798: 1281–1284.

88. Stahlman, M.T., M.P. Gray, M.W. Falconieri, J. a Whitsett, and T.E. Weaver. 2000. Lamellar body formation in normal and surfactant protein B-deficient fetal mice. Lab. Invest. 80: 395–403.

89. Clark, J.C., S.E. Wert, C.J. Bachurski, M.T. Stahlmant, B.R. Stripp, T.E. Weaver, J.A. Whitsett, and J.A. Clements. 1995. Targeted disruption of the surfactant protein B gene disrupts surfactant homeostasis, causing respiratory failure in newborn mice. Cell Biol. 92: 7794–7798.

90. Hobi, N., M. Giolai, B. Olmeda, P. Miklavc, E. Felder, P. Walther, P. Dietl, M. Frick, J. Pérez-Gil, and T. Haller. 2016. A small key unlocks a heavy door: The essential function of the small hydrophobic proteins

SP-B and SP-C to trigger adsorption of pulmonary surfactant lamellar bodies. Biochim. Biophys. Acta - Mol. Cell Res. 1863: 2124–2134.

91. Potter, S., S. Orgeig, S. Donnellan, and C.B. Daniels. 2007. Purifying selection drives the evolution of surfactant protein C (SP-C) independently of body temperature regulation in mammals. Comp. Biochem. Physiol. - Part D Genomics Proteomics. 2: 165–176.

92. Korfhagen, T.R., S.W. Glasser, S.E. Wert, M.D. Bruno, C.C. Daugherty, J.D. McNeish, J.L. Stock, S.S. Potter, and J.A. Whitsett. 1990. Cis-acting sequences from a human surfactant protein gene confer pulmonary-specific gene expression in transgenic mice. Proc. Natl. Acad. Sci. U. S. A. 87: 6122–6126.

93. Johansson, J., T. Szyperski, T. Curstedt, and K. Wuthrich. 1994. The NMR structure of the pulmonary surfactant-associated polypeptide SP-C in an apolar solvent contains a valyl-rich alpha-helix. Biochemistry. 33: 6015–6023.

94. Chou, P.Y., and G.D. Fasman. 1978. Prediction of the Secondary Structure of Proteins from their Amino Acid Sequence. In: Advances in Enzymology and Related Areas of Molecular Biology. . pp. 45–148.

95. Johansson, J., T.E. Weaver, and L.O. Tjernberg. 2004. Proteolytic generation and aggregation of peptides from transmembrane regions: Lung surfactant protein C and amyloid β-peptide. Cell. Mol. Life Sci. 61: 326–335.

96. Johansson, J. 2001. Membrane properties and amyloid fibril formation of lung surfactant protein C. Biochem. Soc. Trans. 29: 601–606.

97. Beers, M.F., and S. Mulugeta. 2005. Surfactant Protein C Biosynthesis and Its Emerging Role in Conformational Lung Disease. Annu. Rev. Physiol. 67: 663–696.

98. Plasencia, I., L. Rivas, C. Casals, K.M.W. Keough, and J. Pérez-Gil. 2001. Intrinsic structural differences in the N-terminal segment of pulmonary surfactant protein SP-C from different species. Comp. Biochem. Physiol. - A Mol. Integr. Physiol. 129: 129–139.

99. Plasencia, I., L. Rivas, K.M. Keough, D. Marsh, and J. Perez-Gil. 2004. The N-terminal segment of pulmonary surfactant lipopeptide SP-C has intrinsic propensity to interact with and perturb phospholipid bilayers. Biochem J. 377: 183–193.

100. Morrow, M.R., S. Taneva, G.A. Simatos, L.A. Allwood, and K.M.W. Keough. 1993. 2H NMR Studies of the Effect of Pulmonary Surfactant SP-C on the Headgroup : A Model for Transbilayer Peptides in Surfactant and Biological Membranes ? Biochemistry. .

101. Dico, A.S., S. Taneva, M.R. Morrow, and K.M. Keough. 1997. Effect of calcium on phospholipid interaction with pulmonary surfactant protein C. Biophys J. 73: 2595–602 ST–Effect of calcium on phospholipid i.

102. Possmayer, F., K. Nag, K. Rodriguez, R. Qanbar, and S. Schürch. 2001. Surface activity in vitro: role of surfactant proteins. Comp. Biochem. Physiol. A. Mol. Integr. Physiol. 129: 209–20.

103. Wang, L., P. Cai, H.J. Galla, H. He, C.R. Flach, and R. Mendelsohn. 2005. Monolayer-multilayer transitions in a lung surfactant model: IR reflection-absorption spectroscopy and atomic force microscopy. Eur. Biophys. J. 34: 243–254.

104. Creuwels, L.A.J.M., R.A. Demel, L.M.G. Van Golde, B.J. Benson, and H.P. Haagsman. 1993. Effect of acylation on structure and function of surfactant protein C at the air-liquid interface. J. Biol. Chem. 268: 26752–26758.

105. Lukovic, D., A. Cruz, A. Gonzalez-Horta, A. Almlen, T. Curstedt, I. Mingarro, and J. Perez-Gil. 2012. Interfacial behavior of recombinant forms of human pulmonary surfactant protein SP-C. Langmuir. 28: 7811–7825.

106. Plasencia, I., a Cruz, C. Casals, and J. Pérez-Gil. 2001. Superficial disposition of the N-terminal region of the surfactant protein SP-C and the absence of specific SP-B-SP-C interactions in phospholipid bilayers. Biochem. J. 359: 651–9.

107. Gonzalez-Horta, A., D. Andreu, M.R. Morrow, and J. Perez-Gil. 2008. Effects of palmitoylation on dynamics and phospholipid-bilayer-perturbing properties of the N-terminal segment of pulmonary surfactant protein SP-C as shown by 2H-NMR. Biophys.J. 95: 2308–2317.

108. Amin, R.S., S.E. Wert, R.P. Baughman, J.F. Tomashefski, L.M. Nogee, a S. Brody, W.M. Hull, and J. a Whitsett. 2001. Surfactant protein deficiency in familial interstitial lung disease. J. Pediatr. 139: 85–92.

109. Nogee, L.M. 2004. Alterations in SP-B and SP-C expression in neonatal lung disease. Annu. Rev. Physiol. 66: 601–623.

110. Glasser, S.W., M.S. Burhans, T.R. Korfhagen, C.L. Na, P.D. Sly, G.F. Ross, M. Ikegami, and J.A. Whitsett. 2001. Altered stability of pulmonary surfactant in SP-C-deficient mice. Proc. Natl. Acad. Sci. U. S. A. 98: 6366–71.

111. Glasser, S.W., E.A. Detmer, M. Ikegami, C.L. Na, M.T. Stahlman, and J.A. Whitsett. 2003. Pneumonitis and emphysema in sp-C gene targeted mice. J. Biol. Chem. 278: 14291–14298.

112. Glasser, S.W., A.P. Senft, J.A. Whitsett, M.D. Maxfield, G.F. Ross, T.R. Richardson, D.R. Prows, Y. Xu, and T.R. Korfhagen. 2008. Macrophage dysfunction and susceptibility to pulmonary pseudomonas aeruginosa infection in surfactant protein C-deficient mice. J. Immunol. 181: 621–628.

113. Glasser, S.W., T.L. Witt, A.P. Senft, J.E. Baatz, D. Folger, M.D. Maxfield, H.T. Akinbi, D.A. Newton, D.R. Prows, and T.R. Korfhagen. 2009. Surfactant protein C-deficient mice are susceptible to respiratory syncytial virus infection. Am. J. Physiol. Lung Cell. Mol. Physiol. 297: L64-72.

114. Glasser, S.W., M.D. Maxfield, T.L. Ruetschilling, H.T. Akinbi, J.E. Baatz, J.A. Kitzmiller, K. Page, Y. Xu, E.L. Bao, and T.R. Korfhagen. 2013. Persistence of LPS-induced lung inflammation in surfactant protein-C-deficient mice. Am. J. Respir. Cell Mol. Biol. 49: 845–854.

115. Lawson, W.E., V. V Polosukhin, G.T. Stathopoulos, O. Zoia, W. Han, K.B. Lane, B. Li, E.F. Donnelly, G.E. Holburn, K.G. Lewis, R.D. Collins, W.M. Hull, S.W. Glasser, J.A. Whitsett, and T.S. Blackwell. 2005. Increased and prolonged pulmonary fibrosis in surfactant protein C-deficient mice following intratracheal bleomycin. Am. J. Pathol. 167: 1267–77.

116. Kim, K., S.Q. Choi, Z.A. Zell, T.M. Squires, and J.A. Zasadzinski. 2013. Effect of cholesterol nanodomains on monolayer morphology and dynamics. Proc Natl Acad Sci U S A. 110: E3054-60.

117. Leonenko, Z., S. Gill, S. Baoukina, L. Monticelli, J. Doehner, L. Gunasekara, F. Felderer, M. Rodenstein, L.M. Eng, and M. Amrein. 2007. An elevated level of cholesterol impairs self-assembly of pulmonary surfactant into a functional film. Biophys J. 93: 674–683.

118. Gunasekara, L., S. Schurch, W.M. Schoel, K. Nag, Z. Leonenko, M. Haufs, and M. Amrein. 2005. Pulmonary surfactant function is abolished by an elevated proportion of cholesterol. Biochim Biophys Acta. 1737: 27–35.

119. Keating, E., L. Rahman, J. Francis, A. Petersen, F. Possmayer, R. Veldhuizen, and N.O. Petersen. 2007. Effect of cholesterol on the biophysical and physiological properties of a clinical pulmonary surfactant. Biophys. J. 93: 1391–401.

120. Gomez-Gil, L., D. Schurch, E. Goormaghtigh, and J. Perez-Gil. 2009. Pulmonary surfactant protein SP-C counteracts the deleterious effects of cholesterol on the activity of surfactant films under physiologically relevant compression-expansion dynamics. Biophys J. 97: 2736–2745.

121. Baumgart, F., O.L. Ospina, I. Mingarro, I. Rodriguez-Crespo, and J. Perez-Gil. 2010. Palmitoylation of pulmonary surfactant protein SP-C is critical for its functional cooperation with SP-B to sustain compression/expansion dynamics in cholesterol-containing surfactant films. Biophys J. 99: 3234–3243.

122. Gomez-Gil, L., J. Perez-Gil, and E. Goormaghtigh. 2009. Cholesterol modulates the exposure and orientation of pulmonary surfactant protein SP-C in model surfactant membranes. Biochim Biophys Acta. 1788: 1907–1915.

123. Mulugeta, S., and M.F. Beers. 2006. Surfactant protein C: Its unique properties and emerging immunomodulatory role in the lung. Microbes Infect. 8: 2317–2323.

124. Augusto, L.A., M. Synguelakis, J. Johansson, T. Pedron, R. Girard, and R. Chabyl. 2003. Interaction of pulmonary surfactant protein C with CD14 and lipopolysaccharide. Infect. Immun. 71: 61–67.

125. Olmeda, B., M. Martínez-Calle, and J. Pérez-Gil. 2017. Pulmonary surfactant metabolism in the alveolar airspace: Biogenesis, extracellular conversions, recycling. Ann. Anat. - Anat. Anzeiger. 209: 78–92.

126. Batenburg, J.J. 1992. Surfactant phospholipids: synthesis and storage. Am. J. Physiol. 262: L367-85.

127. Agassandian, M., and R.K. Mallampalli. 2013. Surfactant phospholipid metabolism. Biochim. Biophys. Acta - Mol. Cell Biol. Lipids. 1831: 612–625.

128. Nakanishi, H., H. Shindou, D. Hishikawa, T. Harayama, R. Ogasawara, A. Suwabe, R. Taguchi, and T. Shimizu. 2006. Cloning and characterization of mouse lung-type acyl-CoA:lysophosphatidylcholine acyltransferase 1 (LPCAT1). Expression in alveolar type II cells and possible involvement in surfactant production. J. Biol. Chem. 281: 20140–7.

129. Orgeig, S., and C.B. Daniels. 2001. The roles of cholesterol in pulmonary surfactant: insights from comparative and evolutionary studies. Comp Biochem Physiol A Mol Integr Physiol. 129: 75–89.

130. Milos, S., J. Qua Hiansen, B. Banaschewski, Y.Y. Zuo, L.J. Yao, L.A. McCaig, J. Lewis, C.M. Yamashita,

and R.A.W. Veldhuizen. 2016. The effect of diet-induced serum hypercholesterolemia on the surfactant system and the development of lung injury. Biochem. Biophys. Reports. 7: 180–187.

131. Doyle, I.R., M.E. Jones, H.A. Barr, S. Orgeig, A.J. Crockett, C.F. Mcdonald, and T.E. Nicholas. 1994. Composition of human pulmonary surfactant varies with exercise and level of fitness. Am. J. Respir. Crit. Care Med. 149: 1619–1627.

132. Besnard, V., S.E. Wert, M.T. Stahlman, A.D. Postle, Y. Xu, M. Ikegami, and J.A. Whitsett. 2009. Deletion of Scap in alveolar type II cells influences lung lipid homeostasis and identifies a compensatory role for pulmonary lipofibroblasts. J. Biol. Chem. 284: 4018–4030.

133. Torday, J., and V. Rehan. 2011. Neutral lipid trafficking regulates alveolar type II cell surfactant phospholipid and surfactant protein expression. Exp. Lung Res. 37: 376–86.

134. Batenburg, J.J., and H.P. Haagsman. 1998. The lipids of pulmonary surfactant: dynamics and interactions with proteins. Prog. Lipid Res. 37: 235–276.

135. Baker, A.D., A. Malur, B.P. Barna, M.S. Kavuru, A.G. Malur, and M.J. Thomassen. 2010. PPARgamma regulates the expression of cholesterol metabolism genes in alveolar macrophages. Biochem. Biophys. Res. Commun. 393: 682–7.

136. Roszell, B.R., J.-Q. Tao, K.J. Yu, S. Huang, and S.R. Bates. 2012. Characterization of the Niemann-Pick C pathway in alveolar type II cells and lamellar bodies of the lung. AJP Lung Cell. Mol. Physiol. 302: L919–L932.

137. Vockeroth, D., L. Gunasekara, M. Amrein, F. Possmayer, J.F. Lewis, and R.A.W. Veldhuizen. 2010. Role of cholesterol in the biophysical dysfunction of surfactant in ventilator-induced lung injury. : 117–125.

138. Foster, C.D., P.X. Zhang, L.W. Gonzales, and S.H. Guttentag. 2003. In vitro surfactant protein B deficiency inhibits lamellar body formation. Am. J. Respir. Cell Mol. Biol. 29: 259–266.

139. Akinbi, H.T., J.S. Breslin, M. Ikegami, H.S. Iwamoto, J.C. Clark, J.A. Whitsett, A.H. Jobe, and T.E. Weaver. 1997. Rescue of SP-B knockout mice with a truncated SP-B proprotein. Function of the C-terminal propeptide. J. Biol. Chem. 272: 9640–9647.

140. Serrano, A.G., E.J. Cabré, and J. Pérez-Gil. 2007. Identification of a segment in the precursor of pulmonary surfactant protein SP-B, potentially involved in pH-dependent membrane assembly of the protein. Biochim. Biophys. Acta - Biomembr. 1768: 1059–1069.

141. Guttentag, S.H., M.F. Beers, B.M. Bieler, P.L. Ballard, G. S.H., B. M.F., B. B.M., and B. P.L. 1998. Surfactant protein B processing in human fetal lung. Am. J. Physiol. 275: L559-66.

142. Brasch, F., M. Ochs, T. Kahne, S. Guttentag, V. Schauer-Vukasinovic, M. Derrick, G. Johnen, N. Kapp, K.M. Muller, J. Richter, T. Giller, S. Hawgood, and F. Buhling. 2003. Involvement of napsin A in the C- and N-terminal processing of surfactant protein B in type-II pneumocytes of the human lung. J. Biol. Chem. 278: 49006–49014.

143. Guttentag, S., L. Robinson, P. Zhang, F. Brasch, F. Bühling, and M. Beers. 2003. Cysteine protease activity is required for surfactant protein B

processing and lamellar body genesis. Am. J. Respir. Cell Mol. Biol. 28: 69–79.

144. Zhou, L., L. Lim, R.H. Costa, and J.A. Whitsett. 1996. Thyroid transcription factor-1, hepatocyte nuclear factor-3beta, surfactant protein B, C, and Clara cell secretory protein in developing mouse lung. J. Histochem. Cytochem. 44: 1183–1193.

145. Keller, A., H.R. Eistetter, T. Voss, and K.P. Schafer. 1991. The pulmonary surfactant protein C (SP-C) precursor is a type II transmembrane protein. Biochem. J. 277 (Pt 2: 493–499.

146. Mulugeta, S., and M.F. Beers. 2003. Processing of Surfactant Protein C Requires a Type II Transmembrane Topology Directed by Juxtamembrane Positively Charged Residues. J. Biol. Chem. 278: 47979–47986.

147. Vorbroker, D.K., W.F. Voorhout, T.E. Weaver, and J.A. Whitsett. 1995. Posttranslational processing of surfactant protein C in rat type II cells. Am. J. Physiol. 269: L727-33.

148. Conkright, J.J., J.P. Bridges, C. Na, W.F. Voorhout, B. Trapnell, S.W. Glasser, and T.E. Weaver. 2001. Secretion of Surfactant Protein C, an Integral Membrane Protein, Requires the N-terminal Propeptide. 276: 14658–14664.

149. Wang, W.J., S.J. Russo, S. Mulugeta, and M.F. Beers. 2002. Biosynthesis of surfactant protein C (SP-C). Sorting of SP-C proprotein involves homomeric association via a signal anchor domain. J Biol Chem. 277: 19929–19937.

150. Ten Brinke, A., J.J. Batenburg, B.M. Gadella, H.P. Haagsman, A.B. Vaandrager, and L.M.G. Van Golde. 2001. The juxtamembrane lysine and arginine residues of surfactant protein C precursor influence palmitoylation via effects on trafficking. Am. J. Respir. Cell Mol. Biol. 25: 156–163.

151. ten Brinke, A., A.B. Vaandrager, H.P. Haagsman, A.N.J. a Ridder, L.M.G. van Golde, and J.J. Batenburg. 2002. Structural requirements for palmitoylation of surfactant protein C precursor. Biochem. J. 361: 663–71.

152. ten Brinke, A., J.J. Batenburg, H.P. Haagsman, L.M.G. van Golde, and A.B. Vaandrager. 2002. Differential effect of brefeldin A on the palmitoylation of surfactant protein C proprotein mutants. Biochem. Biophys. Res. Commun. 290: 532–8.

153. Vorbroker, D.K., C. Dey, T.E. Weaver, and J.A. Whitsett. 1992. Surfactant protein C precursor is palmitoylated and associates with subcellular membranes. BBA - Biomembr. 1105: 161–169.

154. Beers, M.F., and C. Lomax. 1995. Synthesis and processing of hydrophobic surfactant protein C by isolated rat type II cells. Am. J. Physiol. 269: L744-53.

155. Sánchez-Pulido, L., D. Devos, and A. Valencia. 2002. BRICHOS: A conserved domain in proteins associated with dementia, respiratory distress and cancer. Trends Biochem. Sci. 27: 329–332.

156. Johansson, H., M. Eriksson, K. Nordling, J. Presto, and J. Johansson. 2009. The Brichos domain of prosurfactant protein C can hold and fold a transmembrane segment. Protein Sci. 18: 1175–1182.

157. Gustafsson, M., W.J. Griffiths, E. Furusjö, and J. Johansson. 2001. The palmitoyl groups of lung surfactant protein C reduce unfolding into a

fibrillogenic intermediate. J. Mol. Biol. 310: 937–50.

158. Beers, M.F., C.Y. Kim, C. Dodia, and A.B. Fisher. 1994. Localization, synthesis, and processing of surfactant protein SP-C in rat lung analyzed by epitope-specific antipeptide antibodies. J. Biol. Chem. 269: 20318–20328.

159. Johnson, A.L., P. Braidotti, G.G. Pietra, S.J. Russo, A. Kabore, W.J. Wang, and M.F. Beers. 2001. Post-translational processing of surfactant protein-C proprotein: Targeting motifs in the NH2-terminal flanking domain are cleaved in late compartments. Am. J. Respir. Cell Mol. Biol. 24: 253–263.

160. Brasch, F., A. Ten Brinke, G. Johnen, M. Ochs, N. Kapp, K.M. Müller, M.F. Beers, H. Fehrenbach, J. Richter, J.J. Batenburg, and F. Bühling. 2002. Involvement of cathepsin H in the processing of the hydrophobic surfactant-associated protein C in type II pneumocytes. Am. J. Respir. Cell Mol. Biol. 26: 659–670.

161. Osanai, K., R.J. Mason, and D.R. Voelker. 2001. Pulmonary surfactant phosphatidylcholine transport bypasses the brefeldin A sensitive compartment of alveolar type II cells. Biochim. Biophys. Acta - Mol. Cell Biol. Lipids. 1531: 222–229.

162. Veldhuizen, R., and F. Possmayer. 2004. Phospholipid metabolism in lung surfactant. Subcell. Biochem. 37: 359–388.

163. Takahashi, K., Y. Kimura, K. Nagata, A. Yamamoto, M. Matsuo, and K. Ueda. 2005. ABC proteins: Key molecules for lipid homeostasis. Med. Mol. Morphol. 38: 2–12.

164. Cerrada, A., T. Haller, A. Cruz, and J. Pérez-Gil. 2015. Pneumocytes Assemble Lung Surfactant as Highly Packed/Dehydrated States with Optimal Surface Activity. Biophys. J. 109: 2295–2306.

165. Malacrida, L., S. Astrada, A. Briva, M. Bollati-Fogol??n, E. Gratton, and L.A. Bagatolli. 2016. Spectral phasor analysis of LAURDAN fluorescence in live A549 lung cells to study the hydration and time evolution of intracellular lamellar body-like structures. Biochim. Biophys. Acta - Biomembr. 1858: 2625–2635.

166. Dietl, P., and T. Haller. 2005. Exocytosis of lung surfactant: from the secretory vesicle to the air-liquid interface. Annu. Rev. Physiol. 67: 595–621.

167. Young, S.L., E.K. Fram, and E.W. Larson. 1992. Three-dimensional reconstruction of tubular myelin. Exp. Lung Res. 18: 497–504.

168. Schürch, S., F.H.Y. Green, and H. Bachofen. 1998. Formation and structure of surface films: Captive bubble surfactometry. Biochim. Biophys. Acta - Mol. Basis Dis. 1408: 180–202.

169. Whitsett, J.A., and T. Alenghat. 2015. Respiratory epithelial cells orchestrate pulmonary innate immunity. Nat. Immunol. 16: 27–35.

170. Günther, A., R. Schmidt, A. Feustel, U. Meier, C. Pucker, M. Ermert, and W. Seeger. 1999. Surfactant subtype conversion is related to loss of surfactant apoprotein B and surface activity in large surfactant aggregates: Experimental and clinical studies. Am. J. Respir. Crit. Care Med. 159: 244–251.

171. Rider, E.D., M. Ikegami, and A.H. Jobe. 1992. Localization of alveolar surfactant clearance in rabbit lung cells. Am. J. Physiol. 263: L201–L209.

172. Bates, S. 2010. P63 (CKAP4) as an

SP-A receptor: Implications for surfactant turnover. Cell. Physiol. Biochem. 25: 41–54.

173. Bates, S.R., C. Dodia, J.-Q. Tao, and A.B. Fisher. 2008. Surfactant protein-A plays an important role in lung surfactant clearance: evidence using the surfactant protein-A gene-targeted mouse. Am. J. Physiol. Lung Cell. Mol. Physiol. 294: L325-33.

174. Ikegami, M., W.M. Hull, M. Yoshida, S.E. Wert, and J. a Whitsett. 2001. SP-D and GM-CSF regulate surfactant homeostasis via distinct mechanisms. Am. J. Physiol. Lung Cell. Mol. Physiol. 281: L697–L703.

175. Postle, A.D., N.G. Henderson, G. Koster, H.W. Clark, and A.N. Hunt. 2011. Analysis of lung surfactant phosphatidylcholine metabolism in transgenic mice using stable isotopes. Chem. Phys. Lipids. 164: 549–555.

176. Ikegami, M., C.L. Na, T.R. Korfhagen, and J.A. Whitsett. 2005. Surfactant protein D influences surfactant ultrastructure and uptake by alveolar type II cells. Am J Physiol Lung Cell Mol Physiol. 288: L552-61.

177. Bortnick, A.E., E. Favari, J.-Q. Tao, O.L. Francone, M. Reilly, Y. Zhang, G.H. Rothblat, and S.R. Bates. 2003. Identification and characterization of rodent ABCA1 in isolated type II pneumocytes. Am. J. Physiol. - Lung Cell. Mol. Physiol. 285: L869–L878.

178. Zhou, J., Y. You, A.J. Ryan, and R.K. Mallampalli. 2004. Upregulation of surfactant synthesis triggers ABCA1-mediated basolateral phospholipid efflux. J. Lipid Res. 45: 1758–67.

179. Trapnell, B.C., and J.A. Whitsett. 2002. Gm-CSF regulates pulmonary surfactant homeostasis and alveolar macrophage-mediated innate host defense. Annu. Rev. Physiol. 64: 775–802.

180. Baker, A.D., A. Malur, B.P. Barna, S. Ghosh, M.S. Kavuru, A.G. Malur, and M.J. Thomassen. 2010. Targeted PPAR{gamma} deficiency in alveolar macrophages disrupts surfactant catabolism. J. Lipid Res. 51: 1325–1331.

181. Malur, A., A.D. Baker, A.J. McCoy, G. Wells, B.P. Barna, M.S. Kavuru, A.G. Malur, and M.J. Thomassen. 2011. Restoration of PPARγ reverses lipid accumulation in alveolar macrophages of GM-CSF knockout mice. Am. J. Physiol. Lung Cell. Mol. Physiol. 300: L73–L80.

182. Thomassen, M.J., B.P. Barna, A.G. Malur, T.L. Bonfield, C.F. Farver, A. Malur, H. Dalrymple, M.S. Kavuru, and M. Febbraio. 2007. ABCG1 is deficient in alveolar macrophages of GM-CSF knockout mice and patients with pulmonary alveolar proteinosis. J. Lipid Res. 48: 2762–8.

183. Bonfield, T.L., C.F. Farver, B.P. Barna, A. Malur, S. Abraham, B. Raychaudhuri, M.S. Kavuru, and M.J. Thomassen. 2003. Peroxisome proliferator-activated receptor-gamma is deficient in alveolar macrophages from patients with alveolar proteinosis. Am J Respir Cell Mol Biol. 29: 677–682.

184. Kitamura, T., N. Tanaka, J. Watanabe, Uchida, S. Kanegasaki, Y. Yamada, and K. Nakata. 1999. Idiopathic pulmonary alveolar proteinosis as an autoimmune disease with neutralizing antibody against granulocyte/macrophage colony-stimulating factor. J. Exp. Med. 190: 875–80.

185. Tanaka, N., J. Watanabe, T. Kitamura, Y. Yamada, S. Kanegasaki, and K. Nakata. 1999. Lungs of patients with idiopathic pulmonary alveolar proteinosis express a factor which neutralizes granulocyte-

macrophage colony stimulating factor. FEBS Lett. 442: 246–50.

186. Nishinakamura, R., R. Wiler, U. Dirksen, Y. Morikawa, K. Arai, A. Miyajima, S. Burdach, and R. Murray. 1996. The pulmonary alveolar proteinosis in granulocyte macrophage colony-stimulating factor/interleukins 3/5 beta c receptor-deficient mice is reversed by bone marrow transplantation. J Exp Med. 183: 2657–2662.

187. Malur, A., I. Huizar, G. Wells, B.P. Barna, A.G. Malur, and M.J. Thomassen. 2011. Lentivirus-ABCG1 instillation reduces lipid accumulation and improves lung compliance in GM-CSF knock-out mice. Biochem. Biophys. Res. Commun. 415: 288–293.

188. Abe, A., M. Hiraoka, S. Wild, S.E. Wilcoxen, R. Paine, and J.A. Shayman. 2004. Lysosomal phospholipase A2 is selectively expressed in alveolar macrophages. J. Biol. Chem. 279: 42605–42611.

189. Schneider, C., S.P. Nobs, M. Kurrer, H. Rehrauer, C. Thiele, and M. Kopf. 2014. Induction of the nuclear receptor PPAR-γ by the cytokine GM-CSF is critical for the differentiation of fetal monocytes into alveolar macrophages. Nat. Immunol. 15: 1026–1037.

190. Meaney, S., T.L. Bonfield, M. Hansson, A. Babiker, M.S. Kavuru, and M.J. Thomassen. 2004. Serum cholestenoic acid as a potential marker of pulmonary cholesterol homeostasis: increased levels in patients with pulmonary alveolar proteinosis. J. Lipid Res. 45: 2354–2360.

191. Wang, X., H.L. Collins, M. Ranalletta, I. V. Fuki, J.T. Billheimer, G.H. Rothblat, A.R. Tall, and D.J. Rader. 2007. Macrophage ABCA1 and ABCG1, but not SR-BI, promote macrophage reverse cholesterol transport in vivo. J. Clin. Invest. 117: 2216–2224.

192. Bates, S.R., J.-Q. Tao, H.L. Collins, O.L. Francone, and G.H. Rothblat. 2005. Pulmonary abnormalities due to ABCA1 deficiency in mice. Am. J. Physiol. Lung Cell. Mol. Physiol. 289: L980–L989.

193. Out, R., M. Hoekstra, R.B. Hildebrand, J.K. Kruit, I. Meurs, Z. Li, F. Kuipers, T.J.C. Van Berkel, and M. Van Eck. 2006. Macrophage ABCG1 deletion disrupts lipid homeostasis in alveolar macrophages and moderately influences atherosclerotic lesion development in LDL receptor-deficient mice. Arterioscler. Thromb. Vasc. Biol. 26: 2295–2300.

194. Wojcik, A.J., M.D. Skaflen, S. Srinivasan, and C.C. Hedrick. 2008. A critical role for ABCG1 in macrophage inflammation and lung homeostasis. J. Immunol. 180: 4273–82.

195. Schwartz, K., R.M. Lawn, and D.P. Wade. 2000. ABC1 gene expression and ApoA-I-mediated cholesterol efflux are regulated by LXR. Biochem. Biophys. Res. Commun. 274: 794–802.

196. Venkateswaran, a, B. a Laffitte, S.B. Joseph, P. a Mak, D.C. Wilpitz, P. a Edwards, and P. Tontonoz. 2000. Control of cellular cholesterol efflux by the nuclear oxysterol receptor LXR alpha. Proc. Natl. Acad. Sci. U. S. A. 97: 12097–12102.

197. Griese, M., F. Brasch, V.R. Aldana, M.M. Cabrera, U. Goelnitz, E. Ikonen, B.J. Karam, G. Liebisch, M.D. Linder, P. Lohse, W. Meyer, G. Schmitz, A. Pamir, J. Ripper, A. Rolfs, A. Schams, and F.J. Lezana. 2010. Respiratory disease in Niemann-Pick type C2 is caused by pulmonary alveolar proteinosis. Clin. Genet. 77:

119–130.

198. Hamvas, A., L.M. Nogee, F. V. White, P. Schuler, B.P. Hackett, C.B. Huddleston, E.N. Mendeloff, F.F. Hsu, S.E. Wert, L.W. Gonzales, M.F. Beers, and P.L. Ballard. 2004. Progressive lung disease and surfactant dysfunction with a deletion in surfactant protein C gene. Am. J. Respir. Cell Mol. Biol. 30: 771–776.

199. Blanco, O., and J. Perez-Gil. 2007. Biochemical and pharmacological differences between preparations of exogenous natural surfactant used to treat Respiratory Distress Syndrome: role of the different components in an efficient pulmonary surfactant. Eur J Pharmacol. 568: 1–15.

200. Zimmermann, L.J.I., D.J.M.T. Janssen, D. Tibboel, A. Hamvas, and V.P. Carnielli. 2005. Surfactant metabolism in the neonate. In: Biology of the Neonate. . pp. 296–307.

201. Dushianthan, A., M.P.W. Grocott, A.D. Postle, and R. Cusack. 2011. Acute respiratory distress syndrome and acute lung injury. Postgrad. Med. J. 87: 612–22.

202. Günther, a, C. Ruppert, R. Schmidt, P. Markart, F. Grimminger, D. Walmrath, and W. Seeger. 2001. Surfactant alteration and replacement in acute respiratory distress syndrome. Respir. Res. 2: 353–364.

203. Markart, P., C. Ruppert, M. Wygrecka, T. Colaris, B. Dahal, D. Walmrath, H. Harbach, J. Wilhelm, W. Seeger, R. Schmidt, and A. Guenther. 2007. Patients with ARDS show improvement but not normalisation of alveolar surface activity with surfactant treatment: putative role of neutral lipids. Thorax. 62: 588–594.

204. Whitsett, J.A., S.E. Wert, and T.E. Weaver. 2015. Diseases of pulmonary surfactant homeostasis. Annu. Rev. Pathol. 10: 371–93.

205. Silva, A., A. Moreto, C. Pinho, A. Magalhães, A. Morais, and C. Fiuza. 2014. Bilateral whole lung lavage in pulmonary alveolar proteinosis - A retrospective study. Rev. Port. Pneumol. 20: 254–259.

206. Happle, C., N. Lachmann, J. Skuljec, M. Wetzke, M. Ackermann, S. Brennig, A. Mucci, A.C. Jirmo, S. Groos, A. Mirenska, C. Hennig, T. Rodt, J.P. Bankstahl, N. Schwerk, T. Moritz, and G. Hansen. 2014. Pulmonary transplantation of macrophage progenitors as effective and long-lasting therapy for hereditary pulmonary alveolar proteinosis. Sci. Transl. Med. 6: 250ra113.

207. Pastrana, B., A.J. Mautone, and R. Mendelsohn. 1991. Fourier transform infrared studies of secondary structure and orientation of pulmonary surfactant SP-C and its effect on the dynamic surface properties of phospholipids. Biochemistry. 30: 10058–10064.

208. Vandenbussche, G., A. Clercx, T. Curstedt, J. Johansson, H. Jornvall, and J.M. Ruysschaert. 1992. Structure and orientation of the surfactant-associated protein C in a lipid bilayer. Eur J Biochem. 203: 201–209.

209. Wang, Z., O. Gurel, J.E. Baatz, and R.H. Notter. 1996. Acylation of pulmonary surfactant protein-C is required for its optimal surface active interactions with phospholipids. J Biol Chem. 271: 19104–19109.

210. Dluhy, R.A., S. Shanmukh, J.B. Leapard, P. Kruger, and J.E. Baatz. 2003. Deacylated pulmonary surfactant protein SP-C transforms

from alpha-helical to amyloid fibril structure via a pH-dependent mechanism: an infrared structural investigation. Biophys J. 85: 2417–2429.

211. Veldhuizen, E.J., J.J. Batenburg, G. Vandenbussche, G. Putz, L.M. van Golde, and H.P. Haagsman. 1999. Production of surfactant protein C in the baculovirus expression system: the information required for correct folding and palmitoylation of SP-C is contained within the mature sequence. Biochim Biophys Acta. 1416: 295–308.

212. Luy, B., A. Diener, R.P. Hummel, E. Sturm, W.R. Ulrich, and C. Griesinger. 2004. Structure and potential C-terminal dimerization of a recombinant mutant of surfactant-associated protein C in chloroform/methanol. Eur J Biochem. 271: 2076–2085.

213. Na Nakorn, P., M.C. Meyer, C.R. Flach, R. Mendelsohn, and H.J. Galla. 2007. Surfactant protein C and lung function: new insights into the role of alpha-helical length and palmitoylation. Eur Biophys J. 36: 477–489.

214. Perez-Gil, J. 2008. Structure of pulmonary surfactant membranes and films: the role of proteins and lipid-protein interactions. Biochim Biophys Acta. 1778: 1676–1695.

215. Baumgart, F., O.L. Ospina, I. Mingarro, I. Rodriguez-Crespo, and J. Perez-Gil. 2010. Palmitoylation of pulmonary surfactant protein SP-C is critical for its functional cooperation with SP-B to sustain compression/expansion dynamics in cholesterol-containing surfactant films. Biophys J. 99: 3234–3243.

216. Goormaghtigh, E., V. Raussens, and J.M. Ruysschaert. 1999. Attenuated total reflection infrared spectroscopy of proteins and lipids in biological membranes. Biochim Biophys Acta. 1422: 105–185.

217. Lukovic, D., I. Plasencia, F.J. Taberner, J. Salgado, J.J. Calvete, J. Perez-Gil, and I. Mingarro. 2006. Production and characterisation of recombinant forms of human pulmonary surfactant protein C (SP-C): Structure and surface activity. Biochim Biophys Acta. 1758: 509–518.

218. Colthup Daly, L. H. & Wiberley, S. E., N.B., and . 1975. Introduction to Infrared and Raman Spectroscopy. 2nd edition. New York: Academic Press.

219. Hübner A., W. and B. 1998. Interactions at the lipid–water interface. Chem. Phys. Lipids. 96: 99–123.

220. Johansson, J. 1998. Structure and properties of surfactant protein C. Biochim Biophys Acta. 1408: 161–172.

221. Gustafsson, M., M. Palmblad, T. Curstedt, J. Johansson, and S. Schurch. 2000. Palmitoylation of a pulmonary surfactant protein C analogue affects the surface associated lipid reservoir and film stability. Biochim Biophys Acta. 1466: 169–178.

222. Kramer, A., A. Wintergalen, M. Sieber, H.J. Galla, M. Amrein, and R. Guckenberger. 2000. Distribution of the surfactant-associated protein C within a lung surfactant model film investigated by near-field optical microscopy. Biophys J. 78: 458–465.

223. Szyperski, T., G. Vandenbussche, T. Curstedt, J.M. Ruysschaert, K. Wuthrich, and J. Johansson. 1998. Pulmonary surfactant-associated polypeptide C in a mixed organic solvent transforms from a monomeric alpha-helical state into

insoluble beta-sheet aggregates. Protein Sci. 7: 2533–2540.

224. Barth, A. 2007. Infrared spectroscopy of proteins. Biochim Biophys Acta. 1767: 1073–1101.

225. Nag, K., J. Perez-Gil, A. Cruz, and K.M. Keough. 1996. Fluorescently labeled pulmonary surfactant protein C in spread phospholipid monolayers. Biophys J. 71: 246–256.

226. Wustneck, R., J. Perez-Gil, N. Wustneck, A. Cruz, V.B. Fainerman, and U. Pison. 2005. Interfacial properties of pulmonary surfactant layers. Adv Colloid Interface Sci. 117: 33–58.

227. Lang, C.J., A.D. Postle, S. Orgeig, F. Possmayer, W. Bernhard, A.K. Panda, K.D. Jurgens, W.K. Milsom, K. Nag, and C.B. Daniels. 2005. Dipalmitoylphosphatidylcholine is not the major surfactant phospholipid species in all mammals. Am J Physiol Regul Integr Comp Physiol. 289: R1426-39.

228. Bernardino de la Serna, J., R. Vargas, V. Picardi, A. Cruz, R. Arranz, J.M. Valpuesta, L. Mateu, and J. Perez-Gil. 2013. Segregated ordered lipid phases and protein-promoted membrane cohesivity are required for pulmonary surfactant films to stabilize and protect the respiratory surface. Faraday Discuss. 161: 535–548.

229. Seymour, J.F., and J.J. Presneill. 2002. Pulmonary alveolar proteinosis: progress in the first 44 years. Am J Respir Crit Care Med. 166: 215–235.

230. Nystrom, J.H., M. Lonnfors, and T.K. Nyholm. 2010. Transmembrane peptides influence the affinity of sterols for phospholipid bilayers. Biophys J. 99: 526–533.

231. Perez-Gil, J., C. Casals, and D. Marsh. 1995. Interactions of hydrophobic lung surfactant proteins SP-B and SP-C with dipalmitoylphosphatidylcholine and dipalmitoylphosphatidylglycerol bilayers studied by electron spin resonance spectroscopy. Biochemistry. 34: 3964–3971.

232. Shiffer, K., S. Hawgood, H.P. Haagsman, B. Benson, J. a. Clements, and J. Goerke. 1993. Lung surfactant proteins, SP-B and SP-C, alter the thermodynamic properties of phospholipid membranes: A differential calorimetry study. Biochemistry. 32: 590–597.

233. Bernardino de la Serna, J., G. Oradd, L.A. Bagatolli, A.C. Simonsen, D. Marsh, G. Lindblom, and J. Perez-Gil. 2009. Segregated phases in pulmonary surfactant membranes do not show coexistence of lipid populations with differentiated dynamic properties. Biophys J. 97: 1381–1389.

234. Scheidt, H.A., P. Muller, A. Herrmann, and D. Huster. 2003. The potential of fluorescent and spin-labeled steroid analogs to mimic natural cholesterol. J Biol Chem. 278: 45563–45569.

235. Bjorkqvist, Y.J., T.K. Nyholm, J.P. Slotte, and B. Ramstedt. 2005. Domain formation and stability in complex lipid bilayers as reported by cholestatrienol. Biophys J. 88: 4054–4063.

236. De La Serna, J.B., G. Orädd, L.A. Bagatolli, A.C. Simonsen, D. Marsh, G. Lindblom, and J. Perez-Gil. 2009. Segregated phases in pulmonary surfactant membranes do not show coexistence of lipid populations with differentiated dynamic properties. Biophys. J. 97: 1381–1389.

237. Engberg, O., H. Nurmi, T.K. Nyholm, and J.P. Slotte. 2015. Effects of cholesterol and saturated

sphingolipids on acyl chain order in 1-palmitoyl-2-oleoyl-sn-glycero-3-phosphocholine bilayers--a comparative study with phase-selective fluorophores. Langmuir. 31: 4255–4263.

238. Oosterlaken-Dijksterhuis, M.A., M. van Eijk, L.M. van Golde, and H.P. Haagsman. 1992. Lipid mixing is mediated by the hydrophobic surfactant protein SP-B but not by SP-C. Biochim Biophys Acta. 1110: 45–50.

239. Fugler, L., S. Clejan, and R. Bittman. 1985. Movement of cholesterol between vesicles prepared with different phospholipids or sizes. J Biol Chem. 260: 4098–4102.

240. Creuwels, L.A., R.A. Demel, L.M. van Golde, and H.P. Haagsman. 1995. Characterization of a dimeric canine form of surfactant protein C (SP-C). Biochim Biophys Acta. 1254: 326–332.

241. Kairys, V., M.K. Gilson, and B. Luy. 2004. Structural model for an AxxxG-mediated dimer of surfactant-associated protein C. Eur J Biochem. 271: 2086–2092.

242. McMahon, H.T., and J.L. Gallop. 2005. Membrane curvature and mechanisms of dynamic cell membrane remodelling. Nature. 438: 590–596.

243. Johansson, J., T. Szyperski, T. Curstedt, and K. Wuthrich. 1994. The NMR structure of the pulmonary surfactant-associated polypeptide SP-C in an apolar solvent contains a valyl-rich alpha-helix. Biochemistry. 33: 6015–6023.

244. Plasencia, I., F. Baumgart, D. Andreu, D. Marsh, and J. Perez-Gil. 2008. Effect of acylation on the interaction of the N-Terminal segment of pulmonary surfactant protein SP-C with phospholipid membranes. Biochim Biophys Acta. 1778: 1274–1282.

245. Gómez-Gil, L., J. Pérez-Gil, and E. Goormaghtigh. 2009. Cholesterol modulates the exposure and orientation of pulmonary surfactant protein SP-C in model surfactant membranes. Biochim. Biophys. Acta - Biomembr. 1788: 1907–1915.

246. Dico, A.S., S. Taneva, M.R. Morrow, and K.M.W. Keough. 1997. Phospholipid Interaction with Pulmonary Surfactant. 73: 2595–2602.

247. Simatos, G.A., K.B. Forward, M.R. Morrow, and K.M. Keough. 1990. Interaction between perdeuterated dimyristoylphosphatidylcholine and low molecular weight pulmonary surfactant protein SP-C. Biochemistry. 29: 5807–5814.

248. Pérez-Gil, J., C. Casals, and D. Marsh. 1995. Interactions of hydrophobic lung surfactant proteins SP-B and SP-C with dipalmitoylphosphatidylcholine and dipalmitoylphosphatidylglycerol bilayers studied by electron spin resonance spectroscopy. Biochemistry. 34: 3964–71.

249. Lafleur, M., B. Fine, E. Sternin, P.R. Cullis, and M. Bloom. 1989. Smoothed orientational order profile of lipid bilayers by 2H-nuclear magnetic resonance. Biophys. J. 56: 1037–1041.

250. Knight, C., A. Rahmani, and M.R. Morrow. 2016. Effect of an Anionic Lipid on the Barotropic Behavior of a Ternary Bicellar Mixture. Langmuir. 32: 10259–10267.

251. Singh, H., J. Emberley, and M.R. Morrow. 2008. Pressure induces interdigitation differently in DPPC and DPPG. Eur. Biophys. J. 37: 783–792.

252. Rahmani, A., C. Knight, and M.R.

Morrow. 2013. Response to hydrostatic pressure of bicellar dispersions containing an anionic lipid: Pressure-induced interdigitation. Langmuir. 29: 13481–13490.

253. Linseisen, F.M., J.L. Thewalt, M. Bloom, and T.M. Bayerl. 1993. 2H-NMR and DSC study of SEPC-cholesterol mixtures. Chem. Phys. Lipids. 65: 141–149.

254. Davis, J.H., J.J. Clair, and J. Juhasz. 2009. Phase equilibria in DOPC/DPPC-d62/cholesterol mixtures. Biophys. J. 96: 521–539.

255. Dufourc, E.J., E.J. Parish, S. Chitrakorn, and I.C.P. Smith. 1984. Structural and dynamical details of cholesterol-lipid interaction as revealed by deuterium NMR. Biochemistry. 23: 6062–6071.

256. Rinia, H.A., J.W.P. Boots, D.T.S. Rijkers, R.A. Kik, M.M.E. Snel, R.A. Demel, J.A. Killian, J.P.J.M. Van der Eerden, and B. De Kruijff. 2002. Domain formation in phosphatidylcholine bilayers containing transmembrane peptides: Specific effects of flanking residues. Biochemistry. 41: 2814–2824.

257. Plasencia, I., K.M.W. Keough, and J. Perez-Gil. 2005. Interaction of the N-terminal segment of pulmonary surfactant protein SP-C with interfacial phospholipid films. Biochim. Biophys. Acta - Biomembr. 1713: 118–128.

258. Whitsett, J.A., and T.E. Weaver. 2002. Hydrophobic surfactant proteins in lung function and disease. N. Engl. J. Med. 347: 2141–2148.

259. Jordanova, A., G.A. Georgiev, S. Alexandrov, R. Todorov, and Z. Lalchev. 2009. Influence of surfactant protein C on the interfacial behavior of phosphatidylethanolamine monolayers. Eur. Biophys. J. 38: 369–379.

260. Skipski, V.P., M. Barclay, E.S. Reichman, and J.J. Good. 1967. Separation of acidic phospholipids by one-dimensional thin-layer chromatography. Biochim. Biophys. Acta - Lipids Lipid Metab. 137: 80–89.

261. Skipski, V.P., R.F. Peterson, and M. Barclay. 1964. Quantitative analysis of phospholipids by thin-layer chromatography. Biochem. J. 90: 374–378.

262. Skipski, V.P., R.F. Peterson, J. Sanders, and M. Barclay. 1963. Thin-layer chromatography of phospholipids using silica gel without calcium sulfate binder. J. Lipid Res. 4: 227–228.

263. Allan, D., and S. Cockcroft. 1982. A modified procedure for thin-layer chromatography of phospholipids. J Lipid Res. 23: 1373–1374.

264. Weerheim, A.M., A.M. Kolb, A. Sturk, and R. Nieuwland. 2002. Phospholipid composition of cell-derived microparticles determined by one-dimensional high-performance thin-layer chromatography. Anal Biochem. 302: 191–198.

265. Gilfillan, A.M., A.J. Chu, D.A. Smart, and S.A. Rooney. 1983. Single plate separation of lung phospholipids including disaturated phosphatidylcholine. J Lipid Res. 24: 1651–1656.

266. Scarim, J., H. Ghanbari, V. Taylor, and G. Menon. 1989. Determination of phosphatidylcholine and disaturated phosphatidylcholine content in lung surfactant by high performance liquid chromatography. J. Lipid Res. 30:

607–11.

267. Iwamori, M., K. Hirota, T. Utsuki, K. Momoeda, K. Ono, Y. Tsuchida, K. Okumura, and K. Hanaoka. 1996. Sensitive method for the determination of pulmonary surfactant phospholipid/sphingomyelin ratio in human amniotic fluids for the diagnosis of respiratory distress syndrome by thin-layer chromatography-immunostaining. Anal. Biochem. 238: 29–33.

268. Hall, S.B., Z. Wang, and R.H. Notter. 1994. Separation of subfractions of the hydrophobic components of calf lung surfactant. J. Lipid Res. 35: 1386–1394.

269. Tsai, M.Y., and J.G. Marshall. 1979. Phosphatidylglycerol in 261 samples of amniotic fluid from normal and diabetic pregnancies, as measured by one-dimensional thin-layer chromatography. Clin. Chem. 25: 682–685.

270. Spillman, T., D.B. Coton, and E. Golunski. 1988. Detection frequency by thin-layer chromatography of phosphatidylglycerol in amniotic fluid with clinically functional pulmonary surfactant. Clin. Chem. 34: 1976–1982.

271. Mitnick, M.A., B. DeMarco, and J.M. Gibbons. 1980. Amniotic fluid phosphatidylglycerol and phosphatidylinositol separated by stepwise-development thin-layer chromatography. Clin. Chem. 26: 277–281.

272. Cernansky, G., D.F. Liau, S.A. Hashim, and S.F. Ryan. 1980. Estimation of phosphatidylglycerol in fluids containing pulmonary surfactant. J. Lipid Res. 21: 1128–1131.

273. Perez-Gil, J., A. Cruz, and C. Casals. 1993. Solubility of hydrophobic surfactant proteins in organic solvent/water mixtures. Structural studies on SP-B and SP-C in aqueous organic solvents and lipids. Biochim Biophys Acta. 1168: 261–270.

274. Lee, A.. 2003. Lipid–protein interactions in biological membranes: a structural perspective. Biochim. Biophys. Acta - Biomembr. 1612: 1–40.

275. Killian, J.A., and G. Von Heijne. 2000. How proteins adapt to a membrane-water interface. Trends Biochem. Sci. 25: 429–434.

276. Segrest, J.P., H. De Loof, J.G. Dohlman, C.G. Brouillette, and G.M. Anantharamaiah. 1990. Amphipathic helix motif: Classes and properties. Proteins Struct. Funct. Bioinforma. 8: 103–117.

277. Leonenko, Z., S. Gill, S. Baoukina, L. Monticelli, J. Doehner, L. Gunasekara, F. Felderer, M. Rodenstein, L.M. Eng, and M. Amrein. 2007. An Elevated Level of Cholesterol Impairs Self-Assembly of Pulmonary Surfactant into a Functional Film. Biophys. J. 93: 674–683.

278. Romero, F., D. Shah, M. Duong, R.B. Penn, M.B. Fessler, J. Madenspacher, W. Stafstrom, M. Kavuru, B. Lu, C.B. Kallen, K. Walsh, and R. Summer. 2015. A Pneumocyte-Macrophage Paracrine Lipid Axis Drives the Lung toward Fibrosis. .

279. Hayes, D., S. Kirkby, K.S. Mccoy, H.M. Mansour, M. Khosravi, H. Strawbridge, and J.D. Tobias. 2013. Reduction of lipid-laden macrophage index after laparoscopic Nissen fundoplication in cystic fibrosis patients after lung transplantation. Clin. Transplant. 27: 121–125.

280. Basset-Léobon, C., L. Lacoste-Collin, J. Aziza, J.C. Bes, S. Jozan, and M. Courtade-Saïdi. 2010. Cut-off values and significance of Oil Red O-positive cells in bronchoalveolar lavage fluid. Cytopathology. 21: 245–250.

281. Tangirala, R.K., W.G. Jerome, N.L. Jones, D.M. Small, W.J. Johnson, J.M. Glick, F.H. Mahlberg, and G.H. Rothblat. 1994. Formation of cholesterol monohydrate crystals in macrophage-derived foam cells. J. Lipid Res. 35: 93–104.

282. Moore, K.J., and I. Tabas. 2011. Macrophages in the pathogenesis of atherosclerosis. Cell. 145: 341–355.

283. Mora, A.L., E. Torres-González, M. Rojas, C. Corredor, J. Ritzenthaler, J. Xu, J. Roman, K. Brigham, and A. Stecenko. 2006. Activation of alveolar macrophages via the alternative pathway in herpesvirus-induced lung fibrosis. Am. J. Respir. Cell Mol. Biol. 35: 466–473.

284. Homma, S., A. Miyamoto, S. Sakamoto, K. Kishi, N. Motoi, and K. Yoshimura. 2005. Pulmonary fibrosis in an individual occupationally exposed to inhaled indium-tin oxide. Eur. Respir. J. 25: 200–204.

285. Duewell, P., H. Kono, K.J. Rayner, C.M. Sirois, G. Vladimer, F.G. Bauernfeind, G.S. Abela, L. Franchi, G. Nuñez, M. Schnurr, T. Espevik, E. Lien, K.A. Fitzgerald, K.L. Rock, K.J. Moore, S.D. Wright, V. Hornung, and E. Latz. 2010. NLRP3 inflammasomes are required for atherogenesis and activated by cholesterol crystals. Nature. 464: 1357–1361.

286. Moulakakis, C., and C. Stamme. 2009. Role of clathrin-mediated endocytosis of surfactant protein A by alveolar macrophages in intracellular signaling. Am. J. Physiol. Lung Cell. Mol. Physiol. 296: L430-41.

287. Schagat, T.L., M.J. Tino, and J.R. Wright. 1999. Regulation of protein phosphorylation and pathogen phagocytosis by surfactant protein A. Infect. Immun. 67: 4693–4699.

288. Kuhn, D.A., D. Vanhecke, B. Michen, F. Blank, P. Gehr, A. Petri-Fink, and B. Rothen-Rutishauser. 2014. Different endocytotic uptake mechanisms for nanoparticles in epithelial cells and macrophages. Beilstein J. Nanotechnol. 5: 1625–1636.

289. Wang, N., D.L. Silver, C. Thiele, and a R. Tall. 2001. ATP-binding cassette transporter A1 (ABCA1) functions as a cholesterol efflux regulatory protein. J. Biol. Chem. 276: 23742–7.

290. Anzinger, J.J., J. Chang, Q. Xu, C. Buono, Y. Li, F.J. Leyva, B.C. Park, L.E. Greene, and H.S. Kruth. 2010. Native low-density lipoprotein uptake by macrophage colony-stimulating factor-differentiated human macrophages is mediated by macropinocytosis and micropinocytosis. Arterioscler. Thromb. Vasc. Biol. 30: 2022–2031.

291. Augusto, L., K. Le Blay, G. Auger, D. Blanot, and R. Chaby. 2001. Interaction of bacterial lipopolysaccharide with mouse surfactant protein C inserted into lipid vesicles. Am. J. Physiol. Lung Cell. Mol. Physiol. 281: L776–L785.

292. Augusto, L. a, J. Li, M. Synguelakis, J. Johansson, and R. Chaby. 2002. Structural basis for interactions between lung surfactant protein C and bacterial lipopolysaccharide. J. Biol. Chem. 277: 23484–92.

293. Gautier, E.L., A. Chow, R. Spanbroek, G. Marcelin, M. Greter, C. Jakubzick, M. Bogunovic, M.

Leboeuf, N. van Rooijen, A.J. Habenicht, M. Merad, and G.J. Randolph. 2012. Systemic analysis of PPARγ in mouse macrophage populations reveals marked diversity in expression with critical roles in resolution of inflammation and airway immunity. J. Immunol. 189: 2614–2624.

294. Moore, K.J., E.D. Rosen, M.L. Fitzgerald, F. Randow, L.P. Andersson, D. Altshuler, D.S. Milstone, R.M. Mortensen, B.M. Spiegelman, and M.W. Freeman. 2001. The role of PPAR-gamma in macrophage differentiation and cholesterol uptake. Nat. Med. 7: 41–47.

295. Liscum, L., and S.L. Sturley. 2004. Intracellular trafficking of Niemann-Pick C proteins 1 and 2: obligate components of subcellular lipid transport. Biochim. Biophys. Acta. 1685: 22–27.

296. Vance, J.E., and K.B. Peake. 2011. Function of the Niemann-Pick type C proteins and their bypass by cyclodextrin. Curr. Opin. Lipidol. 22: 204–209.

297. Hiraoka, M., A. Abe, Y. Lu, K. Yang, X. Han, R.W. Gross, and J.A. Shayman. 2006. Lysosomal phospholipase A2 and phospholipidosis. Mol. Cell. Biol. 26: 6139–6148.

298. Poelma, D.L., L.J. Zimmermann, W.A. van Cappellen, J.J. Haitsma, B. Lachmann, and J.F. Van Iwaarden. 2004. Distinct effects of SP-B and SP-C on the uptake of surfactant-like liposomes by alveolar cells in vivo and in vitro. Am. J. Physiol. Lung Cell. Mol. Physiol. 287: L1056–L1065.

299. Poelma, D.L.H., L.J.I. Zimmermann, H.H. Scholten, B. Lachmann, and J.F. van Iwaarden. 2002. In vivo and in vitro uptake of surfactant lipids by alveolar type II cells and macrophages. Am. J. Physiol. Lung Cell. Mol. Physiol. 283: L648-54.

300. Quintero, O.A., and J.R. Wright. 2000. Metabolism of phosphatidylglycerol by alveolar macrophages in vitro. Am. J. Physiol. Lung Cell. Mol. Physiol. 279: L399–L407.

301. Poelma, D.L., M.R. Ju, S.C. Bakker, L.J. Zimmermann, B.F. Lachmann, and J.F. Van Iwaarden. 2004. A common pathway for the uptake of surfactant lipids by alveolar cells. Am. J. Respir. Cell Mol. Biol. 30: 751–758.

302. Justice, M.J., D.N. Petrusca, A.L. Rogozea, J.A. Williams, K.S. Schweitzer, I. Petrache, S.R. Wassall, and H.I. Petrache. 2014. Effects of lipid interactions on model vesicle engulfment by alveolar macrophages. Biophys. J. 106: 598–609.

303. Schwendener, R.A., P.A. Lagocki, and Y.E. Rahman. 1984. The effects of charge and size on the interaction of unilamellar liposomes with macrophages. BBA - Biomembr. 772: 93–101.

304. Kelly, C., C. Jefferies, and S.-A. Cryan. 2011. Targeted Liposomal Drug Delivery to Monocytes and Macrophages. J. Drug Deliv. 2011: 1–11.

305. Gross, N.J., and K.R. Narine. 1989. Surfactant subtypes in mice: characterization and quantitation. J. Appl. Physiol. 66: 342–9.

306. Brenner, T.A., T.A. Rice, E.D. Anderson, C.M. Percopo, and H.F. Rosenberg. 2016. Immortalized MH-S cells lack defining features of primary alveolar macrophages and do not support mouse pneumovirus replication. Immunol. Lett. 172: 106–112.

307. Gustafsson, M., J. Thyberg, J. Naslund, E. Eliasson, and J. Johansson. 1999. Amyloid fibril formation by pulmonary surfactant protein C. FEBS Lett. 464: 138–142.

308. Gonzalez-Horta, A., D. Andreu, M.R. Morrow, and J. Perez-Gil. 2008. Effects of palmitoylation on dynamics and phospholipid-bilayer-perturbing properties of the N-terminal segment of pulmonary surfactant protein SP-C as shown by 2H-NMR. Biophys J. 95: 2308–2317.

309. Mbawuike, I.N., and H.B. Herscowitz. 1989. MH-S, a murine alveolar macrophage cell line: morphological, cytochemical, and functional characteristics. J. Leukoc. Biol. 46: 119–127.

310. Fischer, R.T., F.A. Stephenson, A. Shafiee, and F. Schroeder. 1984. delta 5,7,9(11)-Cholestatrien-3 beta-ol: a fluorescent cholesterol analogue. Chem Phys Lipids. 36: 1–14.

311. Mason, J.T., A. V Broccoli, and C. Huang. 1981. A method for the synthesis of isomerically pure saturated mixed-chain phosphatidylcholines. Anal Biochem. 113: 96–101.

312. Ramstedt, B., and J.P. Slotte. 1999. Interaction of cholesterol with sphingomyelins and acyl-chain-matched phosphatidylcholines: a comparative study of the effect of the chain length. Biophys J. 76: 908–915.

313. Taeusch, H.W., J. Bernardino de la Serna, J. Perez-Gil, C. Alonso, and J.A. Zasadzinski. 2005. Inactivation of pulmonary surfactant due to serum-inhibited adsorption and reversal by hydrophilic polymers: experimental. Biophys J. 89: 1769–1779.

314. Bligh, E.G., and W.J. Dyer. 1959. A rapid method of total lipid extraction and purification. Can J Biochem Physiol. 37: 911–917.

315. Plasencia, I., a Cruz, J.L. López-Lacomba, C. Casals, and J. Pérez-Gil. 2001. Selective labeling of pulmonary surfactant protein SP-C in organic solution. Anal. Biochem. 296: 49–56.

316. Rouser, G., A.N. Siakotos, and S. Fleischer. 1966. Quantitative analysis of phospholipids by thin-layer chromatography and phosphorus analysis of spots. Lipids. 1: 85–86.

317. Zarzycki, P., M. Bartoszuk, and A. Radziwon. 2006. Optimization of TLC detection by phosphomolybdic acid staining for robust quantification of cholesterol and bile acids. JPC - J. Planar Chromatogr. - Mod. TLC. 19: 52–57.

318. Fringeli, U.P., and H.H. Gunthard. 1981. Infrared membrane spectroscopy. Mol Biol Biochem Biophys. 31: 270–332.

319. Byler, D.M., and H. Susi. 1986. Examination of the secondary structure of proteins by deconvolved FTIR spectra. Biopolymers. 25: 469–487.

320. Tsamaloukas, A., H. Szadkowska, P.J. Slotte, and H. Heerklotz. 2005. Interactions of cholesterol with lipid membranes and cyclodextrin characterized by calorimetry. Biophys J. 89: 1109–1119.

321. Davis, J.H., K.R. Jeffrey, M. Bloom, M.I. Valic, and T.P. Higgs. 1976. Quadrupolar echo deuteron magnetic resonance spectroscopy in ordered hydrocarbon chains. Chem. Phys. Lett. 42: 390–394.

322. Prosser, R.S., J.H. Davis, F.W. Dahlquist, and M.A. Lindorfer. 1991. 2H nuclear magnetic resonance of the gramicidin A backbone in a

phospholipid bilayer. Biochemistry. 30: 4687–4696.

323. Livak, K.J., and T.D. Schmittgen. 2001. Analysis of Relative Gene Expression Data Using Real-Time Quantitative PCR and the 2−ΔΔCT Method. Methods. 25: 402–408.